CZECH TECHNICAL UNIVERSITY IN PRAGUE

Faculty of Civil Engineering

Department of Concrete and Masonry Structures

Diploma Thesis on

Mlynske Nivy Bus Terminal – Dilatation of A5

Study Program: Civil Engineering

Field of Study: Building Structure

Supervisor: doc. Ing. Marek Foglar, Ph.D.

Prague, 2023 Patil Durgesh Sakharam

CZECH TECHNICAL UNIVERSITY IN PRAGUE
Faculty of Civil Engineering
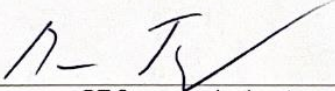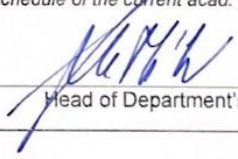Thákurova 7, 166 29 Prague 6, Czech Republic

CTU
CZECH TECHNICAL
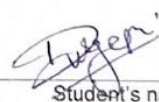UNIVERSITY
IN PRAGUE

DIPLOMA THESIS ASSIGNMENT FORM

I. PERSONAL AND STUDY DATA

Surname: PATIL   Name: Durgesh Sakharam   Personal number: 506366

Assigning Department: Department of concrete and masonry structures

Study programme: Civil Engineering

Study branch/spec.: Building Structures

II. DIPLOMA THESIS DATA

Diploma Thesis (DT) title: Mlýnské Nivy bus terminal - Diltation A5

Diploma Thesis title in English: Mlýnské Nivy bus terminal - Diltation A5

Instructions for writing the thesis:
Static assesment of the entire dilatation A5
- Preliminary desing of post-tensioned building of Mlynske Nivy bus terminal
- Construction drawings (concrete details drawings, prestressing details, reinforcement sketches)

List of recommended literature:
Navrátil,J.: Prestressed concrete structures, CERM Brno, ISBN 80-7204-462-1, 2006

Name of Diploma Thesis Supervisor: doc. Ing. Marek Foglar, Ph.D.

DT assignment date: 19.9.2022   DT submission date in IS KOS: 9.1.2023
see the schedule of the current acad. year

_____   _____
DT Supervisor's signature   Head of Department's signature

III. ASSIGNMENT RECEIPT

I declare that I am obliged to write the Diploma Thesis on my own, without anyone's assistance, except for provided consultations. The list of references, other sources and consultants' names must be stated in the Diploma Thesis and in referencing I must abide by the CTU methodological manual "How to Write University Final Theses" and the CTU methodological instruction "On the Observation of Ethical Principles in the Preparation of University Final Theses".

19.09.2022
_____   _____
Assignment receipt date   Student's name

Affidavit:

I declare that I have prepared this master's thesis independently with the guidance of my supervisor doc. Ing. Marek Foglar, Ph. D and I have listed all information sources from which I drew.

In Prague 08/01/2023 ……………·…………·.

Patil Durgesh Sakharam

Abstract

The subject of this thesis is the pre-stressing design of Mlynske Nivy bus terminal, section AS. Prestressed concrete is specific construction technology extensively used especially for bridges, but it is possible to use it for a variety of large-span structures similar to floor slabs or beams. The preface focuses on the subject of the specifics of prestressed concrete in erecting structures. The thesis also compactly describes the design of a bus station as a multifunctional house, its location, and disposition, likewise, the task is the evaluation of the load-bearing concrete structure. Along with this, topic of this project is software analysis of the most complicated floor slab, first designed in reinforced concrete, then in prestressed concrete. The element of the analysis is the explanation of the use of prestressed concrete in the project. In this part, the thesis smoothly passes to the commented structural analysis of the slab & beam in detail. The beam was chosen so that the principles of its design could be applied to other segments of the slab, even other floors of the building. Eventually, the subject is a design of concrete structure reinforcement in parts of the slab where prestress was designed so that the solution of a typical section of the slab is complete. Furthermore, the design of the staircase, ramps, columns, shear wall (core wall), analysis of sheeting walls and checks, and then the design of the group pile is done using the software for the prestressed concrete structure. Lastly, drawings of prestressing and reinforcement of the solved parts of this all discussed elements are attached to this thesis.

Keywords

prestressed concrete, reinforced concrete, expansion joint, provision of prestressed structure, code dependent deflection, tendons, load acting, short-term and long-term losses, stresses, design check, staircase, ramp, column, shear wall, sheeting walls, pile group

Content

List of figures

1. INTRODUCTION

1.1 Introduction

Concrete is most substantially used as a construction material because of its ease of vacuity, malleability, severity, and continuity. It consists of binding material, fine and coarse aggregate, and water, in which the seashore is usually used as an excellent total. Concrete has pretty high compressive electricity, however a whole lot lower tensile strength in ordinary reinforced cement concrete, compressive stresses are taken up through concrete and tensile stresses by way of the metal alone. The concrete below the impartial axis is left out in view that it is susceptible to stress and is presently a major venture for all masterminds. The only manner to look for druther cloth that may be absolutely or incompletely changed in construction is prestressed concrete, the shipment sporting ability of similar concrete sections may be elevated if metallic and concrete are each confused before the operations of outside loads, that is the theory of prestressed concrete. Prestressed concrete is utilized in a huge range of systems. Its bettered performance can permit longer spans, reduced structural density, and fabric financial savings compared with easily reinforced concrete. regular operations consist of high-upward thrust structures, home crossbeams, basis structures, ground and levee systems, silos and tanks, synthetic pavements, and nuclear constraint systems. [1]

The introductory precept of prestressing changed into carried out to construction, maybe centuries agone whilst ropes or essence bands have been wound around the rustic staves to form a barrel(see figure 1). whilst the bands were tensed, they had been underneath tensile prestress, which in turn created compressive prestress between the staves and enabled them to repel circle stress produced through internal liquid strain. In other phrases, the bands and the staves had been prestressed before they have been subordinated to any service loads.[2]

Figure 1: Introductory principle of prestressing

Therefore an disquisition is demanded to identify suitable cover that's better for strength and continuity performance. In this connection the use of prestressed concrete with partial or full relief may be a promising volition in concrete timber.

1.2 Objective of discussion

The end of this discussion is to analyze and design the structure of the Mlynské Nivy Bus Terminal. originally, to get familiar with the pre-stressing technology, construction process and continuity considerations applied to erecting construction. The alternate ideal is to demonstrate that the structural design of the typical arbor of this structure using conventional concrete isn't possible in order to prove the limitations of this technology in comparison with pre-stressed concrete. Likewise, to estimate the capability of the software SCIA to model and dissect complex structures like the one assessed in this thesis. Also, the last ideal is to present a result for the structural design of the below-pronounced arbor using PSC.

1.3 Organization

The report is organized in five chapters

Chapter 1: Gives brief description of preface of Prestressed concrete. It also includes objective, and association.

Chapter 2: It gives detailed description of Mlynské Nivy Bus terminal which includes its position, complete layout of structure, result of part A, loads acting on the structure, part of structure on which farther dilation is performed. theme, work, material, styles and losses of PSC.

Chapter 3: It discusses back history of use of PSC in structure.

Chapter 4: It includes theme, work and latterly performance analysis (Static solution)

Chapter 5: It describes the conclusion and unborn compass of the design.

2. Mlynské Nivy Bus Terminal

2.1 General

The Mlynské Nivy bus station was the largest bus station in Bratislava, the capital of Slovakia, until the end of 2017. Together with Nivy Mall and Nivy Bus Station, the work has brought a new life and a specific atmosphere to the surroundings and the Slovak capital itself. It helps shape a new vibrant civic street and brings ultramodern systems designed by world notorious and Slovak engineers to an area which was neglected for a long time. It's a large multi-functional structure, it serves plethora of different services, it include a shopping center, office space, requests and a parking lot. The structure is also dominated by a green roof with numerous rest conditioning similar as running track and drill field. The structure will thus be part of the Nové Niva zone, which also includes bordering structures of the Twin City executive complex – structures A, B, C and Twin City Tower. Part of the multi-functional structure design is also the new high- rise office structure, Nivy Tower conterminous from the west, the altitudinous current structure in Bratislava with a height of 125m.[3].

Figure 2: Mlynské Nivy bus station

Data and numbers:

1. Bus station area 30,000 m² – 36 platforms for getting on the motorcars and 7 for getting off Nivy Tower area, shopping Centre 70,000 m ².
2. Number of parking spaces,150

3. Diurnal number of passengers about,000
4. Diurnal number of machine departures advents,100
5. Green roof,000 m ² with further than 130 trees
6. Number of shops 200

2.2 Location

It's located in the megacity quarter Bratislava II – Ružinov. As one of the main trip capitals of Bratislava, the position of the station is suitable for long- distance transport, it's located in the wider megacity center at an imaginary crossroad between the literal center, the main road station and the field. The near D1 trace, the business roadway of Slovakia, also has a accessible position. The structure is framed on the south side by Mlýnská nivy road – a six-lane megacity street. Nivy is one of the stoutly developing sections of Bratislava, in the future it'll clearly be an artistic and social center offering the requirements of everyday life.[4]
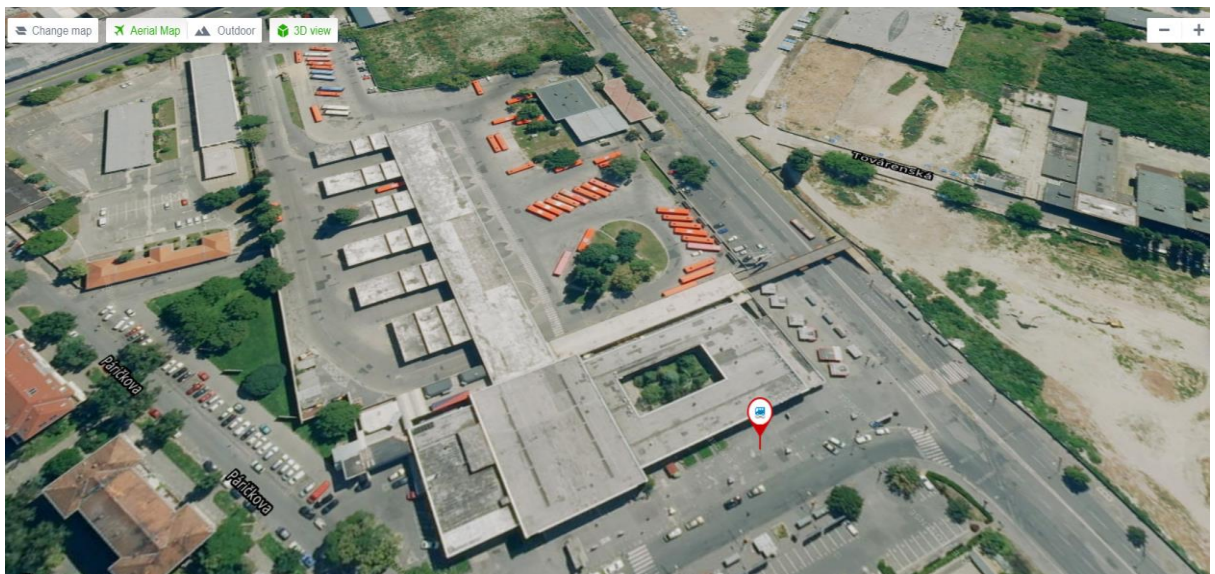
Figure 3: Aerial view of Mlynské Nivy bus station

2.3 Layout of Building

The maximum bottom plan confines of the entire SPV1 installation, i.e. the aggregate of both corridor "A+B", are vastly over standard, approx. 350 m in the longitudinal direction and approx. 140 m in the transverse direction. The multi-functional object being enforced is designed as a reinforced concrete monolithic shell (with a combination of corroborated concrete and prestressed load - bearing elements), which, from the perpetration point of view, consists of three functional units, which are virtually enforced as independent structures

• From the part in which garages and a machine station are located underground, and a shopping gallery(hereinafter A) is located above ground. Part A has two underground and over to six above- ground bottoms.

• From the part in which there are underground garages and a deals gallery above ground(hereafter B). Part B has three underground and five above- ground bottoms.

• From a high- rise executive structure that has three underground and 32 above- ground bottoms.

The internal structures of the underground bottoms, i.e. the ceiling crossbeams and partition walls of individual units SPV1.A and SPV1.B are separated from each other by the so- called by object dilation and latterly they're farther dilated into lower dilation units. All over-base bottoms have the same dilatations in height as internal underground structures. This results in a fairly complicated system from the point of view of icing the structure's watertightness, where the expansion joints in the ceiling structures are terminated four measures before the border wall, which is no longer expanded.

2.3.1 Part A

The part of structure A is divided into two underground and six above- ground bottoms. In 2PP, there are garages, in 1PP there's the machine outstation itself. Both underground bottoms are supplemented with specialized apartments or storages. The below-ground bottoms are substantially the spaces of the shopping center, the request, and the last bottom is a green roof. The main part of the boardwalk is the first below ground bottom where there are 3 main entrances to the complex and also the alternate below ground bottom where we can find fashion stores. On the third bottom is the catering area, which includes not only the formerly mentioned request, but also cafes and fast food. The communication element between the individual bottoms is a system of stairs, ramps for motorcars and buses and especially elevators and escalators. The position of the upper edge of the 1NP bottom determines the height position of the object ±0.000 = 137.500m.a.s.l.[4]
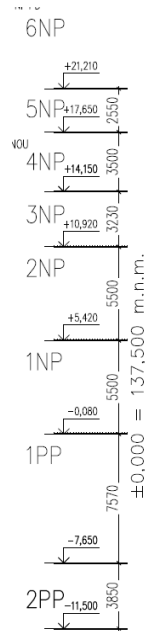
Figure 4: Position of each floor

The answered part of the multifunctional object SPV1.A is designed as a monolithic concrete structure, realized from a combination of reinforced concrete and prestressed load-bearing crossbeams, wall and bar perpendicular and vertical rudiments (columns and shafts). The use of a prestressed structure for the ceilings of the below-ground bottoms needed vastly large module distances of the columns, related to the functional conditions of the communication corridors and individual platforms of the machine station itself, located at the position of the first underground bottom. The structural heights of the individual bottoms are in the range between approx.2.5 to7.5 m. The third to sixth bottoms have a sword structure located at different height situations.
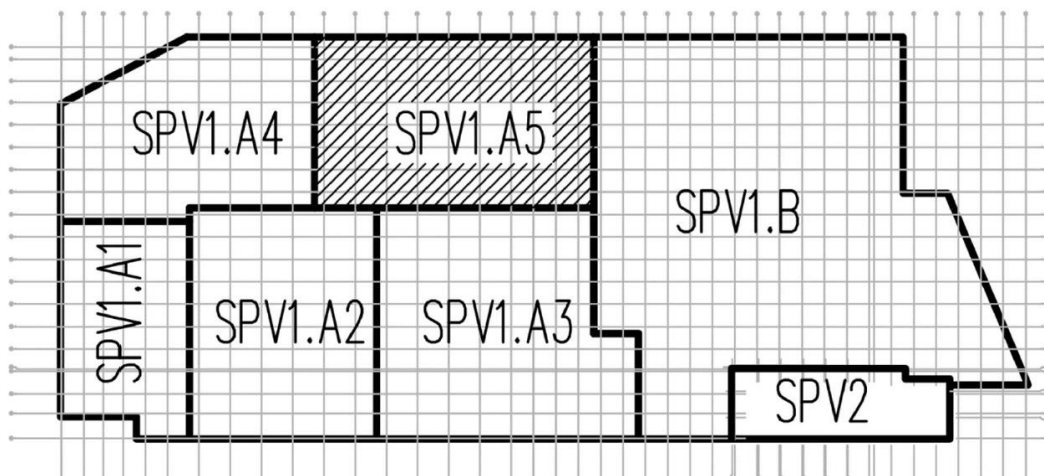
Figure 5: Layout of the Building A with marked expansion

Both corridor A and B together form one object SPV1, each part is further divided into several sections. Part A is divided into 5 expansion units with their own support system. Dilation SPV1.A5, i.e. the fifth dilation section of part A is the subject of this work. Both units are connected by a common base plate. All expansion units are connected by expansion joints enabling vertical movement of the structure. As it's clear from figure, the answered part of the object SPV1.A has a roughly blockish bottom plan with external confines of approx. 194x142 m, with column modulation in the longitudinal direction of 8.1 to 11.3 m and in the transverse direction of 8.1 to 16.2 m. The structure expansion between units SPV1.A and SPV1.B runs along the entire height across the structure, 2.5 m from the left wing of the module axis" 21/ T- F"(towards the axis" 20") and also continues 2.5 m from the left wing of the module axis" 23/ F- A". The range of the expansion joint between the objects and also the expansion joint between individual units A.1 to A.5 will be wider in the direction of height, taking into account the acceptance of the seismic standard in connection with possible distortions of individual units during a seismic event. From the 2nd bottom, this part of the structure will begin to retire in the direction of range from approx. 60 m to 22m.

2.3.1.1 Expansion Joints

In agreement with the acceptance of the request in question, only the expansion of the alternate underground bottom will be handed with system shear legs icing a movement of 20 mm, and in all advanced bottoms, the expansions will be answered through the tooth in concrete constructions, enabling the larger needed relegation of the conterminous expansion units. Expansions in wall constructions are answered on all bottoms through system shear super studs. The position of the individual expansion joints must accept, in addition to the static conditions assessed on the supporting structure, the conditions of the functional, functional and layout of the individual bottoms. With regard to the considerable hugeness of the object complex SPV1.A, indeed after its division into 5 lower units, the individual expansion sections are relatively large (up to 100 measures). In agreement with the below, the construction requires acceptable underpinning of the supporting rudiments and also the gradational concreting of individual sections (shots) with the operation of buffer strips, with fresh concreting at intervals. At the same time, the individual stage- off belts must admire the conditions for prestressing the vertical supporting structures. In agreement with the acceptance of the request in question, only the expansion of the alternate underground bottom will be handed with system shear legs icing a movement of 20 mm, and in all advanced bottoms, the expansions will be answered through the tooth in concrete constructions,

enabling the larger needed relegation of the conterminous expansion units. Expansions in wall constructions are answered on all bottoms through system shear super studs.

2.4 Geological Profile

Originally, detailed geological check was carried out for the structure, which determined the foundation conditions of this structure in detail. The result without expansion joints of the border structures, i.e. the base plate and the border basement walls, was chosen with regard to the considerable depth of "drowning" of the structure in the groundwater, which at the maximum position can rise to a position of over to133.5m.a.s.l., which means up to7.5 m above the position of the bottom of the alternate bottom underground bottom. The structure is grounded on a combination of mat and deep foundation construction, which consists of a base plate supported by large-periphery wearied piles. Piles are designed not only for active and unresistant pressure transfer from perpendicular structures, but also for uplift pressure caused by groundwater. The base plate is substantially of invariant consistence, without expansion. In places of columns, the consistence of the base plate is increased due to the increase in cargo. In these places there are responses from the superstructure transferred with the help of piles to the topsoil. The design of the foundation structures corresponds to the static design of the foundation of the structure.

2.5 Vertical support system

The perpendicular support system in the alternate underground bottom consists of border basement walls, harshening walls, walls of communication cores and columns positioned in the modular grid of the structure. Locally, steel columns are used in the upper bottoms as an fresh perpendicular structure for transferring eccentrically positioned corridor outside the module system(e.g. supporting the so- called "stones"). In the 2PP bottom plan, the wall harshening rudiments are arranged so that in a given bottom, stressed by vertical force goods, they completely take over the vertical goods from earth and hydrostatic pressure, from the goods of wind, temperature goods and seismicity, in collective combinations according to standard conditions. In the first underground bottom, harshening walls are virtually barred due to the needed layout(its own machine station), and vertical goods are transmitted by the walls of the communication cores and, in particular, massive columns with a sampling of over to 1000x1000 mm, which, together with the shafts, form rigid frames in both directions of the structure, in the longitudinal and transverse. analogous to 1PP, the vertical stiffness of

individual expansion units is also assured in the upper above- ground bottoms. The sampling of the columns is acclimated to the conditions of the armature, i.e. indirect columns are used in communication spaces, and square columns are used outside them, or blockish sampling(at least around the border of the object). The size of the columns in the advanced bottoms is gradationally reduced in agreement with the dwindling stress.

The consistence of the separate stiffening walls is 400 mm, and the wall density in the communication cores are 300, 250, independently. 200 mm. Other original wall structures are designed in the edging of communication ramps and in below- ground bottoms as a partial border wall, or as citadels around the border of the structure and also citadels lining large installation holes in ceiling boards. The border basement walls are completely designed with a consistence of 400 mm and, together with the base plate, fulfill the function of the so-called white-tub i.e. all waterproofing protection of the underground part of the building is provided by the reinforced concrete structure itself with maximum admissible cracks.

2.6 Horizontal support system

The 2PP ceiling board is designed as a reinforced concrete point-supported board with a consistence of 350 mm with heads of a total consistence together with a board of 600 mm. The ceiling arbor will be realized with a pitch, interspersing trough and crest to insure thorough drainage of the upper face, stressed by the nonstop business of motorcars. With regard to the given operation, there's a serious problem of the concrete face stressed by imported road swab, i.e. influence of carbonation and chloride erosion. In the given space, it's necessary to constantly apply a suitable face protection system (OS) of classes OS8 and OS11. A flexible system must be suitable to cover both static and dynamic cracks. The defensive system must be enforced as late as possible, so that utmost of the dividing cracks formerly live. The face of the concrete must meet the conditions for the operation of the named defensive system. Internal ramps for motorcars and ramps for passenger buses must also be defended. From the point of view of the range of the cracks, the ceiling boards are designed according to the written request of the client of the structure with the possibility of tone-sealing, or with the operation of original fresh injection of possible cracks, or the operation of face impregnation of concrete (crystalline sequestration). Depending on the nature of the structure and the position of the terrain, the client's demand for maximum cracks in the individual cargo- bearing structures is as follows

- For perimeter walls of basements and base plate, w<0.25mm

- For ceiling board above 2.PP, w<0.30mm

- For ceiling slab above 1.PP and above-ground floors, w<0.40mm

The ceiling structures of the below-ground bottoms are designed as a combination of post-tensioned, bidirectionally corroborated nonstop crossbeams, supported by post-tensioned shafts located in both orthogonal directions. At the point where the shafts cross, the ceiling structure is supported by columns. Where it's necessary to change (shift) the perpendicular support system along the height of the object, important prestressed transfer shafts are used.

2.6.1 Ceiling of SPV1.A

The ceiling prestressed construction of the SPV1.A part of the structure is divided into five expansion units, just like the corroborated concrete ceiling arbor 2PP. The expansion of the 2PP ceiling is answered with the help of system shear legs, and the other bottoms are answered with the help of a nonstop storehouse type (through the toothing of the supporting side. Individual working frames are divided into lower areas by working joints or loss strips, in which the fresh prestressing of the structure is realized. The loss strips are designed extents of 1.0 and 1.5 m, depending on the underpinning used in the given working section. The size of one working shot is assumed to be roughly 30.0 m x30.0m.

For the supporting structure grid of 16.2x11.30 m and 8.10x11.30 m in the ceilings above the 1st bottom, 1st bottom, 2nd bottom, 3rd bottom, 4th bottom and 5th bottom, the consistence of the prestressed board is 250 m and locally at advanced loads, or a consistence of 300 mm is used for a larger span. These are substantially ceilings under landscaping and intimately accessible spaces above the 1st PP, which will have a minimal consistence of 300 mm or further depending on the size of the cargo. fresh prestressed crossbars for spans of 16.20 m and co-acting crossbars with a span of 8.10 m are designed with a blockish sampling with a height of 750 mm and a range of 2000 mm. shafts for spans of11.30 m are designed 600 mm high and 1500 mm wide. Locally used so-called transfer shafts when changing the perpendicular support system have a significantly larger sampling.

2.7 Explanation of the spans - 2PP & 1PP

2PP- Locally supported ceiling arbor which transfer loads from machine and the layout of the parking allows fairly small spans- up to 11m. For the provision of 1PP(machine station), it was necessary to increase the spans due to the examination of the minimal range of the

parking lot and the minimal range of the business lane, thus one whole row of columns is take out compared to 2PP, and the module span rises to 16 m in these places. Such a grid is also on the other upper bottoms of the structure, where the span is justified by the use of internal gallerias, which are among the popular and typical layout rudiments of shopping centers. The gallerias are rounded by so- called voids, indirect penetrations in the ceiling crossbeams, frequently also establishing perpendicular communication across the structure in the form of escalators.
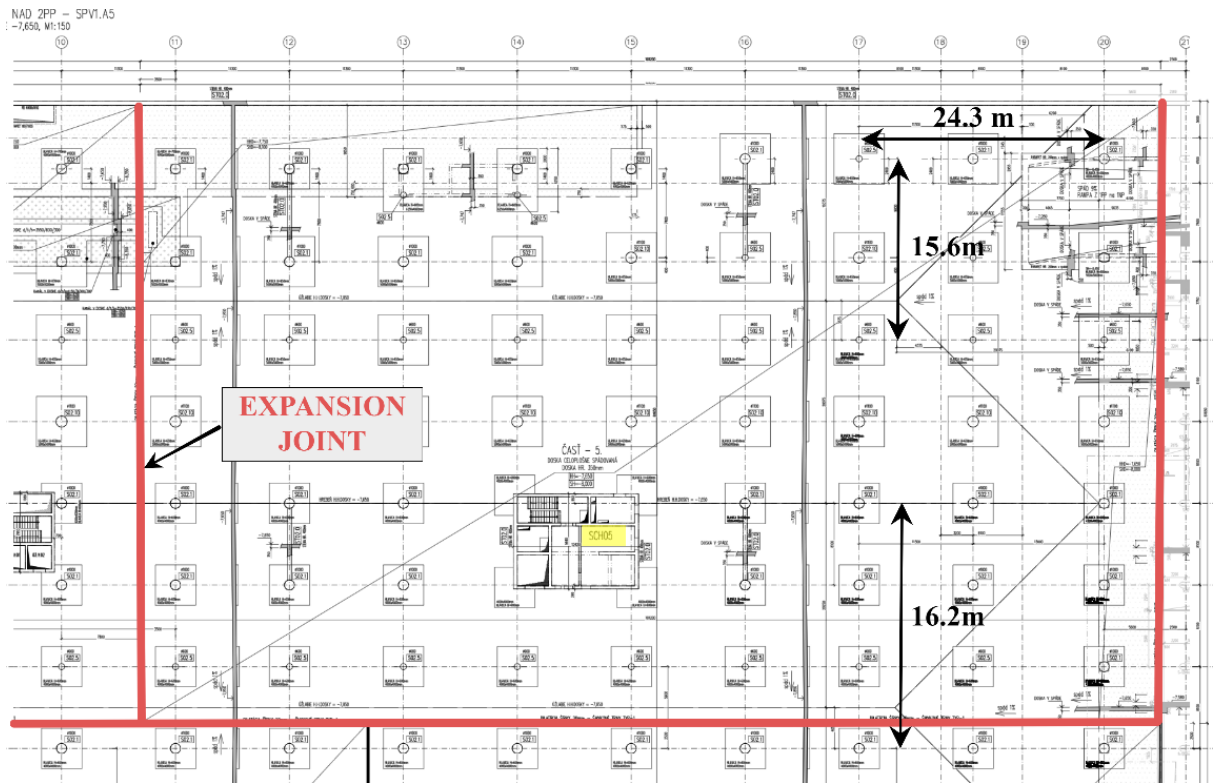
Figure 6: Layout diagram of 2PP with marked maximum spans and stiffening core
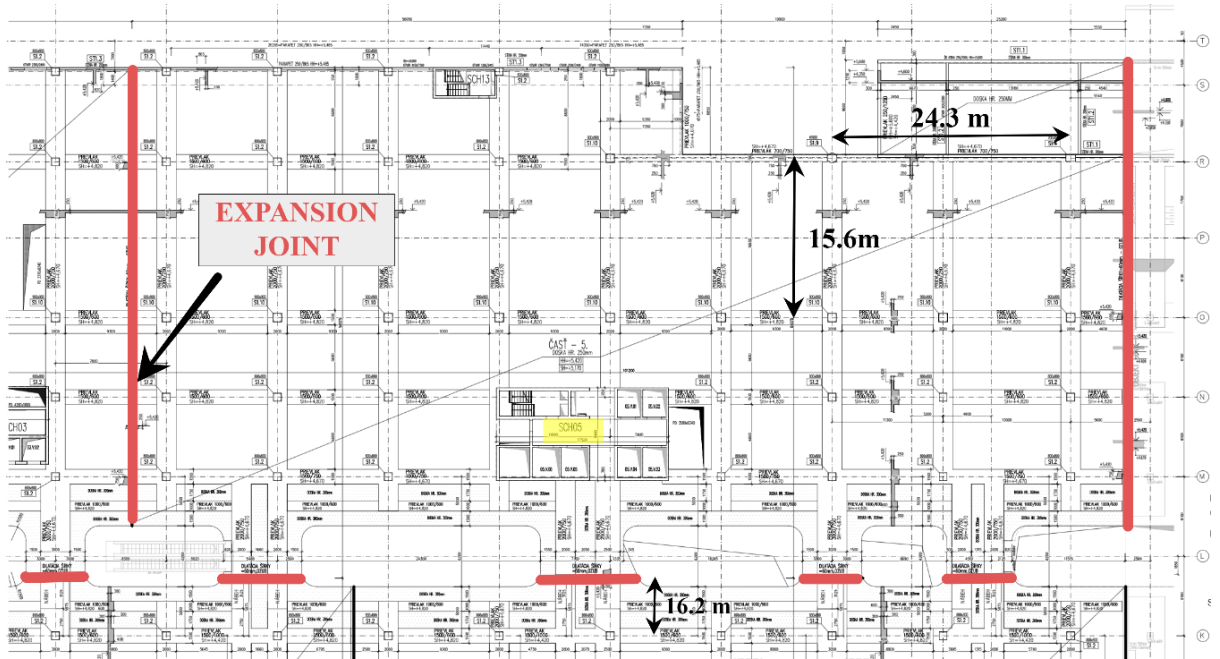
Figure 7: Layout diagram of 1NP with marked maximum spans and stiffening core

3. LITERATURE SURVEY

3.1 General

This chapter gives a comprehensive review of the work carried out by various researchers in the field of using prestressed concrete in structure.

Cyclic shear behavior and strength capacity of prestressed concrete walls in high-rise buildings

Xiaowei Cheng, Xiaodong Ji, Ziguo Xu, Yixiu Wan, Tao Wang.

They used prestressed concrete partitions in high-upward push systems to enhance the coupled axial stress-shear geste of structural walls. three low-issue-charge wall samples have been examined to probe the seismic geste of pc walls below colorful lading styles. the following conclusions are drawn from this observation lading patterns had sizeable items at the failure modes and hysteresis responses of laptop walls. comparison between a computer wall and RC wall indicated that the laptop wall displayed more suitable seismic overall performance because of the original prestressed pressure helping to govern the development of cracks, thereby precluding the sliding failure and significantly improving the facet stiffness and electric potential of the wall. The stilt idealization machine affords an affordable estimate for the cracked shear stiffness of a pc wall under coupled axial strain-shear lading, at the same time as it underestimates the cracked shear stiffness of a PC wall below coupled axial contraction-shear lading [5].

State-of-the-Art Report on Partially-Prestressed Concrete Earthquake-Resistant Building Structures for Highly-Seismic Region

I Gusti Putu Rakaa, Tavioa, Made Dharma Astawaa

The motive of their paper was to study the operation of prestressed concrete to seismic-resistant multi-tale systems. Nonetheless, this paper were studied bearing in thoughts the truth that the widest operation of prestressed concrete(to the ground and kindred systems) has been within the countries concerned with earthquakes and operative seismic canons. inside the paper, the rearmost seismic layout method for prestressed concrete systems in Indonesia is brought. The cutting-edge layout device is grounded at the rearmost Indonesian structure regulation for Structural Concrete and Seismic law, videlicet SNI 28472013 and SNI 17262012, independently. The design system itself isn't always a novelty to those who are acquainted with the capacity layout advanced for times. This paper is also supposed to carry the eye of structural contrivers and other masterminds to the option of the use of

incompletely- prestressed concrete in structures. The outcomes of a disquisition into the seismic resistance of incompletely- prestressed concrete frames are defined. The experimental part of the design worried the trying out of six close to full-scale ray-indoors column assemblies below desk-bound cyclic lading to benefit statistics for seismic layout [6].

Experimental study of prestressed steel-concrete composite beams with profiled steel decking

Marcela Moreira da Rocha Almeida, Alex Sander Clemente de Souza, Augusto Teixeira de Albuquerque

The prevailing work delved into the geste of the prestressed sword- concrete compound shafts with sword trapezoidal decking under high-quality moment by way of the improvement of an experimental and numerical take look. Grounded on the provided effects, the following conclusions have been drawn using prestressing in compound shafts can significantly ameliorate their geste , adding the yielding and final hundreds and decreasing diversions underneath carrier hundreds. The experimental data showed an increase of 19 in the last ability on the prestressed ray while compared to the manipulated ray without prestressing. Prestressing losses represented 21 of the authentic prestressing force that became applied, which become formerly 5 more advanced than the designed unique prestressing pressure. To achieve the requested growth inside the strength of the compound shafts, superior losses should be taken into consideration while making use of prestressing. The arbor failed domestically at the ray's stop in which there was a placed caricature, but no massive goods on the closing resistance of the shafts were linked. The arbor needs to quit with the portion in which there's no cool animated film with only the arbor cover, or suitable underpinning needs to be located to avoid localized damage. throughout the rigors, no unique failure medium turned into related in each shaft, but the numerical models suggest that the failure medium comported in the yielding of the slackened sword ray[7].

Experimental and numerical study on the axial compression performance of the prestressed sleeved members

Peng Gong, Wenhao Liu, Bin Zeng, Zhen Zhou

In this, axial lading checks had been conducted on samples, and the axial contraction performance and buckling modes of the prestressed sleeved contributors were attained. likewise, parametric analyses of five critical parameters and theoretical analyses of trade-order buckling have been completed. the principle conclusions are epitomized as follows a

new prestressed sleeved member with an excessive shipment capacity, big secondary stiffness, and slight restoration capability is proposed to aid the damaging contraction participants in big-span spatial systems. The experimental effects display that most cargo capabilities of M1 and M2 are7. four and 6.7 instances of the maximum shipment capability of M0. in addition, the prestressed sleeved contributors parade two buckling modes first-order and alternate-order buckling. The parametric analyses discovered that the maximum cargo capacity decreases because the authentic fault breadth charge increases, and the buckling mode adjustments from trade-order to first-order buckling. once more, as the beach the front move-sectional vicinity rate increases inside a moderate variety, the elastic stiffness, most cargo potential of the elastic degree, and last shipment ability growth, and the buckling mode changes from first-order to 2nd- order buckling. whilst the beachfront move-sectional place price is small, the final cargo capacity increases with the imperative help plate unique top charge, and the buckling mode changes from first-order to 2d- order buckling. because the inner and external tube move-sectional stiffness prices growth and the inner tube period to slenderness rate decreases, the axial pressure–relegation wind turns into large as an entire, and all the buckling modes are of change-order buckling. The operating medium of trade-order buckling for the pre-burdened sleeved members is brought, which can be divided into 4 stages elastic level, internal tube buckling stage, contact degree of the inner and external half of- tubes, and external 1/2- tubes buckling degree. The comparison of the theoretical and FE effects confirmed that the most errors of the axial relegation and axial pressure would not exceed 15. The beachfront pressure, the touch force, and the aspect deviation of the middle phase of the inner half of- the tube are largely harmonious. This result accordingly verifies that the relevant hypotheticals and theoretical computation formulae are affordable[8].

Serviceability Performance of Prestressed Concrete Buildings Taking into Account Long Term Behavior and Construction Sequence

H. L. YIP, F. T. K. AU, S. T. SMITH

The geste of a normal submit-tensioned concrete structure is studied numerically. while the products of time-structured geste and construction sequence are taken into consideration, the results of discrimination axial shortening, column moments and tendon stresses parade certain unanticipated trends. some of the differences are minor while a few others are sizeable. The time-established goods should accordingly be taken into consideration as it brings about destructive goods on the structural performance in several cases. in the case of the everyday shape studied, discriminational axial shortening seems to be decreased through

time-dependent geste and the development sequence. it is, still, important to perform further disquisition a good way to discover if it is typically applied to other instances. Modeling of creation collection is important for columns because the successional jacking of bottoms will increase the column moments mainly on the decrease of a part of the shape. The column moments are substantially tormented by the boundary conditions at the muse. To advantage of practical estimates of the column moments mainly, correct modeling of the principles of the soil-structure commerce is usually recommended. Tendon stresses are in large part stricken by time-based geste however now not so vital with the aid of the construction series. In summary, the development series and time-structured geste play crucial places inside the long-term geste of prestressed concrete structure structures and they ought to be duly taken into consideration in the design degree[9].

Experimental and numerical study on seismic behavior of prestressed concrete composite shear wall

Xin Zhang, Guangqiang Zhou, Shurong Li, Fang Zhang, Shuai Zhang

Four prestressed concrete compound shear partitions and one cast-in-situ shear wall were tested on this observation to assess the seismic geste of the prestressed concrete compound shear wall. latterly, finite detail models had been mounted, and the geste of the walls below high axial compressive lading was expected. the following conclusions had been drawn from the experimental and numerical outcomes The proposed prestressed concrete compound shear wall displayed the same failure mode, and all samples were dominated by means of flexural distortion. The concrete at the lowest of the boundary detail changed into overwhelmed and the longitudinal mounts within the boundary columns buckled and fractured. because of the vertical prestressed bars in the compound wall, the slant cracks in the precast compound wall have been decreased. The hysteretic angles and cargo–relegation shell angles for each compound shear wall and solid-in situ had been analogous. The power dispersion capability of the compound shear wall extended in comparison to that of instance CW. at some stage in the test, the precast arbor of PW1 labored collectively with the cast-in-situ component, and no separation was handed within the major wall. some of the compound shear walls, PW1 had the loftiest pressure component. Specimen PW1 with a boundary element of kind A, whose boundary rudiments were absolutely forged- in situ, displayed better seismic performance. it may be located from the numerical outcomes that the seismic geste of the compound shear wall under excessive axial compressive lading bettered drastically. under high axial compressive loading, for instance, CW displayed brittle bending-shear failure, and the

vertical bars yielded. Specimen PW1 displayed bending failure, indicating that the vertical prestressed bars in the precast arbor led to huge improvements in shear capacity. as the authentic prestress extended below high axial compressive lading, the pressure of the compound shear wall bettered. Failure mode from bending-shear failure to bending failure [10].

Nonlinear numerical analysis of prestressed concrete beams and slabs

Amilton Rodrigues da Silva, João Paulo de Souza Rosa

In their work, a finite detail version was enforced for nonlinear numerical analysis of prestressed concrete shafts and crossbeams submitted to their ultimate potential. The structural geste of concrete crossbeams became dissembled by way of plate finite rudiments thinking about the orthotropic geste of concrete after cracking. The structural geste of the concrete shafts was dissembled by bar finite rudiments considering the nonlinearity of the concrete thru the concrete strain–stress wind underneath axial lading. For the active underpinning used inside the prestressed shafts and crossbeams, associated finite rudiments have been used to faux their structural geste as well as the relationship among the tendon and the concrete element. The effectiveness of the phrasings enforced changed into confirmed with the aid of evaluating the results attained with outcomes from numerous exemplifications in the literature. In some exemplification, the methodology cautioned on this work supplied higher outcomes than the numerical model offered inside the literature. In others exemplifications, the right agreement changed into found with the experimental responses, appreciably in terms of the remaining shipment supported by the anatomized shape. some small differences set up within the numerical and experimental responses can be defined due to the use of a simplified concrete harm version recommended by means of Huang etal. (Nonlinear analysis of corroborated concrete crossbeams subordinated to the hearth). in addition intricate harm models, similar to the control of the crack conformation and crack commencing using the concrete fracture energy, undergo an extra unique and three-dimensional discretization of the prestressed concrete arbor or ray. for this reason, the numerical models developed in this work have been applicable to dissect the proposed troubles, offering a simple modeling and coffee computational cost [11].

3.2 Basic Terminologies of Prestressed Concrete (PSC)

3.2.1 What's Prestressing?

Prestressing is a system of buttressing concrete, neutralizing applied loads by placing it in a state of contraction previous to the operation of loads.

3.2.2 What's prestressed concrete?

Pre-stressed concrete is a form of concrete where original contraction is given in the concrete before applying the external cargo so that stress from external loads is canceled in the asked way during the service period. This original contraction is introduced by high-strength sword lines or blends (called ' tendons') located in the concrete section.

3.2.3 How Pre-Stressed Concrete works?

The high tensile strength sword cables are fitted into the ray section and they're stretched and anchored, also released. Now the sword tendon wants to gain its original length and tensile stresses are converted into compressive stress in the concrete. Now after loading there are two kinds of forces on the ray i.e., Internal prestressing force and External forces(Dead load, Live load, etc.)
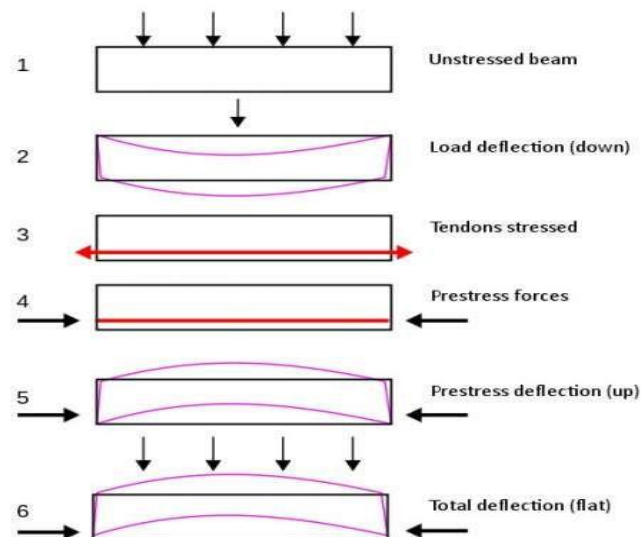
Figure 8: How prestress concrete work

The prestressed element is suitable to repel much-advanced load before crack development. At the same lading, no crack develops, or their number range is limited. While crack number/ range reduction limits the doorway of aggressive agents, the structural rudiments are more durable. No stiffness reduction due to crack development as the rudiments are stiffer and thus

can be more slender or ground advanced spans.
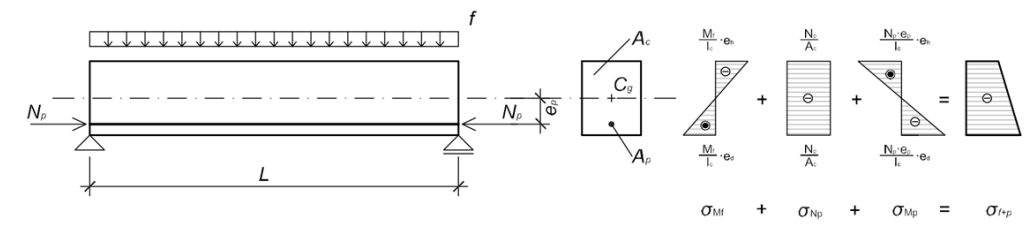
Figure 9: Principle of prestressed concrete

3.2.4 Materials used for PSC

Concrete and steel are the introductory accouterments of construction of prestressed concrete.

3.2.4.1 Concrete

Since high tensile steel is used in PSC, the concrete used should also be of good quality and high strength this is because of the trouble to reduce the influence of creep and loss because concretes with advanced strength aren't subject to similar great distortion from these rheological changes. thus, the law recommends a minimal blend of M40 for the pre-tensioned system and M30 for post slackened system. These composites have high strength and a high value of modulus of elasticity of concrete which results in lower deviation. The concrete used in PSC should be well compacted. High-strength concrete is used in PSC for the following reasons Use of high strength concrete results in lower sections, High strength concrete offers high resistance in pressure, shear, bond, bearing, and lower loss of prestressing occurs with high-strength concrete.

3.2.4.2 Steel

Ordinary mild steel and misshaped bars used in R.C.C. aren't used in PSC (Prestressed concrete) because their yield strength isn't veritably high. In the PSC, loss of prestress(about 20) occurs due to numerous factors. If mild sword or HYSD bars are used also veritably little prestress will be left after the losses and will be of no use to us. thus, high tensile strength sword is used for prestressing. In addition to the high-strength, the sword used in prestressing must have an advanced ultimate extension. colorful forms of sword used for prestressing are as follows

(a) Tendons: Tendons are high-strength tensile cables available in colorful periphery from 1.5 mm to 8 mm.

(b) Wire Strands or Cables: A strand or cable is made of a pack of cables spun together. The overall periphery of a string or stage is from 7 to 17 mm. They're used for post-

tensioning systems.

(c) Bars: High tensile steel bars of diameter 10mm or more are also used in prestressed concrete.

3.2.5 Methods of prestressing
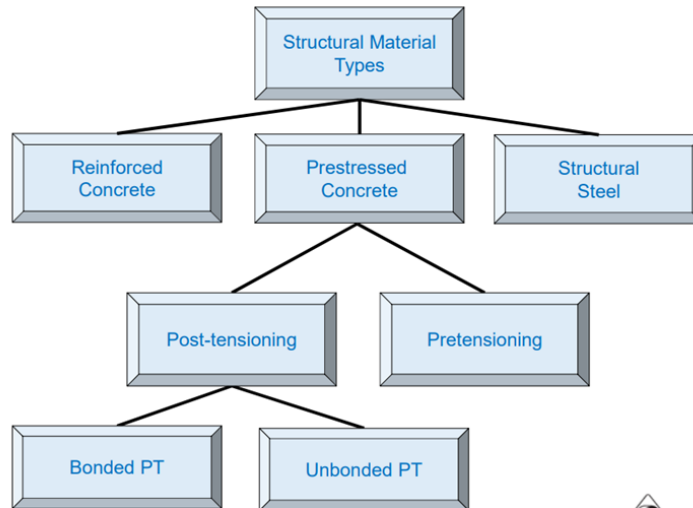
Figure 10: Method of prestressing

a) Pre-Tensioning Method

Pre-tensioning consists in stretching the tendons against an anchored formwork before the concrete is poured. Also, the tendons are released when the concrete has hardened and reached sufficient strength. The force is transferred to the element by the bond between the concrete and the beaches. Pre-tensioning is applied in products like roof crossbeams, bottom crossbeams, piles, poles, ground crossbars, etc.
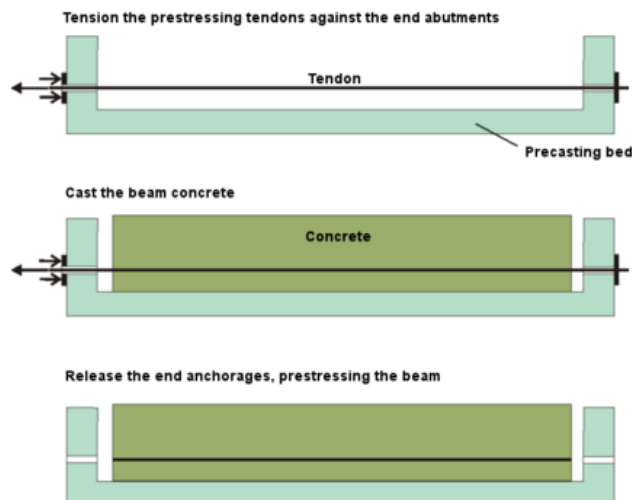
Figure 11: Pre-tensioned method

This process involves the stressing of cables or lines by anchoring them at the end of an essential form, which may be over 120m in length. Hydraulic jacks stress the line as needed, frequently adding 10 to accommodate creep and other pre-stress losses that may be incurred. Side molds are also fixed and the concrete is placed around the slackened cables. The concrete hardens and shrinks, gripping the sword along its length, transferring the pressure from the jacks to ply a compressive force in the concrete. Once the concrete has reached the asked strength, the slackened cables are released from the jacks. Typical concrete strength of 28N/mm2 can be achieved by 24-hour brume curing, as well as using complements. To produce shorter members, dividing plates can be placed at any point along the member which, when removed, permits the slice of the cables.

b) Post-Tensioning Method

Post-tensioning consists in stretching the tendons after the concrete is formerly hardened. Post-tensioning is used in structural products like large crossbars, pavements, pressure vessels, bottom crossbeams, and shells, among others. It's veritably protean and generally used in cast-in-place rudiments but it can also be used for plant-made products.
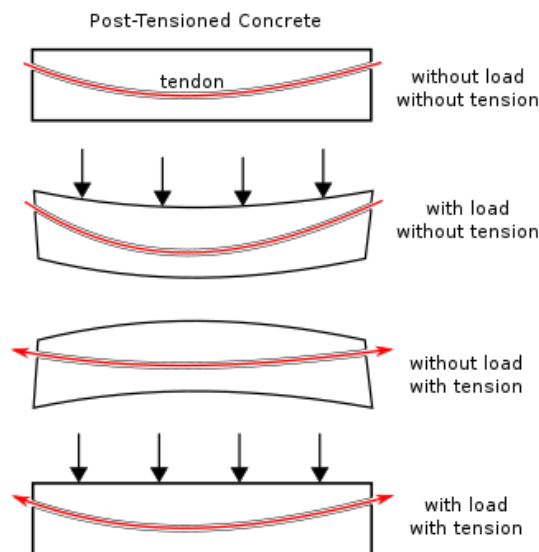
Figure 12: Post-tensioned method

This follows the rear system to pre-tensioning, whereby the concrete member is cast and the prestressing occurs after the concrete is hardened. This system is frequently used where stressing is to be carried out on a point after casting an in-situ element or where a series of precast concrete units are to be joined together to form the needed member. The cables, lines, or bars may be deposited in the unit before concreting, but cling to the concrete is averted by using a flexible conduit or rubber jacket which is deflated and removed when the concrete has hardened. Stressing is carried out after the concrete has been cured by means of hydraulic

jacks operating from one or both ends of the member. Due to the high original stresses at the harborage positions, it's common for a spiral (helical) underpinning to be included in the design. When the needed stress has been reached, the line or lines are anchored to maintain the prestress. The ends of the unit are sealed with cement mortar to help erosion due to any entrapped humidity and to help in stress distribution.

Figure 13: Anchor of prestressing system with a round anchor shape

There are numerous different post-tensioning systems. For illustration, the Freyssinet system enables the stressing beaches to be slackened contemporaneously using center hole attaching jacks, anchored by phased jaws. This is suitable for pre-stressing rudiments up to 50 m in length. The Macalloy system, on the other hand, involves applying stress to the concrete by means of a solid bar, generally with a periphery of 25- 75 mm. The bar is anchored at each end by a special nut that bears against an end plate to distribute the load.

3.2.6 Losses of Prestress

Forces in prestressing aren't constant as it changes over the length of tendons and time, and this change of force is a loss of prestress.

$$-\Delta\sigma = -\varepsilon.E$$

Losses in prestressing can be divided into two categories:

1. Immediate Losses (Short-term losses): Occur during prestressing of tendon and transfer of prestress to concrete member and,

2. Time-dependent (Long-Term losses): occur during the service life of the structure

Losses are the reason why we use advanced quality accouterments for prestressed concrete. The use of concretes of advanced classes leads to a reduction of losses from rheological changes, which substantially include loss and creep. also, it's also the case with prestressing ropes, if we were to prestress classic concrete underpinning, thanks to losses from rheological changes, the applied stress would be reduced by over to 80, and this is the reason why we use underpinning with multiple times advanced strengths. Due to the fact that not only these

processes in concrete are time-dependent and concrete is affected by colorful influences throughout its continuance, the losses in the prestressing underpinning are also variable with time. It's thus necessary to consider the time course of losses. This is how losses are divided into immediate and long-term.

Pre-Tensioned Concrete		Post-Tensioned Concrete	
Short Term	Long Term	Short Term	Long Term
Elastic Shortening	Shrinkage	Friction	Shrinkage
Short term Relaxation	Relaxation	Short term relaxation	Relaxation
Slip in anchorage	Creep	Anchorage slip	Creep

Table 1: Losses of prestress

4. STATIC ASSESSMENT

The aim of the project is to verify the impact of static analysis between the Prestressed concrete and Reinforced concrete. The details of this in terms of soil data and their properties, material properties, description of each floor in A5, and the static calculation of A5 are discussed in this chapter.

Flow chart of the static assessment:
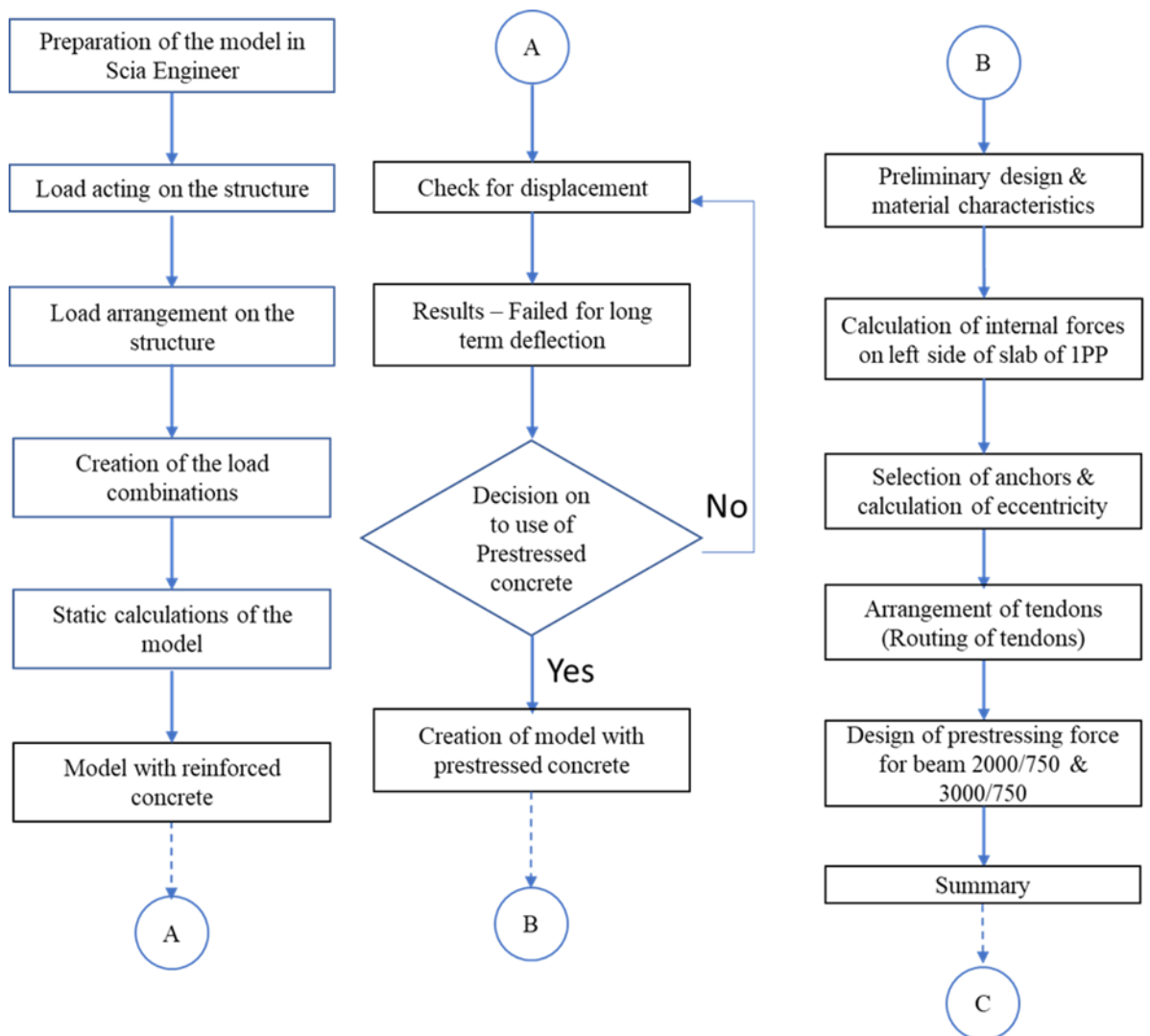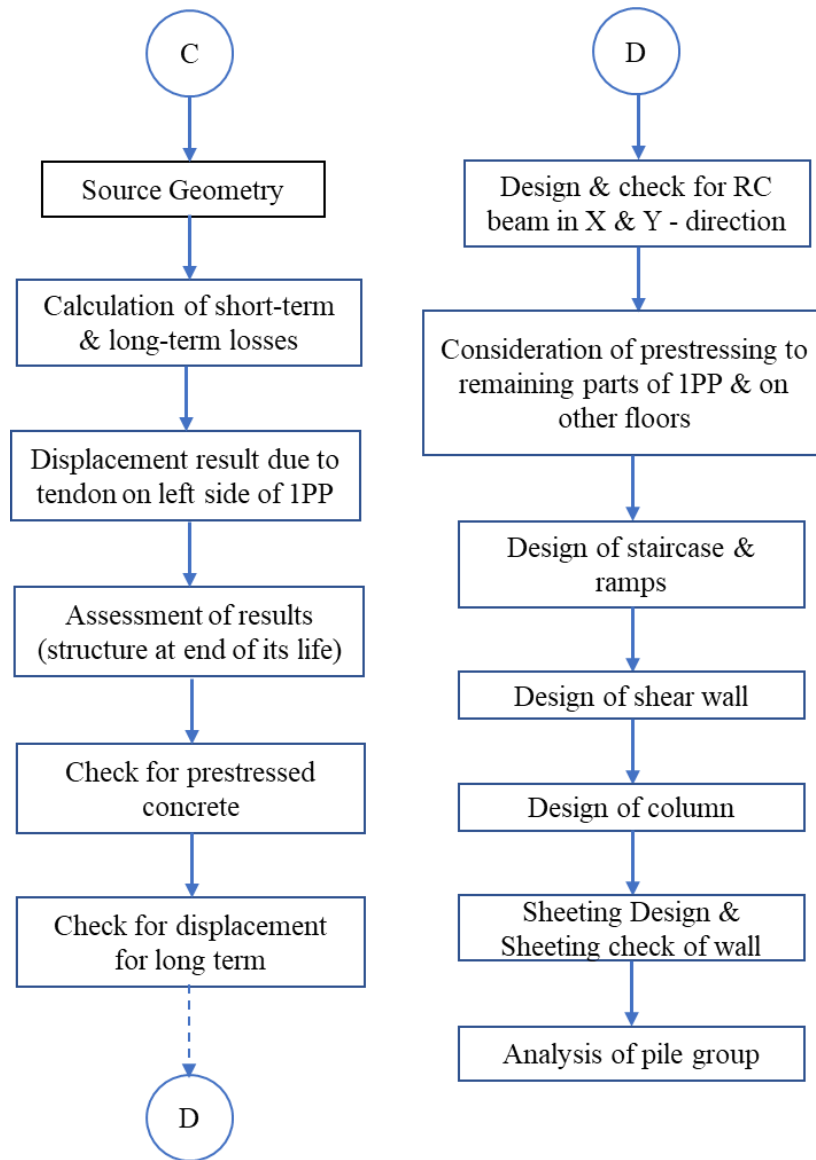
Figure 14: Flowchart of static assessment of the structure

4.1 Material Used

The materials used were taken from the designer's technical report. The marking of concrete corresponds to the Slovak standard.

Perimeter walls of underground floors:

    Concrete: STN EN 206-1-C25/30 XC3, XD1 (SK)-Cl 0.4 - Dmax16-S3

    Reinforcement: B 500 B, cover 30 mm

Ceiling slab 2PP

    Concrete: STN EN 206-1-C30/37 XC3, XD1 (SK)-Cl 0.4 - Dmax16-S3

    Reinforcement: B 500 B, coverage 30 mm

Ceiling slab 1PP and above-ground floors (prestressed ceilings):

Concrete STN EN 206-1-C35/45-XC2, XD1 (SK)-CI 0.4 - Dmax16-S2

Reinforcement: B 500 B, coverage 30 mm

Prestressing steel - ropes 15.7 mm, guaranteed strength 1860 MPa

Stiffening walls and core walls:

Concrete: STN EN 206-1-C35/45 XC1 - Dmax16-S3

 Reinforcement: B 500 B, cover 25 mm

Columns:

Concrete: STN EN 206-1-C45/55 XC1 - Dmax16-S3

Reinforcement: B 500 B, cover 30 mm

4.2 Preparation of Models

Model I

 As part of the original reinforced concrete design, for simplicity, we choose the same shape as the first design. As compared to prestressed structure, the reinforced concrete structure has lower stiffness so we can say hypothetically that structure won't observe.

Geometry of Structure

Originally, in Scia Engineer Software, we prepared the three different sample plate viz., one with normal monolithic slab and beam, another was slab with rib and last was with subregion so that we could got to know which approached is suitable for our model.
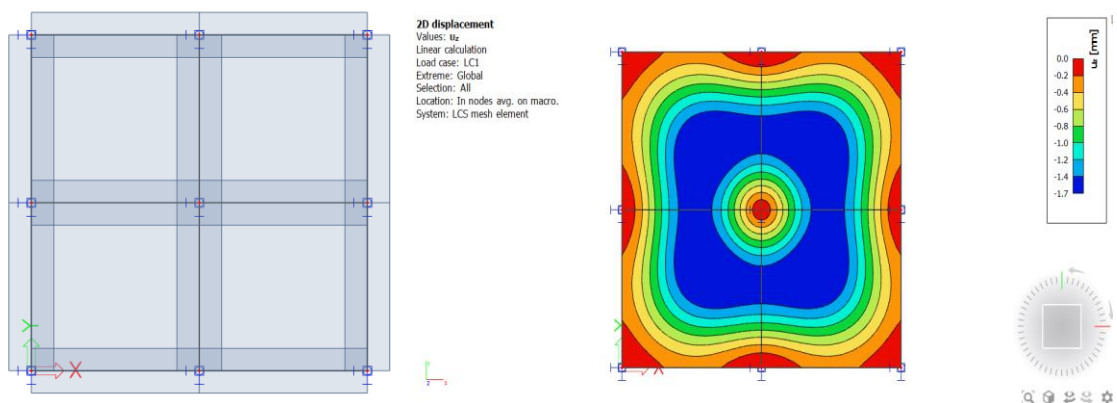
Figure 15:Sample 1 – Monolithic slab with beam

Fig.15 indicates the first approach of the slab with beam, where we could see that load was transferred the entire load to the center of plate that is it only carries its own weight and as a

result the maximum displacement was entirely shifted to the center.
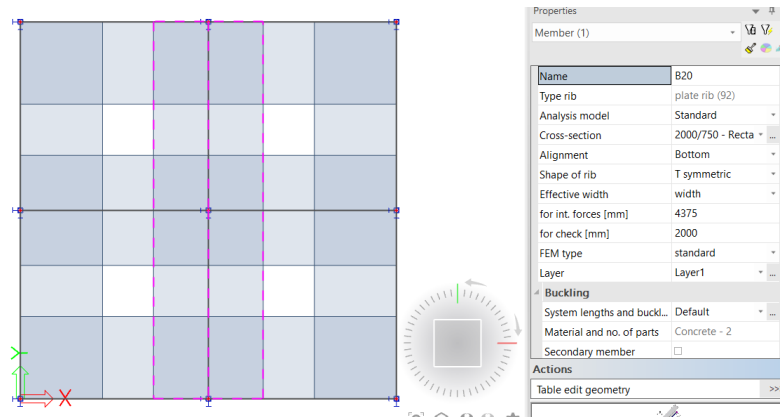
Figure 16: Sample 1 – Slab with rib – Assigning Effective width

Now, in the sample of the slab with ribs, we manually inserted the values for internal forces and for checks so that we could get more accurate results.
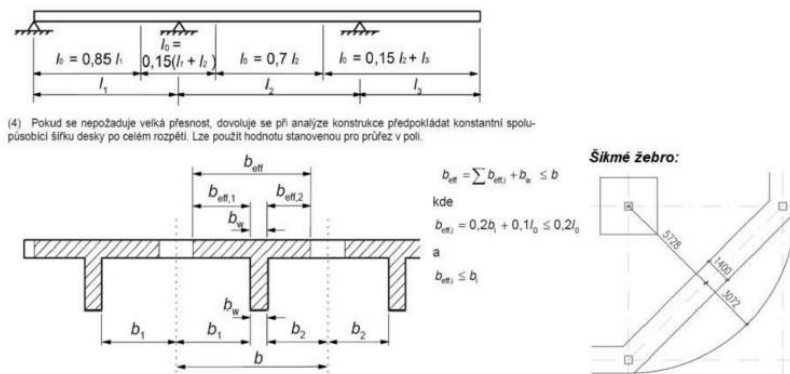
Figure 17: General concept to calculate effective width
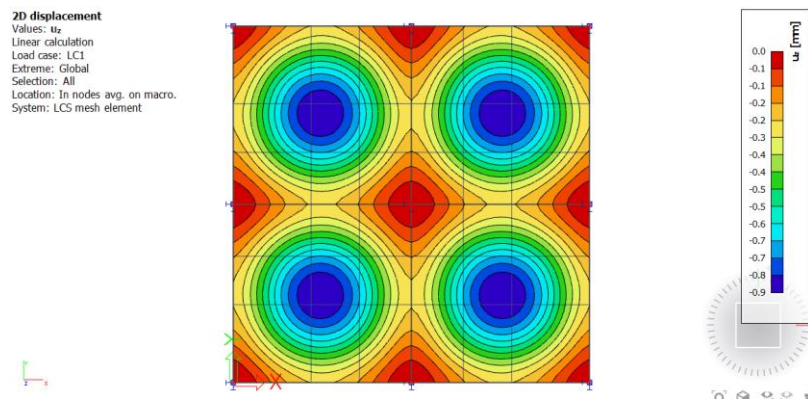
Figure 18: 2D Displacement Result – For Sample slab with ribs

As a consequence, we can state that with ribs (with the manual effective width) fig.18, the beam takes the load from the cooperative width of the slab as a result, we can see the

difference between this strategy and the prior one. If we choose the rib option, the moment will be equal to zero across effective width since it was calculated when the beam is considered as a T-section. In this manner, the same instant was not considered twice. However, a fundamental drawback of the approach is that the program does not use the internal forces or cross-sectional features of the T cross-section; instead, it estimates stress on the beam using just the internal and cross-sectional forces characteristics (without integration of the internal forces acting on the width).
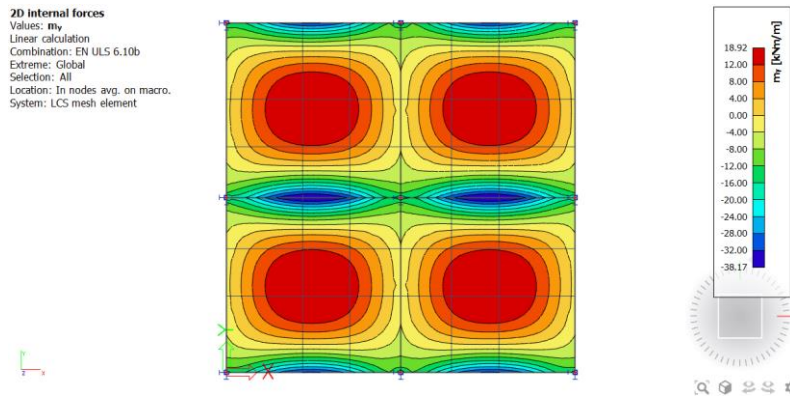
Figure 19: 2D Internal forces (my) Result – For Sample slab with ribs

Aside from that, we modeled the plate/slab with a subregion, where a subregion is a slab defined inside the main slab of different material, thickness, and, so on, it defines local thickening of the slab, to implement area load acting on the part of the slab only, and we obtained more convenient results, similar to the slab with ribs. The program computes stress for a single element - the entire plate, including subregions and co-acting parts. As a result, the subregion method was chosen.
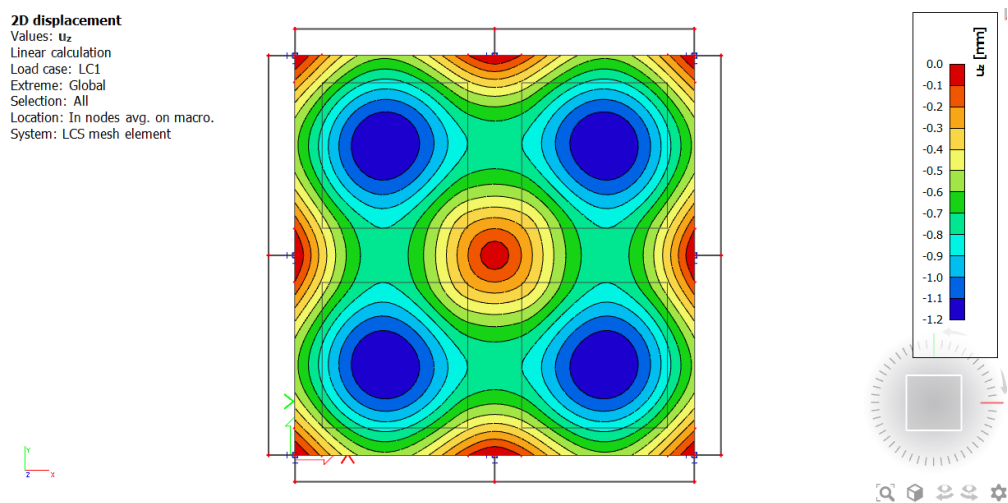
Figure 20: 2D displacement Result – For Sample slab with subregion

Model II: We adopted the identical form of the designer's ceiling in the prestressed variation. Then the construction was evaluated after we designed the preload exclusively in the through holes. We worked with a typical area of the ceiling to acquire the fundamental ideas and apply them in practice to more complex challenges.

4.3 Detailed Building Structure

4.3.1 Base of the structure

The supports of the columns in 2PP are considered to be embedded that is the columns smoothly connect to the base plate with piles.

Interconnection of the model with expansion joints

The most important expansion element in the construction is the placement of the plate on the tooth. Some 2PP expansion joints have expansion pins which are designed in the vertical direction Z. For simplicity, the plate of our expansion unit, which forms the support for the plate of the adjacent expansion unit, will be considered simply as supported. Practically, such a structure would act as a cantilever (shown in figs. 21 and 22) with a continuous load from the plate of the closet unit. Considering our issue, this is not a fundamental change. All boards are thus supported in the Z direction (vertical direction) at the expansion joint locations.
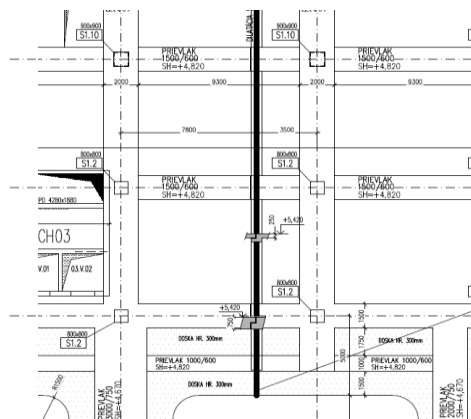
Figure 21: Interconnection of the model with expansion joint

Figure 22: Schematic of deflection for given interconnection in fig.21

4.3.2 2PP

The 2PP model is relatively simple compared to the other floors. Although the 2PP ceiling slab is designed to be sloped over the entire surface, this does not have a significant effect on the results and is therefore considered a constant thickness in the model. The column headers are modeled as sub-areas of the appropriate thicknesses.
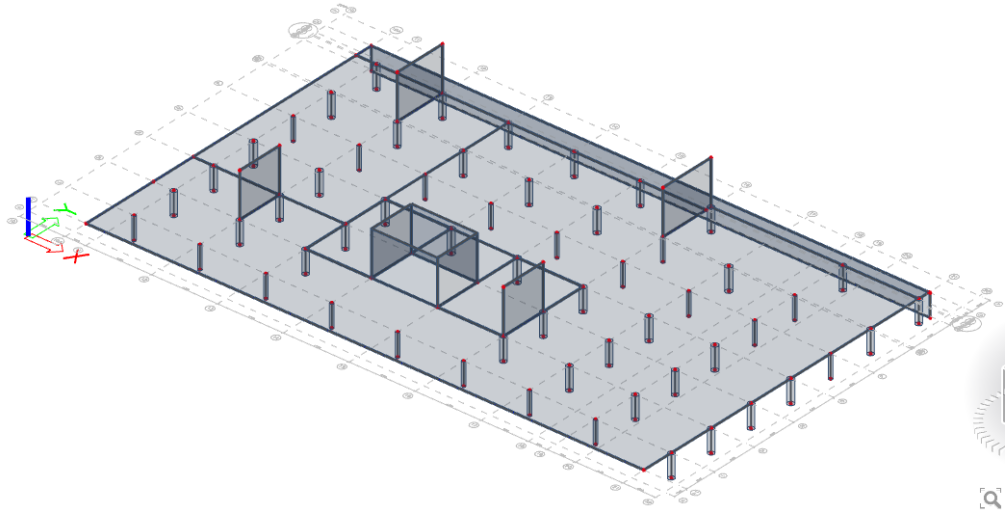
Figure 23: 3D View of the 2PP

4.3.3 1PP

This floor is the most complicated in terms of layout as a floor with a bus station. The slab above 1PP is additionally lowered at the points of supply by trucks. Due to the large spans, the designer designed a plate with through holes that were modeled as plate ribs. Due to the simplicity of the model, the supply docks were neglected, so the lowered part of the slab is modeled without them.
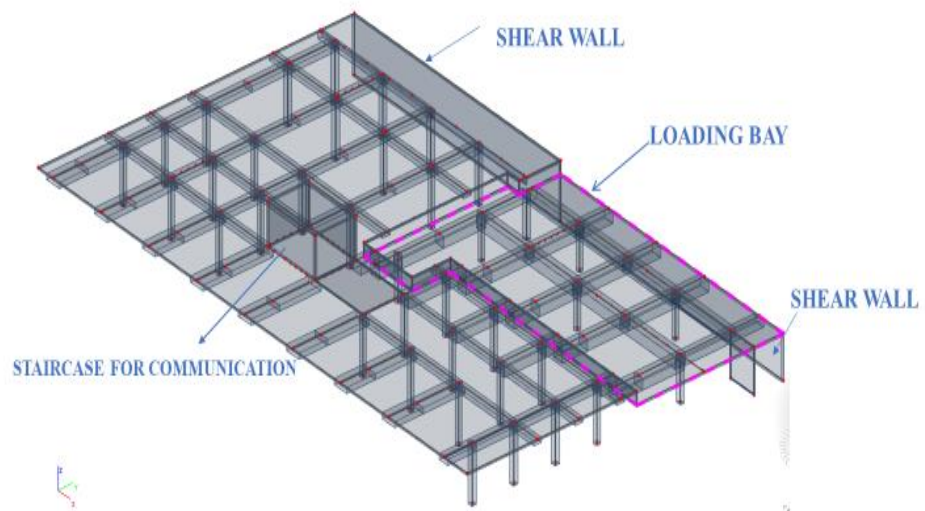
Figure 24: 3D View of the 1PP

41
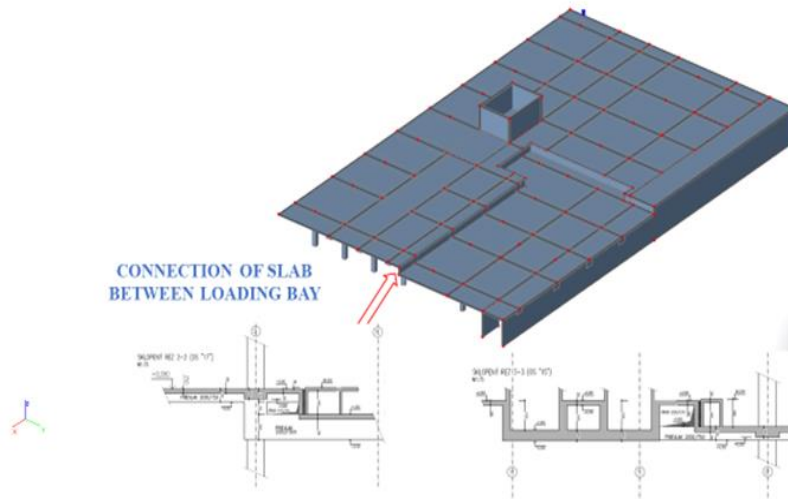
Figure 25: Connection of the slab with loading bay on 1PP

4.3.4 1NP

This is the floor from which it starts to decrease in shape, as a result of the necessity of vertical communication, the slab is supplemented with penetrations. It is also supplemented with through holes. For the simplicity of the model and the topic of the problem, the reduced part of the plate in the receding part was neglected.
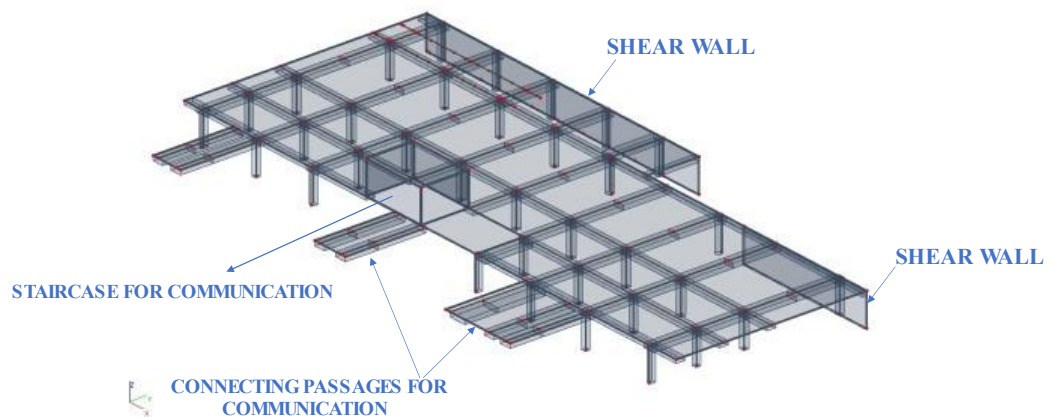
Figure 26: 3D View of the 1NP

4.3.5 2NP

With the coming floors, the slab recedes more and more. From one edge, the slab is only cantilevered and a footbridge is placed on it, this would only be taken into account by the linear load on its edge. On the other side, a smaller part of the plate is supported by a steel structure, which is considered in the model by point supports at the point of support.
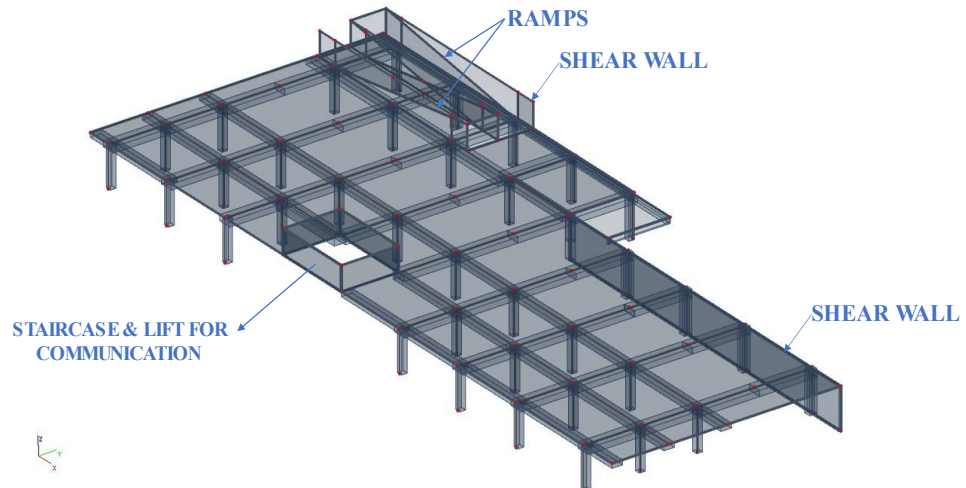
Figure 27: 3D View of the 2NP

Stiffening core with stairwell

The main stairwell and stiffening core of the given dilatation SCH05 was modeled as a multi-story wall structure with plate penetrations. Landings and stairwells were not modeled, they would have been designed as reinforced concrete prefabricated. There is also a stair core SCH013 in the building, it was neglected for the simplicity of the model. The design and assessment of the stair area would not cause problems, and therefore we do not deal with it.
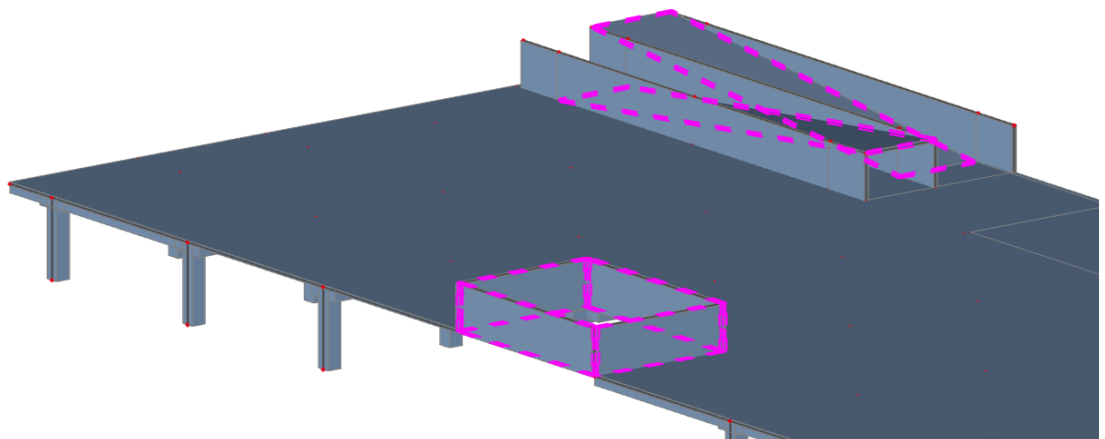
Figure 28: 3D View showing core wall

4.3.6 3NP
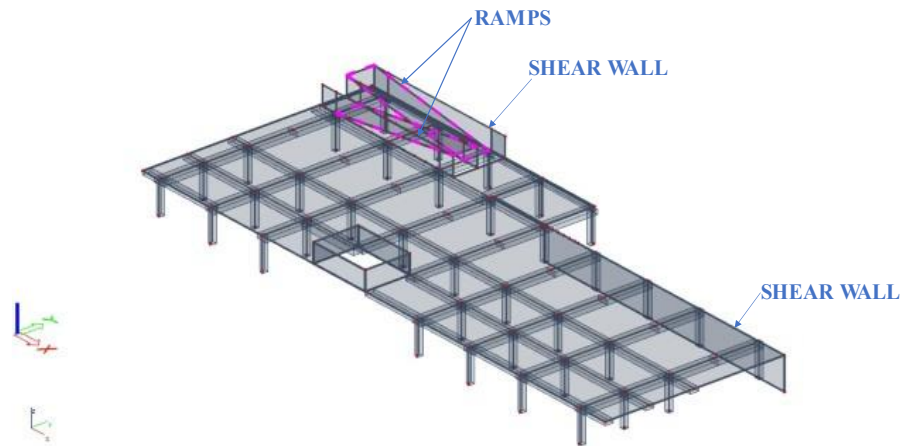
Figure 29: 3D View 3NP

4.3.7 4NP
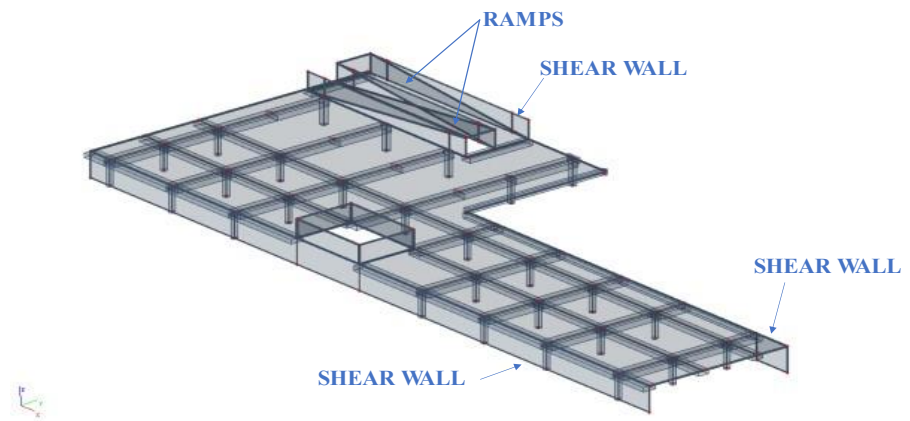
Figure 30: 3D View 4NP

4.3.8 5NP
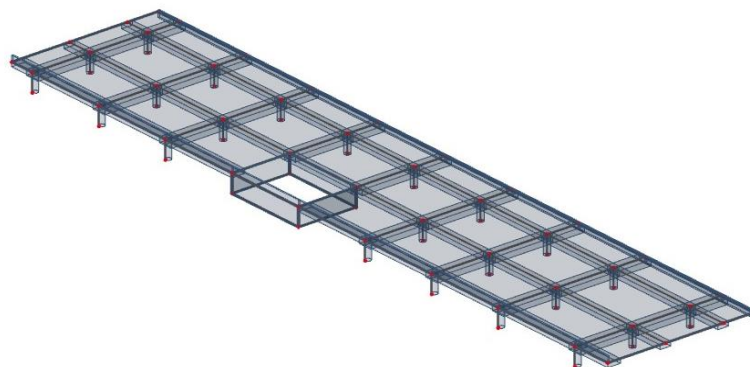
Figure 31: 3D View 5NP

4.4 Loads acting on the structure

4.4.1 Permanent load (or Dead Load)

4.4.1.1 Self-weight of the supporting structure

The self-weight of the reinforced concrete structure was calculated automatically in SCIA Engineer 19.1.

4.4.1.2 Floors, suspended ceilings

a) 2PP, supply area in 1PP

Total floor, suspended ceiling load above 2PP is 0.75 kN/m^2.

b) 1PP

Material	Thickness (mm)	Density (kg/m3)	Gk (kN/m2)
Tread layer	15	2800	0.42
Anhydrite	50	2200	1.1
Separation foil	0.2		
EPS step insulation	50	15	0.01
Suspended ceiling - installation			0.75
Heat insulation	150	78	0.12
Total			2.4kN/m2

Table:2 Total floor load acting on 1PP

c) 1NP – 2NP

Material	Thickness (mm)	Density (kg/m3)	Gk (kN/m2)
Tread layer	15	2800	0.42
Anhydrite	50	2200	1.1
Separation foil	0.2		
EPS step insulation	50	15	0.01
Suspended ceiling - installation			0.75
Total			2.28kN/m2

Table:3 Total floor load acting on 1NP-2NP

But, for simple calculations, we considered it as 2.4kN/m^2.

4.4.2 Variable load

Variable load values were taken from the designer's technical report.

Administrative spaces, corridors: 3.0 + 0.8 (partitions) kN/m^2

Public spaces, entrance halls: 5.0 kN/m^2

Commercial premises: 5.0 kN/m^2

Parking, bus ramps: 9.0 kN/m²

Fire truck, supply: 15.0 kN/m²

4.4.2.1 Snow

Location: Bratislava Snow area II sk = 1.05 kN/m²

Snow Load = 0.8*1.05 = 0.84kN/m²

As per EC 1-1-3: 5.2(3), Snow Load $= s = \mu_i C_e C_t s_k = 0.8 * 1.05 = 0.84 kN/m^2$

Where

μ_i = snow load shape factor, either μ_1 or μ_2

μ_1 = undrifted snow shape factor

μ_2 = drifted snow shape factor

For flat roof, $\mu_1 = \mu_2 = 0.8$

C_e = exposure coefficient = 1.0(For normal topography)

C_t = thermal coefficient = 1.0

S_k = characteristic ground snow load = 1.05kN/m² (As per designer report)

4.4.2.2 Wind

Basic wind speed: 26 m/s, Terrain Category III
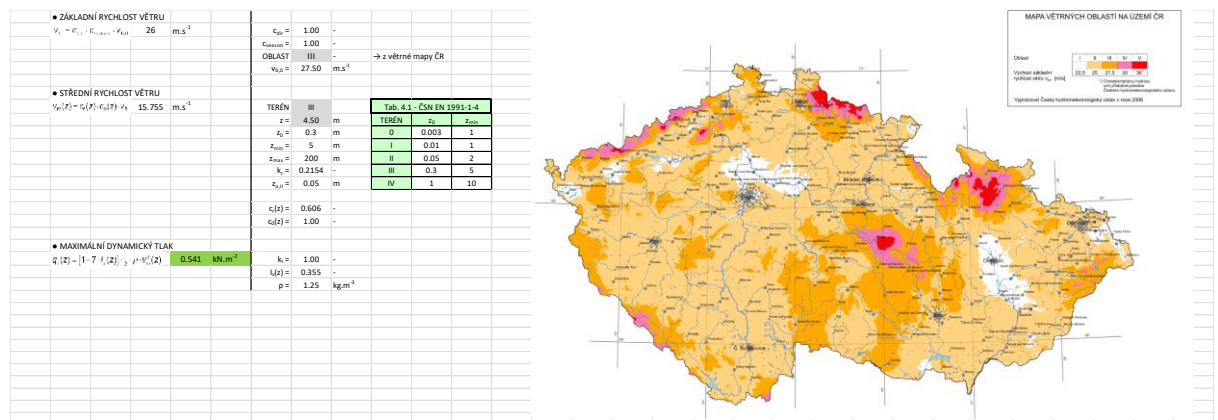
Figure 32: Calculation of the wind pressure

4.5 Load Arrangements on the structure

For load arrangement, it is important to correctly choose the type for load arrangement for their correctness taken into account when building combinations and calculating deformations. There are mainly two basic type for load arrangements viz.,

4.5.1 load acting on entire slab

Most commonly used method of loading for this is load acting on the entire plate (or slab)

because of its quick approach, but this arrangement of loading is false, and the reason for making this statement is explained further. Initially, we prepared the sample model of a slab, and in the beginning, we assigned the variable load to the entire span, as shown in the following fig. 33.
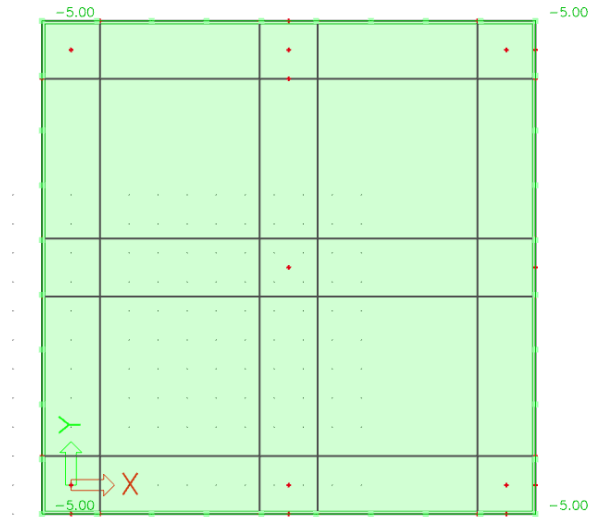
Figure 33: Variable load acting on the entire sample slab

4.5.2 load acting on alternate span of slab (like chessboard pattern)

Then we assigned the variable load on alternate span like chessboard pattern as we can see in the following figure
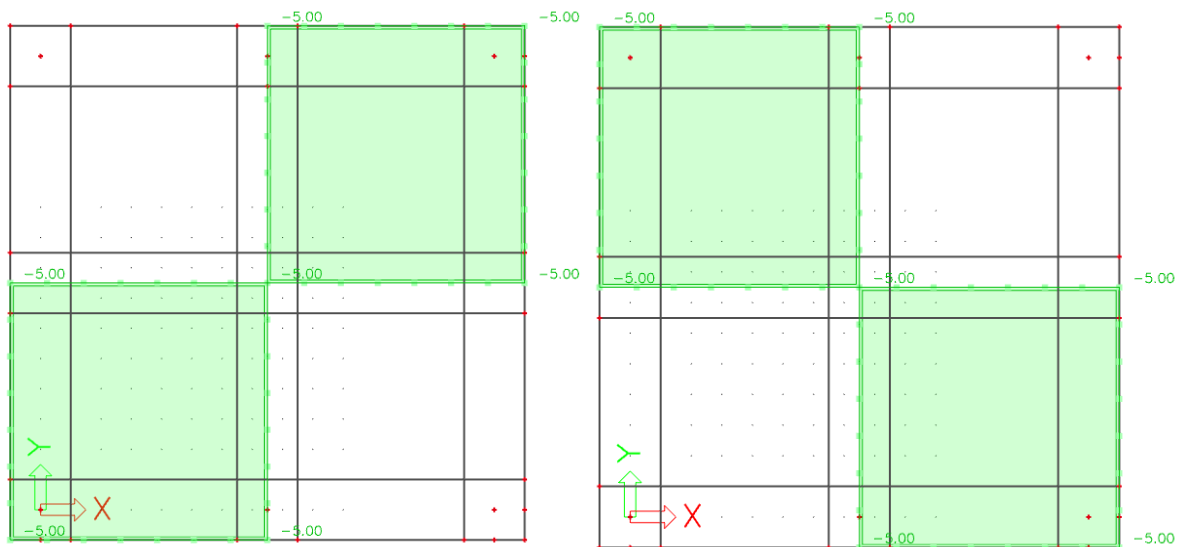
Figure 34: Variable load acting on the alternate span of the sample slab (like chessboard pattern)

After running the calculations, we can see the difference between both types of loading patterns, as due to uplift and punching shear, we need to multiply by some multiplier for safety.

Moreover, we got the maximum sagging moment if we followed the chessboard loading pattern, and loads induce positive moments near where we applied the alternate loading. In general, we can say that a variable load on the entire span was not the correct approach, so we decided to go with a variable load on the alternate span like a chessboard pattern.
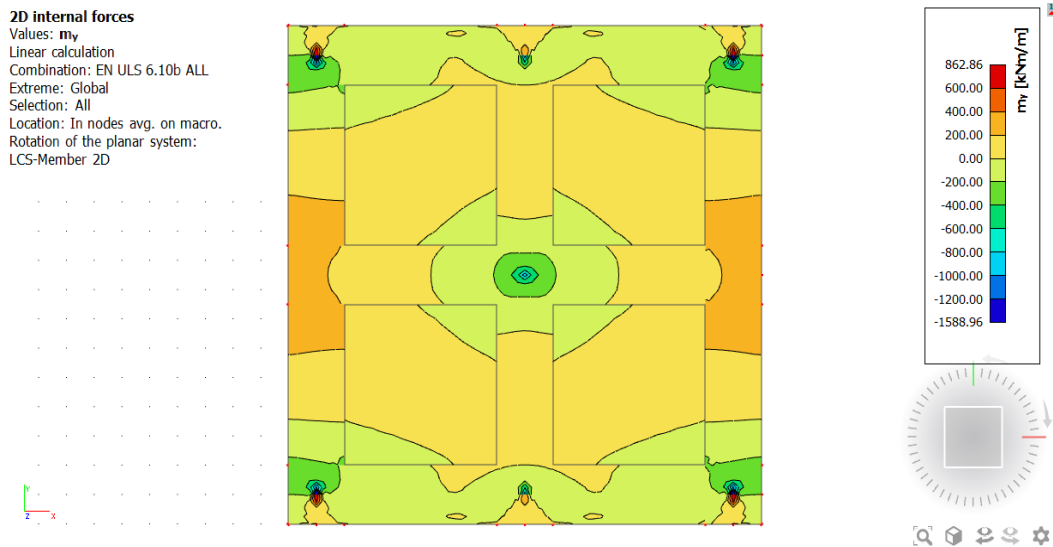
Figure 35: Display of the bending moment my with load acting on entire on sample slab
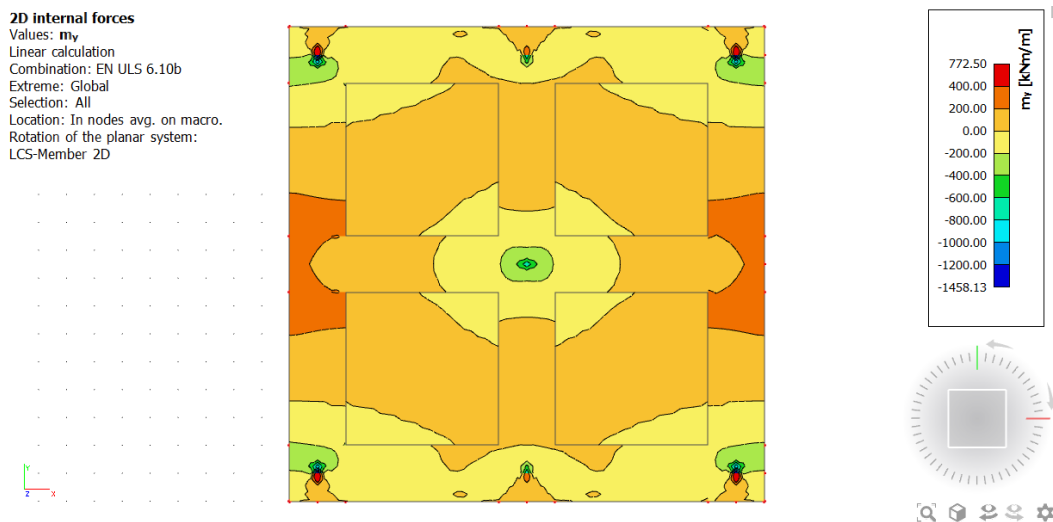
Figure 36: Display of the bending moment my with load acting on alternate span of the sample slab

4.6 Load Combinations

Design load values for permanent and temporary design situations are applied according to the standard "Eurocode - Principles of designing structures...STN EN 1990", table A1.2(B) according to terms 6.10a and 6.10b, the expression 6.10b will normally apply when the permanent actions are not greater than 4.5times the variable actions (except for storage load,

Cat. E in Table A1.1). So, we decided to use the expression 6.10b for load combinations for each floor as well as for the entire model.

6.10b : $1.25G_k + 1.5Q_{k,1} + \sum(\varphi_{0,i}1.5Q_{k,i})$

(3) The combination of actions in brackets { }, in (6.9b) may either be expressed as :

$$\sum_{j\geq1} \gamma_{G,j}G_{k,j} "+" \gamma_P P "+" \gamma_{Q,1}Q_{k,1} "+" \sum_{i>1}\gamma_{Q,i}\psi_{0,i}Q_{k,i} \tag{6.10}$$

or, alternatively for STR and GEO limit states, the less favourable of the two following expressions:

$$\begin{cases} \sum_{j\geq1} \gamma_{G,j}G_{k,j} "+" \gamma_P P "+" \gamma_{Q,1}\psi_{0,1}Q_{k,1} "+" \sum_{i>1}\gamma_{Q,i}\psi_{0,i}Q_{k,i} \tag{6.10a} \\ \sum_{j\geq1} \xi_j\gamma_{G,j}G_{k,j} "+" \gamma_P P "+" \gamma_{Q,1}Q_{k,1} "+" \sum_{i>1}\gamma_{Q,i}\psi_{0,i}Q_{k,i} \tag{6.10b} \end{cases}$$

Where :

"+"	implies "to be combined with"
Σ	implies "the combined effect of"
ξ	is a reduction factor for unfavourable permanent actions G

Figure 37: Load combination for ULS

In expression 6.10a, there is no leading variable action; all the variable actions are taken into account with their combined value, i.e., their value is reduced by the relevant combination factor 0. The permanent actions are taken into account as in expression 6.10, and the unfavorable permanent actions may be considered the leading actor in the combination of actions. All the actions are multiplied by the appropriate safety factor, G or Q. Eq 6.10 is always equal to or more conservative than either 6.10a or 6.10b.

In expression 6.10b, the combination of actions is governed by a leading variable action represented by its characteristic value as in expression 6.10, with the other variable actions being taken into account as accompanying variable actions and being represented by their combination value, i.e., their characteristic value is reduced by the appropriate combination coefficient of a variable action 0. When the envelope of the two expressions showing the less favorable effects of expressions 6.10a and 6.10b is determined, generally expression 6.10a applies to members where the ratio of variable action to total action is low, i.e. for heavier structural materials, and expression 6.10b applies where the same ratio is high, i.e. for lighter structural materials.

For 1PP, Envelope & Linear ULS: $1.25G_k + 1.5Q_{k,1} + \sum(\varphi_{0,i}1.5Q_{k,i})$

Name	1PP_EN-ULS 6.10b		Name	1PP_LN-ULS 6.10b
Description			Description	
Type	Envelope - ultimate		Type	Linear - ultimate
Contents of co...			Amplified Sway M...	☐ no
LC1 - Self weight ...	1.25		Contents of co...	
LC2 - Floor Load [...	1.25		LC1 - Self weight ...	1.25
LC3 - 1-1PPPublic...	1.50		LC2 - Floor Load [...	1.25
LC6 - Fire Truck S...	1.05		LC3 - 1-1PPPublic...	1.50
LC11 - Fire Truck ...	1.05		LC6 - Fire Truck S...	1.05
LC12 - 2-1PPPubli...	1.50		LC11 - Fire Truck ...	1.05
LC14 - Bus Ramp ...	1.05		LC12 - 2-1PPPubli...	1.50
			LC14 - Bus Ramp ...	1.05

Figure 38: Creation of the load combination for given model

Moreover, the load arrangement used for all the floors was an alternative variable load (like a chess pattern), and similarly, we made the envelope and linear combinations for each floor as well as for the entire structure just to check the results on floor 1PP with the load combination on each floor and with the entire floor. [12]
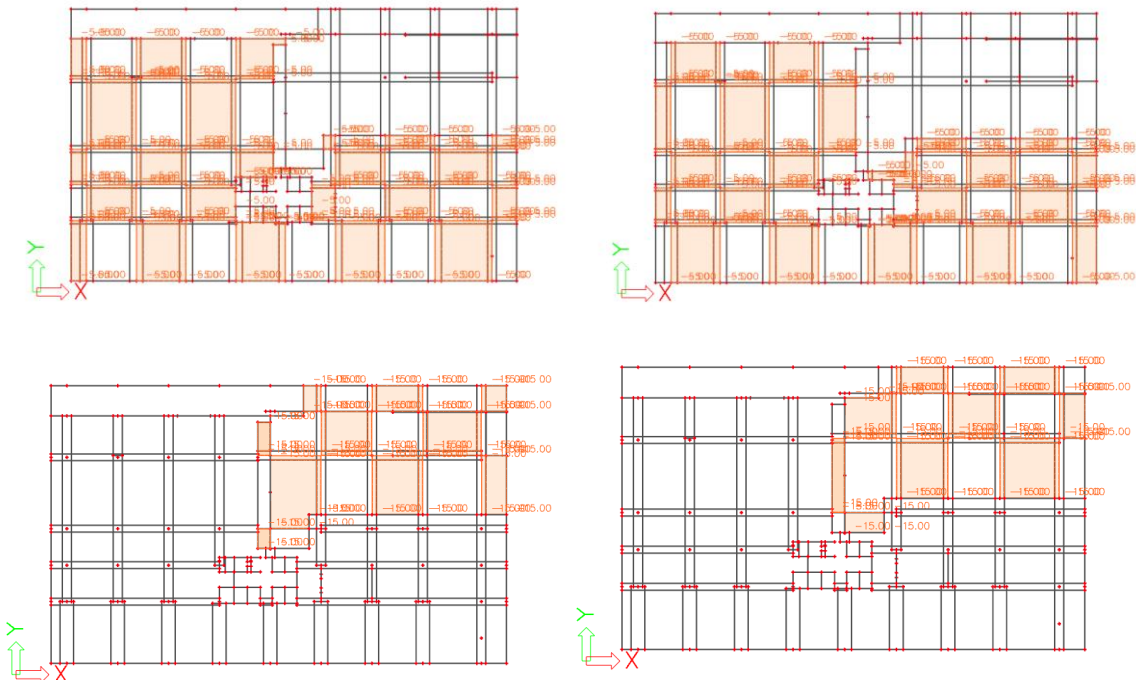
Figure 39: Assigning the load on the alternate span of the floor 1PP
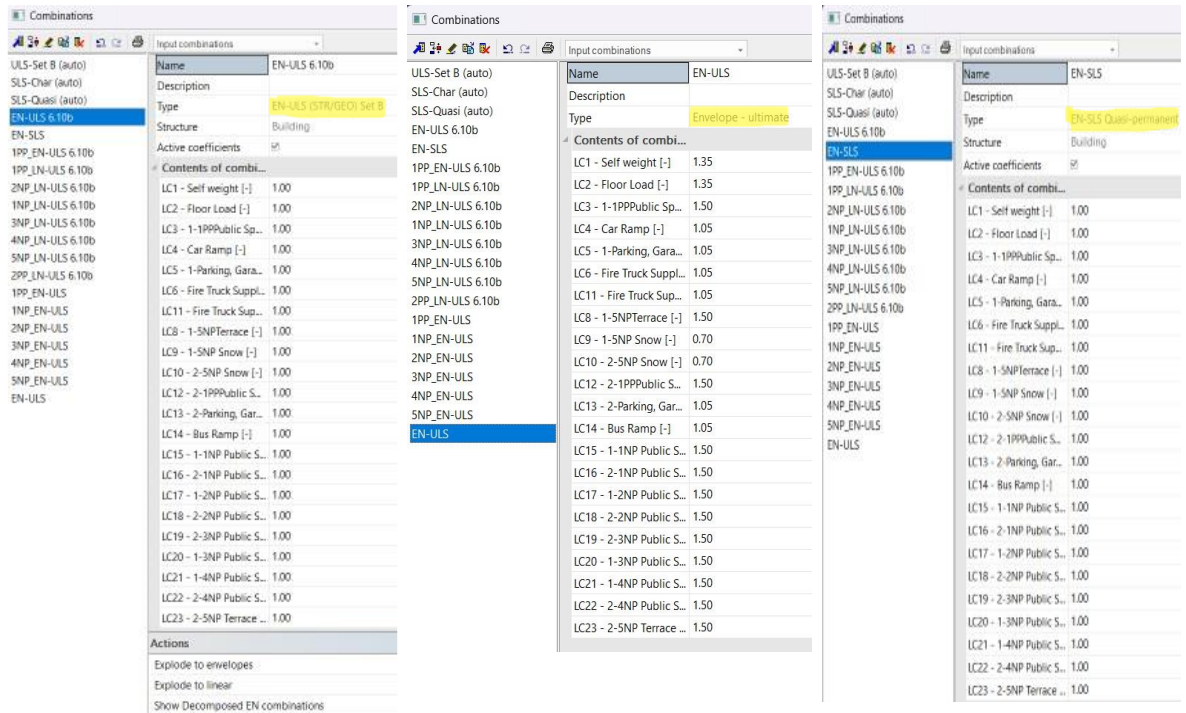
Figure 40: Creation of load combinations for ULS & SLS

Ultimate limit states

Ultimate limit states concern the safety of people and the safety of the structure. Also, the protection of the contents should be classified as Ultimate Limit States. The following ultimate limit states need to be verified when relevant:

• loss of equilibrium of the structure or any part of it, considered as a rigid body

• failure by inordinate distortion, the metamorphosis of the structure or any part of it into a medium, rupture, loss of stability of the structure or any part of it, including supports and foundations

• failure caused by fatigue or other time-dependent goods.

Serviceability limit states

Serviceability limit states concern the functioning of the structure under normal use, the comfort of people, and the appearance(high deviation, expansive cracking). Serviceability limit states correspond to conditions beyond which specified service conditions for a structure or structural member are no longer met. The verification of utility limit countries is grounded on criteria concerning:

• deformations that affect the appearance, the comfort of users, or the functioning of the structure (including machines or services)

• vibrations that cause discomfort to people or that limit the functional effectiveness of the structure

• damage that is likely to adversely affect the appearance, durability or functioning of the structure [12]

4.5 Static Calculations for prepared models

For proper design, calculation of internal forces and assessment, a model was first created in the SCIA Engineer 19.1 software.

4.5.1 Model with Reinforced concrete

In the calculation of RC variant 1, the most complicated slab, i.e. the one above 1PP was assessed. This is a part that is loaded with a useful load of 15 kN/m^2 due to the design of the supply in the lowered places of the slab (see Fig.). The most heavily loaded beam above the support and in the field was assessed. Next, the slab was assessed in the field. The last step was a simplified deflection test.
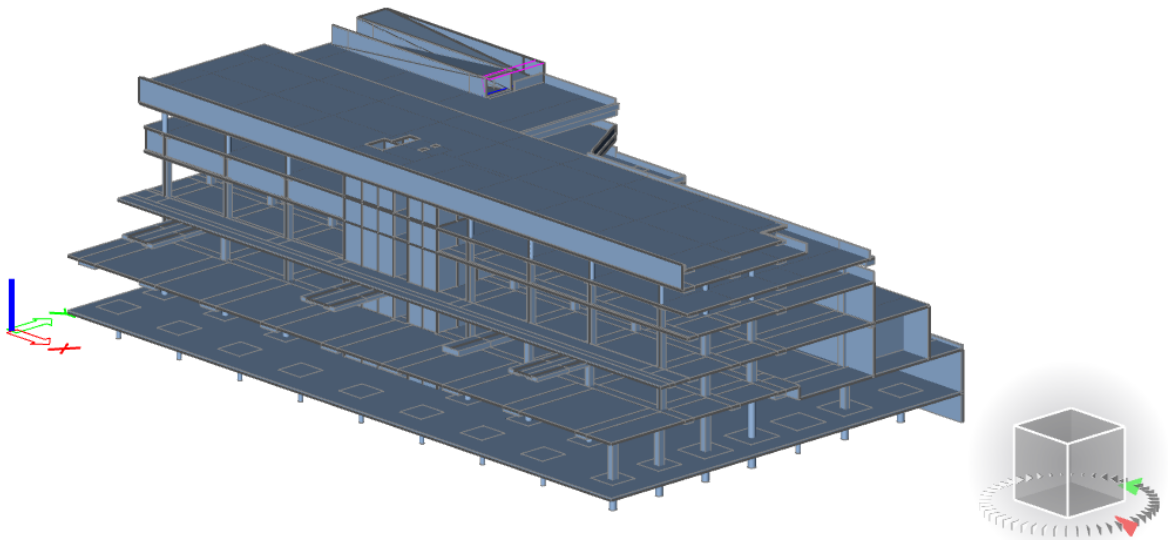
Figure 41: 3D Model of the structure

4.5.1.1 Material characteristics

Concrete

Concrete C35/45, D_{max} 16mm (See 3.1)

Characteristic compressive strength of concrete (f_{ck}) = 35MPa

Design compressive strength of concrete (f_{cd}) $= \dfrac{f_{ck}}{\gamma_d} = \dfrac{35}{1.5} = 23.33 MPa$

Steel

Steel B500B

Characteristic yield strength of reinforcement (f_{yk}) = 35MPa

Design yield strength of reinforcement (f_{yd}) = $\dfrac{f_{yk}}{\gamma_s} = \dfrac{500}{1.15} = 435 MPa$

Mesh Setup:

For further calculation, the finer mesh was used, and the basic thumb rule to calculate the size of the mesh element is 1 to 2 times the thickness of the slab [22], or for a more accurate result, the size of the mesh element is equal to the thickness of the slab. But, due to the speed of the calculation during the modeling, instead of using the thickness of the slab or 1-2 times the thickness of the slab, we chose 0.75 m for a smooth calculation. The reason why we did so was due to the low processor (RAM) available in the computer. As a result, initially, when we selected the mesh size as 0.25 m and 0.5 m, it was not able to run the model, and as a result, we went with 0.75 m.

4.5.1.2 Displacement on 1PP

Displacement due to self-weight:
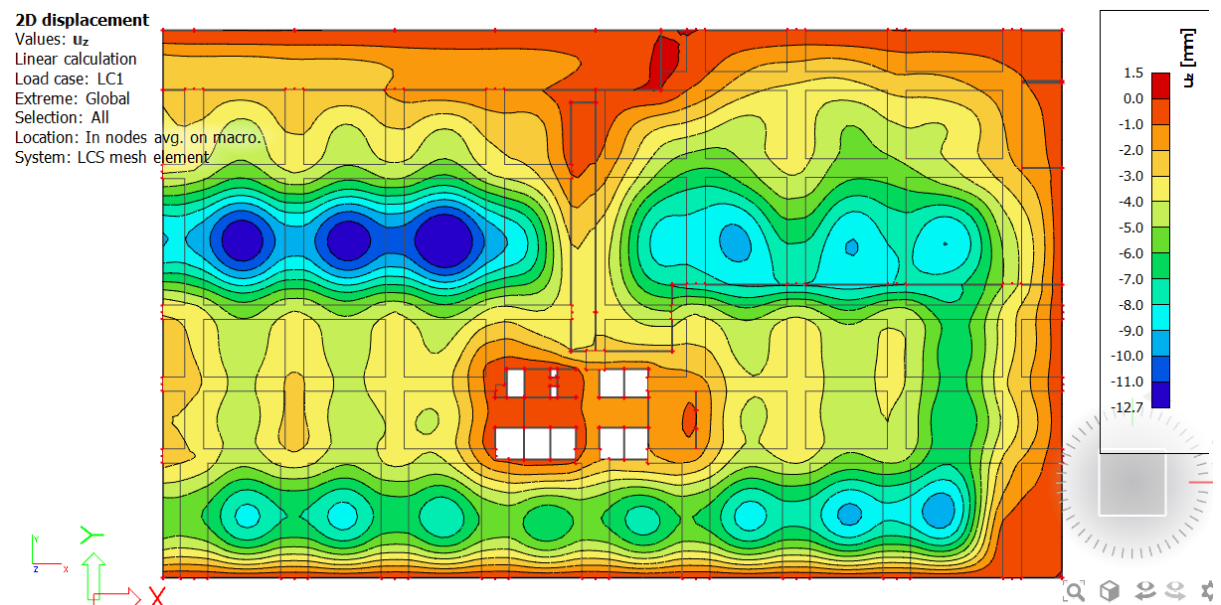
Figure 42: 2D Displacement of 1PP due to self-weight

If we look the vertical displacement from the quasi-permanent load combination on the whole plate above 1PP, we got to know that with SLS combination the maximum displacement is

19.0mm.
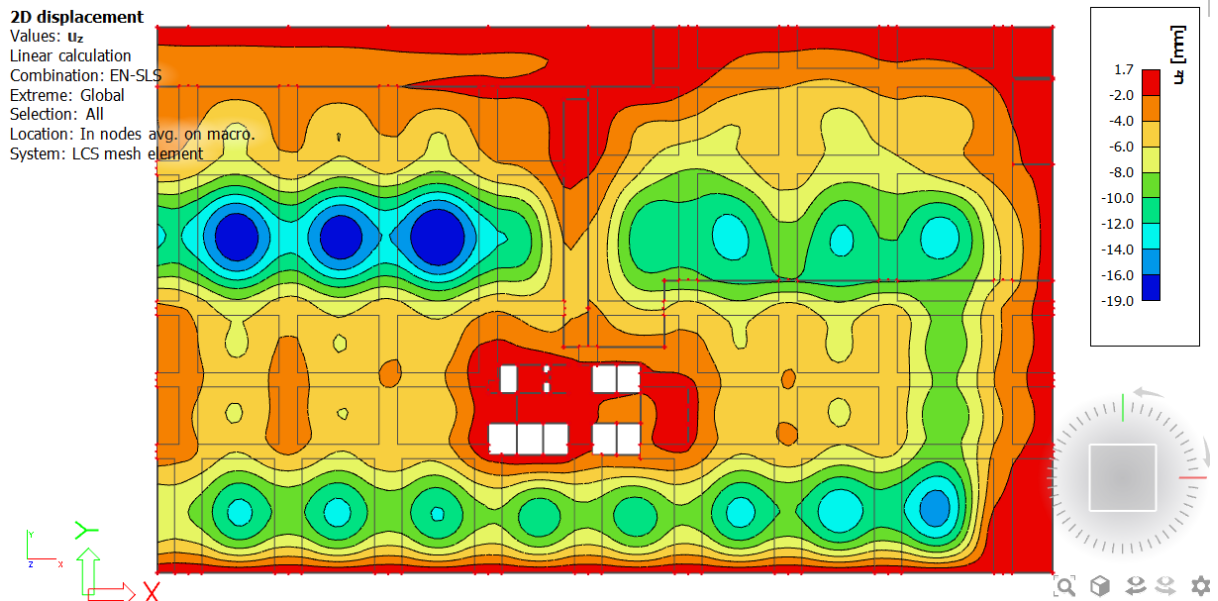
Figure 43: 2D Displacement of 1PP due to SLS-Quasi Permanent combination

Proof why we should use PSC:

Vertical deformation from quasi-steady load combination g under **short-term action**:

$$w_{g,st,1} = 19.0 \; mm$$

Rough estimation of vertical deformation from quasi-steady load combination g under **long-term action**:

$$w_{g,lt,1} = \left(4 \; to \; 5 \; times \; of \; w_{g,st,1}\right) = 95.0 \; mm \; (Say)$$

Limit deflection under quasi-steady load combination:

$$w_{g,lim,1} = \frac{1}{250}.l = \frac{11300}{250} = 45.2 \; mm$$

So,

$$w_{g,lt,1} = 95.0 \; > \; w_{g,lim,1} = 45.2 \; mm \; NOT \; ok$$

To verify this, we run the model for code dependent deflection so that we can check the deflection for short as well as long term.

Code dependent deflection (CDD):

The calculation of code-dependent deflection (CDD) was done according to chapter 7.4.3 from EN 1992-1-1. It should perform the verification of diversions because of the following reasons::

1. Inferior deviation (Unacceptable deflection) shouldn't affect the proper function of the structure or aesthetic- limit or total deviation

2. To avoid damage to partitions and homestretches because of supplements in deviation following their construction- limit for fresh deviation
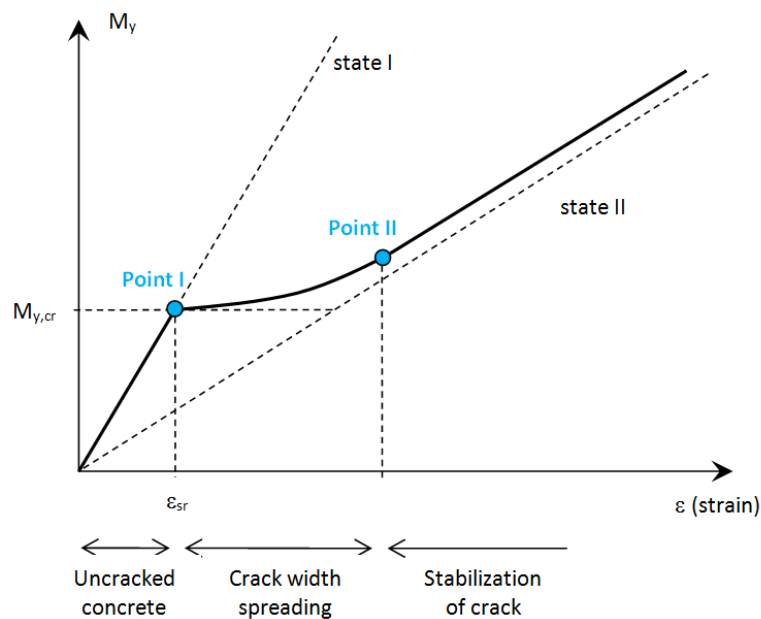
Figure 44: Graph of reliance of cracking moment on strain in concrete

Influence of deviation values:

Generally, there are three main goods that affect the values of distortion

1. Effect of load

In concrete structures, diversions increase with time under sustained load. The lesser part of the deviation typically occurs under sustained loads. Thus, long-term diversions are calculated under a stylish estimate of the sustained cargo during the continuance of the structure. The design cargo for calculating long-term diversions is the endless cargo.

2. Effect of cracking

The effect of concrete cracking is an unrecoverable process. Thus, it's necessary to calculate long-term diversions using an effective tensile concrete strength which corresponds to the worst cracking during the continuance of the structure.

3. Effect of creep

In fact, creep is the nonstop distortion of a member under sustained cargo. As it's mentioned in" hypotheticals", the creep effect is covered in computation via effective modulus of pliantness (elasticity) which is calculated using creep measure.[22]
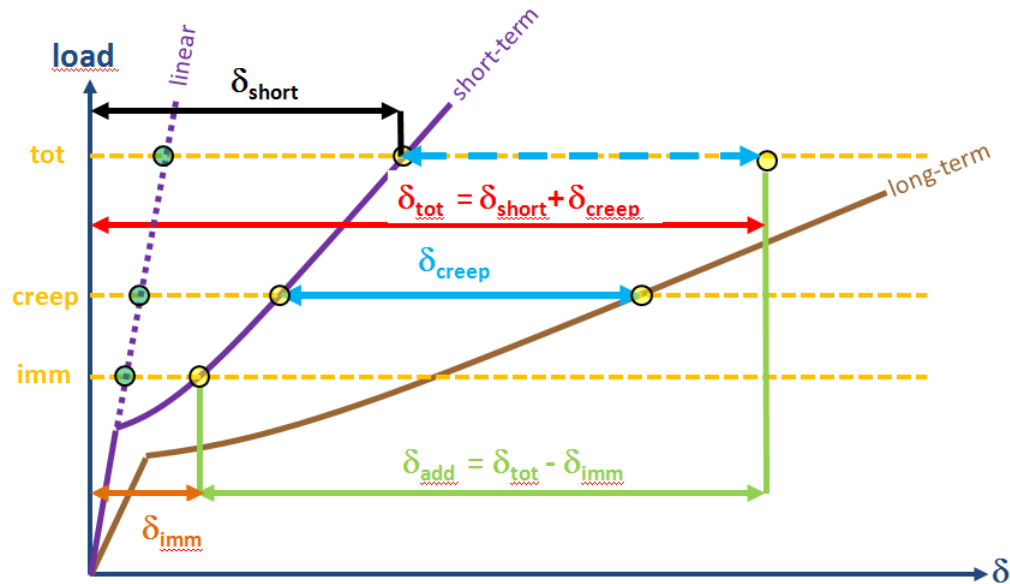
Figure 45: Graph showing deflection variation for long and short term due to creep, shrinkage, imm

Limitation:

1. The Plane generator and Absences are not supported in structures
2. Only deflection in z-axis of LCS of 2D member is calculated (deflection perpendicular for plane of 2D member)
3. Deflection in the y and z axis of LCS of 1D member is supported shrinkage is not taken into account
4. It is not possible run code-dependent deflection for non-linear combination

It is extreme that a reinforced concrete structure cannot "sensibly" act on such a span, the results calculated above also correspond to this. Although this designed and reinforced structure passed at ULS but won't pass SLS. As we know that the ceiling slab above 1PP in the reinforced concrete variant didn't meet the SLS- deviation (although we calculated in a simplified way, the deviation came out to be nearly 2 times higher than its limit value), we would propose a revision of the sampling of the ray so that indeed with a veritably simplified computation we meet this condition.
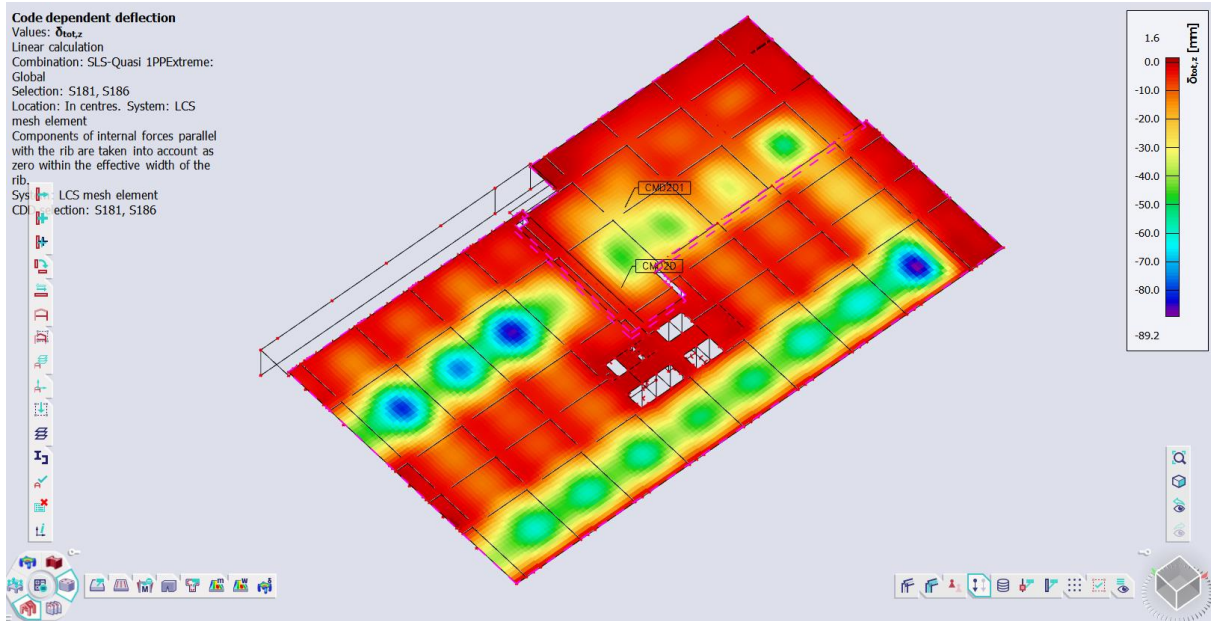
Figure 46: Long-term deflection due to SLS Quasi on the entire floor of 1PP

After running the model for long-term using the code-dependent deflection function in the Scia Engineer software v.21, it can be said that the quick rough estimate that we made earlier was correct. From fig.46, we got the displacement for the long-term was almost 90mm, which was greater than the limiting value which was not a suitable approach to design the model as reinforced concrete. Hence, we decided to go with prestressed concrete.
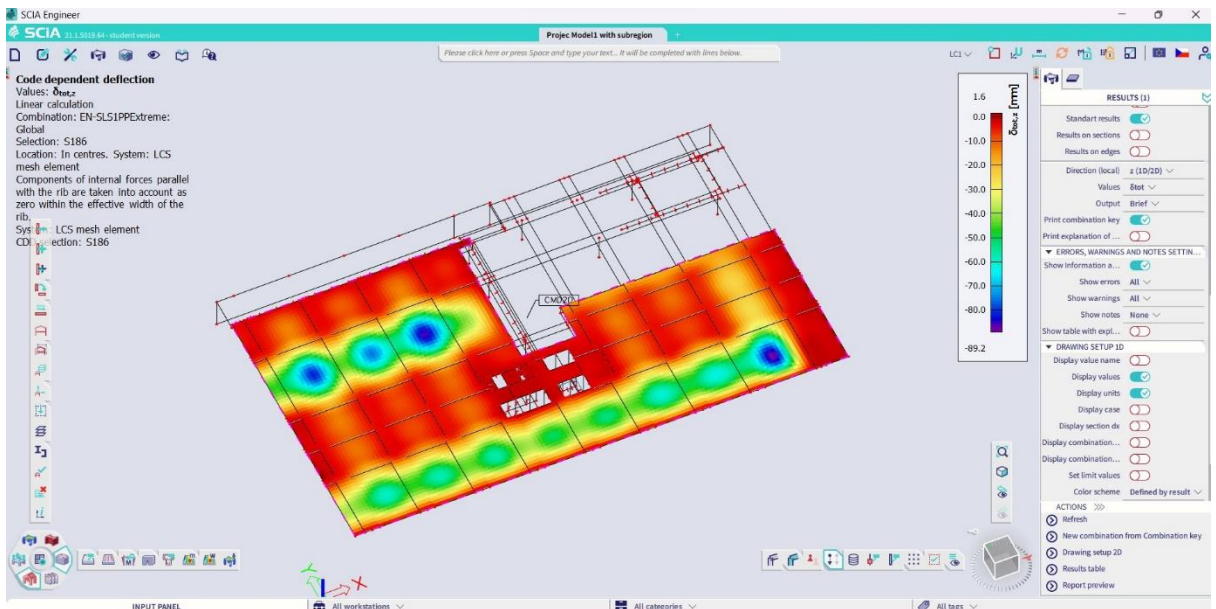
Figure 47: Long-term deflection due to SLS Quasi on the left part of 1PP
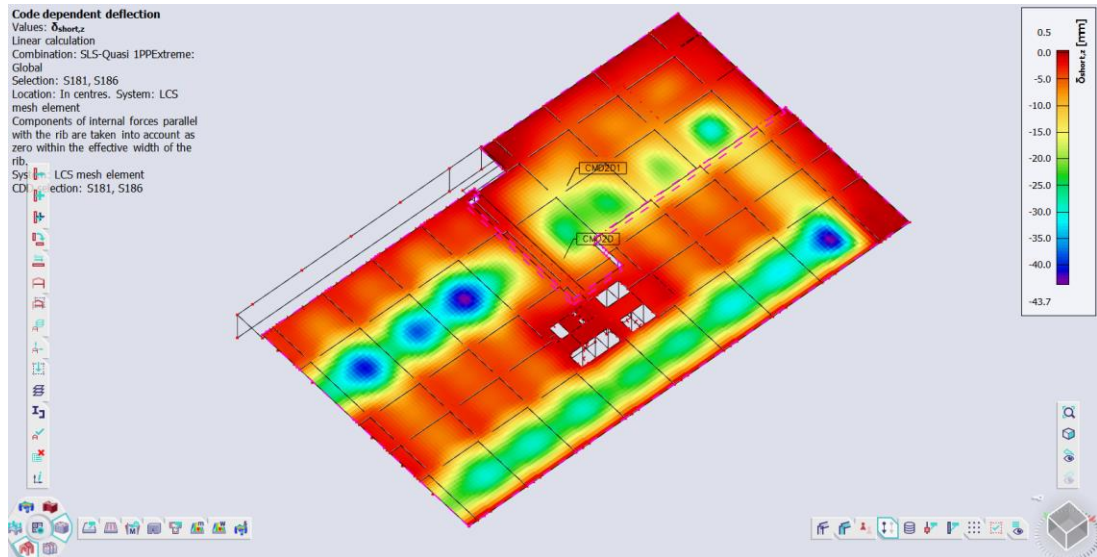
Figure 48: Short term deflection due to SLS Quasi on the entire floor of 1PP
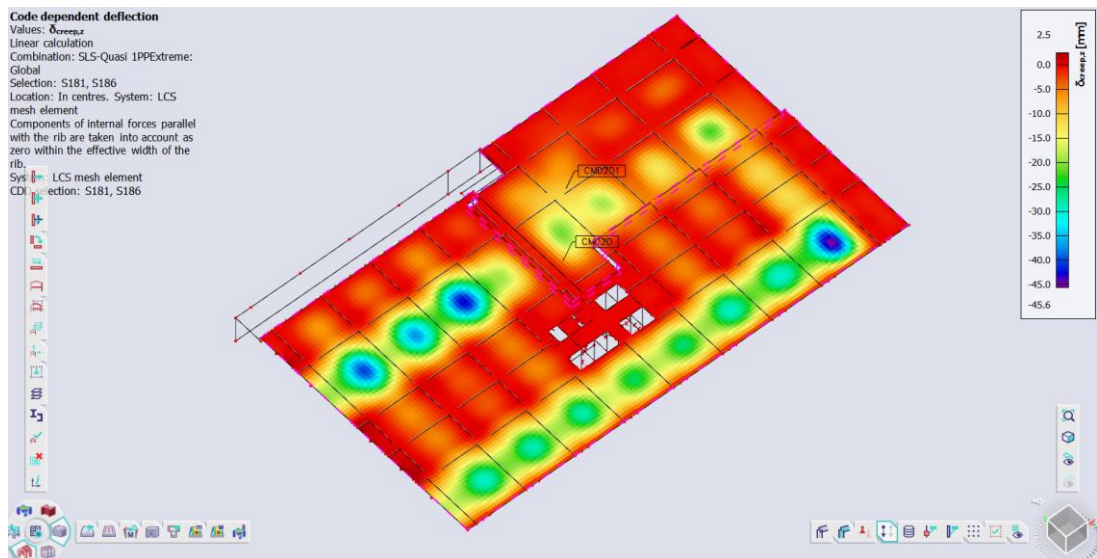
Figure 49: Deflection for creep due to SLS Quasi on the entire floor of 1PP

Solution:

Piecemeal from this, if we change the cross section, there will be change in the volume of A5 and as a result it will also affect in the overall cost. But, we can lower (decreased) the price of model if we use the prestressed concrete technology.

Apart from this, when we looked for the crack width check due to SLS for the reinforced model, we got the following results shown in Fig. 50. From this, it can be say that to minimize the cracks, we need to provide additional steel or change the cross-section of the beam which is not economical. Hence, this was also one of the reasons why we decided to design the model as a prestressed model.
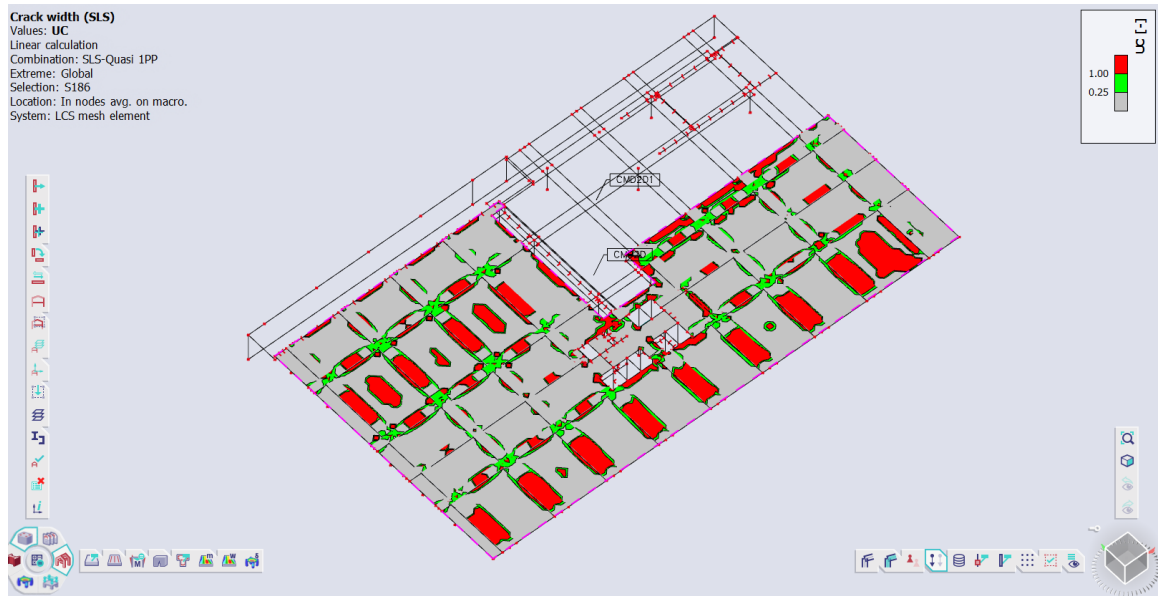
Figure 50: Display showing the crack width for 1PP due to SLS Quasi

4.5.2.3   Design and reinforcement of Beam on 1PP – Left Side of slab (ULS)

For the design, initially we choose the left side (West side) of slab, as shown in the following fig.51 on left side there are four beams of size 2000/750 and at one edge size of beam is 3000/750, which is highlighted by green color namely A1, A2, A3 and A4. Then we calculated the values of the moments on the A1 – A4 for further measurements.

Beam 2000/750
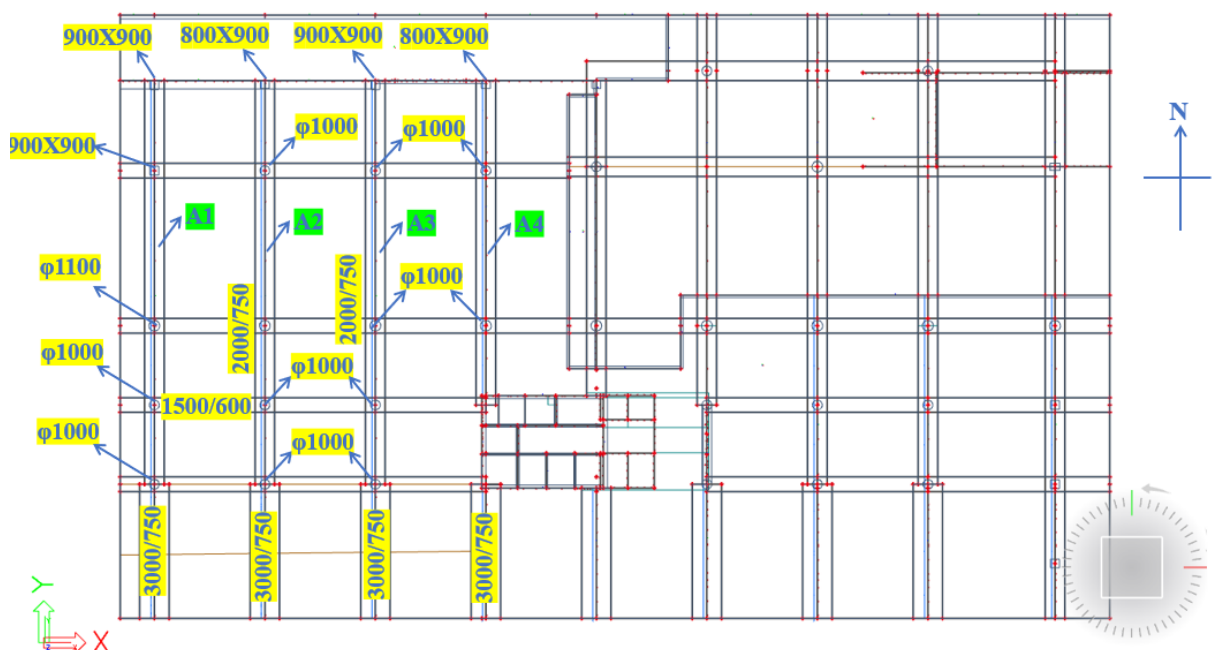
Figure 51: Layout of 1PP showing the position of the beam on left side of slab

Cross-section

Height of beam: $h_T = 750\ mm$

Beam width: $b_T = 2000mm$

Plate thickness: $h_d = 250mm$

2D internal forces
Values: $\mathbf{m_y}$
Linear calculation
Combination: ULS-Set B (auto)
Extreme: Mesh
Selection: S186, SE1
Location: In nodes avg. on macro.
System: LCS mesh element
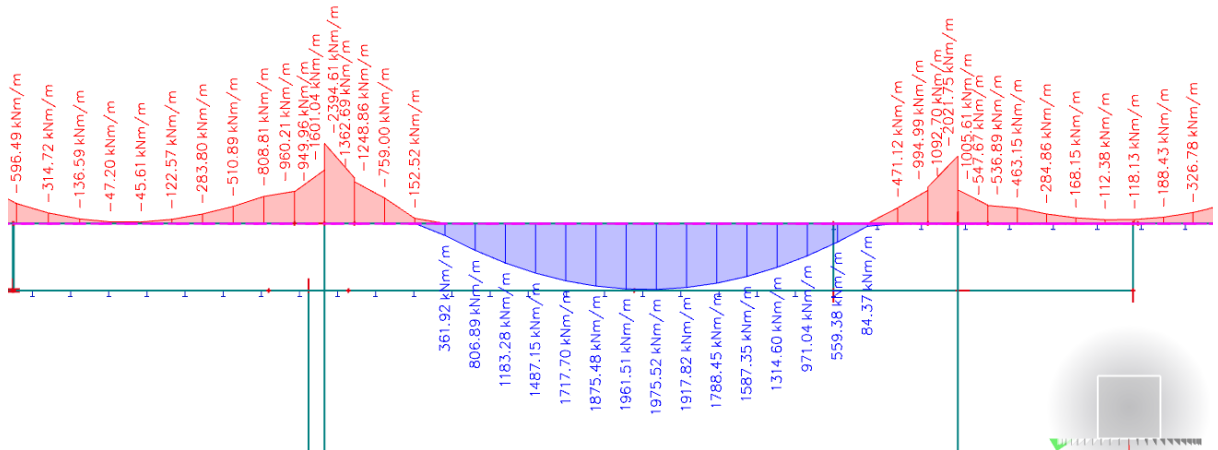
Figure 52: Display of 2D internal forces my for beam 2000/750 (A2) for ULS combination

Over Support:

Assume $\emptyset = 25mm$, $\emptyset_{stirrups} = 10mm$, $C_{nom} = 30mm$

Moment over support $\left|M_{Ed,support}\right| = 2394.61kNm$

Effective cross-section height:

$$d_t = h_t - C_{nom} - \emptyset_{stirrups} - \emptyset - \frac{\emptyset}{2} = 700 - 30 - 10 - 12.5 = 697.5mm$$

$$A_{s,req} = \frac{M_{Ed}}{0.87 * fy * z} = \frac{2394.61 * 10^6}{0.87 * 435 * 0.9 * 697.5} = 10079.51mm^2$$

$Say\ 21\emptyset25mm\ at\ 95mm,\ A_{s,prov} = 10308.35mm^2$

Check

1) $M_{Rd} \geq M_{Ed}$

$$x = \frac{f_{yd} * A_{s,prov}}{0.8 * b * f_{cd}} = \frac{435 * 10308.35}{0.8 * 2000 * 23.33} = 120.13mm$$

$$z = d - 0.4x = 697.5 - (0.4 * 120.13) = 649.448 mm$$

$$M_{Rdy} = A_{s,prov} * f_{yd} * z = 10308.35 * 435 * 649.448 = 2912.21 kNM$$

So, $M_{Rd}(= 2912.21) > M_{Ed}(= 2394.61) ... ... OK$

2) $\varepsilon \leq \varepsilon_{bal} \approx 0.64$

$$\varepsilon = \frac{x}{d} = 0.17 < 0.64 ... ... OK$$

3) $\rho_{min} \leq \rho \leq \rho_{max}$

$$0.0015 \leq \frac{A_{s,prov}}{bd} \leq 0.4$$

$$0.0015 \leq \frac{10308.35}{2000 * 697.5} = 0.007 < 0.4 ... ... OK$$

4) $\varepsilon_s \leq \varepsilon_{cu}(5\%)$

$$\varepsilon_s = \frac{0.0035(d - x)}{x} = \frac{0.0035(697.5 - 120.13)}{120.13} = 1.68\% < 5\% ... ... OK$$

In field (midspan):

Assume $\emptyset = 25mm, \emptyset_{stirrups} = 10mm, C_{nom} = 30mm$

Moment over support $|M_{Ed}| = 1975.52 kNm$

Effective cross-section height:

$$d_t = h_t - C_{nom} - \emptyset_{stirrups} - \emptyset - \frac{\emptyset}{2} = 700 - 30 - 10 - 12.5 = 697.5mm$$

$$A_{s,req} = \frac{M_{Ed}}{0.87 * fy * z} = \frac{1975.52 * 10^6}{0.87 * 435 * 0.9 * 697.5} = 8315.458mm^2$$

$Say\ 18\emptyset25mm\ at\ 110mm, A_{s,prov} = 8835.73mm^2$

Check

1) $M_{Rd} \geq M_{Ed}$

$$x = \frac{f_{yd} * A_{s,prov}}{0.8 * b * f_{cd}} = \frac{435 * 8835.73}{0.8 * 2000 * 23.33} = 205.93mm$$

$$z = d - 0.4x = 697.5 - (0.4 * 205.93) = 615.128mm$$

$$M_{Rdy} = A_{s,prov} * f_{yd} * z = 8835.73 * 435 * 615.128 = 2364.27kNM$$

So, $M_{Rd}(= 2364.27) > M_{Ed}(= 1975.52) \dots \dots \dots \dots \dots \dots OK$

2) $\varepsilon \leq \varepsilon_{bal} \approx 0.64$

$$\varepsilon = \frac{x}{d} = 0.33 < 0.64 \dots \dots \dots \dots \dots OK$$

3) $\rho_{min} \leq \rho \leq \rho_{max}$

$$0.0015 \leq \frac{A_{s,prov}}{bd} \leq 0.4$$

$$0.0015 \leq \frac{8835.73}{2000 * 697.5} = 0.014 < 0.4 \dots \dots \dots \dots OK$$

4) $\varepsilon_s \leq \varepsilon_{cu}(5\%)$

$$\varepsilon_s = \frac{0.0035(d - x)}{x} = \frac{0.0035(697.5 - 205.93)}{205.93} = 0.695\% < 5\% \dots \dots \dots OK$$

4.5.2.4 *Design and check for reinforcement of slab on 1PP – Left Side of slab (SLS)*

Slab thickness = 250mm

Assume $\emptyset = 12mm, \emptyset_{stirrups} = 10mm, C_{nom} = 30mm$

2D internal forces
Values: m_y
Linear calculation
Combination: SLS-Quasi (auto)
Extreme: Mesh
Selection: S186, SE3
Location: In nodes avg. on macro.
System: LCS mesh element
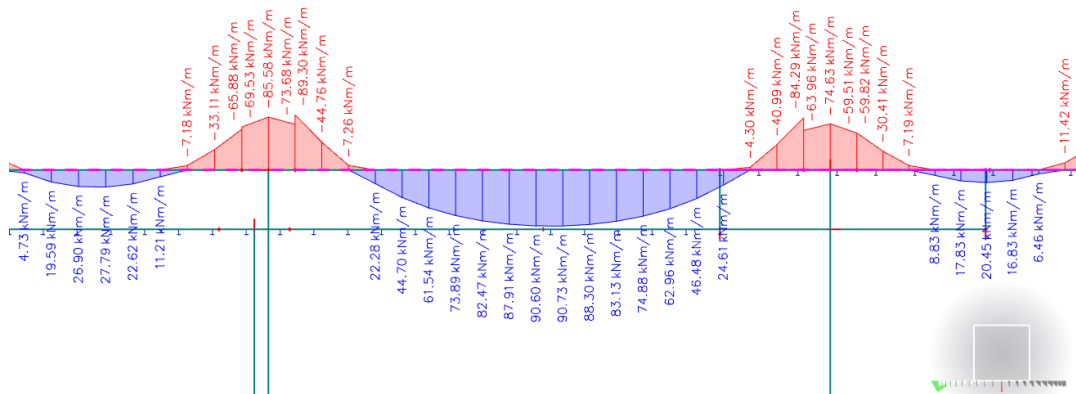
Figure 53: Display of 2D internal forces my for slab (=250mm) for SLS combination

Moment $\left| M_{Ed,y} \right| = 85.58 kNm$

Effective cross-section height:

$$d_y = h_y - C_{nom} - \emptyset_{stirrups} - \emptyset - \frac{\emptyset}{2} = 250 - 30 - 12 - 6 = 202mm$$

$$A_{s,req} = \frac{M_{Ed}}{0.87 * fy * z} = \frac{85.58 * 10^6}{0.87 * 435 * 0.9 * 202} = 1243.855mm^2$$

$Say \ 11\emptyset 12mm \ at \ 90mm, A_{s,prov} = 1244.07mm^2$

Spacing $s = \frac{a_s * b}{A_s} = 90.92 \approx 90$

$$s \leq s_{max,slab} \gg 3h \leq 400 \gg 750 \leq 400$$

$$\frac{l_y}{l_x} < 2 \dots \dots \dots \dots Two \ Way \ Slab$$

Check

1) $M_{Rd} \geq M_{Ed}$

$$x = \frac{f_{yd} * A_{s,prov}}{0.8 * b * f_{cd}} = \frac{435 * 1244.07}{0.8 * 1000 * 23.33} = 28.99mm$$

$$z = d - 0.4x = 202 - (0.4 * 28.99) = 190.404mm$$

$$M_{Rdy} = A_{s,prov} * f_{yd} * z = 1244.07 * 435 * 190.404 = 103.04kNM$$

So, $M_{Rd}(= 103.04) > M_{Ed}(= 85.58) \dots \dots \dots \dots \dots \dots OK$

2) $\varepsilon \leq \varepsilon_{bal} \approx 0.64$

$$\varepsilon = \frac{x}{d} = 0.144 < 0.64 \dots \dots \dots \dots OK$$

3) $\rho_{min} \leq \rho \leq \rho_{max}$

   % of req tensile r/f

$$0.0015 \leq \frac{A_{s,prov}}{bd} \leq 0.4$$

$$0.0015 \leq \frac{1244.07}{1000 * 202} = 0.006158 \leq 0.4 \dots \dots \dots \dots OK$$

4) $\varepsilon_s \leq \varepsilon_{cu}(5\%)$

$$\varepsilon_s = \frac{0.0035(d - x)}{x} = \frac{0.0035(202 - 28.99)}{28.99} = 2.088\% < 5\% \dots \dots \dots OK$$

SLS – Deflection Check (7.4EN 1992-1-1)

$$\frac{l}{d} = k \left[11 + 1.5\sqrt{f_{ck}}\frac{\rho_0}{\rho} + 3.2\sqrt{f_{ck}}\left(\frac{\rho_0}{\rho} - 1\right)^{3/2} \right] = 334.3465$$

$$\left(\frac{l}{d_{allowable}}\right) = 334.3465 * 1 * \frac{1244.07}{1243.855} = 334.404$$

$$\left(\frac{L}{d_{actual}}\right) = 272.3 > 234.404 \dots \dots \dots \dots NOT Ok$$

SLS – Shear Check

$$k = \left(1 + \sqrt{\frac{200}{d}} \right) = 1.995 > 2$$

$$\rho_1 = 0.006158$$

$$V_{Rd,c} = \left[0.12k(100 * \rho_1 * f_{ck})^{1/3}\right]b_w * d = 117.56kN > V_{Ed} = 63.95kN$$

$$V_{Rd,cmin} = 9.76kN$$

2D internal forces
Values: v_y
Linear calculation
Combination: ULS-Set B (auto)
Extreme: Mesh
Selection: S186, SE3
Location: In nodes avg. on macro.
System: LCS mesh element
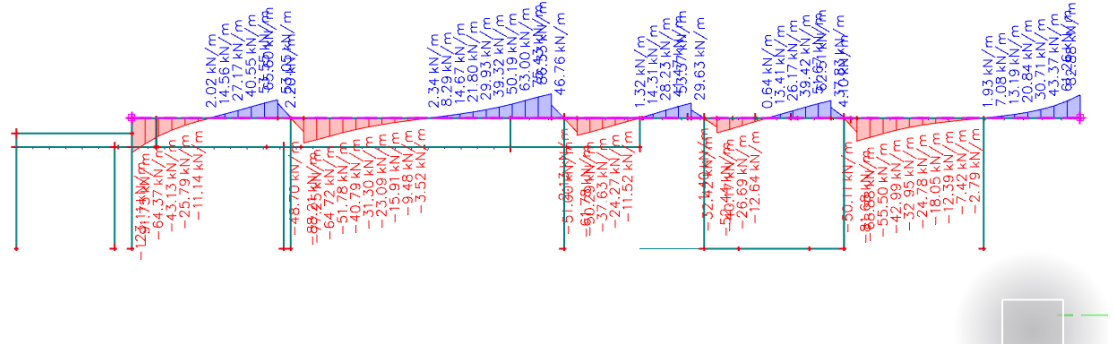
Figure 54: Display of 2D internal forces Vy for slab on 1PP

4.5.2.5   Design of Beam on 1PP – Right Side of slab

Fig. 43 shows the two most heavily loaded parts with the maximum displacement: one on the left side and another on the right side, so we chose the right side of the slab, as shown in fig. 55, with beams of sizes 2000/1500 and 2000/1000 on the right side. Then we calculated the values of the moments on this beam and looked for the maximum value for further measurements.
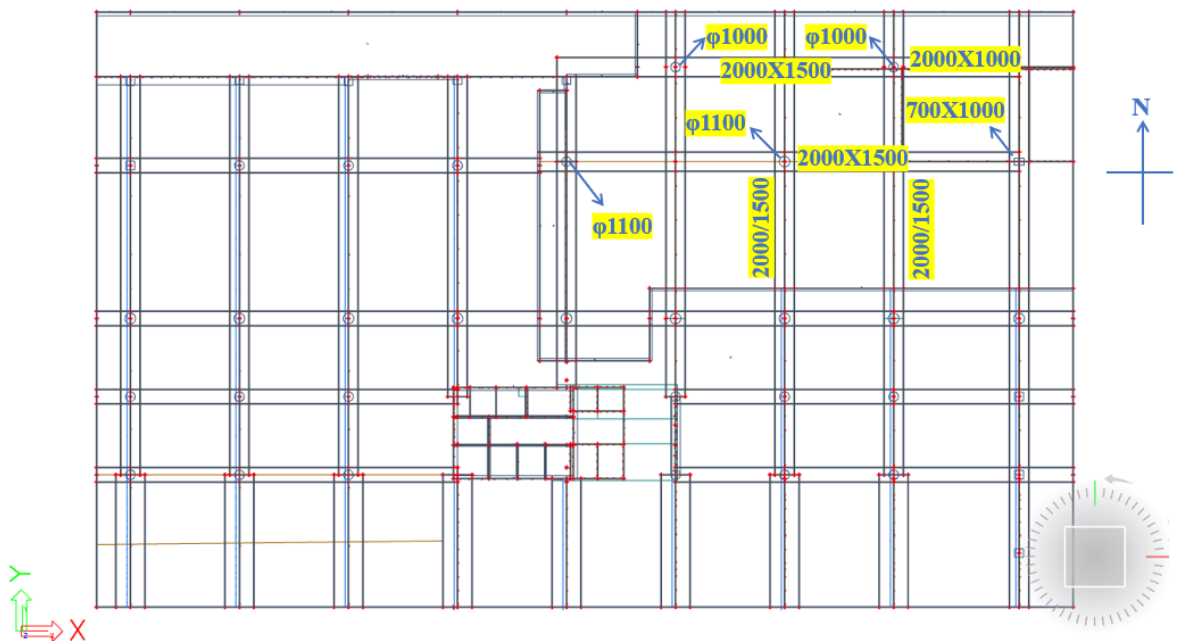
Figure 55: Layout of 1PP showing the position of beam and column on right side of slab

Cross-section

Height of beam: $h_T = 1500\ mm$

Beam width: $b_T = 2000mm$

Plate thickness: $h_d = 300mm$

Bending Moment

The software calculated bending moment (M_y) by considering the wall which is above the beam (see Fig.53).
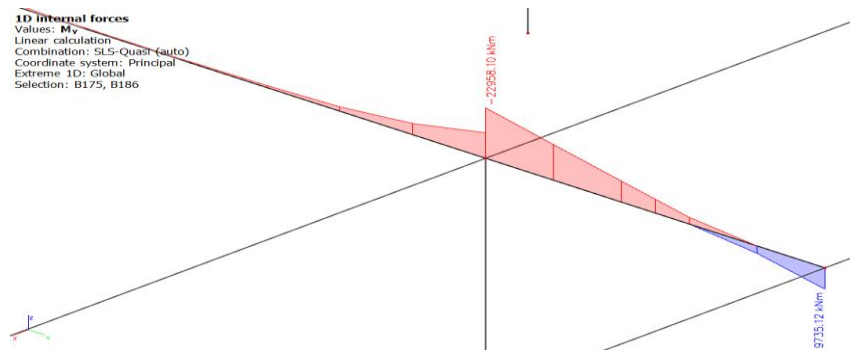
Figure 56: Display of the bending moment my from SLS combination on the most heavily loaded beam on right side of slab on 1PP

Moment in the field ($M_{Ed,filed}$) = 8468.8kNm

Moment over support ($M_{Ed,support}$) = −14807.5kNm

Design Check for moment over support

Trial 1:

Say $\emptyset = 32mm$

$\emptyset_{stirrups} = 12mm$

Cover I $= 30mm$

$M_{Ed,support} = -14807.5kNm$

Effective cross-sectional height

$$= d_T = h_T - c - \frac{\emptyset}{2} - \emptyset_{stirrups} = 1500 - 30 - \frac{32}{2} - 12 = 1442mm$$

Required reinforcement area $= A_{st,req} = \frac{b_T.d_T.f_{cd}}{f_{yd}}.(1 - \sqrt{1 - \frac{2.M_{Ed,support}}{b_T.d_T^2.f_{cd}}})$

$$= \frac{2000*1442*23.3}{435}.(1 - \sqrt{1 - \frac{2*14807.5}{2000*(1442)^2*23.3}}) * 10^6 = 23606.3\ mm^2$$

$$x = \frac{A_{s,prov}*f_{yd}}{0.8*b_T*f_{cd}} = \frac{27344*435}{0.8*2000*23.3} = 318.6mm ,$$

$$z = d_T - 0.4*x = 1442 - (0.4*318.6) = 1314.6mm,$$

Bearing Moment

$$M_{Rd} = A_{s,prov}*f_{yd}*z = 27344*435*1314.6*10^{-6} = 15636.2kNm$$

$$M_{Ed,support} = 14807.5kNm < M_{Rd} = 15636.2kNm \ Ok$$

Number of bars $n_\emptyset = 34 \ no.$

Minimum clear spacing of bar

$$s_{min} = \max(20mm, 1.2*\emptyset. D_{max} + 5mm) = \max(20, 38, 21) = 38mm$$

$$s_c = \frac{b_T - 2*c - 2*\emptyset_{stirrups} - n_\emptyset*\emptyset}{n_\emptyset - 1} = \frac{2000 - 2*30 - 2*12 - 34*32}{34 - 1} = 25mm$$

So, $s_{min} > s_c$, NOT OK

Trial 2:

The smaller diameter of the bars is more advantageous in terms of structural deflections, but we have to design the reinforcement in three rows so that the required area of the reinforcement is preserved.

So Say $\emptyset = 25mm$

$\emptyset_{stirrups} = 12mm$

Cover I = 30mm

|$M_{Ed,support}$ | = 14807.5kNm

Effective cross-sectional height

$$= d_T = h_T - c - \frac{\emptyset}{2} - \emptyset_{stirrups} - s_{min} = 1500 - 30 - \frac{32}{2} - 12 - 25 = 1390.5mm$$

Required reinforcement area $= A_{st,req} = \frac{b_T.d_T.f_{cd}}{f_{yd}}.(1 - \sqrt{1 - \frac{2.M_{Ed,support}}{b_T.d_T^2.f_{cd}}})$

$$= \frac{2000*1390.5*23.3}{435} \cdot (1 - \sqrt{1 - \frac{2*14807.5}{2000*(1390.5)^2*23.3}}) * 10^6 = 25994.8 \text{ mm}^2$$

$$x = \frac{A_{s,prov}*f_{yd}}{0.8*b_T*f_{cd}} = \frac{29452*435}{0.8*2000*23.3} = 344.2mm \,,$$

$$z = d_T - 0.4*x = 1390.5 - (0.4*344.2) = 1252.8mm,$$

Bearing Moment

$$M_{Rd} = A_{s,prov} * f_{yd} * z = 29452.435 * 435 * 1252.8 * 10^{-6} = 16050.4kNm$$

$$M_{Ed,support} = 14807.5kNm \; < \; M_{Rd} = 16050.4kNm \; Ok$$

Number of bars $n_\emptyset = 60 \; no.$

Minimum clear spacing of bar

$$s_{min} = \max(20mm, 1.2*\emptyset. D_{max} + 5mm) = \max(20, 38, 21) = 38mm$$

$$s_c = \frac{b_T - 2*c - 2*\emptyset_{stirrups} - n_\emptyset * \emptyset}{n_\emptyset - 1} = \frac{2000 - 2*30 - 2*12 - 60*32}{60 - 1} = 25mm$$

So, $s_{min} < s_c \,, \;\; OK$

Design Check for $M_{Ed,field}$

Say $\emptyset = 32mm$

$\emptyset_{stirrups} = 12mm$

Cover I = 30mm

b_{eff} = 6m

$M_{Ed,field}$ = 8468.8kNm

Effective cross-sectional height

$$= d_T = h_T - c - \frac{\emptyset}{2} - \emptyset_{stirrups} = 1500 - 30 - \frac{32}{2} - 12 = 1442mm$$

Required reinforcement area $= A_{st,req} = \frac{b_{eff}.d_T.f_{cd}}{f_{yd}} \cdot (1 - \sqrt{1 - \frac{2.M_{Ed,field}}{b_{eff}.d_T^2.f_{cd}}})$

$$= \frac{6000*1442*23.3}{435} \cdot (1 - \sqrt{1 - \frac{2*8468.8}{6000*(1442)^2*23.3}}) * 10^6 = 13501.0 \text{ mm}^2$$

$$x = \frac{A_{s,prov}*f_{yd}}{0.8*b_{eff}*f_{cd}} = \frac{14476*435}{0.8*6000*23.3} = 56.2mm \ ,$$

$$z = d_T - 0.4 * x = 1442 - (0.4 * 56.2) = 1419.5mm,$$

Bearing Moment

$$M_{Rd} = A_{s,prov} * f_{yd} * z = 14476 * 435 * 1419.5 * 10^{-6} = 8938.7kNm$$

$$M_{Ed,support} = 8468.8kNm \ < \ M_{Rd} = 8938.7kNm \ Ok$$

4.5.2.6 Design of Slab on 1PP

From fig.54 slab works with beam having dimension 1500x2000 mm as a results it become very heavy slab as compared to the slab on other floors.

Thickness of slab (h_d) = 300mm
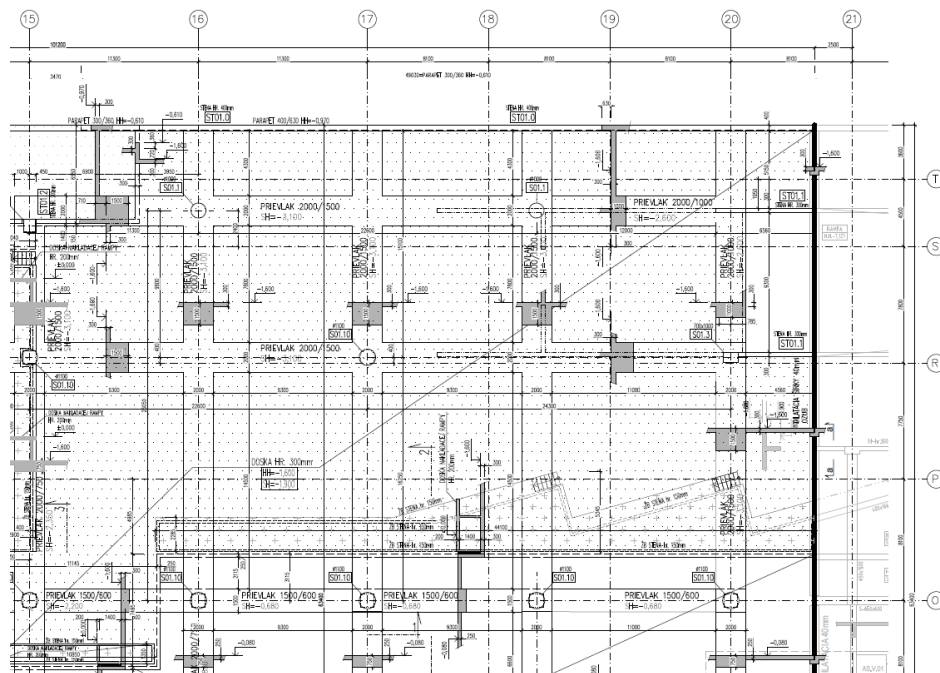
Figure 57: Layout of right side of slab of 1PP

So, as we explained in 4.2 that why we created three different models can be easily understand from the following results.

Result: 2D Internal forces (Moment)

1. Model I – Slab with monolithic beam
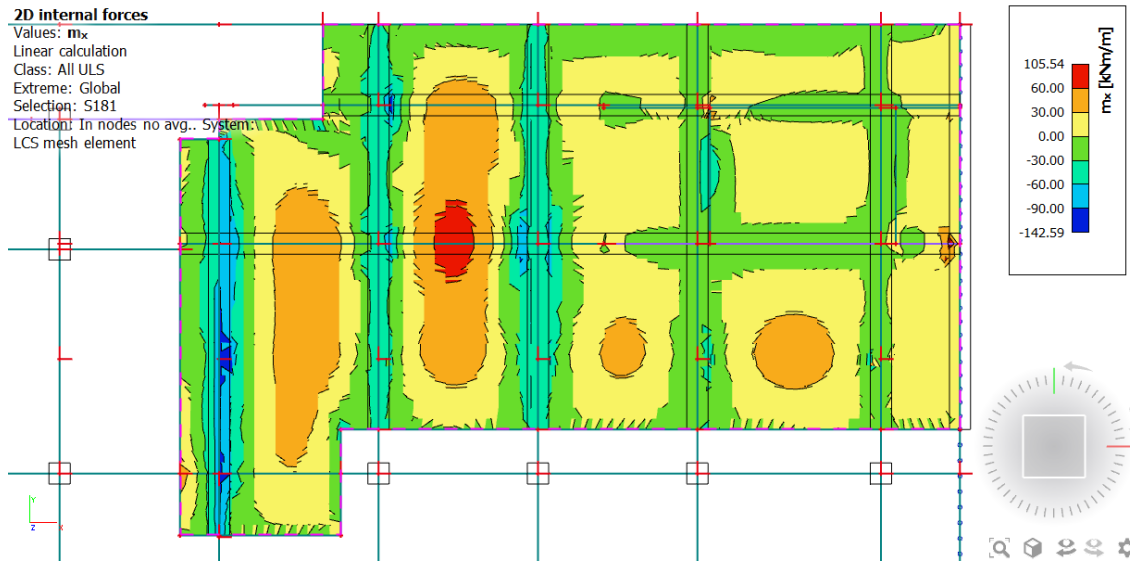
Figure 58: Display of 2D internal forces mx on right side of 1PP with monolithic due to ULS
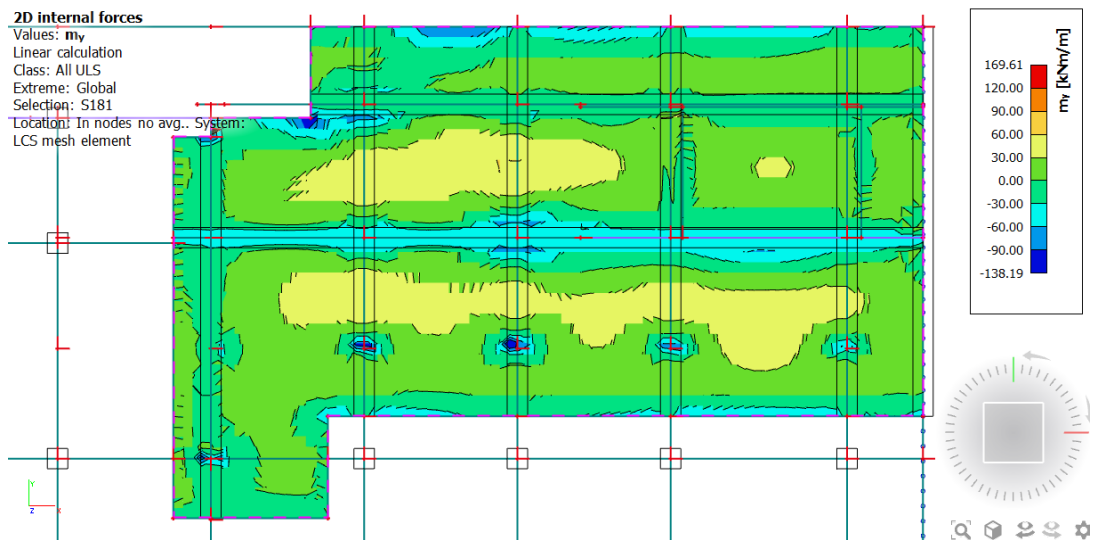
Figure 59: Display of 2D internal forces my on right side of 1PP model with monolithic due to ULS

$Say, \emptyset_x = 16mm$

$C_{nom} = 30mm$

$M_{Ed,x} = 105.54kNm$

Effective cross-sectional height

$$= d = h_d - c - \frac{\emptyset}{2} = 300 - 30 - \frac{16}{2} = 262mm$$

Required reinforcement area $= A_{st,req} = \dfrac{b.d.f_{cd}}{f_{yd}} \cdot (1 - \sqrt{1 - \dfrac{2.M_{Ed,support}}{b..d^2.f_{cd}}})$

$= \dfrac{1000*262*23.3}{435} \cdot (1 - \sqrt{1 - \dfrac{2*105.54}{1000*(262)^2*23.3}}) * 10^6 = 926.033 \text{ mm}^2$

$x = \dfrac{A_{s,prov}*f_{yd}}{0.8*b_T*f_{cd}} = \dfrac{1005.31*435}{0.8*1000*23.3} = 23.46 = 23.5mm$, $4Nos \, \emptyset = 16mm$

$z = d - 0.4 * x = 262 - (0.4 * 23.5) = 252.6mm,$

Bearing Moment

$M_{Rd} = A_{s,prov} * f_{yd} * z = 1005.31 * 435 * 252.6 * 10^{-6} = 110.46kNm$

$$M_{Ed,x} = 105.54kNm < M_{Rd} = 110.46kNm \;\; Ok$$

Similarly,

$$M_{Ed,x} = 169.61kNm < M_{Rd} = 172.81kNm \;\; Ok$$

2. Model II – with ribs
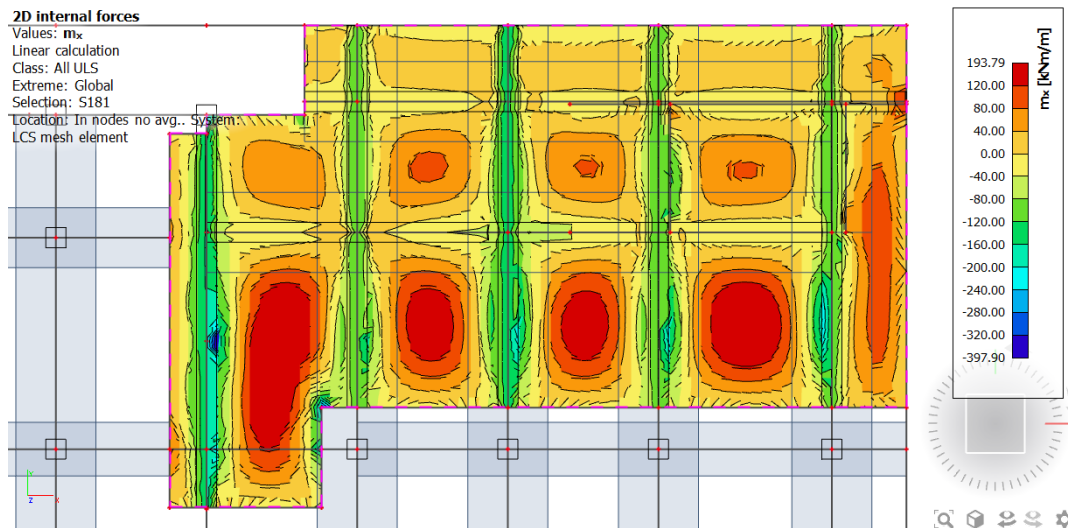
Figure 60: Display of 2D internal forces mx on right side of 1PP model with rib due to ULS

$\emptyset_x = 16mm$

$C_{nom} = 30mm$

$M_{Ed,x} = 2361.16kNm$
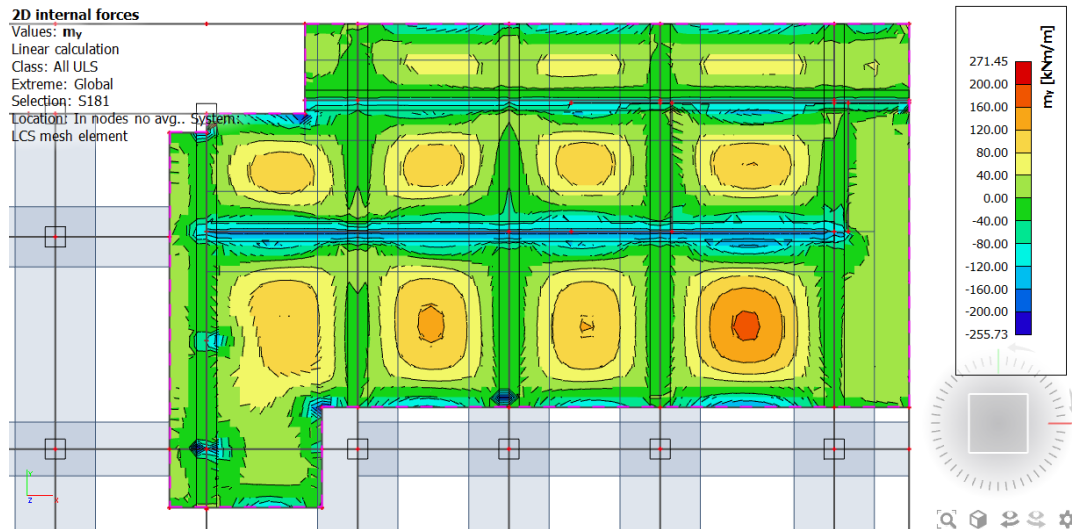
Figure 61: Display of 2D internal forces my on right side of 1PP model with rib due to ULS

Effective cross-sectional height

$$= d = h_d - c - \frac{\emptyset}{2} = 300 - 30 - \frac{16}{2} = 262mm$$

Required reinforcement area $= A_{st,req} = \frac{b.d.f_{cd}}{f_{yd}} \cdot (1 - \sqrt{1 - \frac{2.M_{Ed,support}}{b..d^2.f_{cd}}})$

$$= \frac{1000*262*23.3}{435} \cdot (1 - \sqrt{1 - \frac{2*2361.16}{1000*(262)^2*23.3}}) * 10^6 = 20717.4 \ mm^2$$

$$x = \frac{A_{s,prov}*f_{yd}}{0.8*b_T*f_{cd}} = \frac{20910.44*435}{0.8*1000*23.3} = 488mm \ ,$$

$$z = \ d - 0.4*x = 262 - (0.4*488) = 66.8mm,$$

Bearing Moment

$$M_{Rd} = \ A_{s,prov} * f_{yd} * z = 20910.44 * 435 * 66.8 * 10^{-6} = 607.61kNm$$

$$M_{Ed,x} = 2361.16kNm > M_{Rd} = 607.61kNm \ NOT \ Ok$$

Similarly,

$$M_{Ed,x} = 2178.51kNm > M_{Rd} = 607.61kNm \ NOT \ Ok$$

3. Model III – with subregion
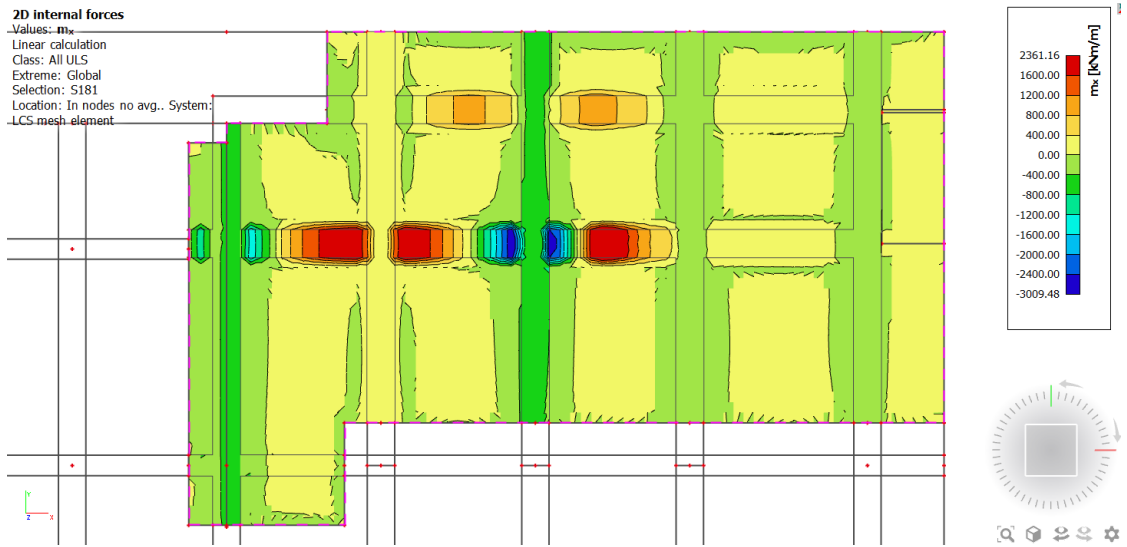
Figure 62: Display of 2D internal forces mx on right side of 1PP model with subregion due to ULS

Moment peaks show the action of the most heavily loaded part of the plate, although the moment values are smaller than when considering the rib.
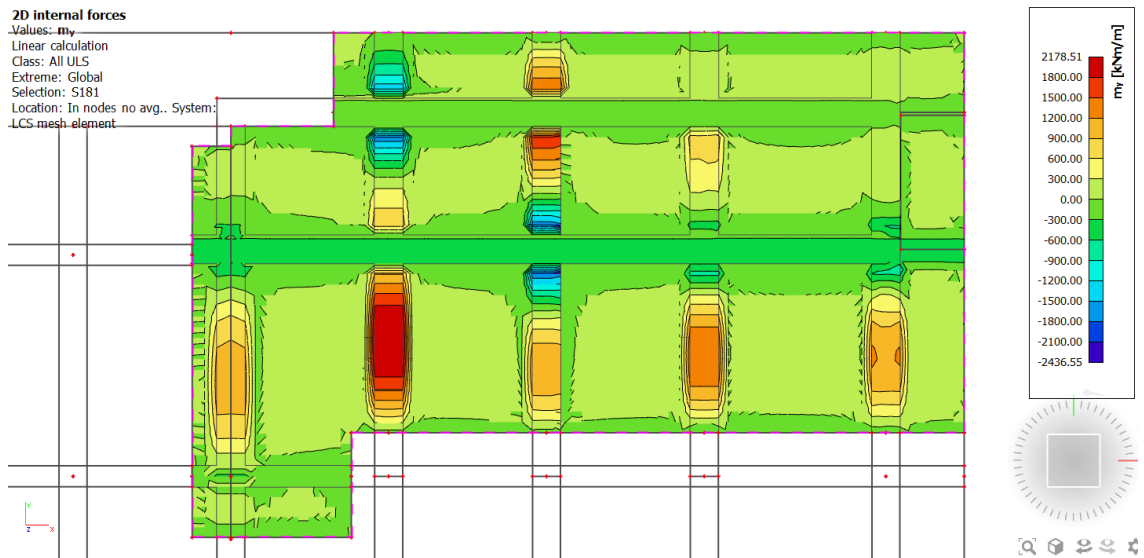
Figure 63: Display of 2D internal forces my on right side of 1PP model with subregion due to ULS

For moments in the other direction, the results also correspond, on the second beam from the left stretched vertically it is easy to see the course of the moment in the placement of the girder on girder (or die on the die).

Using the "cut on the surface" function, we displayed the course of internal forces on the plate/slab, including the transfer of the moment through the vertical wall above the through-

hole.
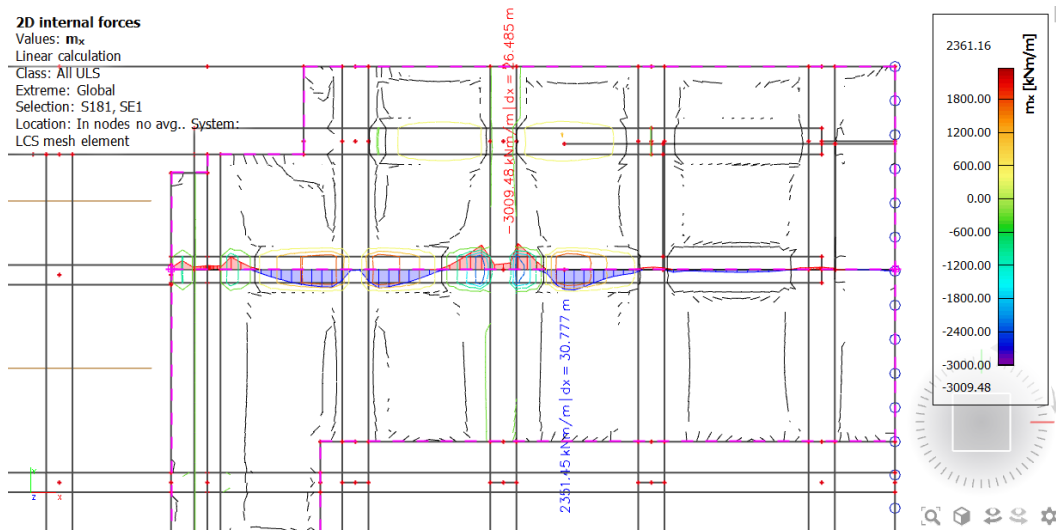
Figure 64: Display of 2D internal forces of maximum mx on right side of 1PP model with subregion due to ULS

Interacting width of the plate for the holes A2 and A3:

$$b_{eff} = \sum b_{eff,i} + b_w \leq b$$

Spacing of zero moments for a quasi-steady load combination : $l_0 = 9.057m$

The width of the beam in the left section of the plate above 1PP: $b_w = 2.0m$

The axial distance of the through-beam in the left side of the plate above 1PP: : $b = 11.3m$

$b_{1,2} = \frac{b-b_w}{2} = \frac{11.3-2}{2} = 5.55\text{m}$

$$b_{eff_{1,2}} = 0.2b_{1,2} + 0.1l_0 \leq \min(0.2l_0, b_{1,2})$$

$$b_{eff_{1,2}} = 2.02 \leq 1.81$$

$$b_{eff} = b_1 + b_2 + b_w \leq \text{b}$$

$$= 6.04 \leq 11.3$$

After calculating the interacting width of plate, we looked into the stress at the bottom of surface of the plate in the perpendicular direction to the calculated beam and we can easily

74

recognize the where compressive stress respectively zero goes. And then, we measured the specific distance of zero isolines so that we obtain the interacting width, although this was a different hole, but, we believe that our estimate explained in 4.5.1 (6 m) was justified. Therefore, we considered the interacting widths of the beam A2 and A3 as a single value as shown below:
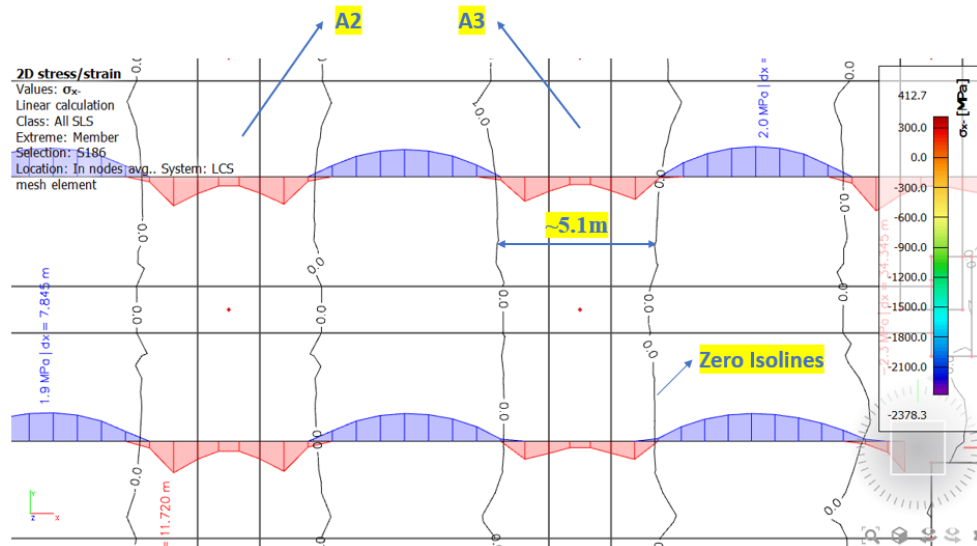
Figure 65: Display of 2D stress on A2 and A3 on right side of 1PP model with subregion due to SLS

4.5.3 Summary

The design of a structure with prestressed concrete was perhaps the main concept of this design, and from the above static simulations of a model with reinforced concrete, we could say that the reason we had to go with the alternate system, i.e., prestressed concrete. It is clear because the design of a structure with reinforced concrete was affected by its usability rather than its load-bearing capacity. Likewise, we also realized that 1PP was the most heavily loaded part of the slab with a large span and the most complex part of the dilation of A5. In Figure 43, we could see that largest displacements shown in the places where one row of columns was neglected, especially in the "southern" part of the arbor. The design of the prestress in the most heavily loaded part would be too complicated at first, so we started with the design of the prestress in the through-shafts A1–A4.

4.5.2 Model with Prestressed concrete

4.5.2.1 Preliminary Design of prestressing

Initially, we did pre-tension only on the plate beam; if it failed to check or was not suitable, we would go for further bias design in the fields of the plate, as shown in figure 63 below:
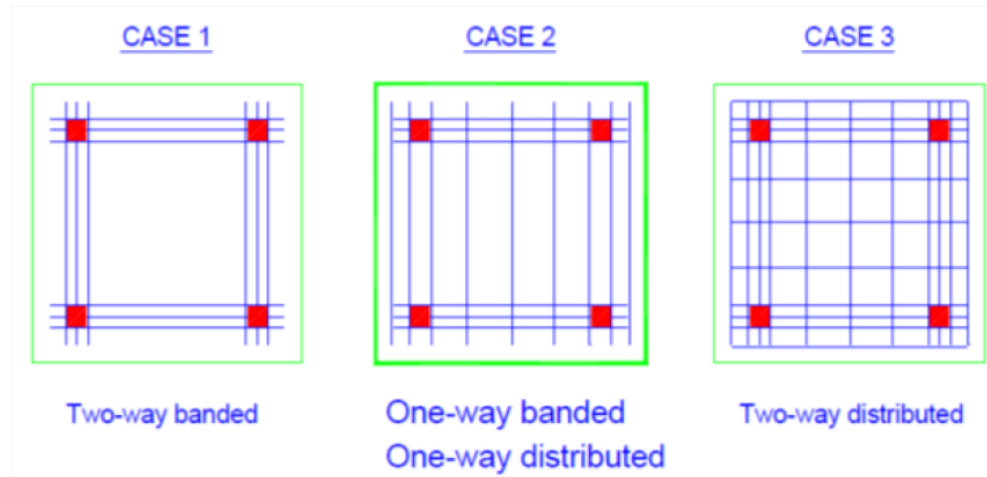
Figure 66: Types of prestressing layout

4.5.2.1.1 Material characteristics

1) Concrete

Concrete C35/45, D_{max} 16mm (See 3.1)

Characteristic compressive strength of concrete (f_{ck}) = 35MPa

Design compressive strength of concrete (f_{cd}) = $\frac{f_{ck}}{\gamma_d} = \frac{35}{1.5} = 23.33 MPa$

2) Prestressing Reinforcement

Prestressing Reinforcement : $Y1860S7 -15.7$

Nominal rope diameter: $\emptyset_p = 15.7mm$

Number of wires in one rope = 7

Characteristic tensile strength: $f_{pk} = 1860 MPa$

Modulus of elasticity: $E_p = 195\ GPa$

Cross-sectional area of one rope: $A_p = 150\ mm^2$

Yield strength: $f_{p,0.1k} = 0.88 * f_{pk} = 1636.8\ MPa$

Design stress: $f_{p,d} = \frac{f_{p,0.1k}}{\gamma_s} = \frac{1636.8}{1.15} = 1423.3\ MPa$

Maximum stress in prestressing reinforcement:

$$\sigma_{p,max} = \min\left(0.8 * f_{pk}, 0.9 * f_{p,0.1k}\right) = \min(1488,1473) = 1473 MPa$$

Maximum tension:

The tension in the prestressing reinforcement immediately after tensioning (after consideration of instantaneous losses – 5%) must not exceed value =

$$\sigma_{p,m,o} = \min(0.75 * f_{pk}, 0.85 * f_{p,0.1k}) = \min(1395, 1391.3) = 1391.3 \, MPa$$

Tension at time t = 50 years (at the end of the structure's lifetime – we consider it as long-term losses, which is 25% of the maximum prestressing force achieved during tensioning,

$$\sigma_{p,\infty} = (1 - 0.25)\sigma_{p,max} = 0.75 * 1473 = 1104.75 MPa$$

Cover of concrete layer: $C_{nom} = C_{min} + \Delta C_{dev}$

Where, allowance for design deviation = $\Delta C_{dev} = 10 \, mm$

Degree of environmental influence:

Corrosion induced by carbonation: $XC2$ (from 4.1)

Corrosion induced by chlorides: $XD1$ (from 4.1)

Construction class : S3

Minimum covering layer in terms of cohesion: $C_{min,b} = 70mm$

$$C_{min} = \max(C_{min,b}; C_{min,dur}, 10) = (70, 35, 10) = 70$$

Total cover for concrete layer = $C_{nom} = C_{min} + \Delta C_{dev} = 70 + 10 = 80mm$

4.5.3.3.3   Solved part of the slab – A2 (2000/750 & 3000/750)

For the design, initially, we chose the left side (west side) of the slab as shown in the following fig. 67, on the left side, there are four beams of size 2000/750, and at one edge, the size of the beam is 3000/750, which had been highlighted by green colour, namely A1, A2, A3, and A4. Then we calculated the values of the moments on the A1–A4 for further measurements.

Cross Section

Cross-section 2000/750

Height (h_t)= 750 mm

Width (b_t) = 2000 mm

Thickness of plate = 250mm

Effective width (b_{eff}) = 5100mm
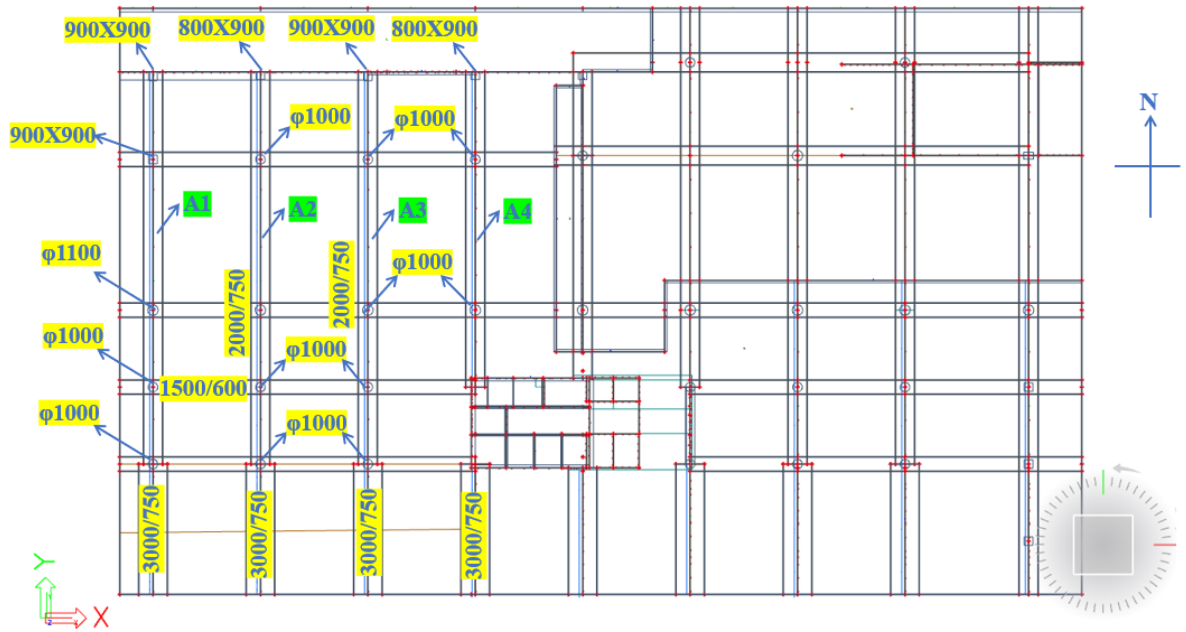
Figure 67: Schematic of a simplified drawing of the shape of the solved part of the left side of slab on 1PP

T-Section (2000/750) – in field
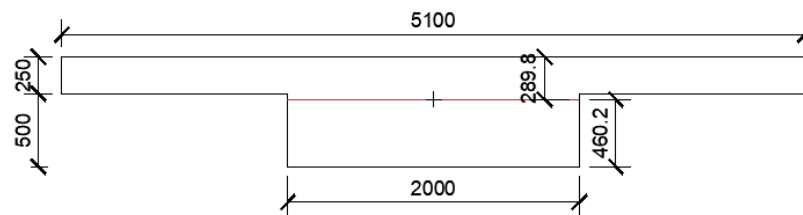
Figure 68: Cross section of 2000/750

Cross sectional area (A_c) = 2.275m²

Position of CG from upper fiber (e_h) = 289.8mm

Position of CG from bottom fiber (e_d) = 460.2mm

Moment of Inertia (I_y) = 0.106286m⁴

Section (2000/750) – above support

Cross sectional area (A_c) = 1.5m²

Position of CG from upper and lower fiber ($e_h = e_d$) = 375mm

Moment of Inertia (I_y) = 0.0703125m⁴

2) Cross-section 3000/750

Height (h_t)= 750 mm

Width (b_t) = 3000 mm

Thickness of plate = 250mm

Effective width (b_{eff}) = 5100mm

T-Section (3000/750) – in field
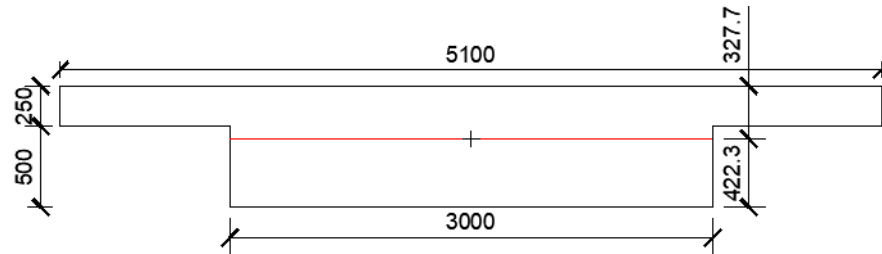
Figure 69: Cross section of 3000/750

Cross sectional area (A_c) = 2.775m^2

Position of CG from upper fiber (e_h) = 327.7mm

Position of CG from bottom fiber (e_d) = 423.3mm

Moment of Inertia (I_y) = 0.134808m^4

Section (3000/750) – above support

Cross sectional area (A_c) = 2.25m^2

Position of CG from upper and lower fiber ($e_h = e_d$) = 375mm

Moment of Inertia (I_y) = 0.10546875m^4

Internal forces:

For the design, we used the values from the quasi-permanent combination for the bending moment of internal forces in the model with ribs. The values of the moments on the A1-A4 was almost similar, and hence we chose A2 for further calculations. From the figure 70, it can be see that the most heavily loaded beam A2 has a moment of 2000/750 of 1316.13 kNm in the field and 1987.13 kNm above the support, and a moment of 3000/750 was 1901.42 kNm in the field and 2020.08 kNm above the support.

1D internal forces
Values: M_y
Linear calculation
Combination: SLS-Quasi2
Coordinate system: Principal
Extreme 1D: Member
Selection: B1023..B1030
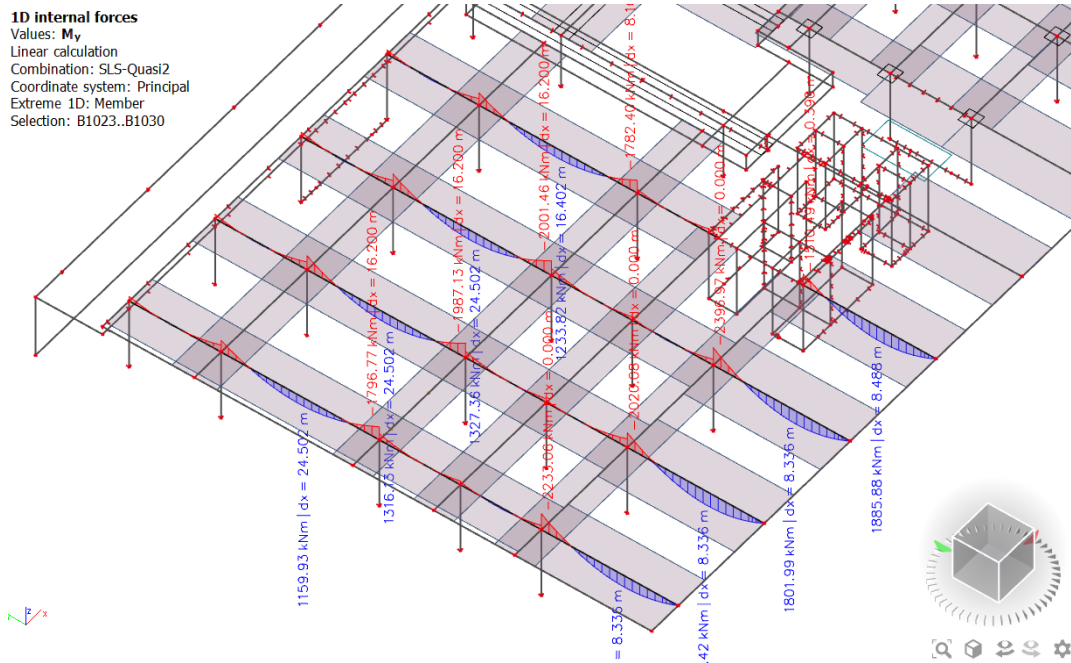
Figure 70: Display of internal forces My on left side of 1PP due to SLS

Selection of anchors & cable for prestressing system:

For prestressing design, we used a multi-cable system with circular cross-section anchors. We chose the anchors with 9 strand from the manual of freyssinet pre-switching system [21] that was 9C15 as shown in fig.68, Where, A=225mm, B=185mm, C=260mm, D=150mm, H=56mm, and outer diameter = 70mm (page 7 of manual 21)

Figure 71: Manual of freyssinet pre-switching system showing different sizes of tendons, page7

Eccentricity:

Eccentricity is a critical value for preload design. In the places of the greatest bending moment, the maximum eccentricity with respect to the center of gravity of the cross-section must be designed to guarantee the maximum effectiveness of the prestressing. In the field, the channel with the cables was near to the lower fibers, and above the support was near to the upper fibers. We assumed that cover of 80 mm and a channel diameter of 70 mm then the center of gravity of the reinforcement is far from the upper/lower fibers:

$$d_{1,2} = \frac{\emptyset_k}{2} + c_{nom} = \frac{70}{2} + 80 = 115mm$$

$$e_{p,n} = e_t - c - \frac{\emptyset_d}{2} = e_{h/d} - d_{1,2}$$

Over 2000/750 & 3000/750

Maximum eccentricity from the centre of gravity above the support:

$$e_{p,max,h} = e_t - c - \frac{\emptyset_d}{2} = e_d - d_{1,2} = 375 - 115 = 260 \ mm$$

Maximum eccentricity from the centre of gravity above the field:

$$e_{p,max,d} = e_t - c - \frac{\emptyset_d}{2} = e_h - d_{1,2} = 460.2 - 115 = 345.2 \ mm$$

A2- SLS Quasi My		
Moment		Position of Prestressing Force (ep,n)
$M_{Ed,0}$	-629.19	0
$M_{Ed,1}$	123.03	0
$M_{Ed,2}$	-1942.92	260
$M_{Ed,3}$	1316.13	345.2
$M_{Ed,4}$	-1987.13	260
$M_{Ed,5}$	25.34	0
$M_{Ed,6}$	-549.47	0
$M_{Ed,7}$	52.69	0
$M_{Ed,8}$	-2020.08	260
$M_{Ed,9}$	1901.42	307
$M_{Ed,10}$	12.34	0

Table 4: Position of prestressing forces for A2 due to SLS Quasi

Routing of cable or arrangement of tendons:

In the specific design of the cable route, we first calculated the course of bending moments from a quasi-permanent combination of loads on the beam (without preload). Due to the nature of creating the model with ribs, we took the values of internal forces from the model

with ribs.

We proposed the maximum eccentricity in the locations of the greatest bending moments (in the fields with the maximum spans), as shown in the figure below. In other cases, we preloaded the center of gravity as a result there was no danger of tensile stresses in the cross-section.
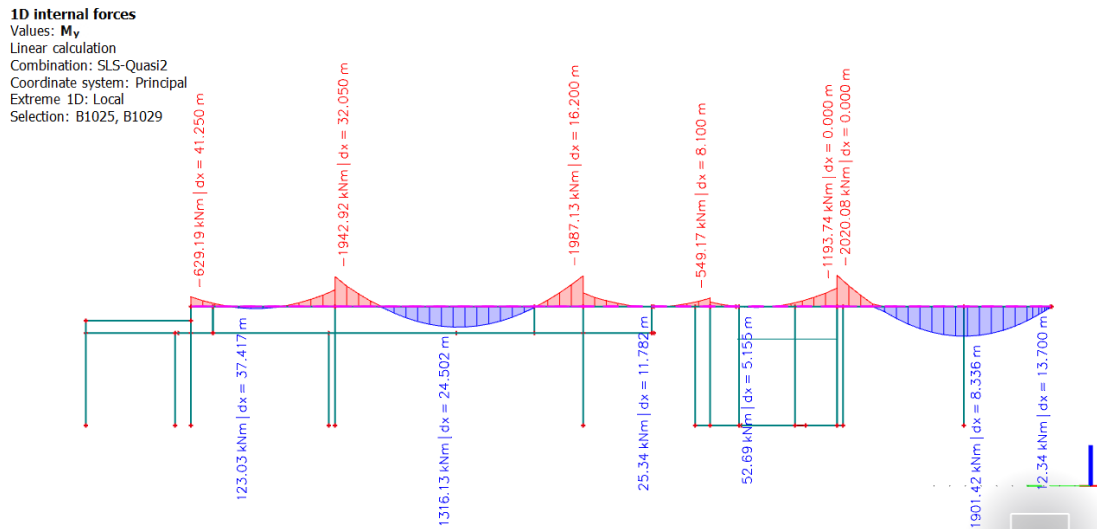
Figure 72: Bending moments My from a quasi-steady load combination without prestressing on the holes in the left tract of the slab

The arrangement of the prestressing tendon along the structure could be designed based on the principle shown in the following fig. 73. The ideal parabolic form of the tendon is approximated using straight lines and circular arcs to simplify the computation. In the first step, a polygon was chosen according to the figures, and then arcs were added. The original polygons were tangents of the arcs.
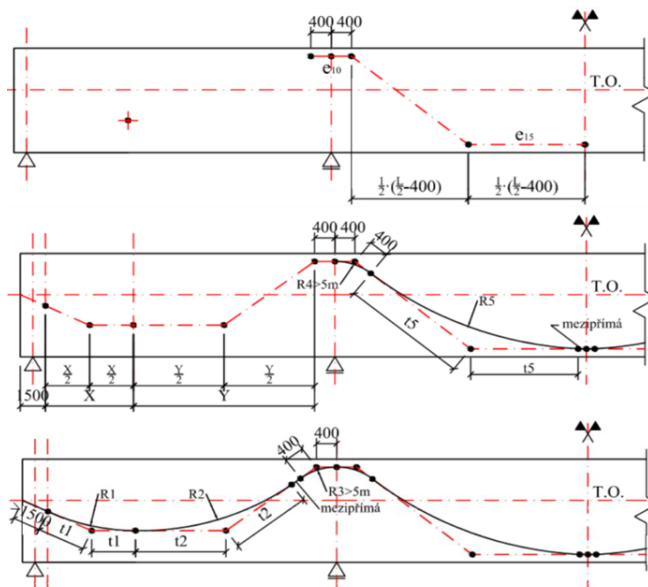
Figure 73: Designed principle for arrangement of tendons [13]

Using this principle, we had created this following arrangement as shown below in the figure:

Figure 74: Arrangement of tendon/cable

Design of prestressing force (2000/750)

First, we used the Balancing Stress Method to create the design, with the resulting tension at the top and bottom fibers equal to zero. We designed the prestressing throughout the length of the beam, and because the beam's width increased, we placed extra anchors (1 anchor from each side) at the point of cross-section change.

Because the eccentricity at sections 0 and 1 was zero, we proceeded to sections 3 and 4 to determine the prestressing force.

Therefore,

Tension at lower fiber:

$$\sigma_{c,d} = \frac{-N_p}{A_c} + \frac{M_{Ed}}{I_y} * e_d + \frac{M_p}{I_y} * e_d = 0$$

Tension at upper fiber:

$$\sigma_{c,h} = \frac{-N_p}{A_c} + \frac{M_{Ed}}{I_y} * e_h + \frac{M_p}{I_y} * e_h = 0$$

Where, $M_p = N_p * e_p + \Delta M_p \ (N_p = N)$

The relationship for lower fiber was then used to design preclamping.

By solving, prestressing force:

$$N_p = P = \frac{M_{Ed}*e_d*A_c}{I_y+(A_c*e_d*e_p)} \ \& \ N_p = P = \frac{M_{Ed}*e_h*A_c}{I_y+(A_c*e_h*e_p)}$$

So, Prestressing force in 3:

$$P_{3,req} = \frac{M_{Ed,3} * e_d * A_c}{I_y + \left(A_c * e_d * e_{p,3,max}\right)} = \frac{1316.13 * 0.4602 * 2.275}{0.106286 + (2.275 * 0.4602 * 0.3452)}$$

$$= 2946.21 kN$$

Prestressing force in 4:

$$P_{4,req} = \frac{M_{Ed,4} * e_h * A_c}{I_y + \left(A_c * e_h * e_{p,4,max}\right)} = \frac{(-1987.13) * (-0.375) * 1.5}{0.0703125 + (1.5 * (-0.375) * (-0.260))}$$

$$= 5161.38 kN$$

Now,

Required reinforcement area $= A_{p,i,req} = \frac{P_{i,req}}{\sigma_{p,\infty}}$

Required area in 3:

$$A_{p,3,req} = \frac{2946.21 * 10^3}{1104.75} = 2666.86 \ mm^2$$

Required area in 4:

$$A_{p,4,req} = \frac{5161.38 * 10^3}{1104.75} = 4671.99 \ mm^2$$

Required number of ropes : $n_{p,i,req} = \frac{A_{i,req}}{A_p}$

$$n_{p,3,req} = \frac{2666.86}{150} = \ 17.78 \sim 18 no.$$

$$n_{p,4,req} = \frac{4671.99}{150} = 31.15 \sim 32no.$$

Due to the cross-section of the beam at the point of prestressing, it was necessary to determine the number of anchors that we would be able to use so that their minimum axial distance was observed. Since we had neglected the indeterminate moment from the prestress, so we would propose a larger number of ropes.

For a cross-section of 2000/750 mm, we will propose 5 nine-strand cables:

$$\frac{n_{p,max,1}}{5} = \frac{32}{5} = 6.4 \sim 9 \, no.$$

$$n_{p,prov,1} = 5 * 9 = 45 \geq n_{p,max,1} \, (= 32)$$

$$A_{p,prov,1} = 45 * A_p = 45 * 150 = 6750mm^2$$

So, design 5 cables from 9 ropes along the entire length of the duct.

The eccentricity at the point No. 3 is too large, we need to reduce it so that the effects of preload are not extreme and we did this after the design so that the structure is not unnecessarily overworked. Moreover, in sections 2 and 4, the cables will be routed with maximum eccentricity.

We know that,

$$P = \frac{M_{Ed} * e_d * A_c}{I_y + (A_c * e_d * e_p)}$$

$$P_{3,req} = \frac{M_{Ed,3} * e_d * A_c}{I_y + (A_c * e_d * e_3)}$$

By rearranging the terms, we get

$$e_3 = \frac{-I_y}{e_d * A_c} + \frac{M_{Ed,3}}{P_{3,req}}$$

To calculate prestressing force at 3 instead of using numbers of ropes the we calculated in the

beginning of design of prestressing force at 3, we used the $n_{p,prov,1} = 45$, to adjust the eccentricity.

$$P_{3,req,2} = 45 * A_p * \sigma_{p,\infty} = 45 * 150 * 1104.75 * 10^{-3} = 7457.1 kN$$

$$e_3 = \frac{-0.106286}{0.4602 * 2.275} + \frac{1316.13}{7457.1} = 0.074975 m = 74.98 mm \sim 100 mm (Say)$$

Verification of minimum axial distances between anchors:
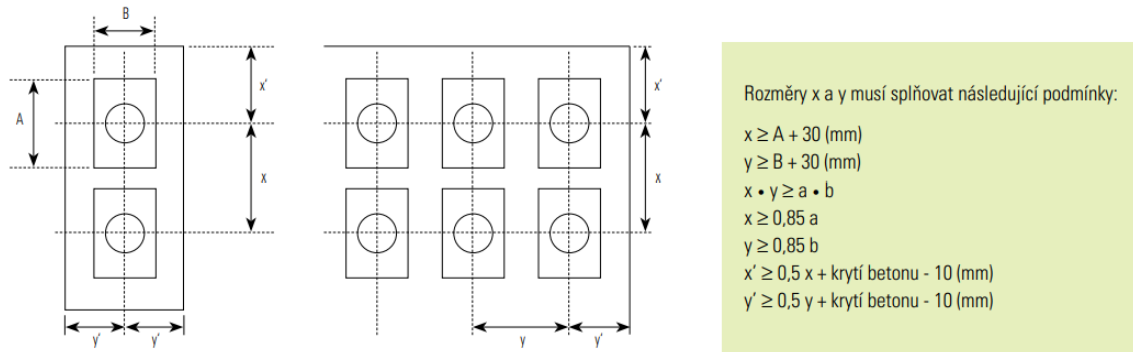
Figure 75: Verification of minimum axial distance between anchors [page10 of 21]

In our case, anchors are distributed in one direction, so

$$x \geq A + 30 \geq 225 + 30 \geq 255$$

$$x' \geq 0.5x + C_{nom} - 10 \geq (0.5 * 350) + 80 - 10 \geq 245 mm$$

Where, x,y = minimum axial distance between two anchors in the structure in the x & y direction

x', y' = min. edge distance between the edge of the spreading pad and nearest outer edge of the structure in x & y direction

x = 350mm

x'= 300mm
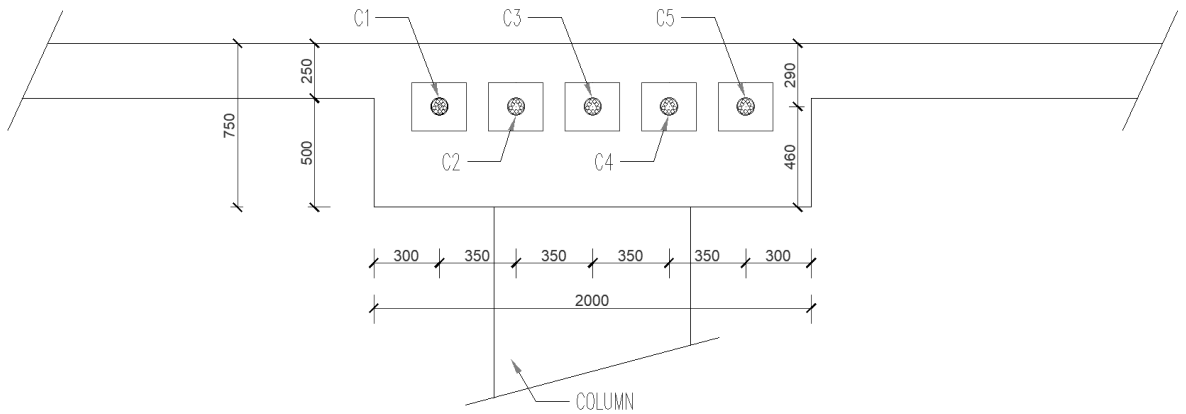
Figure 76: Section of beam 2000/750 showing the position of anchors

Since we had neglected the indeterminate moment from the prestress, so we were propose a larger number of ropes.

For a cross-section of 2000/750 mm, we proposed 5 nine-strand cables:

$$\frac{n_{p,max,1}}{5} = \frac{32}{5} = 6.4 \sim 9 \; no.$$

$$n_{p,prov,1} = 5 * 9 = 45 \geq n_{p,max,1} \; (= 32)$$

$$A_{p,prov,1} = 45 * A_p = 45 * 150 = 6750 mm^2$$

So, design 5 cables from 9 ropes along the entire length of the duct.
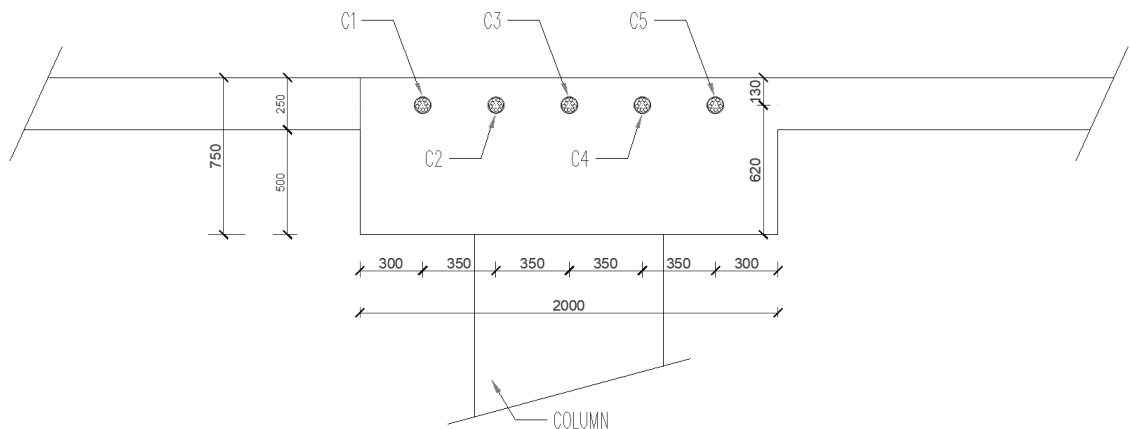
Figure 77: Section of beam 2000/750 showing the position of anchors

Design of prestressing force (3000/750)

Due to the increase in bending moments in the last field of beam (3000/750) and beam has large width so we could use two additional cables for designing to meet the tension requirement $\sigma_c \leq 0$

So, Prestressing force in section 8:

$$P_{8,req} = \frac{M_{Ed,8} * e_h * A_c}{I_y + \left(A_c * e_h * e_{p,8,max}\right)} = \frac{(-2020.08) * (-0.375) * 2.25}{0.105468 + (2.25 * (-0.375) * (-0.260))}$$

$$= 5246.97 kN$$

Prestressing force in 9:

$$P_{9,req} = \frac{M_{Ed,9} * e_d * A_c}{I_y + \left(A_c * e_d * e_{p,9,max}\right)} = \frac{1901.42 * (0.4223) * 2.775}{0.134808 + (2.775 * 0.4223 * 0.3073)}$$

$$= 4502.16 kN$$

Now,

Required reinforcement area $= A_{p,i,req} = \frac{P_{i,req}}{\sigma_{p,\infty}}$

Required area in 8:

$$A_{p,8,req} = \frac{5246.97 * 10^3}{1104.75} = 4749.46 \; mm^2$$

Required area in 9:

$$A_{p,9,req} = \frac{4502.16 * 10^3}{1104.75} = 4075.27 \; mm^2$$

Required number of ropes : $n_{p,i,req} = \frac{A_{i,req}}{A_p}$

$$n_{p,8,req} = \frac{4749.46}{150} = 45.4 \sim 45no.$$

$$n_{p,9,req} = \frac{4075.27}{150} = 27.168 \sim 28no.$$

But, if we look into the eccentricity at section 9, we realized that eccentricity at 9 was again large, so we need to modify the eccentricity by the using the same approach that we used in the section 3.

For a cross-section of 3000/750 mm, we proposed 5 nine-strand and 2 four-strand cables:

$$\frac{n_{p,max,2} - n_{p,prov,1}}{2} = \frac{45.4 - 45}{2} = 0.2 \sim 4 \; no.$$

$$n_{p,prov,2} = 4 * 2 = 8 \geq n_{p,max,2} - n_{p,prov,1} \; (= 0.2)$$

$$A_{p,prov,2} = 8 * A_p = 8 * 150 = 1200 mm^2$$

So, design add 2 cables from 4 ropes in the last field.
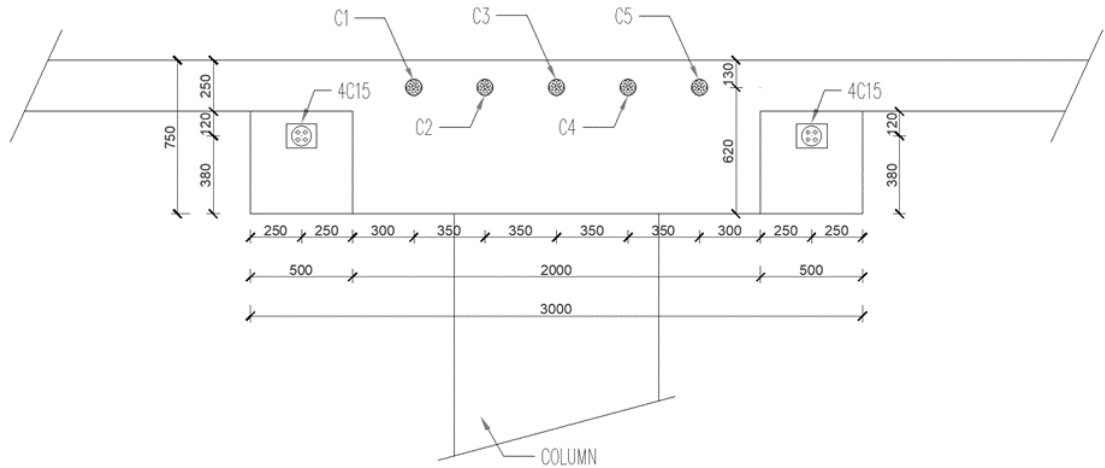
Figure 78: Section of beam showing the axial distances between additional anchors

The eccentricity at the point No. 9:

We know that,

$$P = \frac{M_{Ed} * e_d * A_c}{I_y + (A_c * e_d * e_p)}$$

$$P_{9,req} = \frac{M_{Ed,9} * e_d * A_c}{I_y + (A_c * e_d * e_9)}$$

By rearranging the terms, we get

$$e_9 = \frac{-I_y}{e_d * A_c} + \frac{M_{Ed,9}}{P_{9,req}}$$

We get, $e_9 \cong 200 \; mm \; (say)$

Summary

Due to the similar pattern of the internal forces on beams A1 to A4, it can be said that we can use the same design that we did for beam A2 for all other beams. Also, we would propose a

preload for the entire left tract of the plate in the y direction. Also, in sections 2, 4, and 8, the cables were routed with maximum eccentricity, but in sections 3 and 9, the eccentricity was reduced so that the effects of prestressing were not extreme.

4.5.2.1 Assigning the preload into Scia software

To begin, we needed to assign the prestressing cable to the beam rather than the flat part (because we created the model with subregion), so we first created fictitious (imaginary) ribs of 1x1 mm cross section with unit mass of 0.1 kg/m3 so that these fictive ribs do not affect the global stiffness matrix of the structure, and we could then apply additional prestressed cable with cohesion to it.

Fictive ribs of 1x1 mm
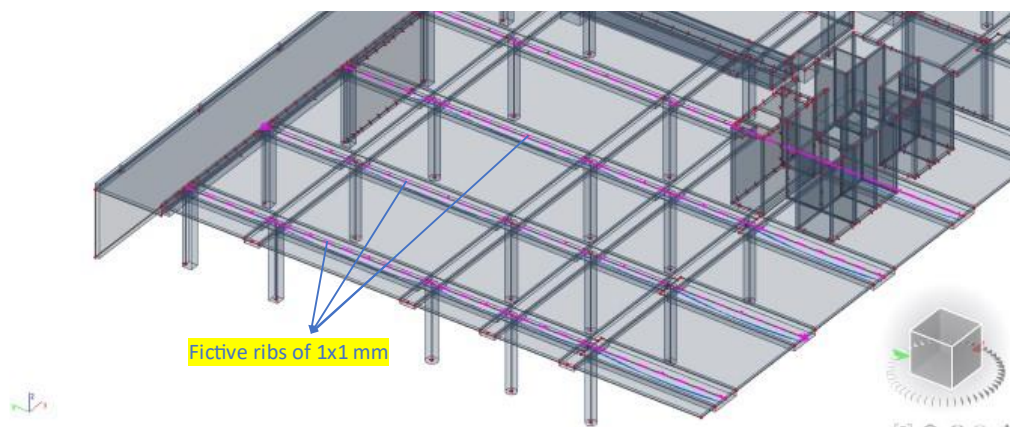
Figure 79: Assigning of the fictive ribs

Moreover, during the assessment of the prestressed ceiling structure, we were mainly interested in the stress at the upper and lower fibers, and the model with ribs does not render the stress as we would need it, so this was also one of the reasons we chose the model with subregion. To display the internal forces on the beams, it was more appropriate to use the model with ribs (see above sample model); therefore, we entered it in the model with ribs as well.

4.5.2.2 Modelling or construction of prestressing cable for A1-A4

For the construction of the tendons, it was very important to know the source geometry (as shown in the following fig.80) so that we could place the tendons in proper position. So, first, we created the source geometry using the values of the eccentricities that we calculated previously, as shown in Fig. 76, and also created an additional route of cable for Beam 3000/750 (Fig. 77).
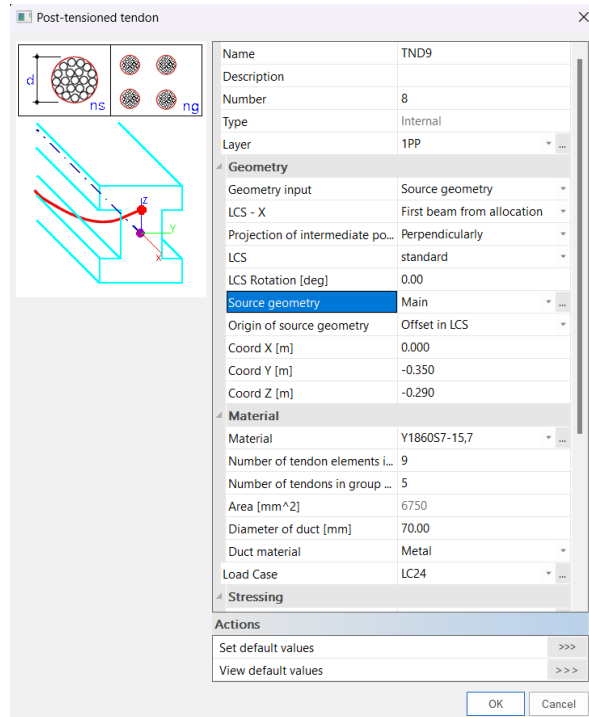
Figure 80: Assigning the source geometry

It is essential to enter the position of the cable in the decisive cross-sections. We will therefore choose the geometry according to the preliminary design of the preload. The cable geometry can be specified in different ways with different parameters. To begin with, we leave the default values of the program, i.e.: Curve type: circle + radius; Curve parameter: 0.8 m, as shown in following fig.81.
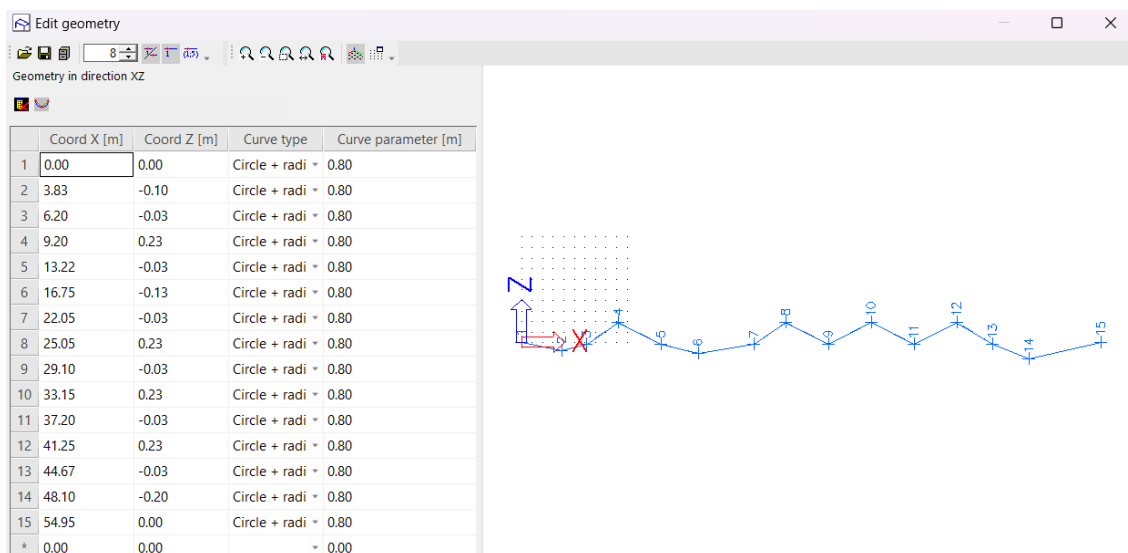
Figure 81: Geometry of the tendons for entire beam in y-direction on left side of 1PP
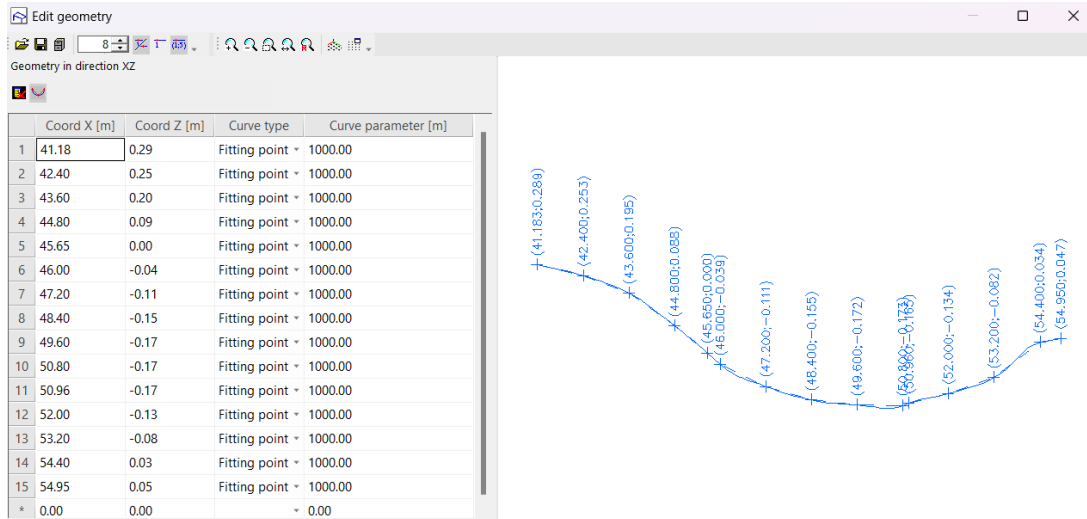
Figure 82: Geometry of the tendons with fitting type curve for beam 3000/750 in y-direction on left side of 1PP

For a significantly better effect, we will choose a smoother route (fig.82), For easier input, by selecting lay the cable points - "fitting type", where we leave the coordinates of the cable from the previous design and the cable in the software will pass through these points, as the name suggests[32, p. 91] This fact has a very positive effect on the course of tension in the decisive fibers of the cross-section.

Verification of the minimum radius of curvature of the cable:

Regarding the radius of curvature of the cable, it is necessary to observe the minimum possible radius. The minimum possible radius of curvature depends on the internal diameter of the cable channel. [32, p. 27] We consider the internal diameter of the cable channel to be $Øk,2 = 80$ mm
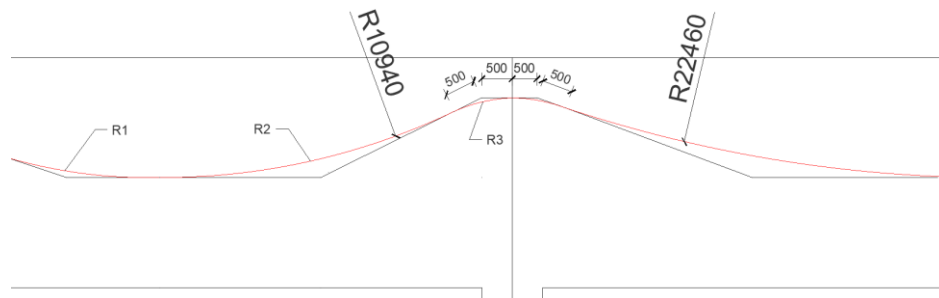
Figure 83: Part of the cable route at ten times the elevation scale with the radii of curvature marked

We measured the cable route from the software and measured the smallest radius used as shown above.

Check: Smallest used radius $= \mathrm{R} \geq R_{min}(= 100 * Ø_{k,2})$

$$R2 = 10940mm > (100 * 80 = 8000mm)$$

$$R4 = 22460mm > (100 * 80 = 8000mm)$$

Moreover, we then entered the designed preload for the through-holes A1–A4, as shown in following figure 84, it shows that the through-holes with pre-tensioning cables (blue), anchors and tensioning directions (black). We analyzed the structure at time t_0 (immediately after tensioning) and at time t_∞ (at the end of the service life).
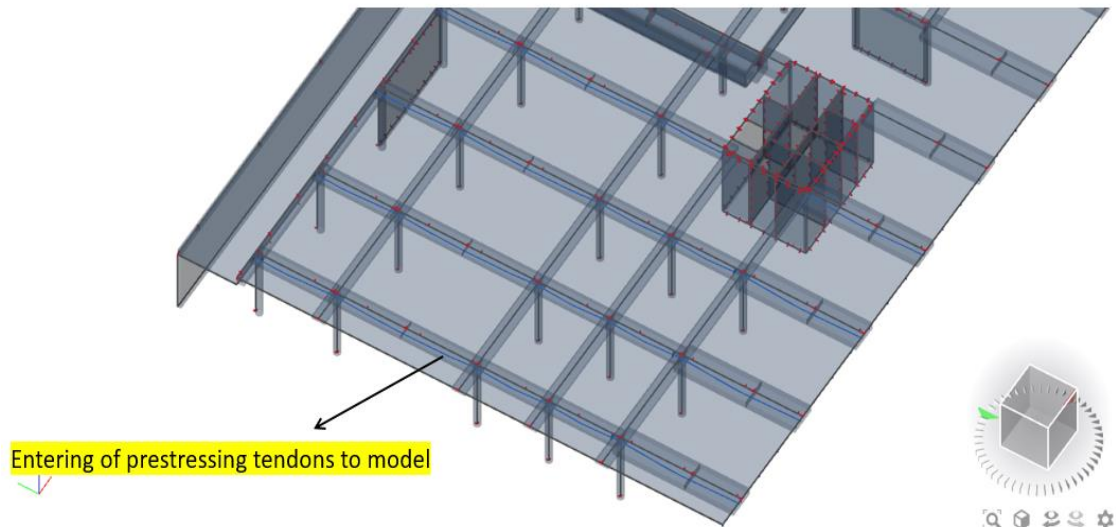
Figure 84: Entering of tendons to model on left side of 1PP

4.5.2.2 Displacement due to tendons on 1PP

If we compared this displacement with displacement without tendons then we could say that there was a rapid decline in the results.
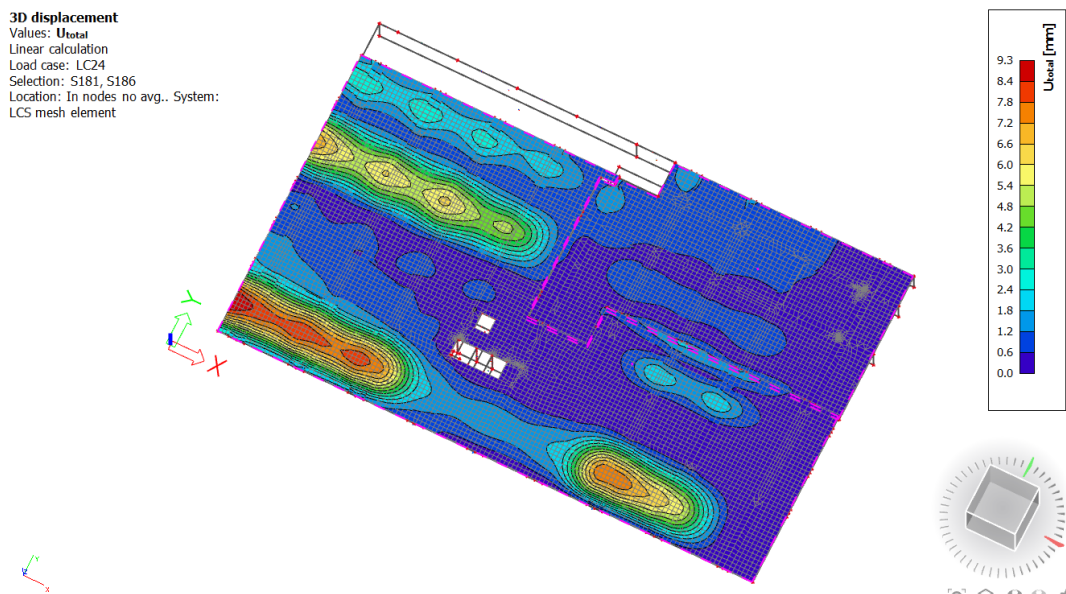
Figure 85: 3D displacement on 1PP due to prestressed tendons

Displacement due to SLS:
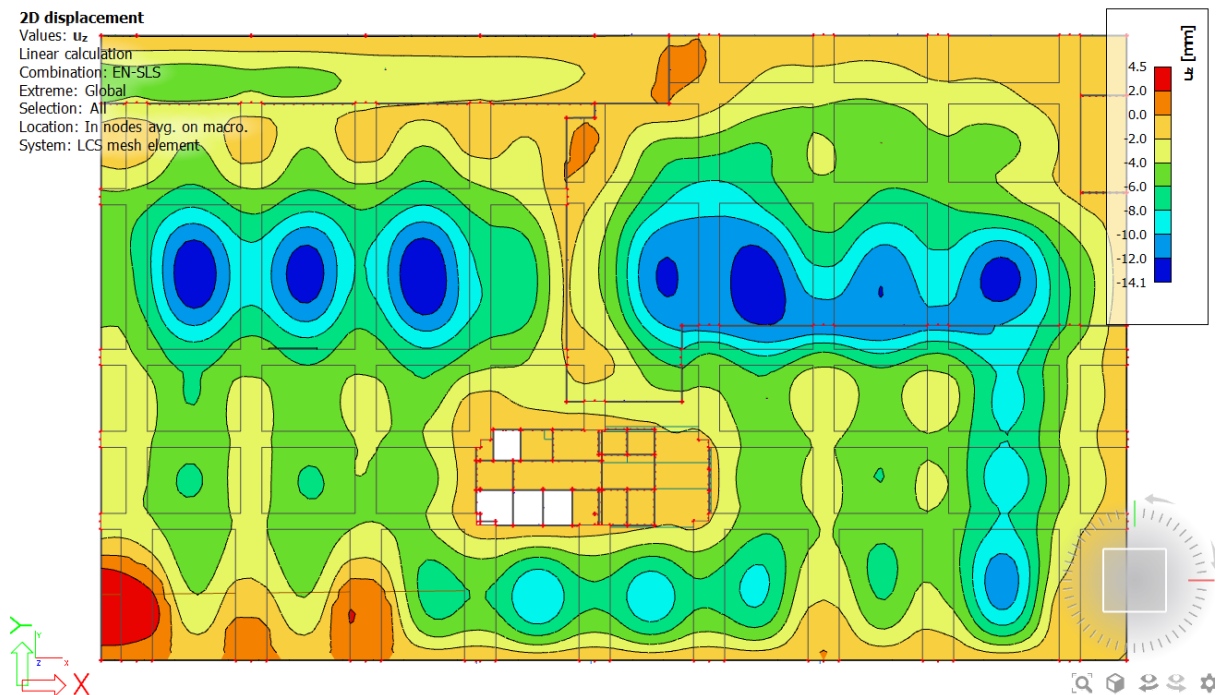
Figure 86: Display of 2D displacement on 1PP due to prestressed tendons

4.5.2.3 Calculation with short-term losses (Verification of the condition of maximum prestressing stress)

We evaluated the beam momentarily during short-term action—tensioning the prestressing reinforcement. The key difference between the short-term and long-term assessments was the tensile stress, which was not covered by long-term losses and was thus much greater. Because of this distinction, we will not be concerned with the critical cross-sections with the highest tensile stresses this time.

Let us assume the prestressing stress $\sigma_p = 1440 MPa$. It is necessary to check whether the tension in the cables after instantaneous losses does not exceed the value $\sigma_p, m, o = 1391.3 MPa$ (from 4.5.2.1.1(2)). If this value gets exceeded, it is necessary to proceed to reduce the tensioning stress. After considering the short-term losses calculated by the software, the maximum stress in the cables was $\sigma_{p,m,o,prov} = 1387.41 MPa$ for cables running along the entire length of the beam and for shorter cables running only in the last field was $\sigma_{p,m,o,prov} = 1359.13 MPa$, which is way below assumed the prestressing value

94
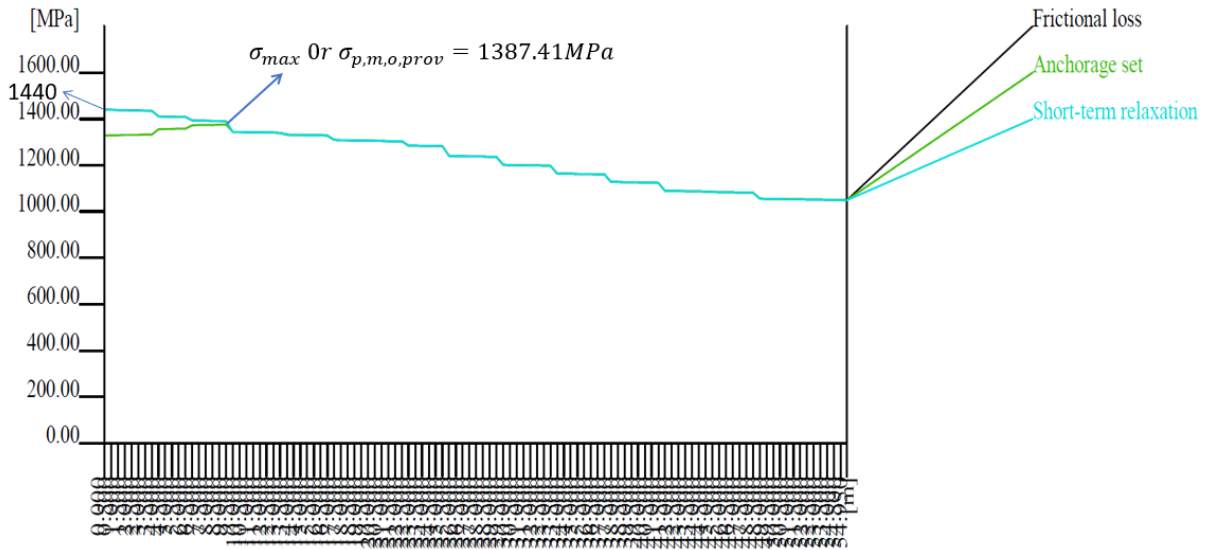
Figure 87: Graph of prestressing short term losses on a cable running along the entire length of a beam

4.5.2.4 Calculation with long-term losses (Verification of the condition of maximum prestressing stress)

Preload losses are generally understood as the reduction of stress in preload cables. In chapter 3, we described the losses and divided them into two categories – immediate and long-term. Immediate losses (friction, slippage in the anchor, etc) were calculated for us by the software (as shown in above figure), long-term losses (mainly creep and shrinkage of concrete) can be estimated at 20% of the applied preload. So we will estimate the losses and artificially reduce the tension stress in the software.

We will thus consider the condition of the structure at the end of its useful life (t = 50 years) and will be able to assess it. Tensile stress reduction to consider long-term losses: σ,
So we write this value in the "Initial stress" column.

Tension reduction to consider long-term losses:
$$\sigma_{p,\infty} = (1 - 0.20) * \sigma_p = 0.8 * 1440 = 1152 \; MPa$$
So we write this value in the "Initial stress".
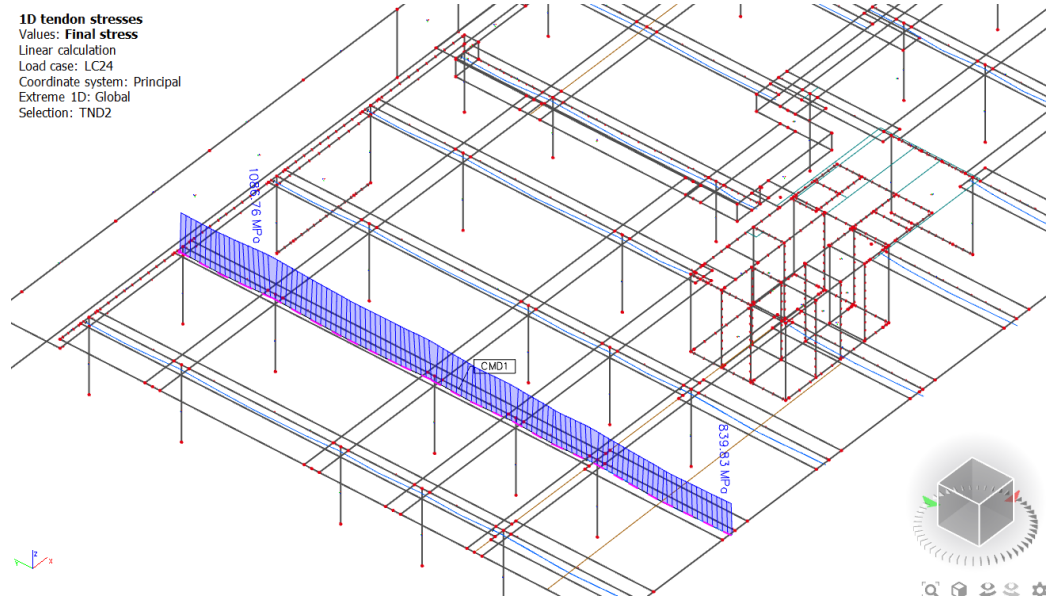
Figure 88: Display of stresses due to prestress on A2 of 1PP

Manual calculation of prestressing losses:

Choose from manufacturer's information, how many tendons shall be used and how many cables will be included at each tendon.

n_1 =	5	pcs	number of tendons
n_2 =	13	pcs	number of cables at each tendon
n =	65	pcs	total number of cables provided
A_p =	9750	mm²	total cross sectional area of prestressing reinforcement provided
σ_p =	1440	MPa	prestressing stress, must be set as less or equal to $\sigma_{p,max}$

Losses of prestressing

Friction *Due to friction in the curved parts at the path of the prestressing reinforcement, a loss of prestressing due to friction has to be considered. The calculation is based on the angular change in the path of the prestressing and friction coefficient. Additional friction due to duct wobble is considered in the straight parts as well.*

Angles can be measured or calculated as shown in the example.

$$\Delta\sigma_{p,1} = -\sigma_{P,max} \cdot \left(1 - e^{-\mu \cdot (\alpha + k \cdot l)}\right)$$

where μ... friction coefficient in curved part
α... central angle of circular arc in particular interval
k... friction coeficient in straight part (related to 1m of length)
l... length of particular interval
$\mu = 0.19$ (for metal duct)
$k = 0.01\ m^{-1}$

α_1 =	0.06527 rad
α_2 =	0.10097 rad
α_3 =	0.10097 rad
α_4 =	0.11835 rad
α_5 =	0.11835 rad

	cable length	angle	loss	stress after losses
section 5	3.83 m	0.06527 rad	-28.705137 MPa	1411.3 MPa
section 10	9.2 m	0.26721 rad	-97.1861 MPa	1342.8 MPa
section 15	16.75 m	0.50391 rad	-176.43021 MPa	1263.6 MPa

Relaxation of prestressing reinforcement

Metal reinforcement bars have "the ability to relax" when elongated. This means, that the stress in the tendon decreases over time even though their elongation was not reduced.

$$\Delta\sigma_{p,r} = -\overline{\sigma_{p0}} \cdot 0.66 \cdot 2.5 \cdot e^{9.1 \cdot \mu} \cdot \left(\frac{t}{1000}\right)^{0.75 \cdot (1-\mu)} \cdot 10^{-5}$$

where t is the time after prestressing *[hours]*

100 days	stress after short term losses		μ	loss	stress after losses
section 5	1411.295	MPa	0.75876068	-27.2004 MPa	1384.1 MPa
section 10	1342.814	MPa	0.72194296	-18.9656 MPa	1323.8 MPa
section 15	1263.57	MPa	0.6793386	-12.4544 MPa	1251.1 MPa

end of service life	stress after short term losses		μ	loss	stress after losses
section 5	1411.295	MPa	0.75876068	-71.4674 MPa	1339.8 MPa
section 10	1342.814	MPa	0.72194296	-57.7466 MPa	1285.1 MPa
section 15	1263.57	MPa	0.6793386	-44.9754 MPa	1218.6 MPa

Concrete creep

"Concrete creep" is the term describing long term strain change with constant stress applied. It is a physical effect that cannot be dismissed. There are various mathematical models that can be used to estimate the long term effect. The amount of creep generally depends on concrete composition, concrete age at loading and conditions of the surrounding environment. The simplified method of calculating creep strain in concrete is described in Eurocode 2 (BS EN 1992-1-1 annex B).

inputs:

RH =	50	%	relative humidity (usually 30-50% for indoor spaces, 70-90 for outdoor environment)
u =	5.5	m	perimeter of the member in contact with atmosphere
h_0 =	290.91	mm	notional size of the member
t_0 =	14	days	age of concrete at loading at days

coefficients:

α_1 =	1.3282	coefficient for concrete strength
α_2 =	1.0845	coefficient for concrete strength
α_3 =	1.1293	coefficient for concrete strength
β_H =	718.7447	coefficient for humidity and member size
$\beta(f_{cm})$ =	3.4779	coefficient for concrete strength
$\beta(t_0)$ =	0.5570	coefficient for concrete age at loading
ϕ_{RH} =	2.1714	coefficient for humidity
ϕ_0 =	4.2067	notional creep coefficient

time	$\beta_c(t,t_0)$	$\phi(t,t_0)$
at 100 days	0.511	2.151
at the end of service life	0.994	4.182

Loss of prestress due to creep

$$\Delta\sigma_{Pc} = -\frac{E_p}{E_c(\tau)} \cdot \sigma_{cP}^{g+P} \cdot \varphi(t;\tau)$$

for simplicity full value of E_{cm} can be considered instead of $E_c(\tau)$

100 days	stress after previous losses	stress in concrete in place of prestressing(Mpa)	loss due to creep
section 5	0.0	0.000	0
section 10	0.0	-14.342	-182.2795243
section 15	0.0	12.899	163.937835

end of service life	stress after previous losses	stress in concrete in place of prestressing	loss due to creep(Mpa)
section 5	1339.8	-16.329	-403.5389554
section 10	1285.1	-54.052	-1335.76972
section 15	1218.6	-42.150	-1041.642559

Concrete shrinkage

The simplified method of calculating drying shrinkage in concrete is described in Eurocode 2 (BS EN 1992-1-1 cl. 3.1.4 and Annex B).

α_{ds1} =	6	for cement type R (assumption)
α_{ds2} =	0.11	for cement type R (assumption)
β_{RH} =	1.35625	coefficient for humidity
$\varepsilon_{cd,0}$ =	0.000785	basic drying shrinkage strain
k_h =	0.7	approximate value (may be interpolated from table 3.3 in BS EN 1992-1-1)
t_s =	3	days curing of concrete
$\varepsilon_{ca,inf}$ =	0.000063	autogeneous shrinkage final value

	$\beta_{as}(t)$	$\varepsilon_{ca}(t)$	$\beta_{ds}(t,t_s)$	$\varepsilon_{cd}(t)$	$\varepsilon_{cs}(t)$	loss due to shrinkage
100 days	0.865	0.000054	0.328289981	0.000258	0.000312	-60.77984133
end of service life	1.000	0.000063	0.994591417	0.000781	0.000843	-164.4005018

Prestressing losses summary

		stress in reinforcement(MPa)	percentage loss %
after prestressing	section 5	1411.3	2.0
	section 10	1342.8	6.7
	section 15	1263.6	12.3
100 days	section 5	-60.8	104.2
	section 10	-243.1	116.9
	section 15	103.2	92.8
end of service	section 5	771.9	46.4
	section 10	-215.1	114.9
	section 15	12.6	99.1

4.5.2.2 Assessment of the results (Structure at the end of its life)

Because the design was based on the resulting tension at the upper and lower fibers being equal to zero (from a quasi-permanent combination of load and preload), we would also evaluate the structure in this way in the software. To begin with, let's plot the stresses in the

model over the entire plate.

4.5.2.2.1 Stress on the plate at the top surface

From figure 89, the red portion of the result at the top surface of the quasi-load combination without prestress indicates tension, and the blue one shows pressure.
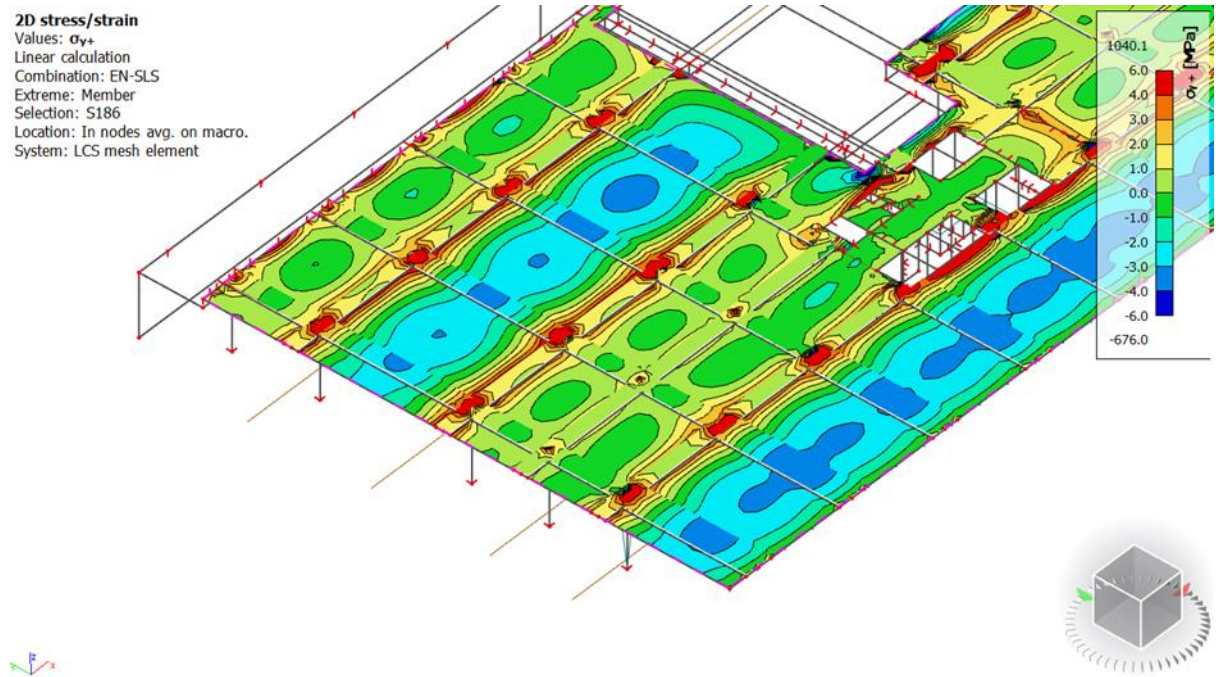
Figure 89: Stresses on the plate at the top surface from a quasi-steady load combination without prestress

However, in the case of stress at top surface from quasi combination with prestressing we can see the less tension as compared to previous case as shown below.
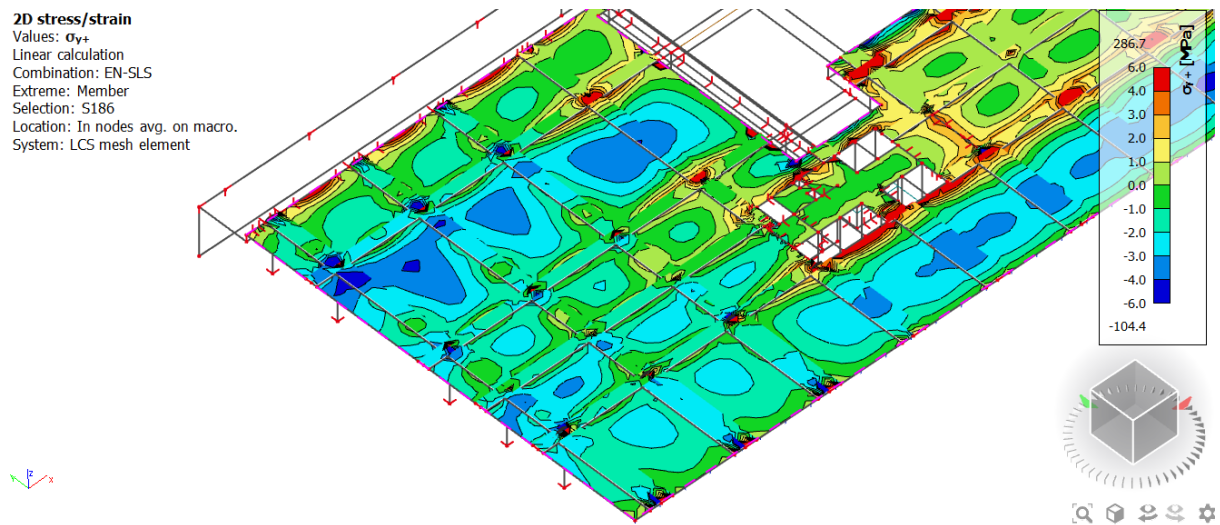
Figure 90: Stresses on the plate at the top surface from a quasi-steady combination of loading and prestressing

4.5.2.2.2 Stress on the plate at the bottom surface

From figure.91, the red portion of the result at the bottom surface from quasi load combination without prestress indicates tension and the blue one shows pressure.
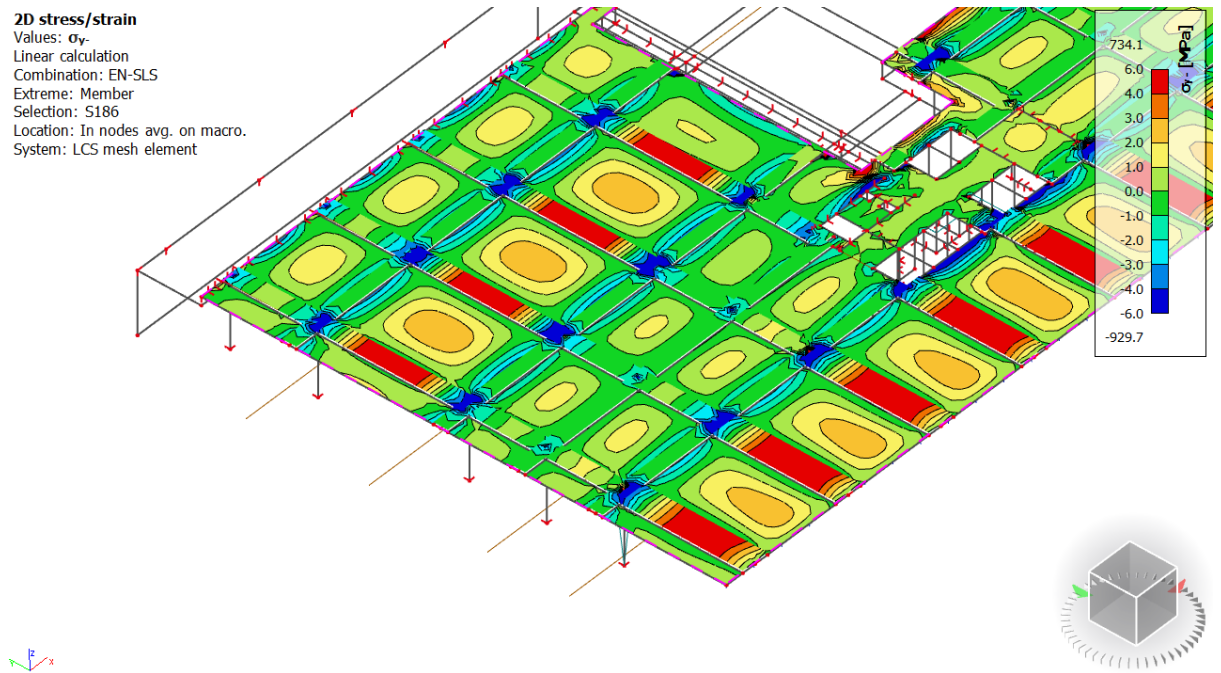
Figure 91: Stresses on the plate at the bottom surface from a quasi-steady load combination without prestressing

However, in the case of stress at bottom surface from quasi combination with prestressing indicates tension in red whereas pressure in blue color as shown below.
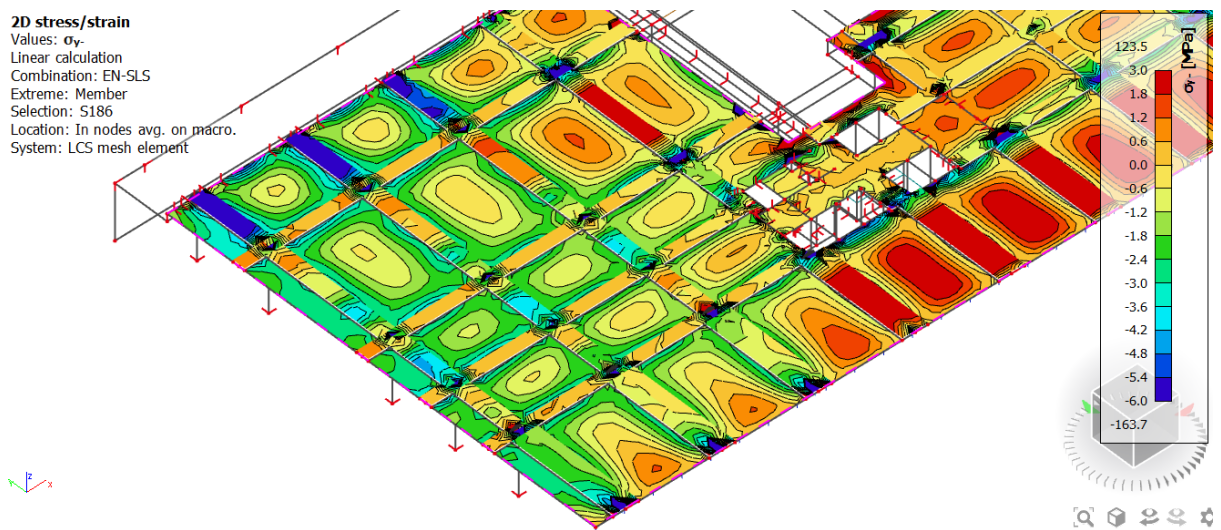
Figure 92: Stresses on the plate at the bottom surface from a quasi-steady combination of loading and prestressing

4.5.2.2.3 Tension on beam

We managed to reduce the tensile stress, but not enough. The emergence of tensile stresses could be attributed to a too-straight line of the prestressing lines or the neglect of the indeterminate element of the moment in the prestressing. We would show the section through beam A2 and reveal the specific cross-sections where tensile stresses arise.

4.5.2.2.4 Evaluation of the stress over the support

Although we previously designed the prestress over the supports with maximum eccentricity (or curiosity), at first we could conclude from the section that the predesigned prestress (due to the pulls arising over the support) wasn't sufficient. But let's dissect the course of the tension above the support in further detail.

2D stress/strain
Values: σ_{y+}
Linear calculation
Combination: EN-SLS
Extreme: Member
Selection: S186, SE12, SE14
Location: In nodes avg. on macro.
System: LCS mesh element
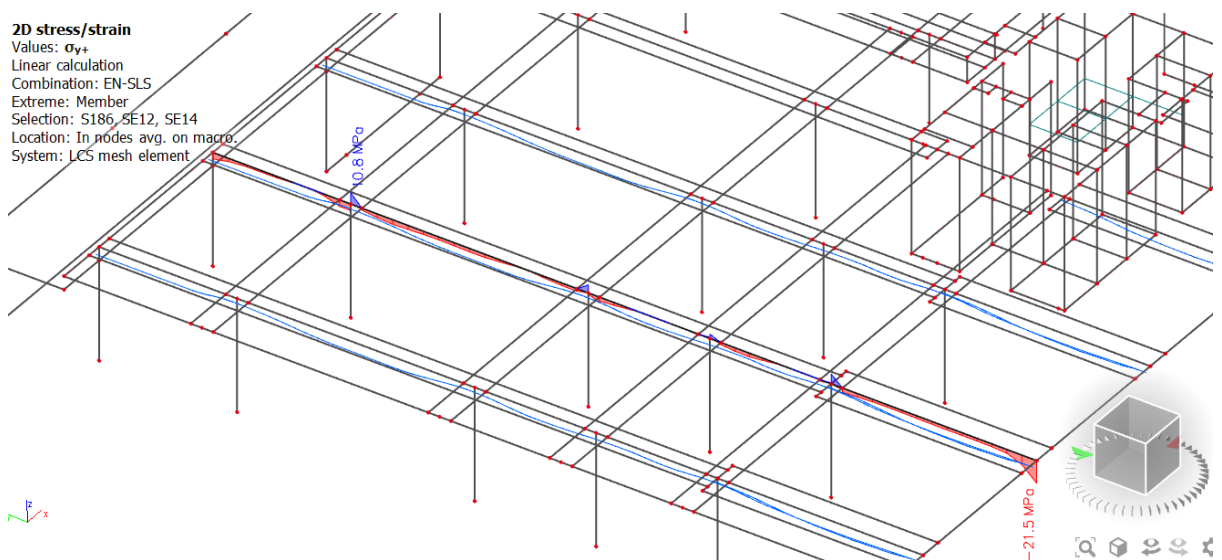
Figure 93: Stress on A2 at top surface from quasi-steady load combination with prestress

The results of the stress above the support were negatively affected by the fact that the software considered the column as a thin rod, and the normal force of the column therefore acts perpendicular to the plate at one point. Thus, a singularity has arisen on the plate accompanied by a very high stress that does not correspond to the actual action. The software allows us to locally thicken the network around the point. If we refined the network at the point of singularity, stress would increase. We did so and displayed the tensile stresses at this point.

Then we can recall the connection with the standard, which tells us about the reduction and redivision of the bending moment over the support due to the specific range of the support. We didn't reduce the necklace in our design; the software also calculates the peak necklace. similar to this procedure, we could do with the voltage assessment. We'll take a conservative approach to this fact and settle for zero pressure in the face of the support.

4.5.2.2.5 Evaluation of the stress over the field

There were no longer any singularities in the field, but tensile tensions appeared. The path of the prestressing cables was somewhat straight - in the cross-sections with the greatest positive moment, the tension approaches zero, but suddenly rises owing to the too rapid decrease of the eccentricity - a pull occurs, as indicated in fig 94. It was established that we would need to smooth out the cables or increase the number of cables in one wire.

Figure 94: Stress on P2 at lower surface from quasi-steady combination of load with prestress

Previously, we had neglected the indeterminate (secondary) moment component of the preload. It might have been this simplification that caused tensile stresses above the support. As has already been described several times above, we, unfortunately, could not afford to neglect the statically indeterminate component of the moment in the preload. Even though the statically indeterminate component of the prestress would change with the increasing designed area of the prestress and the change of the cable route, we would use for the prestress design the sum of the bending moments from the quasi-steady load combination (without prestress) and the statically indeterminate component from the prestress from the first design. We thus commit less inaccuracy than if we neglected this component of the bias.

Figure 95: Stress on P2 at lower surface from quasi-steady combination of load with prestress after change in the geometry of tendons

4.5.2.2.6 Prelimiary assessment of the tension of the beam A2

From the results presented so far, the tensile stress above the support was caused by the insufficient number of prestressing cables used and, in particular, the inappropriate routing of the prestressing cables. So, we adjusted the number of ropes in the cables and their route in such a way that we were assured about the compressive stresses in the cross-section.

$$Stress\ in\ concrete\ \sigma_c \leq 0\ MPa\quad OK$$

4.5.2.3 Check of prestressed concrete

4.5.2.3.1 Stress prior to (before) anchoring

As per EN 1992-1-1, clause 5.10.2.1, Stress in the prestressing tendon prior to and after anchoring was evaluated for combination ULS (short). The stress before anchoring must follow the condition below:

$$\sigma_{p.pa} \leq \sigma_{p,max}$$

$$1440 < 1473 \dots \dots \dots OK$$

$\sigma_{p,max}$ = allowable stress in prestressing before anchoring based on formula 5.41 from EN 1992-1-1 with respect of NA values k1 = 0,8; k2 = 0,9 are NA dependent values.

$$\sigma_{p,max} = \min\left(k_1 * f_{pk},\ k_2 * f_{p0.1k}\right) = \min(1488,1473) = 1473 MPa$$

Value of f_{pk} is taken from 4.5.2.1.1(2)

$\sigma_{p.pa}$ = calculated stress before anchoring = 1440MPa

4.5.2.3.2 Stress prior after anchoring

The stress after anchoring must follow the condition below

$$\sigma_{p,aa} \leq \sigma_{p,m,o}$$

$$1379.28 < 1391.3 \dots \dots \dots OK$$

$\sigma_{p,m,o}$ = allowable stress in prestressing after anchoring based on formula 5.43 from EN 1992-1-1 with respect of NA,

k7 = 0,75; k8 = 0,85 are NA dependent values

$$\sigma_{p,m,o} = \min\left(k_7 * f_{pk}, \ k_8 * f_{p0.1k}\right) = \min(1395, 1391.3) = 1473MPa$$

$\sigma_{p.pa}$ = calculated stress after anchoring with respect of short-term losses = 1379.28MPa

4.5.2.3.3 Stress limitation due to cracks or deformation from characteristic combination (SLS)

As per clause 7.2(5), the stress in reinforcement was verified due to limitation of unacceptable strain existence and thus appearance of cracks in concrete.

$$\sigma_{p,char} \leq \sigma_{p,char,lim}$$

Where, $\sigma_{p,char,lim} = 0.75 * f_{pk} = 0.75 * 1860 = 1395MPa$

$\sigma_{p,char}$ = calculated stress in tendons from characteristic combinations

Cracking status

Before calculation of crack width, the normal concrete stresses on un-cracked section at the most tensioned fiber has to be checked. If condition below is satisfied, the crack width does not create and the crack width is not calculated, if below the condition

$$\sigma_{ct} \leq f_{ct,eff}$$

Where,

σ_{ct} = normal concrete stress on un-cracked section at the most tensioned fibber of concrete cross-section

$f_{ct,eff}$ = the crack width is calculated only in case that normal concrete stress on un-cracked section at the most tensioned fiber of concrete cross-section is greater the mean value of the

tensile strength of the concrete effective

There cracking forces (Ncr, Mcry, Mcrz) are also presented in the in table output. These cracking forces are forces which cause the reaching of value $f_{ct,eff}$ (occurring of crack width in cross-section) in the most tensioned fibre of concrete cross-section in direction of first or second principal stress. For calculation of this cracking forces is used condition, that eccentricity of inputted forces and cracking forces has to be the same.

The crack width is calculated according to EN 1992-1-1, from equation 7.8 (page 124),

$$W_k = S_{r,max}(\varepsilon_{sm} - \varepsilon_{cm})$$

Where,

$S_{r,max}$ = is the maximum crack spacing

ε_{sm} = is the mean strain in the reinforcement under the relevant combination of loads, including the effect of imposed deformations and taking into account the effects of tension stiffening. Only the additional tensile strain beyond the state of zero strain of the concrete at the same level is considered

ε_{cm} = is the mean strain in the concrete between cracks

$$(\varepsilon_{sm} - \varepsilon_{cm}) = \frac{\sigma_s - k_t * \frac{f_{ct,effect}}{\rho_{p.eff}} * (1 + \alpha_e * \rho_{p.eff})}{E_s} \geq 0.6 * \frac{\sigma_s}{E_s}$$

σ_s = is the stress in the tension reinforcement assuming a cracked section. For pretensioned members, σ_s may be replaced by $\Delta\sigma_p$ the stress variation in prestressing tendons from the state of zero strain of the concrete at the same level.

Prestress Crack check N+M (SLS)
Values: **UC**
Linear calculation
Combination: EN-SLS
Coordinate system: Member
Extreme 1D: Global
Selection: B1000
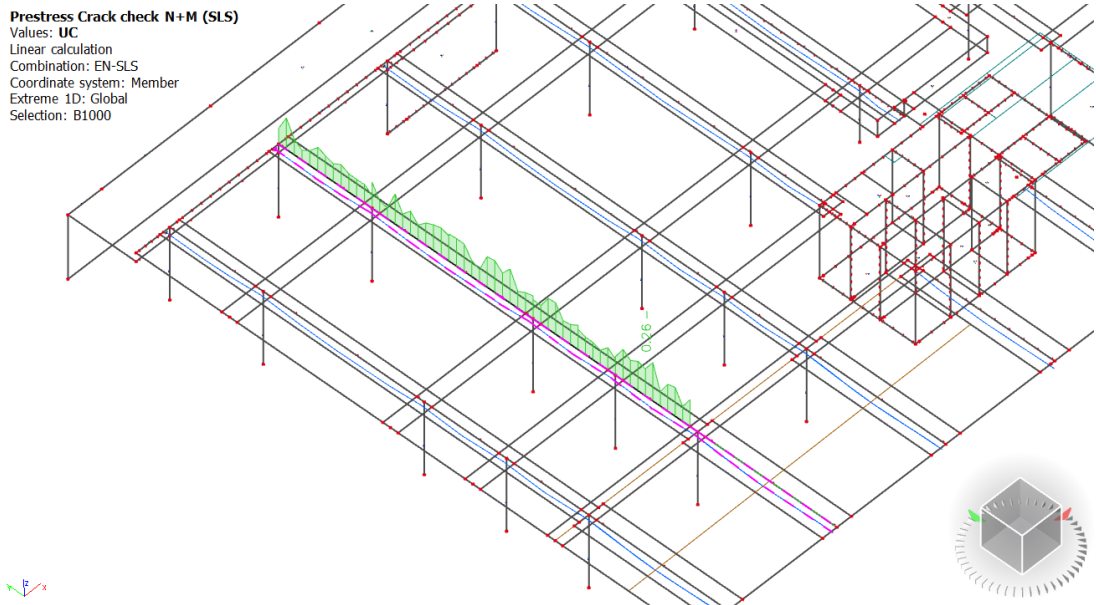
Figure 96: Display showing prestress crack check due to SLS

Crack width (SLS)
Values: **UC**
Linear calculation
Combination: SLS-Quasi 1PP
Extreme: Global
Selection: S186
Location: In nodes avg. on macro.
System: LCS mesh element

Figure 97: Display showing prestress crack width check for entire floor of 1PP due to SLS

As compared to 4.5.1.2, from figure 97, we conclude that there was drastic change in the results of the crack width in case of model with prestressed concrete.

Crack width (SLS)

Linear calculation
Combination: SLS-Quasi 1PP
Extreme: Global
Selection: S186
Location: In nodes avg. on macro. System: LCS mesh element

Upper surface - Standard result

Name	Mesh	Position [m]	Case	m_{1+} [kNm/m] m_{2+} [kNm/m]	n_{1+} [kN/m] n_{2+} [kN/m]	$A_{s,1+}$ [mm²] $A_{s,2+}$ [mm²]	$\sigma_{s,1+}$ [MPa] $\sigma_{s,2+}$ [MPa]	$S_{r,max,1+}$ [mm] $S_{r,max,2+}$ [mm]	$\varepsilon_{(sm-cm),1+}$ [1e-4] $\varepsilon_{(sm-cm),2+}$ [1e-4]	w_{1+} [mm] w_{2+} [mm]	w_{max+} [mm]	UC_{1+} [-] UC_{2+} [-]
S186	Element: 27029 Node: 27195	90.400 28.350 11.420	SLS-Quasi 1PP/1	-686.03 -	-2807.35 -	6 -	161.8 -	25526.530 -	4.9 -	12.387 -	**0.300**	41.29 -
S186	Element: 25805 Node: 26471	79.100 28.821 11.420	SLS-Quasi 1PP/1	- -718.43	- -2846.47	- 10	- 196.8	- 14351.880	- 5.9	- 8.474	0.300	- 28.25

Lower surface - Standard result

Name	Mesh	Position [m]	Case	m_{1-} [kNm/m] m_{2-} [kNm/m]	n_{1-} [kN/m] n_{2-} [kN/m]	$A_{s,1-}$ [mm²] $A_{s,2-}$ [mm²]	$\sigma_{s,1-}$ [MPa] $\sigma_{s,2-}$ [MPa]	$S_{r,max,1-}$ [mm] $S_{r,max,2-}$ [mm]	$\varepsilon_{(sm-cm),1-}$ [1e-4] $\varepsilon_{(sm-cm),2-}$ [1e-4]	w_{1-} [mm] w_{2-} [mm]	w_{max-} [mm]	UC_{1-} [-] UC_{2-} [-]
S186	Element: 24394 Node: 1008	65.125 33.150 11.420	SLS-Quasi 1PP/2	50.03 57.73	608.72 -189.66	0 0	0.0 0.0	0.000 0.000	0.0 0.0	3.000 3.000	**0.300**	3.00 3.00

Name	Combination key
SLS-Quasi 1PP/1	LC1 + LC2 + 0.30*LC11 + LC24
SLS-Quasi 1PP/2	LC1 + LC2 + 0.30*LC6 + 0.60*LC12 + LC24

Table 5: Crack width for 1PP due to SLS Quasi

The check of decompression is done according to chapter 7.3.1(5) EN 1992-1-1 in Scia Engineer. Together with a check of relaxation the limited values of the crack range for prestressed were enforced. Check of relaxation is done only for the prestressed concrete 1D members. The check of relaxation means the prestressing beachfront or tendon lies in the predefined zone(z_{dec}) of the concrete which is in contraction. The relaxation distance($z_{dec,max}$) where the concrete is vindicated is set in the EN1992-1-1 and the dereliction value is 25 mm. This value is measured from the edge of the beachfront(pre-tensioning) or the edge of the conduit(post-tensioning). The idea is to corroborate the distance around the beachfront to be in contraction in proper distance. This check is needed according to chapter 7.3.1 (5) from EN1992-1-1. The check is performed as the following:

 1). computation z_{dec} is the distance from the edge of the beachfront or edge of the conduit to the neutral axis.

2). Value $z_{dec,max}$ is set in NA.

3). computation check value the $z_{dec,max}$ / z_{dec}, If $z_{dec,max}$ / z_{dec} ≤,0 → Check is OK

4.5.2.3.4 Limitation of concrete stress

We would consider the cross-sections with the maximum compressive stresses. We assumed that these would be the cross-sections above the support at the bottom fibers and other places

with peak stresses were certainly in the places of the anchors - they would be captured by the under-anchor reinforcement. For the sake of assessment, we showed a section of the stress at the bottom surface from the self-weight load and from the prestress on beam A2, thereby demonstrating the real effect during implementation.

The maximum value of the compressive stress was therefore $\sigma = -7.1\ MPa$. Finally, the greatest compressive stress occurred in the first field due to the "holding" of the cable at the center of gravity.

As per the EN1992-1-1:Eurocode 2 standards (Clause 5.10.2.2(5).Page77)
For the compressive stress of the concrete during tensioning of the prestressing reinforcement, the following condition should be satisfied:

$$\sigma_c \leq 0.6 f_{ck}\ (t)$$

If the value of concrete compressive stress is exceed than this then nonlinear creep is to be considered.

$$\sigma_c < 0.45 f_{ck}\ (t)$$

where f_{ck} (t) is the concrete strength at the time of tensioning the structure (we choose the time t = 5 days).

As per the EN1992-1-1:Eurocode 2 standards (Clause 3.1.2(5&6).Page27), the value of compressive strength of concrete f_{ck} (t) is

$$f_{ck}(t) = f_{cm}\ (t) - 8MPa$$

$$f_{cm}(t) = \beta_{cc}(t) * f_{cm} = exp\left[s * \left(1 - \sqrt{\frac{28}{t}} \right) \right] * f_{cm}$$

Where,

f_{cm}(t) = is the mean concrete compressive strength at an age of t days

f_{cm} = is the mean (average) compressive strength at 28 days according to Table 3.1 page 29 of EN1992-1-1

β_{cc}(t) = is a coefficient which depends on the age of the concrete (t)

t = is the age of the concrete in days

s = is a coefficient which depends on the type of cement:

= 0.20 for cement of strength Classes CEM 42,5 R, CEM 52,5 Nand CEM 52,5 R (Class R)

= 0.25 for cement of strength Classes CEM 32,5 R, CEM 42,5 N (Class N)

= 0.38 for cement of strength Classes CEM 32,5 N (Class S)

So we choose, s = 0.20 for high-strength fast-hardening cements

For the age of concrete C35/45 at time t = 5 days (tension time) and high-strength fast-hardening cement:

$$f_{cm}(t = 5) = \beta_{cc}(t = 5) * f_{cm} = exp\left[s * \left(1 - \sqrt{\frac{28}{(t = 5)}}\right)\right] * f_{cm}$$

$$f_{cm}(t = 5) = exp\left[0.20 * \left(1 - \sqrt{\frac{28}{(t = 5)}}\right)\right] * (43) = 32.72 MPa$$

Where,

$$f_{cm} = f_{ck} + 8 = 35 + 8 = 43 MPa \ldots \ldots \ldots As\ per\ EN\ 1992 - 1 - 1, Table 3.1\ page\ 29$$
$$f_{ck}(t = 5) = f_{cm}\ (t = 5) - 8 MPa = 32.72 - 8 = 24.72 MPa$$

So,

$$\sigma_c \leq 0.6 f_{ck}\ (t = 5)\ \rightarrow 7 \leq 0.6 * 24.72 = 14.832\ OK$$

$$\sigma_c < 0.45 f_{ck}\ (t = 5)\ \rightarrow 7 < 11.124\ linear\ creeping$$

The assessed cross-section passed, in a more detailed long-term calculation we can consider linear creep. We can declare the construction satisfactory in terms of preload.

4.5.2.3.5 Concrete stress after anchoring (For combination ULS-short)

As per EN 1992-1-1, clause 5.10.2.2(5), $\sigma_{c,aa} = 0.6 * f_{ck}(t)$

For the age of concrete C35/45 at time t = 5 days (tension time) and high-strength fast-hardening cement:

$$f_{cm}(t = 5) = \beta_{cc}(t = 5) * f_{cm} = exp\left[s * \left(1 - \sqrt{\frac{28}{(t = 5)}}\right)\right] * f_{cm}$$

$$f_{cm}(t = 5) = exp\left[0.20 * \left(1 - \sqrt{\frac{28}{(t = 5)}}\right)\right] * (43) = 32.72 MPa$$

Where,

$$f_{cm} = f_{ck} + 8 = 35 + 8 = 43 MPa \ldots \ldots \ldots As\ per\ EN\ 1992 - 1 - 1, Table 3.1\ page\ 29$$

$$f_{ck}(t = 5) = f_{cm}\ (t = 5) - 8 MPa = 32.72 - 8 = 24.72 MPa$$

$$\sigma_{c,aa} = 0.6 * 24.72 = 14.832 MPa$$

Max. value of concrete strength after anchoring is 14.832MPa,
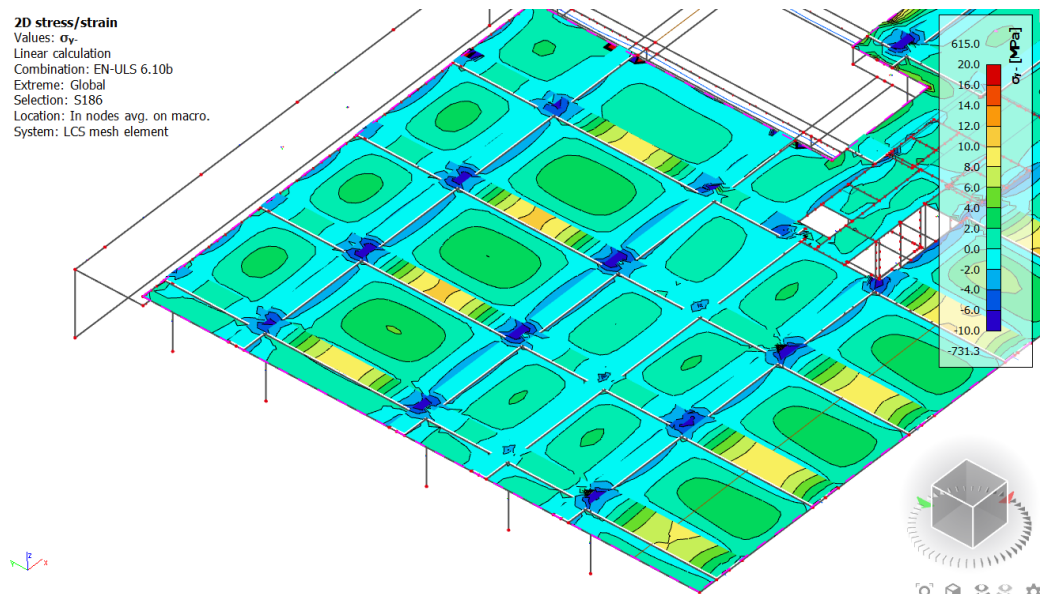
Figure 98: Display showing stresses on lower side due to ULS after prestress
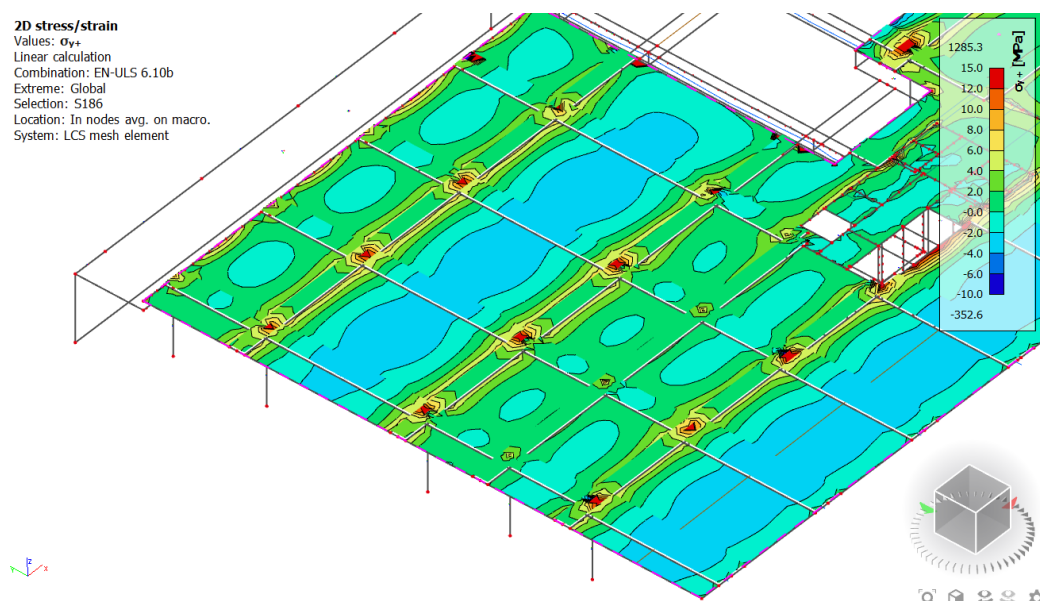
Figure 99: Display showing stresses on upper side due to ULS after prestress

4.5.2.3.6 Concrete stress in characteristics combination – longitudinal cracks -short

Stress in compression:

$$\sigma_{cc,ch} = 0.6 * f_{ck}(t) = 26.47 MPa \dots \dots \dots 7.2(2)$$

Stress in tension:

$$\sigma_{ct,ch} = 0.3 * (f_{ctm}(t))^{\wedge}(\frac{2}{3}) = 3.74 MPa \dots \dots \dots 7.1(2)$$

Strength of concrete in working life of 50 years has to be calculated manually,

$$f_{cm}(t = 18250) = \beta_{cc}(t = 18250) * f_{cm} = exp\left[s * \left(1 - \sqrt{\frac{28}{(t = 18250)}}\right)\right] * f_{cm}$$

$$f_{cm}(t = 18250) = exp\left[0.20 * \left(1 - \sqrt{\frac{28}{(18250)}}\right)\right] * (43) = 44.11 MPa$$
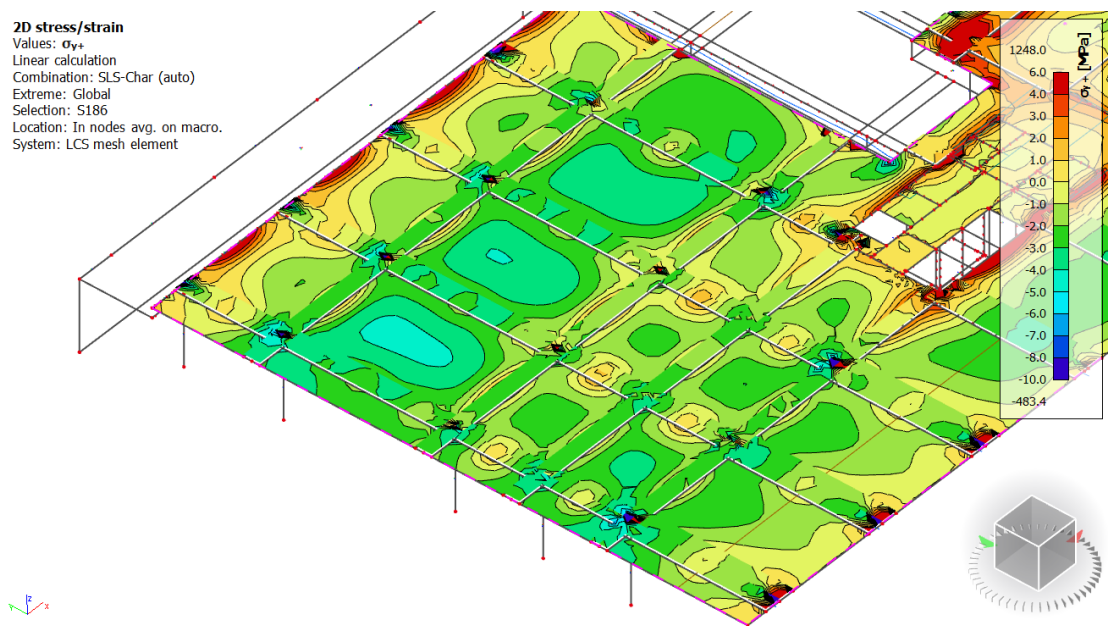
Figure 100: Display showing stresses on upper side due to SLS after prestress

We can see that all compressive stress in concrete was lower than the limit value $\sigma_{cc,ch} = 26.47 MPa$
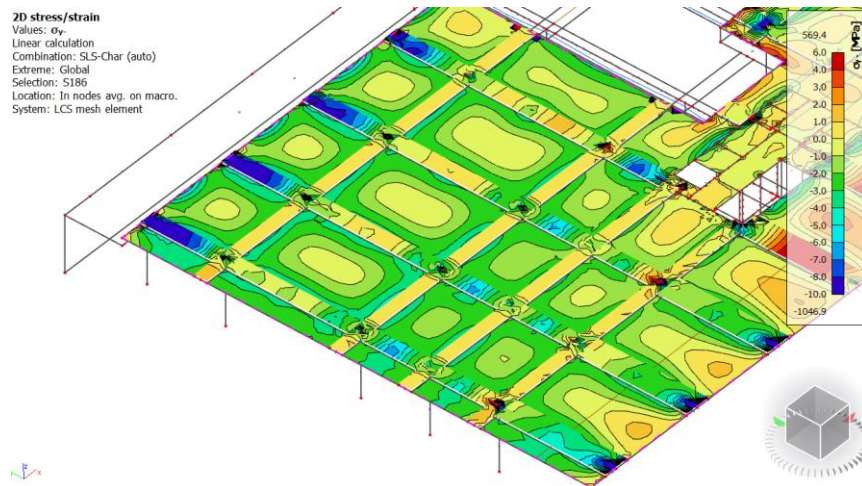
Figure 101: Display showing stresses on lower side due to SLS after prestress

4.5.2.3.6 Concrete stress in quasi – permanent combination (Nonlinear creep)

As per EN 1992-1-1, clause 7.2(3), t=5days

$$\sigma_{cc,qp} = 0.45 * f_{ck}(t) = 0.45 * 24.72 = 11.124 MPa > Comp. Stress (-7.1 MPa)$$
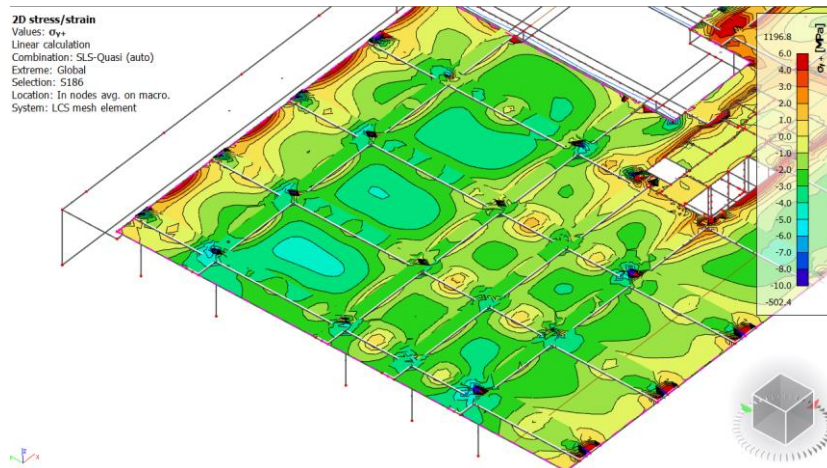
Figure 102: Display showing stresses on upper side due to SLS after prestress
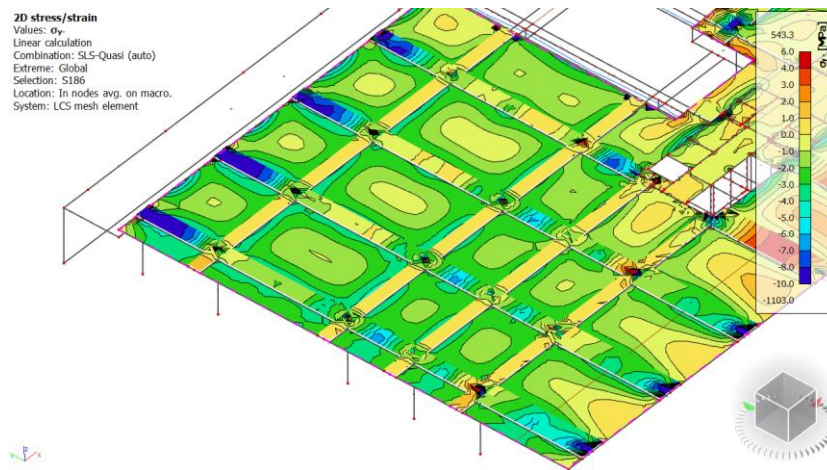
Figure 103: Display showing stresses on lower side due to SLS after prestress

We can see that all compressive stress in concrete was lower than the limit value.

4.5.2.3 Check for code dependent deflection in Scia v21

Earlier we did this check for model with reinforced structure, and we stated why we're going with prestressed model, but, to again justify our supposition we run the code dependent deflection in Scia Engineer software in version 21 -64bit.

Originally, it wasn't easy for us to get the results we anticipated, and the reason why we're saying this is that preliminarily for the utmost of the work(like to check deflection, moments, and stresses) we run the model in version 19 and 20 of Scia, but after assigning the tendons to model, we had another problem and we tried to sort out and when communicated to client service engineer then we got to know that prestressing option wasn't fully working with version 19 & 20 also not suitable to work with subregion in this performances, but after our suggestion, they promised to fix this issue in forthcoming times and as a result plethora of times during the computation for this nonlinear combination software was crashed so numerous times as we can see in the following fig. 104.
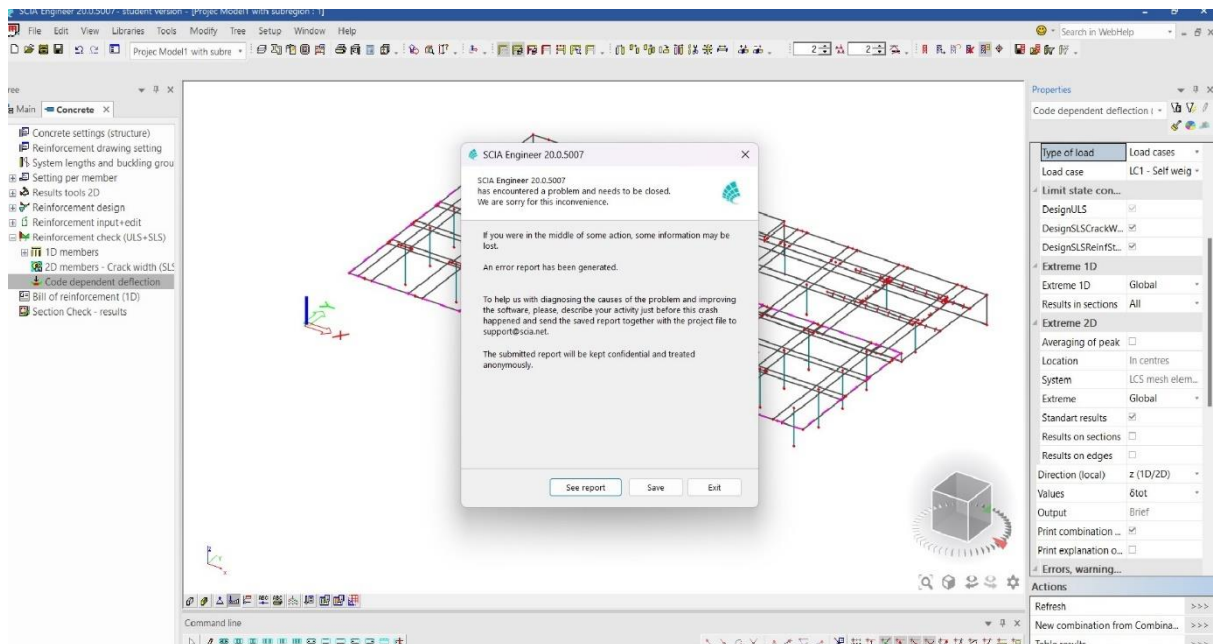
Figure 104: Display showing the crash of program during the code dependent analysis

So, after running the CDF (code dependent deflection) in version 21 for long term, we got this following results,
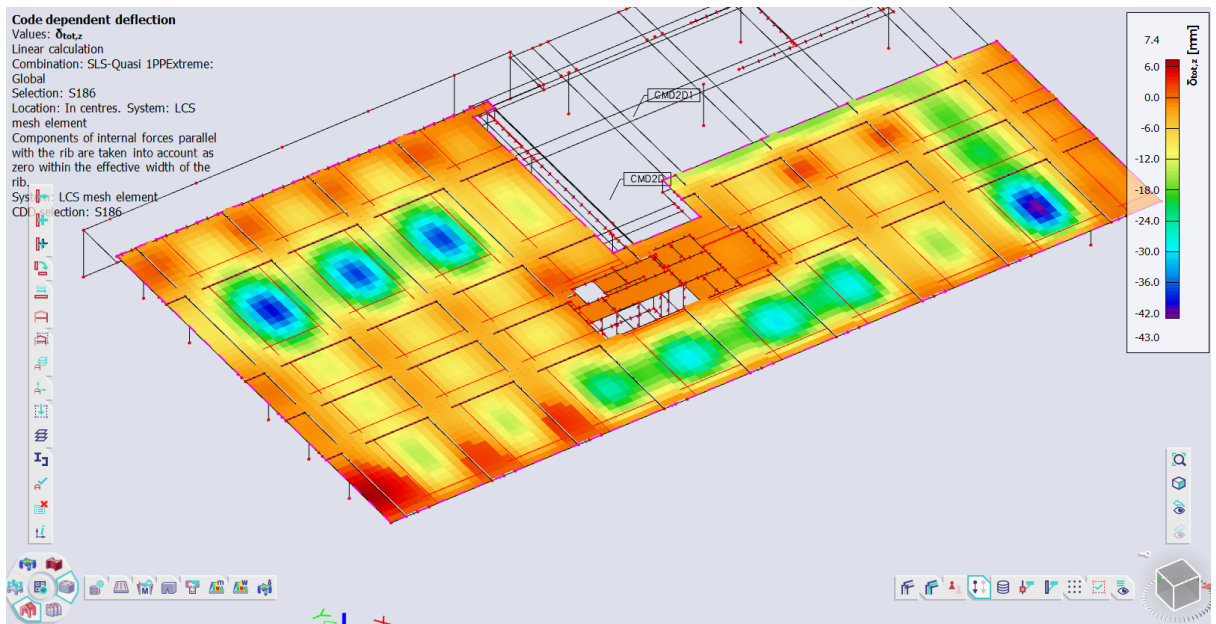
Figure 105: Display showing the long term deflection due to SLS 1PP after prestressing

From the results, we can say that vertical deformation from quasi-steady load combination g under **long-term action** is ok:

$$w_{g,lt,1} = 42.0 \ mm \ (Say)$$

And, Limit deflection under quasi-steady load combination:

$$w_{g,lim,1} = \frac{1}{250} \cdot l = \frac{11300}{250} = 45.2 \ mm$$

So,

$$w_{g,lt,1} = 42.0 < \ w_{g,lim,1} = 45.2 \ mm \ Ok$$

If we compare this result ($w_{g,lt,1} = 42.0 \ mm$) with vertical deflection of long term for model with reinforced structure ($w_{g,lt,1} = 95.0 \ mm$) we can say that model with prestressing is fine for such a complex structure.

4.5.2.4 Design and assessment of reinforced concrete structures (in y-direction)

Here, we designed the reinforcement of a reinforced concrete slab in the same direction as the prestressed girders; we therefore had to consider the effect of the prestress in the slab, i.e., primarily the normal force introduced through the girders. The same part of the plate would be solved again; the scope of the solution was known from the course of the internal forces (4.5.2.4.2).

4.5.2.4.1 Material characteristics

We used the same material characteristics from 4.5.1.1

Modulus of elasticity of reinforcement (E_s) = 200GPa

4.5.2.4.2 Internal forces

We initially presented the software's internal force findings on the entire plate, then divided them into portions and subtracted the numbers for design and assessment. We constructed the reinforcement to have the greatest bending moment possible (without the impact of the normal force) and then evaluated the key sections in the interaction diagram (pressure + bending interaction). We would compare the fields of the A2 and A3 beams.

My from the combination of SLS with preload:
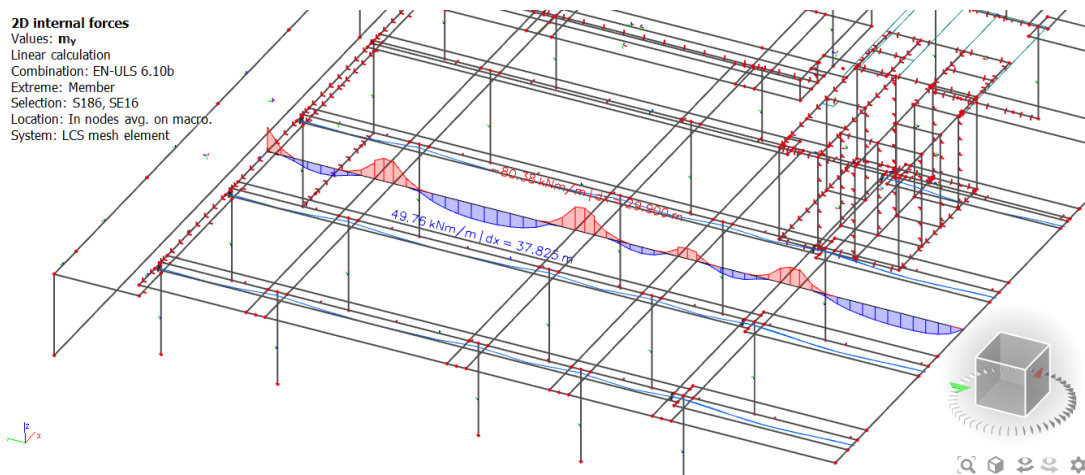
Figure 106: Bending moment my from load combination for EN ULS (6.10b) with prestress (section in fields between A2 and A3)

N_y from the combination of ULS with preload
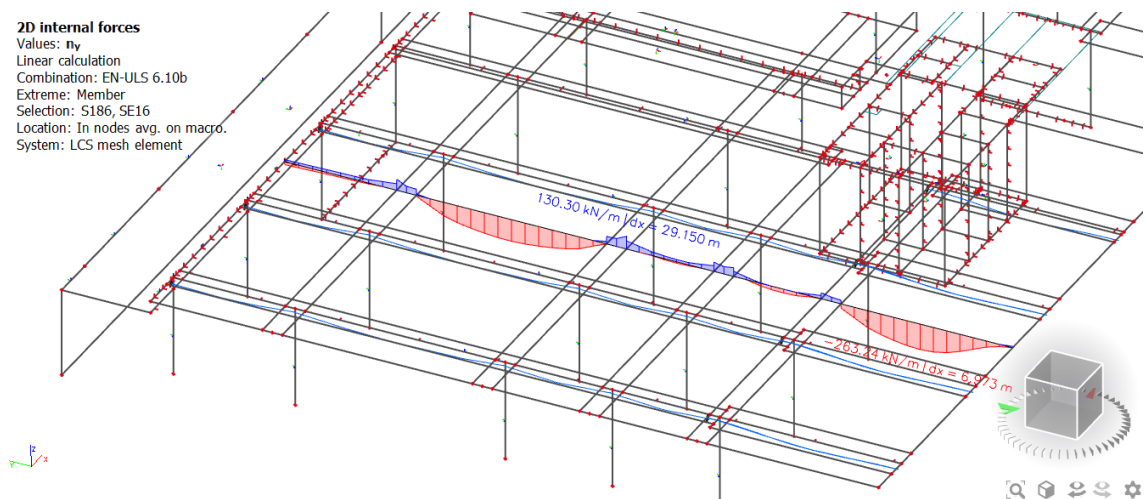
Figure 107: Normal force ny from load combination EN ULS6.10b with prestress (section in the fields between A2 and A3)

114

4.5.2.4.3 Design of reinforcement for the slab

We designed the reinforcement as if the slab were just bent, and we solely considered the impact of normal force throughout the assessment. The design of the reinforcement in the field and above the support would be the same; the only difference would be the position of the reinforcement (for top and bottom threads).

Design (in field, above support)

Let us assume supporting reinforcement : $\emptyset_y = 12mm, \emptyset_x = 14mm$

Cover: $C_{nom} = 30mm$

Maximum torque: $M_{Ed,pole} = 47.09kNm/m'$

Effective cross-sectional height:

$$d = h_d - c_{nom} - \emptyset_x - \frac{\emptyset_y}{2} = 250 - 30 - 14 - \frac{12}{2} = 200mm$$

Required reinforcement area:

$$A_{s,req} = \frac{b * d * f_{cd}}{f_{yd}} * \left(1 - \sqrt{1 - \frac{2 * M_{Ed,x}}{b * d^2 * f_{cd}}}\right)$$

$$= \frac{1000 * 200 * 23.33}{435}\left(1 - \sqrt{1 - \frac{2 * 47.09}{1000 * 200^2 * 23.33}}\right) * 10^6$$

$$= 541.264mm^2$$

$$Try\ 5\emptyset12mm\ at\ 125mm, so\ A_{s,pro} = 565.5mm^2$$

Assessment for interaction diagram

We would construct a point-to-point interaction diagram for the assessment. Considering that we did not consider the upper thrust (structural reinforcement) when assessing the bending of the slab, the interaction diagram would also be calculated without the structural reinforcement. A detailed procedure taken from the diploma thesis [17] would be used to calculate individual points.

Limiting proportional strain of concrete: $\varepsilon_{cu} = 3.5\% = 0.0035$

Limit proportional strain of the reinforcement: $\varepsilon_{sy} = \frac{f_{yd}}{E_s} = \frac{435}{200*10^3} = 2.175\% = 0.002175$

Stress in concrete (at failure in compression): $\sigma_c = -f_{cd} = -23.3333MPa$

Cover: $C_{nom} = 30mm$

Axial distance of the reinforcement from the lower fibers:

$$d_1 = C_{nom} + \emptyset_x + \frac{\emptyset_y}{2} = 30 + 14 + 6 = 50mm$$

115

The width of the assessed cross-section (Assume 1m of width): b = 1m

Concrete area: $A_c = b * h_d = 1 * 0.25 = 0.25mm^2$

Point 0 – central pressure

Lever arm of internal forces: $z = \frac{h_d}{2} - d_1 = \frac{250}{2} - 50 = 75mm$

Deformation of concrete when it reaches its strength: $\varepsilon_{c2} = 2\% = 0.002$

Tension stress in reinforcement: $\sigma_s = -E_s * \varepsilon_{c2} = -200000 * 0.002 = -400MPa$

$$m_{R,d,0} = A_c * \sigma_c + A_s * \sigma_s = 1 * 0.25 * (-23.33 * 10^3) + \left(565.5 * (-400 * 10^3)\right)$$
$$= 6058.7kNm$$

$$m_{R,d,0} = A_s * \sigma_s * z = 565.5 * (-400) * 0.075 * 10^{-3} = -27.14kNm$$

Point 1 – stressed by a positive moment, the neutral axis passes through the reinforcement

$\sigma_s = 0MPa$

$x = h_d - d_1 = 250 - 50 = 200mm$

$n = b * 0.8 * x * \sigma_c = 1 * 0.8 * 0.200 * (-23.33) * 10^3 = -3733.33kN$

$$m_{Rd,1} = b * 0.8 * x * \sigma_c \left(0.4x - \frac{h_d}{2}\right) = 1 * 0.8 * 0.200 * (-23.33) * (-0.045) * 10^3$$
$$= 168kNm$$

Point 2 – stressed by a positive moment, reinforcement for intermediate field

$\sigma_s = f_{yd} = 435MPa$

$x = (h_d - d_1) * \frac{\varepsilon_{cu}}{\epsilon_{cu3} + \varepsilon_{sy}} = (250 - 50) * \frac{0.0035}{0.0035 + 0.002175} = 123.4mm$

$z = \frac{h_d}{2} - d_1 = \frac{250}{2} - 50 = 75mm$

$$n_{Rd,2} = (b * 0.8 * x * \sigma_c) + (A_s * \sigma_s)$$
$$= (1 * 0.8 * 0.1234 * (-23.3) * 10^3) + (565.5 * 435 * 10^{-3})$$
$$= -2057.1451kN$$

$$m_{Rd,2} = b * 0.8 * x * \sigma_c \left(0.4x - \frac{h_d}{2}\right) + (A_s * \sigma_s * z)$$
$$= 1 * 0.8 * 0.1234 * (-23.33) * (-0.0756) * 10^3 + (565.5 * 435 * 0.075$$
$$* 10^{-3}$$

$= 192.57kNm$

Point 3 – simple bend

$x = \frac{A_s * f_{yd}}{0.8 * b * f_{cd}} = \frac{565.5 * 435 * 10^{-3}}{0.8 * 1 * 23.33} = 13.18mm$

$z = h_d - d_1 - 0.4 * x = 250 - 50 - 0.4 * 13.18 = 194.728mm$

$n_{Rd,3} = 0$

$$m_{Rd,3} = A_s * f_{yd} * z = 565.5 * 435 * 0.194728 * 10^{-3} = 47.9 kNm$$

Point 4 = Point 5 (central pull)

$$\sigma_s = f_{yd} = 435 MPa$$

$$z = \frac{h_d}{2} - d_1 = \frac{250}{2} - 50 = 75 mm$$

$$n_{Rd,\frac{4}{5}} = A_s * \sigma_s = 565.5 * 435 * 10^{-3} = 245.99 kNm$$

$$m_{Rd,4/5} = A_s * f_{yd} * z = 565.5 * 435 * 0.075 = 18.44 kNm$$

We used an online program (InDiOn-Interaction Diagram Online) to draw the interaction diagram, verify the correctness of the results, and provide feedback. We symbolically enter the value 0.0001 in columns As1 and d1 so that the program does not take into account structural reinforcement. We were verified the correctness of the results and assess them. We considered all the design points for the assessment in absolute value. For the same reinforcement for the upper and lower fibers (above the support and in the field), therefore we assessed the design in one interaction diagram ($m_{y,Ed}$ = 47.09kNm, $n_{y,Ed}$ -263.24kNm).
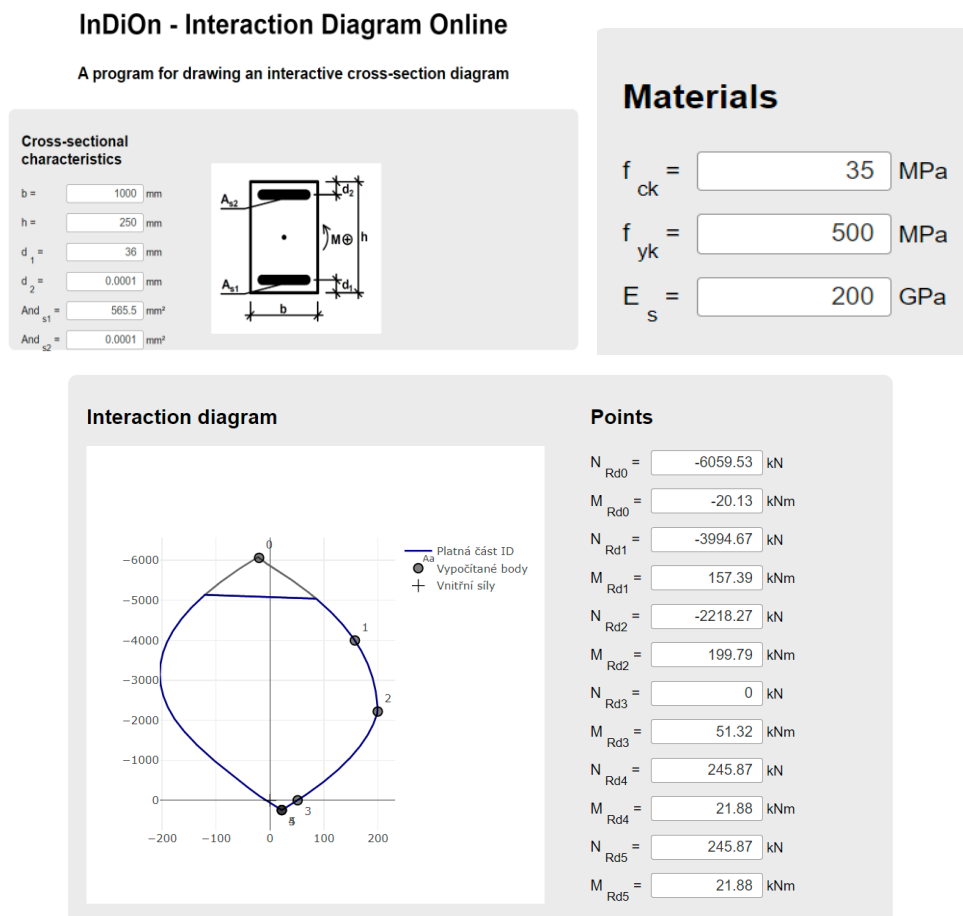
Figure 108: Display showing the interaction diagram with N & M

All selected combinations [myEd; ny,Ed] meet the condition of the interaction diagram.

$$(m_{y,Ed}, n_{y,Ed}) \leq (m_{Rd}, n_{Rd}) \dots\dots\dots OK$$

4.5.2.5 Design and assessment of reinforced concrete structures (direction x)

We created and assessed the most severely loaded reinforced concrete elements that are perpendicular to the prestressed beams - the beam and the slab, which were highlighted in green color shown in fig.109, for the completeness of the design of the left portion of the slab. These elements are A5, A6, A7, and A8.
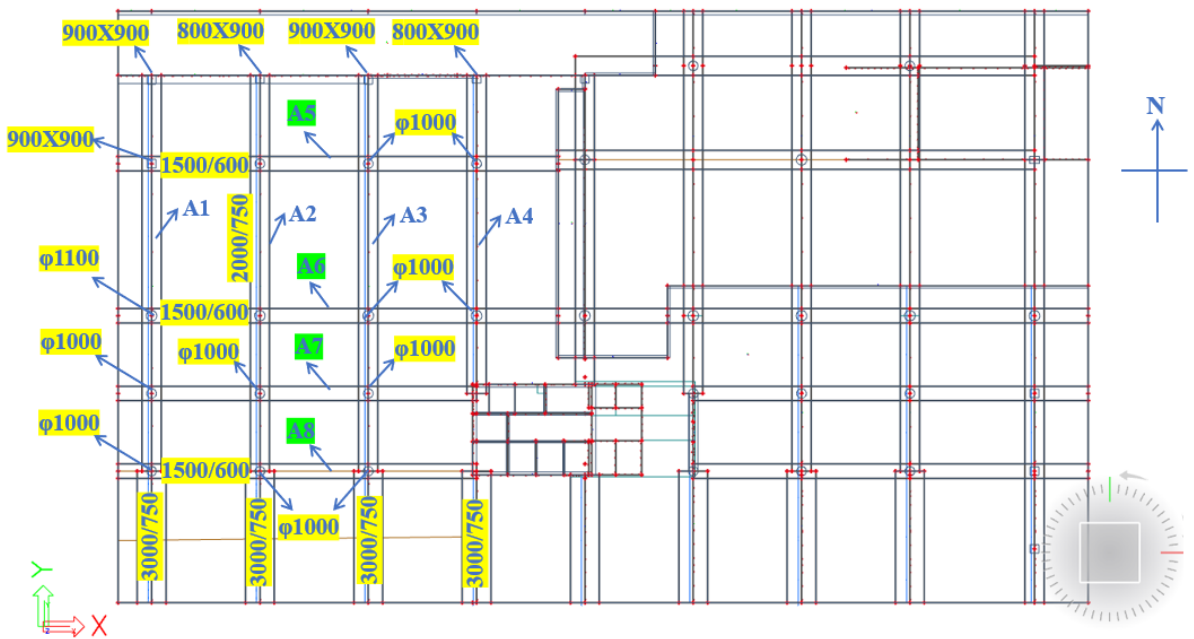
Figure 109: Schematic of a simplified drawing of the shape of the solved part of the slab which is on the left side

4.5.2.5.1 Material characteristics

We would take over the material characteristics from chapters 4.

Let's stimulate the solved part of the slab - the left tract (West Side). We were mark the solved beam A5 – A8 as shown in figure 109. The A8 beam stretches over 3 fields with a length of 11.3 m.

Cross – Section 1500/600
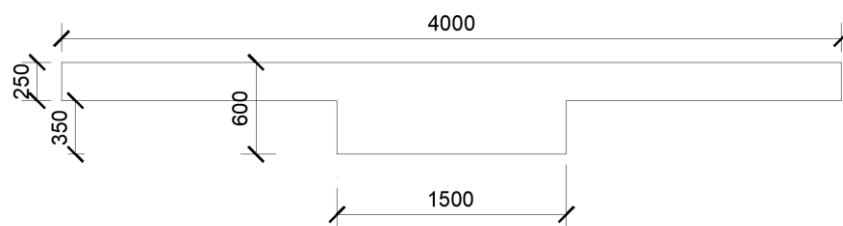
Figure 110: Cross section of 1500/600

Beam height: $h_t = 600mm$

Beam width: $b_t = 1500mm$

Thickness of slab: $h_d = 250mm$

Interacting width of the board in the field: $b_{eff} = 4442mm$

4.5.2.5.2 Internal forces

In the Scia software, we chose the most heavily loaded beam A8 for the internal forces.
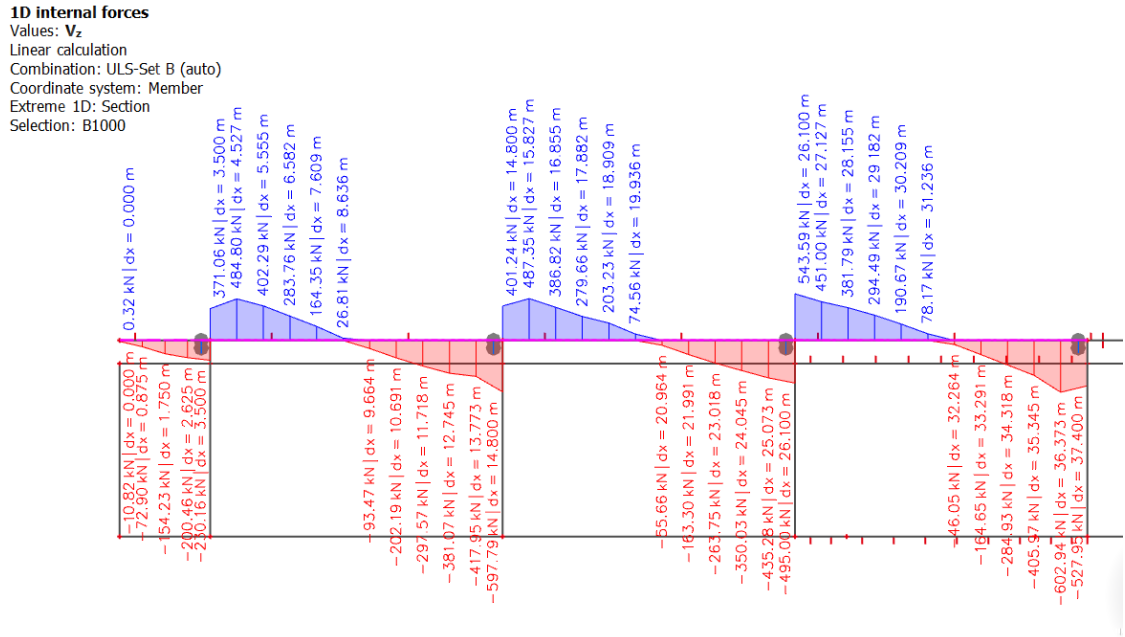
Figure 111: Display showing the internal forces Vx due to SLS on A8
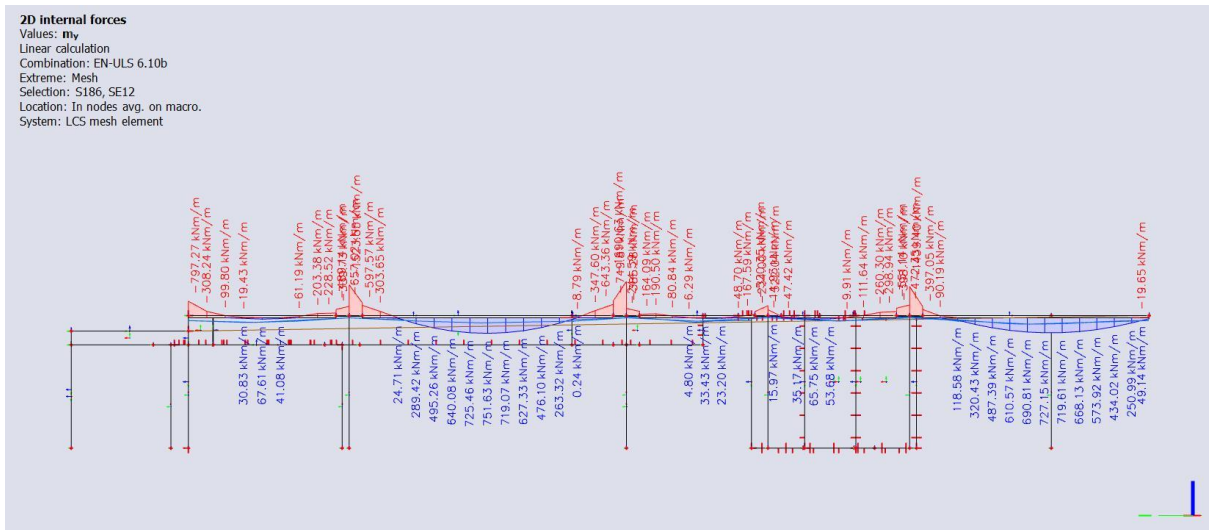
Figure 112: Display showing the internal forces my due to SLS on beam 1500/600

4.5.2.5.3 Design and check of reinforcement (ULS)

For beam 1500/600, (x-direction)

Assume $\emptyset = 25mm$, $\emptyset_{stirrups} = 10mm$, $C_{nom} = 30mm$

Moment over support $\left|M_{Ed,support}\right| = \left|-883.98kNm\right|$,

Effective cross-section height:

$$d_t = h_t - C_{nom} - \emptyset_{stirrups} - \emptyset - \frac{\emptyset}{2} = 600 - 30 - 10 - 12.5 = 547.5mm$$

$$k = \frac{M}{f_{ck} * b_w * d^2} = \frac{883.98 * 10^6}{23.33 * 1500 * 547.5^2} = 0.084 < 0.156 \dots \dots Singly\ r/f\ section$$

Required reinforcement area:

$$A_{s,req} = \frac{M_{Ed}}{0.87 * fy * d} = \frac{883.98 * 10^6}{0.87 * 435 * 0.9 * 547.5} = mm^2$$

$Say\ 10\emptyset25mm\ at\ 150mm$, $A_{s,prov} = 4909mm^2$

Check

1) $M_{Rd} \geq M_{Ed}$

$$x = \frac{f_{yd} * A_{s,prov}}{0.8 * b * f_{cd}} = \frac{435 * 4909}{0.8 * 1500 * 23.33} = 76.275mm$$

$$z = d - 0.4x = 547.5 - (0.4 * 22.92) = 516.99mm$$

$$M_{Rdy} = A_{s,prov} * f_{yd} * z = 4909 * 435 * 516.99 = 1103.98kNM$$

So, $M_{Rd}(= 1104) > M_{Ed}(= 883.98kNm) \dots \dots \dots \dots \dots \dots OK$

2) $\varepsilon \leq \varepsilon_{bal} \approx 0.64$

$$\varepsilon = \frac{x}{d} = 0.139 < 0.64 \dots \dots \dots \dots OK$$

3) $\rho_{min} \leq \rho \leq \rho_{max}$

$$0.0015 \leq \frac{A_{s,prov}}{bd} \leq 0.4$$

$$0.0015 \leq \frac{4909}{1500 * 547.5} = 0.005977 < 0.4 \dots \dots \dots \dots Ok$$

It complies with the design principles.

Design in the Co-acting slab

Interacting width field $b_{eff} = 3234mm$

Moment in the field: $M_{Ed,field} = 268.13kNm$

Effective cross-sectional height:

$$d_t = h_t - C_{nom} - \emptyset_{stirrups} - \frac{\emptyset}{2} = 600 - 30 - 10 - 12.5 = 547.5mm$$

$$k = \frac{M}{f_{ck} * b_f * d^2} = \frac{268.13 * 10^6}{23.33 * 3234 * 547.5^2} = 0.012 < 0.156 \dots \dots Signly \ r/f \ section$$

Required reinforcement area:

$$A_{s,req} = \frac{M_{Ed}}{0.87 * fy * d} = \frac{268.13 * 10^6}{0.87 * 435 * 0.9 * 547.5} = 1437.84mm^2$$

$Say \ 3\emptyset25mm \ at \ 300mm, A_{s,prov} = 1473mm^2$

$$20\% \ of \ bottom \ reinforcement = 0.2 * 1473 = 294.6mm^2$$
$$= top \ reinforcement, say \ 8\emptyset8mm \ at \ 150mm$$

Check

4) $M_{Rd} \geq M_{Ed}$

$$x = \frac{f_{yd} * A_{s,prov}}{0.8 * b * f_{cd}} = \frac{435 * 1473}{0.8 * 1500 * 23.33} = 22.92mm$$

$$z = d - 0.4x = 547.5 - (0.4 * 22.92) = 538.332mm$$

$$M_{Rdy} = A_{s,prov} * f_{yd} * z = 1473 * 435 * 538.332 = 344.94kNM$$

So, $M_{Rd}(= 344.94) > M_{Ed}(= 268.13) \dots \dots \dots \dots \dots \dots OK$

5) $\varepsilon \leq \varepsilon_{bal} \approx 0.64$

$$\varepsilon = \frac{x}{d} = 0.042 < 0.64 \ldots\ldots\ldots\ldots\ldots OK$$

6) $\rho_{min} \leq \rho \leq \rho_{max}$

$$0.0015 \leq \frac{A_{s,prov}}{bd} \leq 0.4$$

$$0.0015 \leq \frac{1473}{1500 * 547.5} = 0.00179 < 0.4 \ldots\ldots\ldots\ldots Ok$$

It complies with the design principles.

4.5.2.5.4 Slab

Let us assess the plate in the x direction (perpendicular to the preload), the combination of SLS.

Thickness of the board h_d = 250mm

Max. design moment over support = -63.58kNm/m'

Max. design moment in the field = 40.45kNm/m'

Design of reinforcement (bending)

Let us assume reinforcement : $\emptyset_x = 12mm$,

Cover: $C_{nom} = 30mm$

Effective cross-sectional height:

$d = h_d - c_{nom} - \frac{\emptyset_x}{2} = 250 - 30 - 12 - \frac{8}{2} = 204mm$

Required reinforcement area:

$$A_{s,req} = \frac{M_{Ed}}{0.87 * fy * d} = \frac{40.45 * 10^6}{0.87 * 435 * 0.9 * 204} = 582.15mm^2$$

$Say\ 6\emptyset12mm\ at\ 150mm,\ A_{s,prov} = 679mm^2$
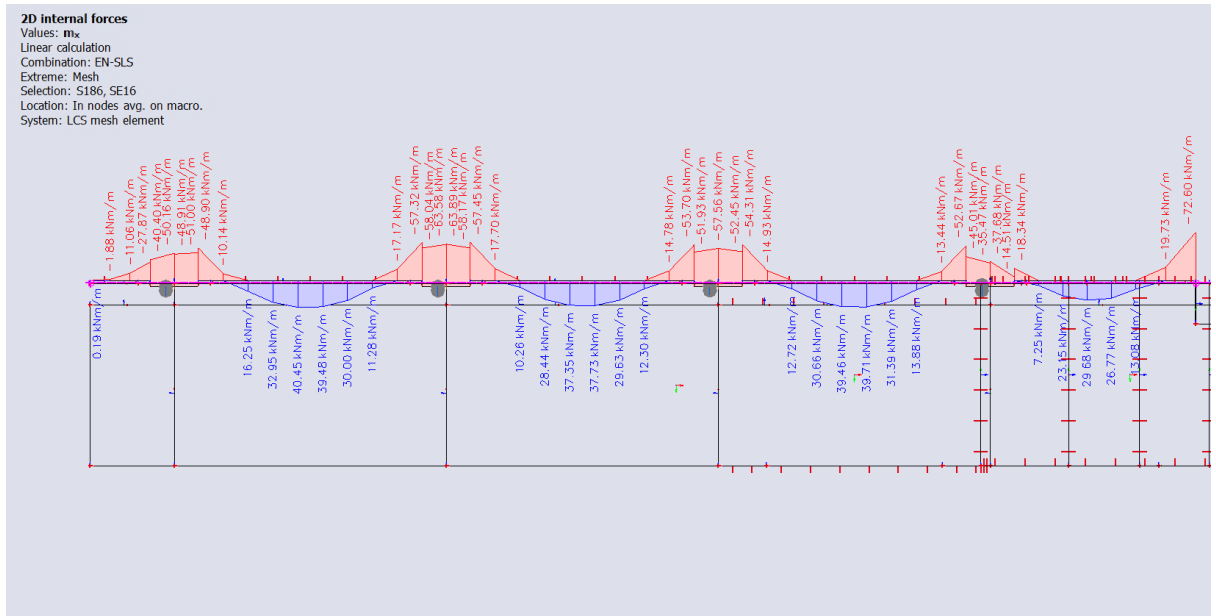
Figure 113: Display showing the internal forces mx due to SLS on left side of slab on 1PP

Check

1) $M_{Rd} \geq M_{Ed}$

$$x = \frac{f_{yd} * A_{s,prov}}{0.8 * b * f_{cd}} = \frac{435 * 679}{0.8 * 1000 * 23.33} = 15.83 mm$$

$$z = d - 0.4x = 204 - (0.4 * 15.83) = 197.668 mm$$

$$M_{Rdy} = A_{s,prov} * f_{yd} * z = 679 * 435 * 197.668 = 58.38 kNM$$

So, $M_{Rd}(= 58.38) > M_{Ed}(= 40.45) \dots \dots \dots \dots \dots \dots \dots OK$

2) $\varepsilon \leq \varepsilon_{bal} \approx 0.64$

$$\varepsilon = \frac{x}{d} = 0.0776 < 0.64 \dots \dots \dots \dots \dots OK$$

3) $\rho_{min} \leq \rho \leq \rho_{max}$

$$0.0015 \leq \frac{A_{s,prov}}{bd} \leq 0.4$$

$$0.0015 \leq \frac{679}{1000 * 204} = 0.0033 < 0.4 \dots \dots \dots \dots OK$$

4) $\varepsilon_s \leq \varepsilon_{cu}(5\%)$

$$\varepsilon_s = \frac{0.0035(d-x)}{x} = \frac{0.0035(204-15.83)}{15.83} = 4.16\% < 5\% \dots \dots \dots OK$$

It complies with the design principles.

Design and assessment for skid

Bearing capacity:

$$V_{Rd,max} = v * f_{cd} * b * z * \frac{cot\theta}{1+cot\theta^2} = 0.516 * 23.33 * 1.5 * 449.28 * \frac{1.5}{1+1.5^2} = 3744.39kN$$

Where,

$$v = 0.6 * \left(1 - \frac{f_{ck}}{250}\right) = 0.516$$

$$cot\theta = 1.5$$

Check, $|V_{Ed}| = 579.79kN \leq V_{Rd,max}(= 3744.39kN) \dots \dots \dots \dots \dots OK$

Design of stirrups

Assume number of stirrups cut be (n) = 6

Stirrup diameter: $\emptyset_{stirrup} = 10mm$

Cross-sectional area of stirrup: $A_{stirrups} = \frac{n*\pi}{4} * \emptyset_{stirrup}^2 = \frac{6*\pi*10^2}{4} = 471.24mm^2$

The required axial distance of stirrups

$$s \leq \frac{A_{stirrups} * f_{yd}}{V_{Ed}} * z * cot\theta$$

$$s = \frac{471.24 * 435}{602.94} * 0.44928 * 1.5 \approx 200mm$$

So, provide stirrups φ10mm at 200mm

Check,

$$V_{Rd} = \frac{A_{stirrups} * f_{yd}}{s} * z * cot\theta = \frac{471.2 * 435 * 0.4615 * 1.5 * 10^{-3}}{0.20} = 709.46kN$$

$$|V_{Ed}| = 579.79 kN \le V_{Rd}(= 709.46 kN) \dots \dots \dots \dots \dots OK$$

It complies with the design principles.

Reinforcement diagram
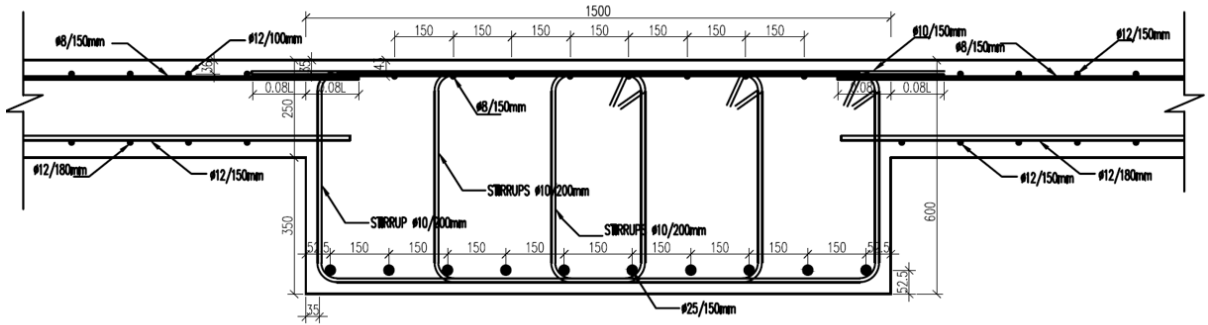
Figure 114: Reinforcement Diagram for section 1500/600

4.5.2.5.5 Assessment of SLS (Deflection - flexural slenderness)

We assessed the beam A8 in the cross-section above the support.

Bending slenderness of beam:

$$\lambda = \frac{L}{d} \le \lambda_d$$

Where, L=11.3m, d=0.5225m,

$$\lambda_d = k_{c,1} * k_{c,2} * k_{c,3} * \lambda_{d,tab}$$

$$k_{c,1} = 1.0$$

$$k_{c,2} = \frac{7}{L} = \frac{7}{11.3} = 0.619$$

$$k_{c,3} = \frac{500 * A_{s,prov}}{f_{yk} * A_{s,req}} = \frac{500 * 11780.97}{500 * 5945.6} = 1.98$$

Value of bending slenderness from table: $\lambda_{d,tab} = 22.86$

$$\rho = \frac{A_{s,prov}}{A_c} = 1.11\%$$

$$\lambda = \frac{L}{d} = \frac{11.3}{0.5225} = 21.6$$

$$\lambda_d = 1 * 0.619 * 1.98 * 22.86 = 28.02$$

$$\lambda \le \lambda_d \dots \dots \dots OK$$

The flexural slenderness assessment works for us, which means that we can say that the deflection assessment was not very necessary. Due to the scope and nature of the work, we would not deal with this. It was possible that the beams in the x direction were also intended by the designer to be prestressed. If we wanted to preserve the shape of the beam, we could reinforce the structure more and thus eliminate its deflection. A simpler solution would be to increase the section of the beam to 750 mm; this would not increase the structural height of the floors, and the beam would comply with deflection (flexural slenderness).

Design and assessment of reinforced concrete structures (direction y)

For beam 2000/750,

Assume $\emptyset = 25mm$, $\emptyset_{stirrups} = 10mm$, $C_{nom} = 30mm$

Moment over support $\left|M_{Ed,support}\right| = |-1690.63kNm|$,

Effective cross-section height:

$$d_t = h_t - C_{nom} - \emptyset_{stirrups} - \emptyset - \frac{\emptyset}{2} = 750 - 30 - 10 - 12.5 = 697.5mm$$

$$k = \frac{M}{f_{ck} * b_w * d^2} = \frac{1690.63 * 10^6}{23.33 * 1500 * 697.5^2} = 0.0744 < 0.156 \dots \dots Singly\ r/f\ section$$

Required reinforcement area:

$$A_{s,req} = \frac{M_{Ed}}{0.87 * fy * d} = \frac{1690.63 * 10^6}{0.87 * 435 * 0.9 * 697.5} = 7116.285mm^2$$

Say $15\emptyset 25mm\ at\ 130mm$, $A_{s,prov} = 7363.11mm^2$

Check

   1) $M_{Rd} \geq M_{Ed}$

$$x = \frac{f_{yd} * A_{s,prov}}{0.8 * b * f_{cd}} = \frac{435 * 7363.11}{0.8 * 2000 * 23.33} = 85.81mm$$

$$z = d - 0.4x = 697.5 - (0.4 * 85.81) = 663.176mm$$

$$M_{Rdy} = A_{s,prov} * f_{yd} * z = 7363.11 * 435 * 663.176 = 2124.12kNM$$

So, $M_{Rd}(= 2124.12) > M_{Ed}(= 1690.63kNm) \dots \dots \dots \dots \dots \dots \dots OK$

2) $\varepsilon \le \varepsilon_{bal} \approx 0.64$

$$\varepsilon = \frac{x}{d} = 0.123 < 0.64 \dots\dots\dots\dots\dots OK$$

3) $\rho_{min} \le \rho \le \rho_{max}$

$$0.0015 \le \frac{A_{s,prov}}{bd} \le 0.4$$

$$0.0015 \le \frac{7363.11}{2000 * 697.5} = 0.0053 < 0.4 \dots\dots\dots\dots Ok$$

It complies with the design principles.

Design in the field

Interacting width field $b_{eff} = 4442mm$

Moment in the field: $M_{Ed,field} = 751.63kNm$

Effective cross-sectional height:

$$d_t = h_t - C_{nom} - \emptyset_{stirrups} - \frac{\emptyset}{2} = 600 - 30 - 10 - 12.5 = 697.5mm$$

$$k = \frac{M}{f_{ck} * b_f * d^2} = \frac{751.63 * 10^6}{23.33 * 4442 * 697.5^2} = 0.0149 < 0.156 \dots\dots Signly\ r/f\ section$$

Required reinforcement area:

$$A_{s,req} = \frac{M_{Ed}}{0.87 * fy * d} = \frac{751.63 * 10^6}{0.87 * 435 * 0.9 * 697.5} = 3163.79mm^2$$

$Say\ 7\emptyset25mm\ at\ 270mm, A_{s,prov} = 3436mm^2$

$$20\%\ of\ bottom\ reinforcement = 0.2 * 3436 = 687.2mm^2$$
$$= top\ reinforcement, say 7\emptyset12mm\ at\ 150mm$$

Check

4) $M_{Rd} \ge M_{Ed}$

$$x = \frac{f_{yd} * A_{s,prov}}{0.8 * b * f_{cd}} = \frac{435 * 3436}{0.8 * 2000 * 23.33} = 40.04mm$$

$$z = d - 0.4x = 697.5 - (0.4 * 40.04) = 681.484mm$$

$$M_{Rdy} = A_{s,prov} * f_{yd} * z = 3436 * 435 * 681.484 = 1018.57kNM$$

So, $M_{Rd}(= 1018.57) > M_{Ed}(= 751.63) \dots \dots \dots \dots \dots \dots \dots OK$

5) $\varepsilon \leq \varepsilon_{bal} \approx 0.64$

$$\varepsilon = \frac{x}{d} = 0.057 < 0.64 \dots \dots \dots \dots \dots OK$$

6) $\rho_{min} \leq \rho \leq \rho_{max}$

$$0.0015 \leq \frac{A_{s,prov}}{bd} \leq 0.4$$

$$0.0015 \leq \frac{3436}{2000 * 697.5} = 0.00246 < 0.4 \dots \dots \dots \dots Ok$$

It complies with the design principles.

4.5.2.6 Consideration of prestress design for an unsolved part of the supporting structure

During the analysis, we started the preliminary design and checked for the prestress from the left side of the slab on 1PP by selecting the A2 beam only, and then we assigned the prestressing tendons to the entire floor of 1PP as shown in the following fig. 115, which was actually typical for the ceiling structures of other floors where we learned to analyze problems in detail and mastered the principles of prestressing on one beam. We would certainly follow this concept and way to design the prestressing of other parts of the structure of 1PP. After such a detailed analysis, we would probably come across new obstacles that we would have to solve, as mentioned in 4.5.2.3, but we managed to create the basic framework for the design of the rest of the dilatation.
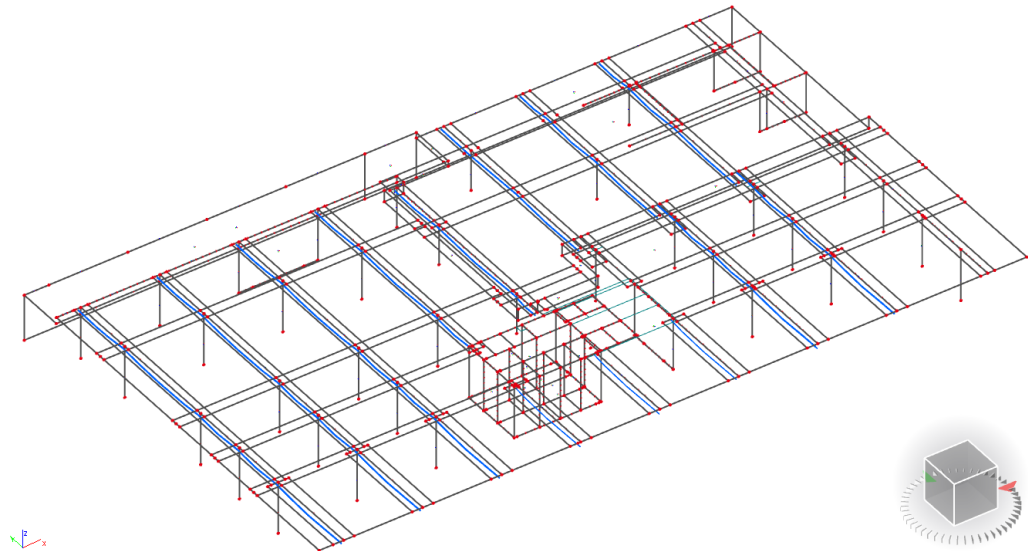
Figure 115: Assigning the tendons on the entire slab of 1PP

All in all, we can say that the concept of the design and check for the prestressing for the beams available on other floors would be the same and repeated, so instead of solving this entire in-depth design again for these additional floors due to repetitive work, we only applied the tendons to the rest of all floors and looked for the overall results like displacements and stresses. From that, we could also say that prestressing is also fine for other floors instead of reinforced concrete.

Here are the results of the other floors after modelling it with prestressing tendons:

1NP:
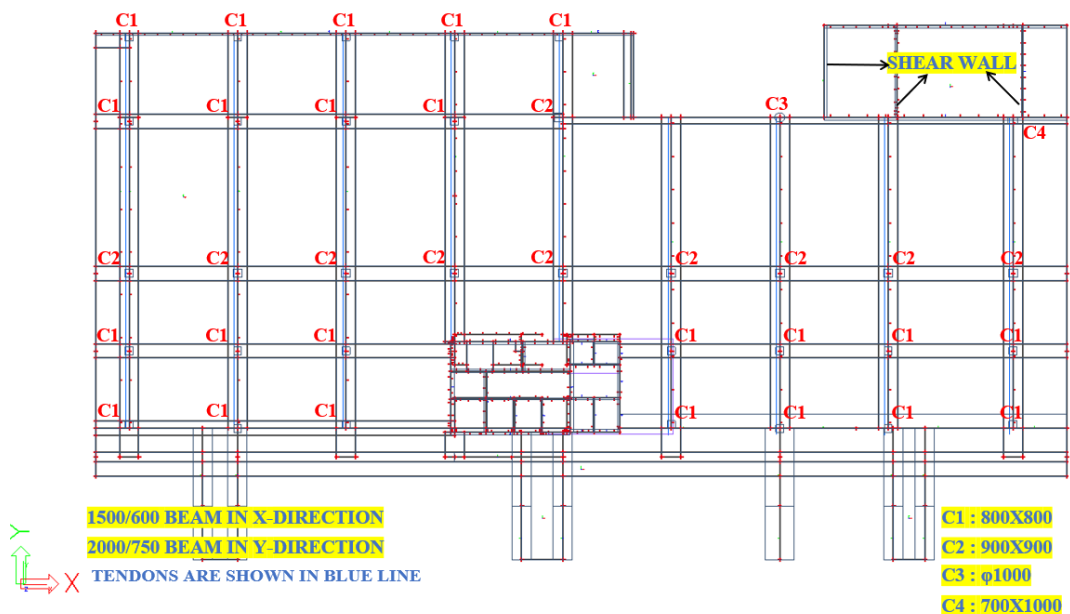
Figure 116: Layout of 1NP with tendons

Fig. 116 shows layout of the 1NP after assigning the tendons to the entire floor. It also shows that the cross section of column is also similar to 1PP. After running the calculations following displacements achieved show in fig. 117.
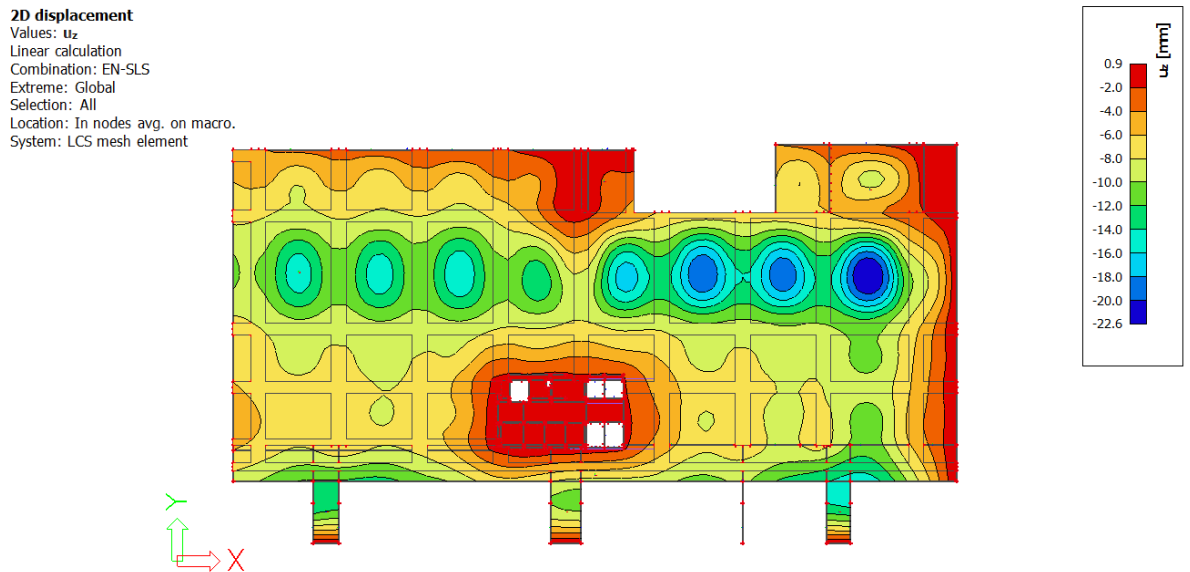

Figure 117: Display of 2D Displacement due to SLS-Quasi on 1NP

2NP:

We repeat the procedure of assigning tendons for floor 2NP as shown in the fig.118. On 2PP, details of beams and columns are also similar to other floors.
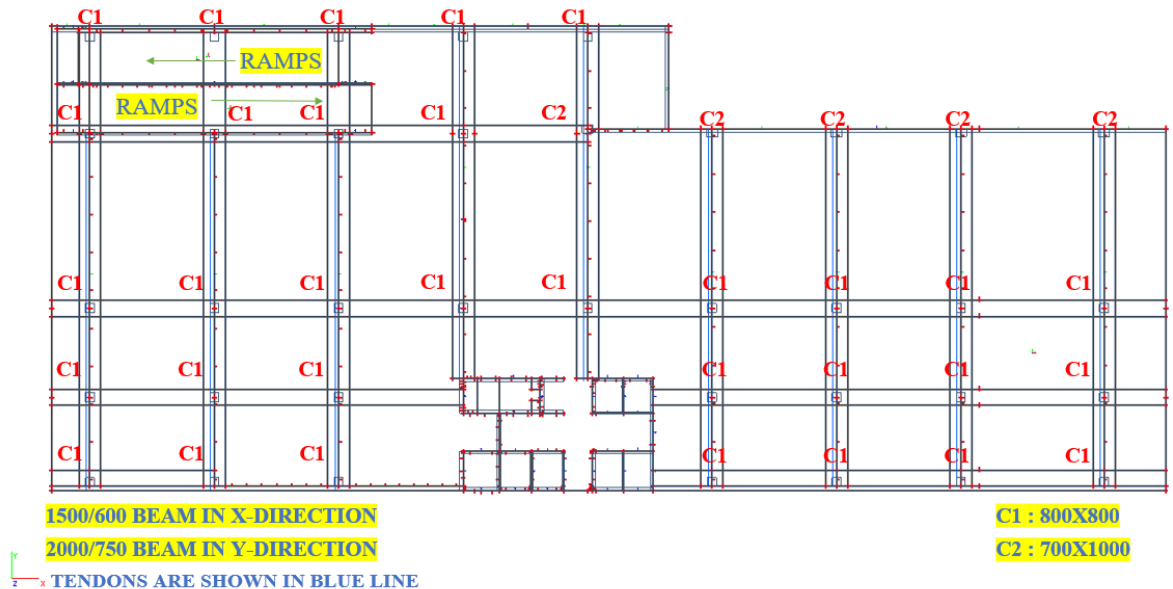

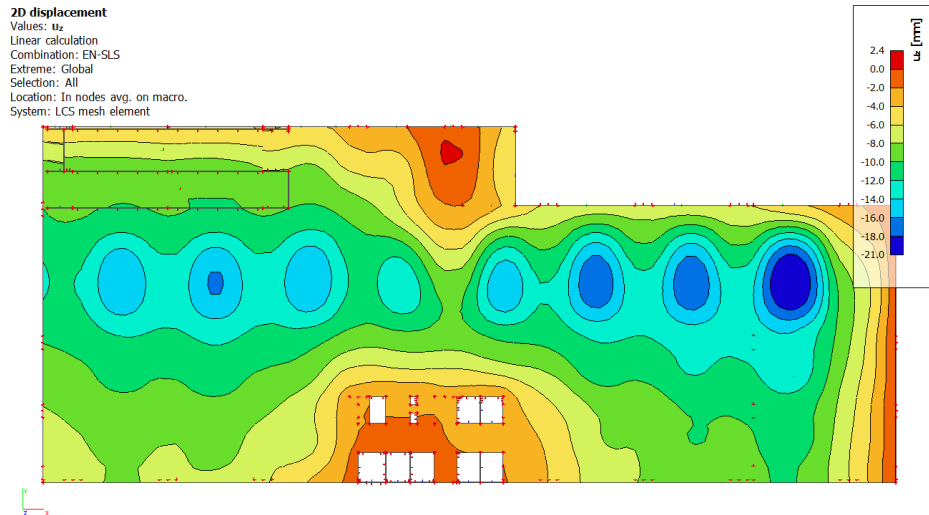*Figure 118: Layout of 2NP with tendons*

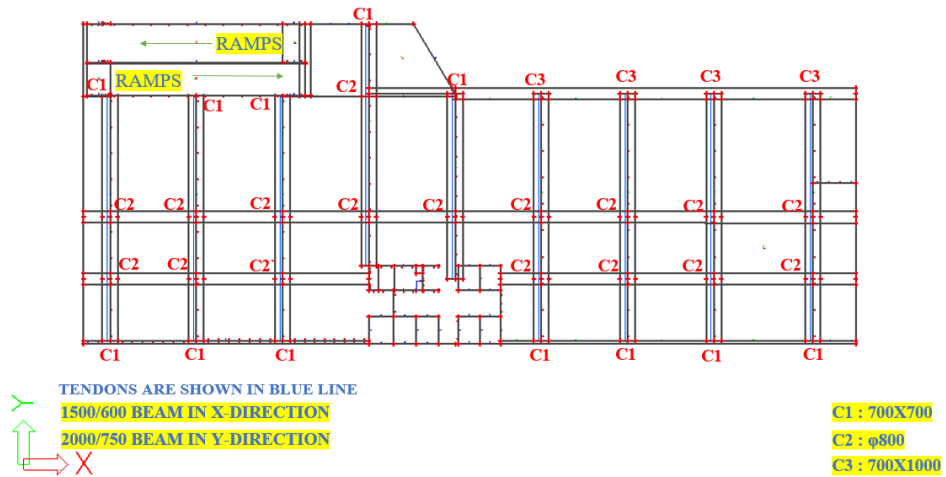*Figure 119: Display of 2D Displacement due to SLS-Quasi on 2NP*

3NP:

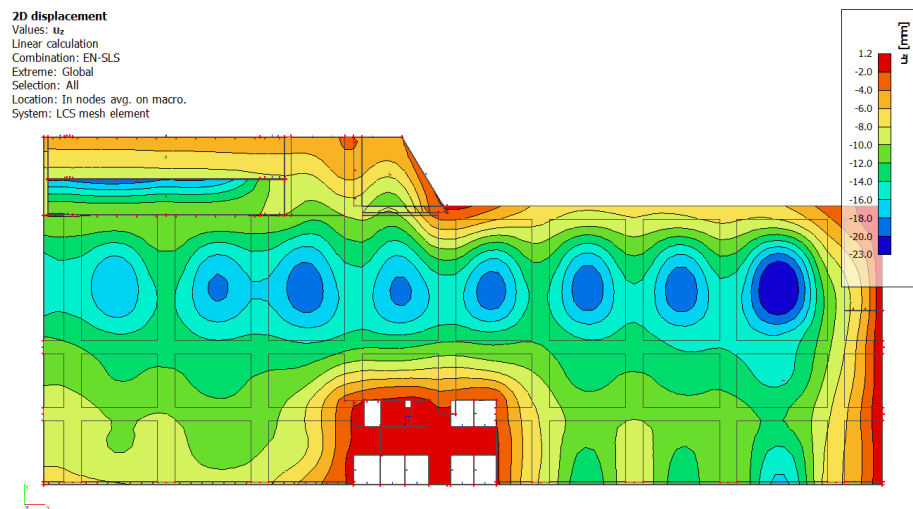*Figure 120: Layout of 3NP with tendons*

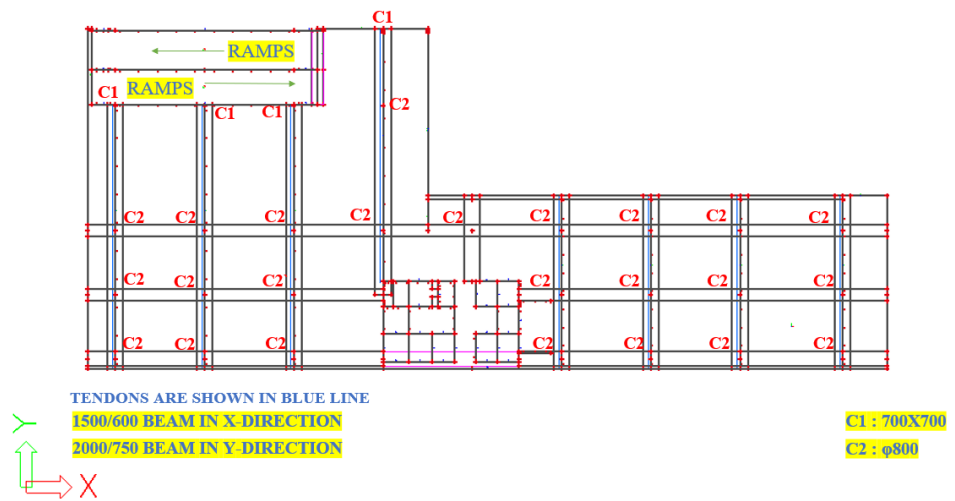*Figure 121: Display of 2D Displacement due to SLS-Quasi on 3NP*

4NP:

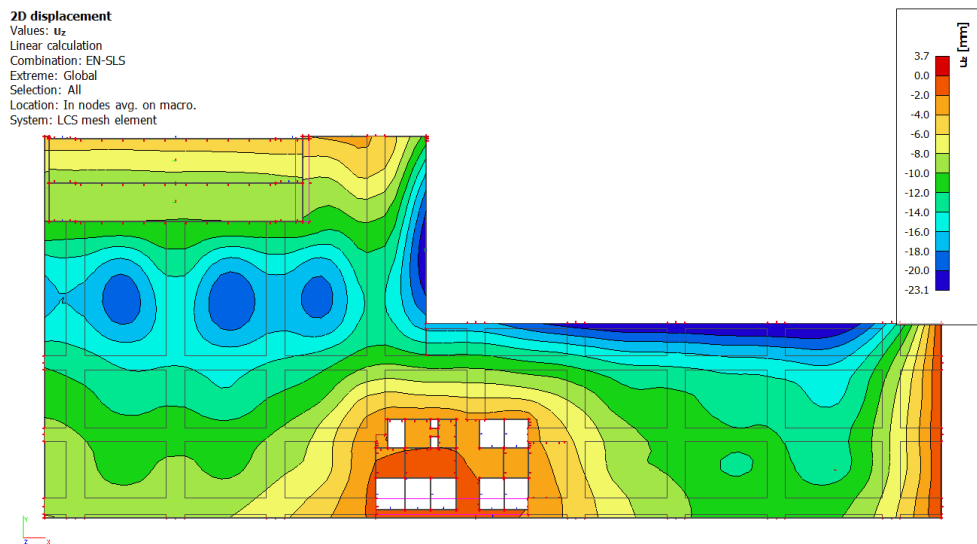*Figure 122: Layout of 3NP with tendons*

Figure 123: Display of 2D Displacement due to SLS-Quasi on 4NP
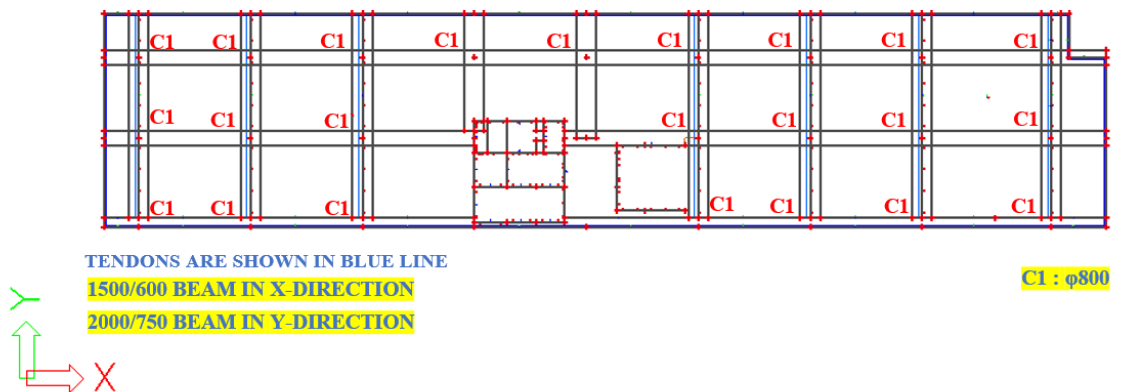
5NP:

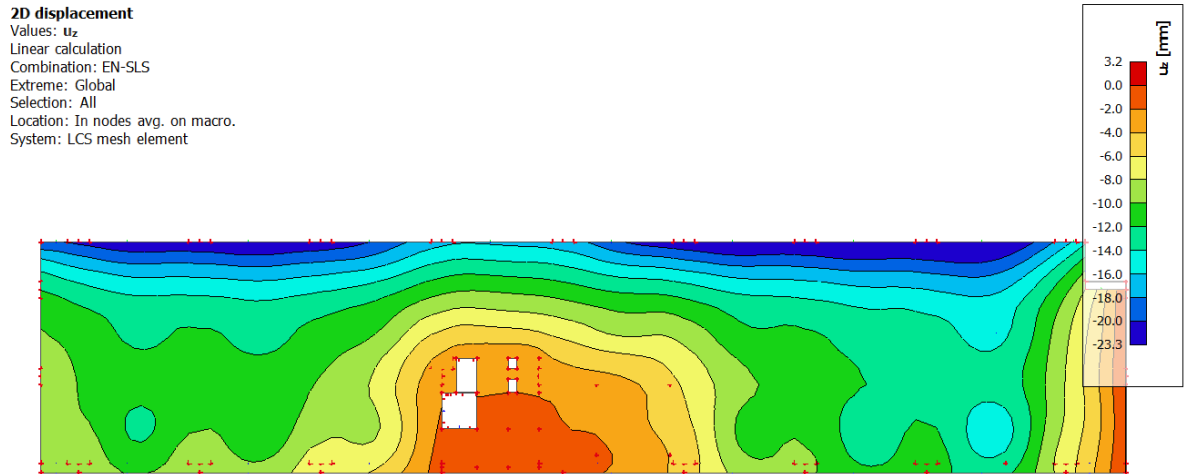*Figure 124: Layout of 5NP with tendons*

Figure 125: Display of 2D Displacement due to SLS-Quasi on 5NP

4.5.3 Design of staircase

4.5.3.1 Geometry

Thickness of main slab = 250mm,

Thickness of flight = 150

Riser (R) = 176 & 172mm (as per given by designer report)

Tread (T) = 270mm (given)

Number of riser per flight = 11nos (given), otherwise we can calculate it by number of riser divided by 2, where number of riser is floor to floor height by riser.

Number of tread per flight = 11-1 = 10 nos

Total going (G) = 10*270=2700mm

Width of flight = 1200mm, Length of flight = 2700mm

Width of landing = 2600mm, Length of landing = 1300mm

Width of gap between the flights = 200mm

Width of staircase = (1200x2) + 200 = 2600mm

Perpendicular and head clearance of the staircase:

- Head clearance has to be more than $1500 + \frac{750}{\cos 45.5256} = 2570.53mm > 2100mm$

Perpendicular clearance has to be more than $750 + 1500 * \cos(45.53) > 1900$

$$h_1 = h_k - h_s - h_f - h = 2750 - 250 - 150 - 270 = 2080mm$$
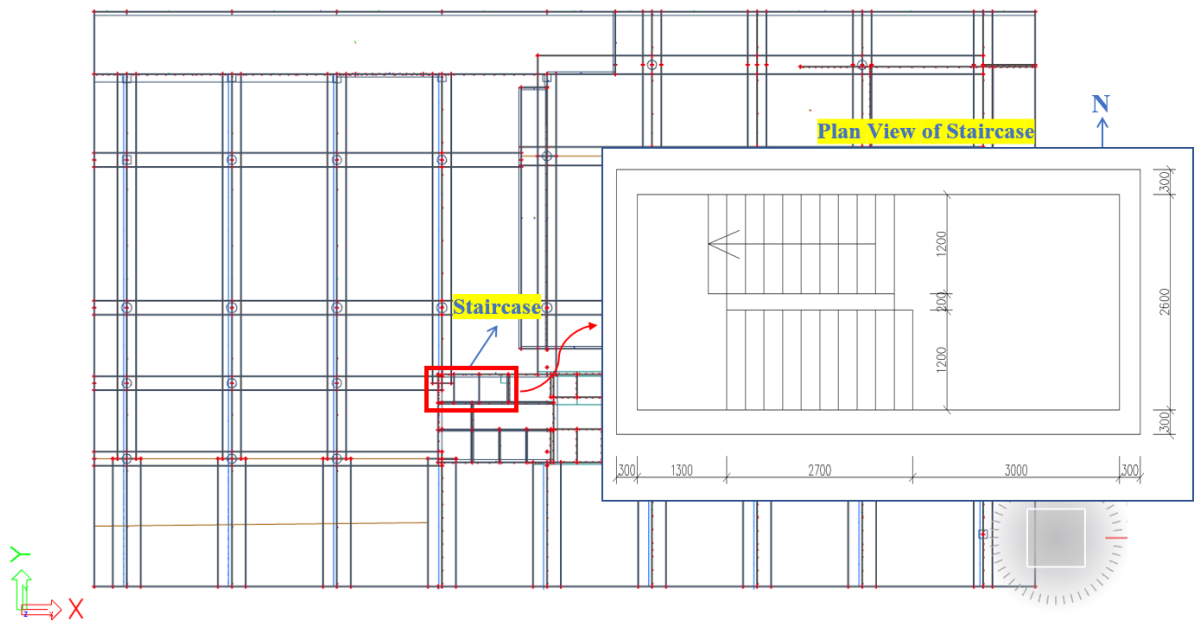
$$h_2 = 2080 * \cos(45.525)$$

Figure 126: Layout of the floor 1PP showing the location of the staircase

Preliminary check of the depth of the slab:

- The staircase is considered as one-way simply supported slab with the span of 7000mm.

- The depth should be at least 7000mm/25 = 280mm.

- The depth of landing is 200mm (given)
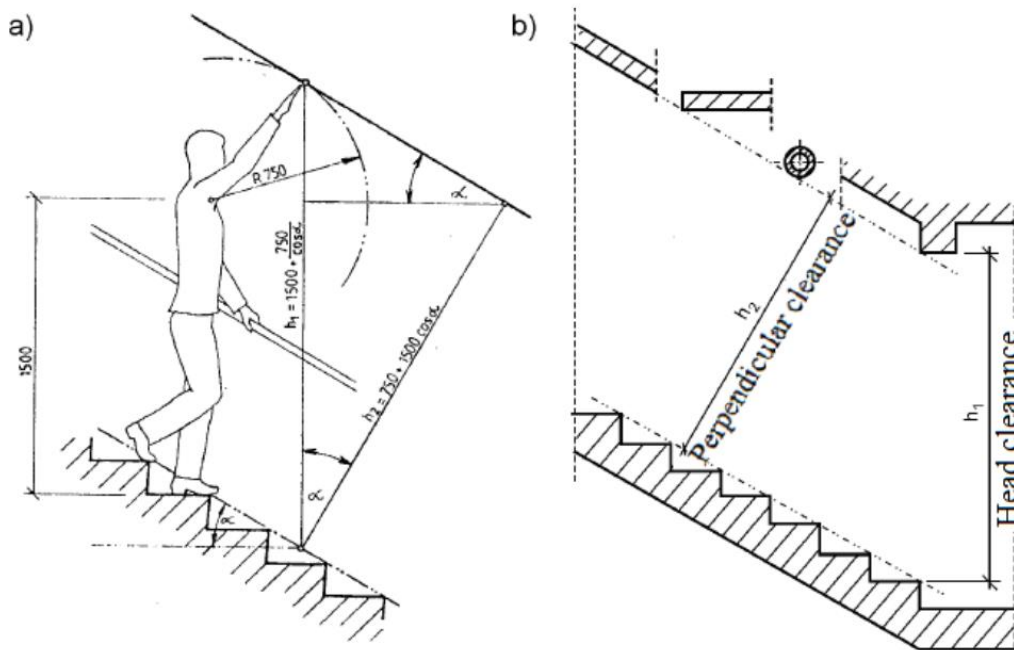
- The depth of flight is 150mm (given)

Figure 127: Basic principle regarding the staircase

Calculation of the loads

Self-weight of waist slab $= \dfrac{h_{waist}}{\cos(32.5)} * 25 * 1 = \dfrac{150}{\cos 32.5} * 25 * 1 = 4.45 kN/m$

Self-weight of step $= \dfrac{R}{2} * 25 * 1 = \dfrac{0.172}{2} * 25 * 1 = 2.15 kN/m$

Self-weight of slab for landing $= 0.2*25 = 5kN/m^2$

Floor load $= 0.75kN/m^2$

Live Load $= 5kN/m^2$

Total load $= f_{d,flight} = 1(6.6 + 0.75 * 1) + (0.30 * 5 * 1) = 8.85 kN/m$

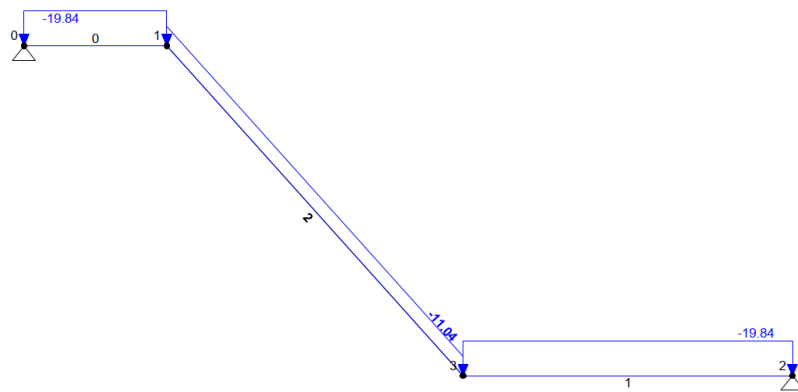$$f_{d,landing} = 1(5 + 0.75 * 1) + (0.30 * 5 * 1) = 7.25 kN/m$$

Figure 128: Schematic of the staircase showing the load acts on it

1D internal forces
Values: M_y
Linear calculation
Combination: SLS-Quasi flight
Coordinate system: Principal
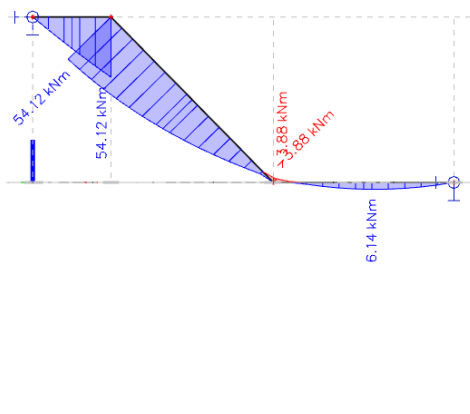Extreme 1D: Member
Selection: All

Figure 129: Display showing the internal forces my due to SLS on staircase

135

M = 54.12kNm

$$d = h_w - C_{nom} - \frac{\emptyset}{2} = 200 - 30 - 6 = 164mm$$

$$A_{s,req} = \frac{M_{Ed}}{0.87 * fy * d} = \frac{54.12 * 10^6}{0.87 * 435 * 0.9 * 697.5} = 968.86mm^2$$

$Say\ 9\emptyset12mm\ at\ 110mm,\ A_{s,prov} = 1017.88mm^2$

Check

5) $M_{Rd} \geq M_{Ed}$

$$x = \frac{f_{yd} * A_{s,prov}}{0.8 * b * f_{cd}} = \frac{435 * 1017.88}{0.8 * 1000 * 23.33} = 23.724mm$$

$$z = d - 0.4x = 164 - (0.4 * 23.724) = 154.51mm$$

$$M_{Rdy} = A_{s,prov} * f_{yd} * z = 1017.88 * 435 * 154.51 = 68.41kNM$$

$So,\ M_{Rd}(= 68.41) > M_{Ed}(= 54.12) \ldots \ldots \ldots \ldots \ldots \ldots OK$

6) $\varepsilon \leq \varepsilon_{bal} \approx 0.64$

$$\varepsilon = \frac{x}{d} = 0.144 < 0.64 \ldots \ldots \ldots \ldots OK$$

7) $\rho_{min} \leq \rho \leq \rho_{max}$

$$0.0015 \leq \frac{A_{s,prov}}{bd} \leq 0.4$$

$$0.0015 \leq \frac{1017.88}{1000 * 164} = 0.006 < 0.4 \ldots \ldots \ldots \ldots OK$$

8) $\varepsilon_s \leq \varepsilon_{cu}(5\%)$

$$\varepsilon_s = \frac{0.0035(d-x)}{x} = \frac{0.0035(164-23.724)}{23.724} = 2\% < 5\% \dots \dots \dots OK$$

Check for deflection:

K = 1, since $\rho < \rho_0$

$$\frac{L}{d} = k \left[11 + 1.5\sqrt{f_{ck}}\frac{\rho_0}{\rho} + 3.2\sqrt{f_{ck}}\left(\frac{\rho_0}{\rho} - 1\right)^{1.5} \right]$$

$$\beta_s = \frac{310}{\sigma_s} = \frac{310}{256.71} = 1.2075$$

$$\sigma_s = \frac{310 * f_{yk} * A_{S_{req}}}{500 A_{S_{prov}}} = 256.71$$

$$Allowable\frac{span}{depth}ratio = \beta_s * \frac{L}{d} = 1.2075 * 7300 = 53.75mm$$

$$Actual\frac{span}{depth}ratio = \frac{7300}{164} = 44.51mm$$

Shear Design:

Figure 130: Display showing the axial force acting on the staircase due to SLS

$V_{Ed} = 55.81kN$

$$C_{Rdc} = \frac{0.18}{1.5} = 0.12$$

$$K = 1 + \sqrt{\frac{200}{d}} = 1 + \sqrt{\frac{200}{164}} = 2.1043$$

$$V_{min} = 0.035k^{1.5} * f_{ck}{}^{0.5} = 0.5160$$

$$V_{Rd,c} = [C_{Rdc} * k(100\rho_1 f_{ck})^{0.33}] = 0.6085 > 0.5160 \dots\dots\dots OK$$

No shear reinforcement is required, shear is ok

Detailed of staircase is given in attached drawings.

4.5.4 Design of Ramp

Figure 131: Layout of the 2NP showing the location of the ramp

Layout of ramp:

Figure 132: Geometry of the ramp

Plate thickness = 250mm

Fall (slope) = 14% given
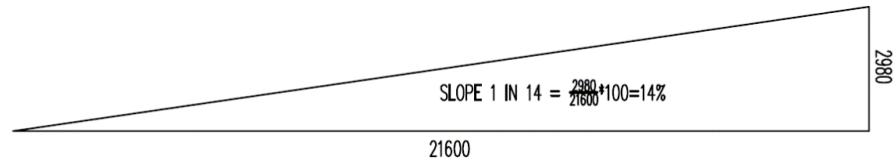
Figure 133: Slope of the ramp

4.5.4.1 Material characteristics

Concrete: C30/37, XC4, XD3, XM2 – CL 0.4, Dmax 16-S3

Steel: B500B

Concrete cover: 35mm

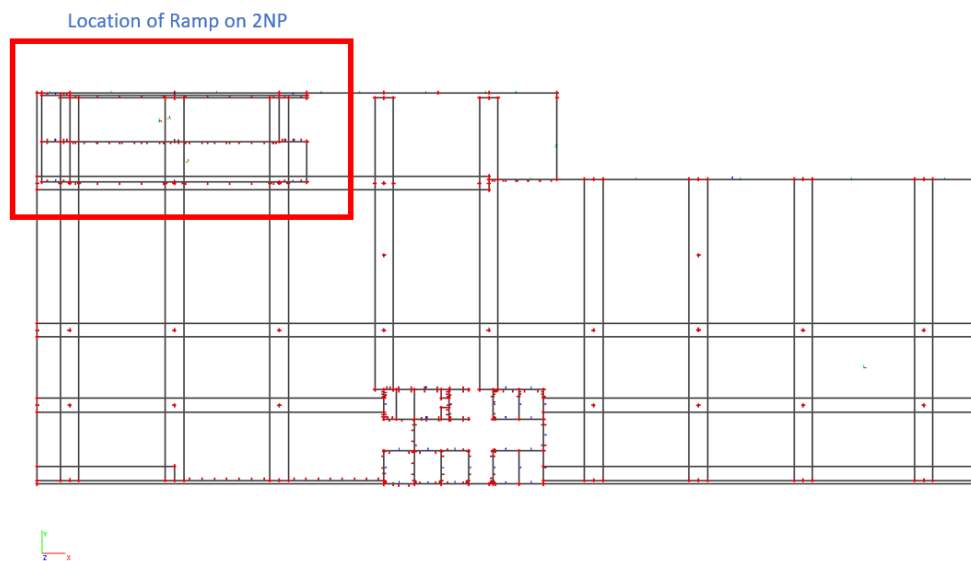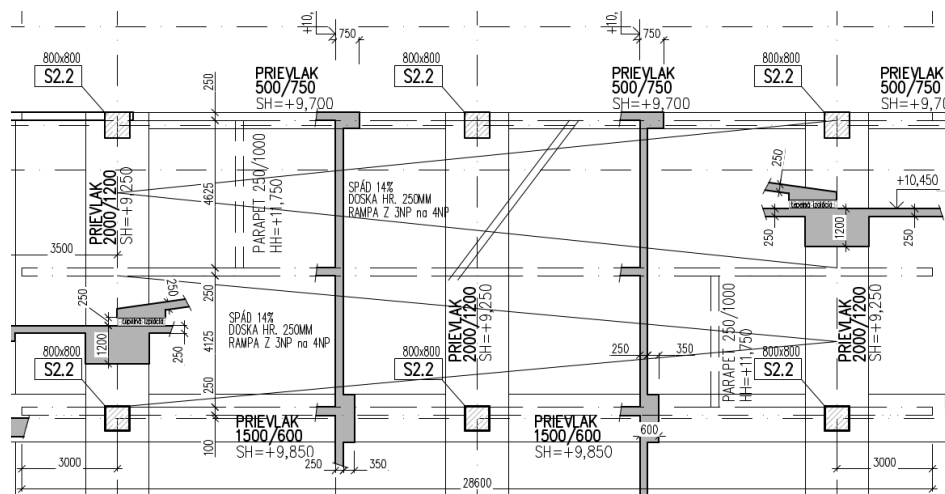Waterproof concrete with seepage max. 50mm,

Thermal insulation is provided at landing of ramp of height 250mm

Concrete

Concrete C30/37, D_{max} 16mm (See 3.1)

Characteristic compressive strength of concrete (f_{ck}) = 30MPa

Design compressive strength of concrete (f_{cd}) = $\frac{f_{ck}}{\gamma_d} = \frac{30}{1.5} = 20MPa$

Steel

Steel B500B

Characteristic yield strength of reinforcement (f_{yk}) = 30MPa

Design yield strength of reinforcement (f_{yd}) = $\frac{f_{yk}}{\gamma_s} = \frac{500}{1.15} = 435MPa$

Cover of concrete layer: $C_{nom} = C_{min} + \Delta C_{dev}$

Where, allowance for design deviation = $\Delta C_{dev} = 10\ mm$

Degree of environmental influence:

Corrosion induced by carbonation: $XC4$

Corrosion induced by chlorides: $XD3$

Construction class : S3

Minimum covering layer in terms of cohesion: $C_{min,b} = 12mm$

$$C_{min} = \max(C_{min,b}; C_{min,dur}, 10) = (12,25,10) = 25$$

Total cover for concrete layer $= C_{nom} = C_{min} + \Delta C_{dev} = 25 + 10 = 35mm$

4.5.4.2 Design and check for reinforcement of slab on 1PP – Left Side of slab (SLS)

Slab thickness = 250mm

Assume $\emptyset = 10mm$, $\emptyset_{stirrups} = 8mm$, $C_{nom} = 35mm$

Moment $\left|M_{Ed,x}\right| = 100.23kNm$

Effective cross-section height:

$$d_x = h_x - C_{nom} - \emptyset_{stirrups} - \emptyset = 250 - 35 - 10 = 210mm$$

$$A_{s,req} = \frac{M_{Ed}}{0.87 * fy * z} = \frac{100.23 * 10^6}{0.87 * 435 * 0.9 * 210} = 1401.29mm^2$$

Say $18\emptyset10mm$ at $150mm$, $A_{s,prov} = 1413.72mm^2$

Check

1) $M_{Rd} \geq M_{Ed}$

$$x = \frac{f_{yd} * A_{s,prov}}{0.8 * b * f_{cd}} = \frac{435 * 1413.72}{0.8 * 1000 * 20} = 38.44mm$$

$$z = d - 0.4x = 210 - (0.4 * 38.44) = 194.624mm$$

$$M_{Rdy} = A_{s,prov} * f_{yd} * z = 1413.72 * 435 * 194.624 = 119.7kNM$$

So, $M_{Rd}(= 119.7) > M_{Ed}(= 100.23kNm) \dots \dots \dots \dots \dots \dots \dots OK$

2) $\varepsilon \leq \varepsilon_{bal} \approx 0.64$

$$\varepsilon = \frac{x}{d} = 0.1830 < 0.64 \dots \dots \dots \dots \dots OK$$

3) $\rho_{min} \leq \rho \leq \rho_{max}$

    % of req tensile r/f

$$0.0015 \leq \frac{A_{s,prov}}{bd} \leq 0.04$$

$$0.0015 \leq \frac{1413.72}{1000 * 210} = 0.00673 \leq 0.04 \ldots \ldots \ldots \ldots OK$$

4) $\varepsilon_s \leq \varepsilon_{cu}(5\%)$

$$\varepsilon_s = \frac{0.0035(d - x)}{x} = \frac{0.0035(210 - 38.44)}{38.44} = 1.56\% < 5\% \ldots \ldots \ldots OK$$

SLS – Deflection Check (7.4EN 1992-1-1)

$$\frac{l}{d} = k\left[11 + 1.5\sqrt{f_{ck}}\frac{\rho_0}{\rho} + 3.2\sqrt{f_{ck}}\left(\frac{\rho_0}{\rho} - 1\right)^{3/2}\right] = 208.17$$

$$\left(\frac{l}{d_{allowable}}\right) = 208.17 * 1 * \frac{1413.72}{1401.288} = 210.02$$

$$\left(\frac{L}{d_{actual}}\right) = \frac{22800}{210} = 108.57 < 234.404 \ldots \ldots \ldots \ldots Ok$$

SLS – Shear Check

$$k = \left(1 + \sqrt{\frac{200}{d}}\right) = 1.995 > 2$$

$$\rho_1 = 0.006158$$

$$V_{Rd,c} = \left[0.12k(100 * \rho_1 * f_{ck})^{1/3}\right]b_w * d = 117.56kN > V_{Ed} = 63.95kN$$

$$V_{Rd,cmin} = 9.76kN$$

SLS – Long Term Deflection Check:

Limit deflection under quasi-steady load combination:

$$w_{g,lim,1} = \frac{1}{250}.l = \frac{4125}{250} = 16.5 \, mm$$

So,

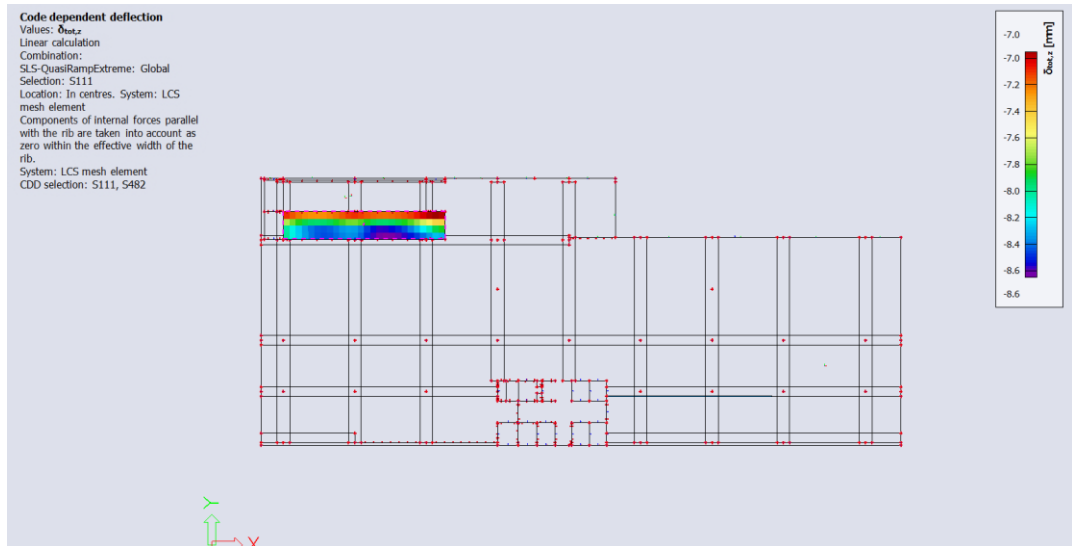$$w_{g,lt,1} = 8.6mm \ < \ w_{g,lim,1} = 45.2 \, mm \ldots \ldots \ldots \ldots Ok$$

Figure 134: Display showing the long term deflection on one side of ramp due SLS Quasi on 2NP
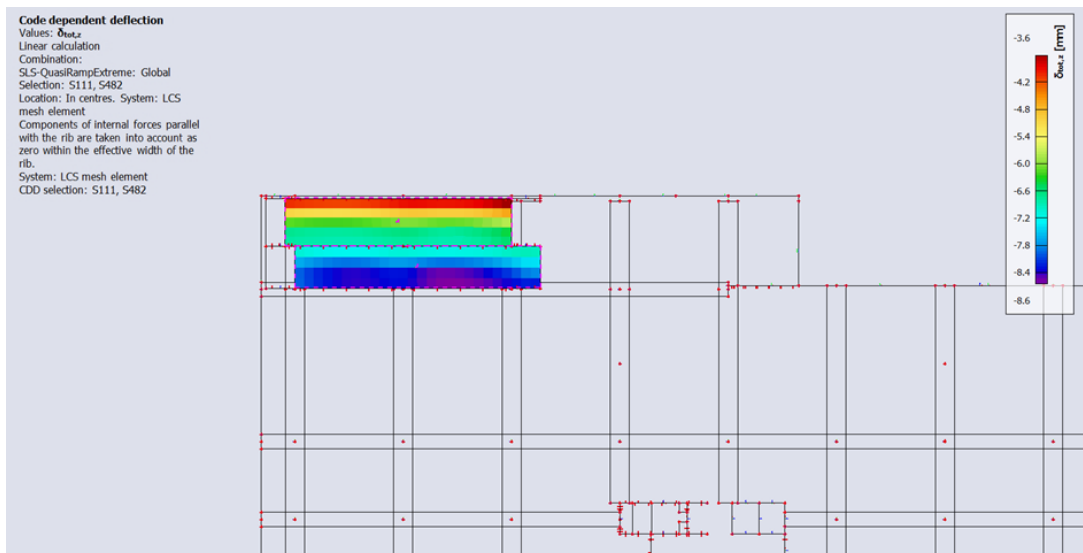

Figure 135: Display showing the long term deflection on both side of ramp due SLS Quasi on 2NP

4.5.5 Design of Shear Wall

The procedure for designing a concrete wall is very similar to the design of concrete columns. Slenderness must be checked about the minor axes of the wall, the design moment determined by considering the effect of imperfections and second-order effect if critical. Finally, reinforcement is provided using column interaction charts.

In our model, shear walls are provided in each floors, but most of the shear walls are not continuous one over other, but the core walls (shear wall) near the staircase and lifts are continuous from ground floor to the roof. So, we choose one of that shear wall for our further designing. Before to proceed, first we analyze the actions required to design the wall but calculating the action on roof as well as on each floor. Previously in 4.4.2, we already calculate the wind pressure so we used that here for further calculations.
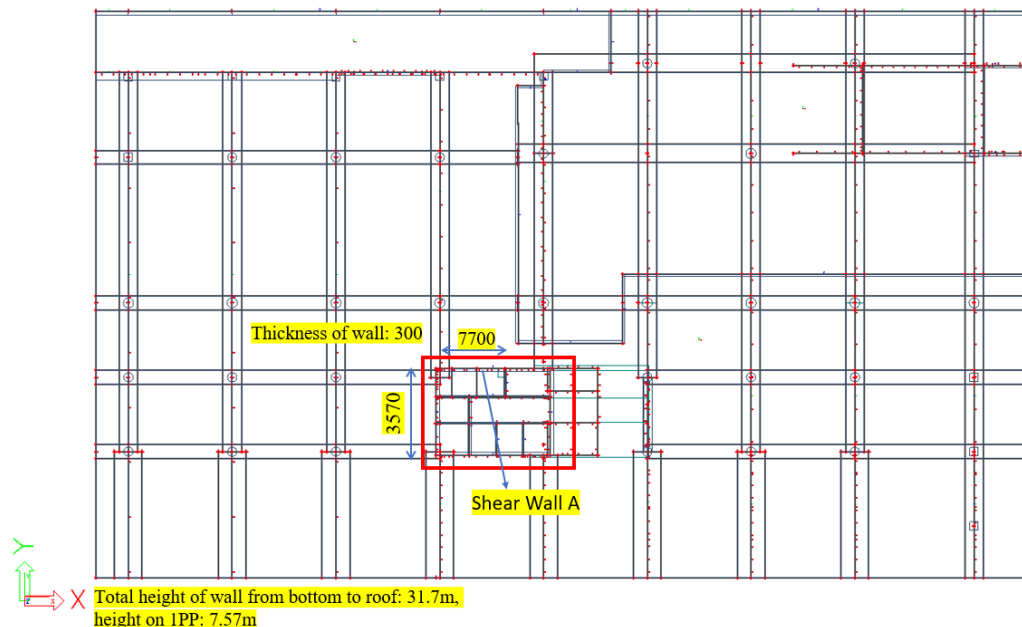
Figure 136: Layout of the 1PP showing the location of shear wall (core wall) near the staircase

Action from roof:

Permanent Action: $Roof\ Load = \left(7.7 + \frac{7.7/2}{2}\right)\left(\frac{7.7}{2} + \frac{7.7/2}{2}\right) * 8.65 = 480.80kN$

On roof: g_k=8.65kN/m^2, q_k=5.84kN/m^2,

$Wall\ weight = (0.3 * 2.55 * 7.7 * 25) = 147.2625kN$

Total $G_{k,roof}$ = 628.06kN

Variable Action: $Roof\ Load = \left(7.7 + \frac{7.7/2}{2}\right)\left(\frac{7.7}{2} + \frac{7.7/2}{2}\right) * 5.84 = 324.61kN$

Action from floor:

Permanent Action: $Floor = \left(7.7 + \frac{7.7/2}{2}\right)\left(\frac{7.7}{2}\right) * 8.65 = 320.54 kN$

$$Stair = \left(\frac{3.85}{2}\right)(7.7) * 8.65 = 128.21 kN$$

$$Wall\ weight\ by\ floor = 4NP = 0.3 * 3.5 * 7.7 * 25 = 202.13 kN$$

Similarly carried out for all other floors and values are shown in following table.

Variable Action: Floor = 185.28kN

Stair = 48.125kN, Total =233.405kN

Imposed load reduction factor can be applied to wall based on number of storeys,

$$\alpha_n = 1 - \frac{n}{10}$$

Where, n = no. of floor supported

Floor	α_n	Gk (kN)	Gk	Qk (kN)	Qk(kN)	Qk(kN)
			Cummulative		Cum.	red.
R-5NP	1	628.06	628.06	324.61	324.61	324.61
5NP-4NP	0.9	650.88	1278.94	233.41	558.02	502.218
4NP-3NP	0.8	633.55	1912.49	233.41	791.43	633.144
3NP-2NP	0.7	766.38	2678.87	233.41	1024.84	717.388
2NP-1NP	0.6	766.38	3445.25	233.41	1258.25	754.95
1NP-1PP	0.5	855.91	4301.16	233.41	1491.66	745.83
1PP-2PP	0.4	671.09	4972.25	233.41	1725.07	690.028

Table 7: Axial load acting on the each floor

Now, we need axial force at mid height and base of wall,

At mid height: G_k = 2678.77kN, Q_k = 1024.84kN

1) Assuming imposed loading is leading variable action and wind is accompanying variable action, then $N_{Ed} = 1.35G_k + 1.5Q_k = 5153.74kN$,

2) Assuming wind loading is leading variable action and imposed loading is accompanying variable action, then $N_{Ed} = 1.35G_k + 1.5\psi Q_k = 4692.52kN$, where ψ = 0.7

Similarly, for at base:

1) N_{Ed} = 9342.14kN

2) N_{Ed} = 8565.41kN

In plane moments:

By inspection, walls are symmetrical about plane of action of wind actions. Therefore, shear centre of wall will coincide with point of application of wind load, hence effect of torsion can be neglected.

Wind is being shared according to stiffness of wall is 0.198~0.20, i.e., 20% of wind load taken by wall. (I $= 7.61$mm^4, I$_{lc}$=23.12).

$$W_k = \frac{0.20}{100} * 0.541 * 101.2 = 0.11 kNm$$

Overturning Moment:

At mid height:

$$M = W_k * \frac{\left(\frac{31.7}{2}\right)^2}{2} = 13.82 kNm$$

Assuming wind loading is leading variable action and imposed loading is accompanying variable action, $M_{Ed,y} = 1.5M = 20.73 kNm$,

Assuming imposed loading is leading variable action and wind action is accompanying variable action, , $M_{Ed,y} = 1.5\varphi M = 1.5 * 0.5 * M = 10.37 kNm$

Similarly,

At base:

$$M = W_k * \frac{(31.7)^2}{2} = 55.27 kNm$$

Assuming wind loading is leading variable action and imposed loading is accompanying variable action, $M_{Ed,y} = 1.5M = 82.91 kNm$,

Assuming imposed loading is leading variable action and wind action is accompanying variable action, , $M_{Ed,y} = 1.5\varphi M = 1.5 * 0.5 * M = 41.45 kNm$

Transverse Moment:

Wall (k$_{w1}$) = I/L $= \frac{7.7*0.3^3}{12*7.57} = 2.2866 x 10^6$, (kw2) $= 3.15 x 10^6$

Slab (k_s) = 1.75×10^6

Imposed load leading = $M_f = 9.625[(1.35*8.65) + (1.5*8)] * \frac{7.7^2}{12} = 911.996 kNm$

$$M_{Ed,z} = \frac{k_w}{(2.2866*10^6*3.15*10^6) + (1.75*10^6)} * M_f = 232.99 \approx 233 kNm$$

Wind load leading = $M_f = 9.625[(1.35*8.65) + (1.5*0.7*5)] * \frac{7.7^2}{12} = 804.99 kNm$

$$M_{Ed,z} = \frac{k_w}{(2.2866*10^6*3.15*10^6) + (1.75*10^6)} * M_f = 205.66 kNm$$

Axial Force in wall:

1) At mid height: $f_t = \frac{N}{Lh} \pm \frac{6M}{hL^2} = \frac{4692.52*10^3}{7700*300} \pm \frac{6*20.73*10^6}{300*7700^2} = 2.04 N/mm^2$

   Force in wall $N_{max} = 2.04 * 300 = 612 kN$

2) At base: $f_t = \frac{N}{Lh} \pm \frac{6M}{hL^2} = \frac{8565.41*10^3}{7700*300} \pm \frac{6*82.91*10^6}{300*7700^2} = 3.75 N/mm^2$

   Force in wall $N_{max} = 3.75 * 300 = 1124.94 kN$

Slenderness verification:

As per clause 5.6.2, slenderness verification is more critical for stack at mid height than base so check will be carried out for base only.

$$\omega = 0.003 * \frac{f_{yk}}{f_{ck}} = 0.033$$

$$\varepsilon = 0.69 * \sqrt{\frac{(1 + 2\omega)(1000hf_{ck})}{Nmax}} \geq 1.0$$

$$\varepsilon = 2.4678 > 1.0$$

$$M_{1,z} = -205.66 kNm, M_{2,z} = 205.66 kNm$$

Now, first we check the wall is slender or not for 1PP,

$$l_{0,z}0.75 * 7.57 = 5.6775 = 5677.5$$

$$\frac{l_{0z}}{h} \leq 4.38\left(1.7 - \frac{M_{1,z}}{M_{2,z}}\right)$$

$$\frac{5677.5}{300} = 18.925 < 29.18 \dots \dots \dots \dots Wall\ is\ NOT\ Slender$$

$$M_{Ed,z} = \max\ (M_2; M_{z,i} + N_{Ed}(e_{2,z} + e_a)$$

$$M_{2,z} = 0.6M_{2z} + 0.4M_{1z} > 0.4M_{2,z}$$

$$M_{2,z} = 41.32 < 82.264$$

$$e_a = \frac{\theta_i * l_{0,z}^2}{2} = \frac{1 * 5677.5}{400 * 2} = 7.096$$

$$So, M_{Ed,z} = 205.66 kNm$$

Design for reinforcement

As per clause 9.6.2(1) and 9.6.3(1) of BS EN 1992-1-1,

$$d_2 = 30 + \frac{16}{2} + 10 + 8 = 56mm$$

$$\frac{d_2}{h} = \frac{56}{300} = 0.28$$

Using d/h chart, we get area of reinforcement,

$$\frac{M}{bh^2 f_{ck}} = \frac{205.66 * 10^6}{1000 * 300^2 * 45} = 0.051$$

$$\frac{N}{bh f_{ck}} = \frac{612 * 10^3}{1000 * 300 * 45} = 0.05$$

$$\frac{A_s * f_{yk}}{bh f_{ck}} = 0.1, (From\ chart)$$

$$A_s = \frac{0.1 * 1000 * 300 * 45}{500} = 2700mm^2$$

This is the area on the both side of wall, so area per face is 2700/2 = 1350mm²/m/face.

So, try 7φ16@150mm c/c, $A_{spro} = 1407.44mm^2$

Check:

Minimum $A_s = 0.002A_s = 0.002 * 1000 * 300 = \frac{600mm^2}{m} = \frac{600}{2} = 300mm^2\ per\ face$

Horizontal r/f = $A_s = \max(0.25A_{sprov}, 0.001A_c) = (351.86, 300) = 351.86mm^2$

So, try 4φ12@250mm c/c, $A_{spro} = 452.4mm^2$

Detailed of reinforcement shown in drawings.

4.5.5 Design of Column

As we saw 4.5.2, first we did the static analysis for 1PP floor by applying the tendons on left side first then on entire slab of 1PP as we got more displacement on this floor particularly on left side so after the complete design and check for reinforcement on left side of 1PP, we decided to follow the same path for designing of the column.

Hence, initially we started by choosing the higher size of column on left side of 1PP which is near to area of maximum displacement, is highlighted by green color in red box, viz., C1, C2 & C3 (fig.137). These columns are continuous from underneath the ground floor (2PP) to 5NP. Though there are many different sizes of column was used in entire structure ranging from 800x900, 900x900, 800x900, φ1000, φ1100, and φ600, but the designing procedure for all these columns are almost similar, only differ in the height of the column based on the floor.
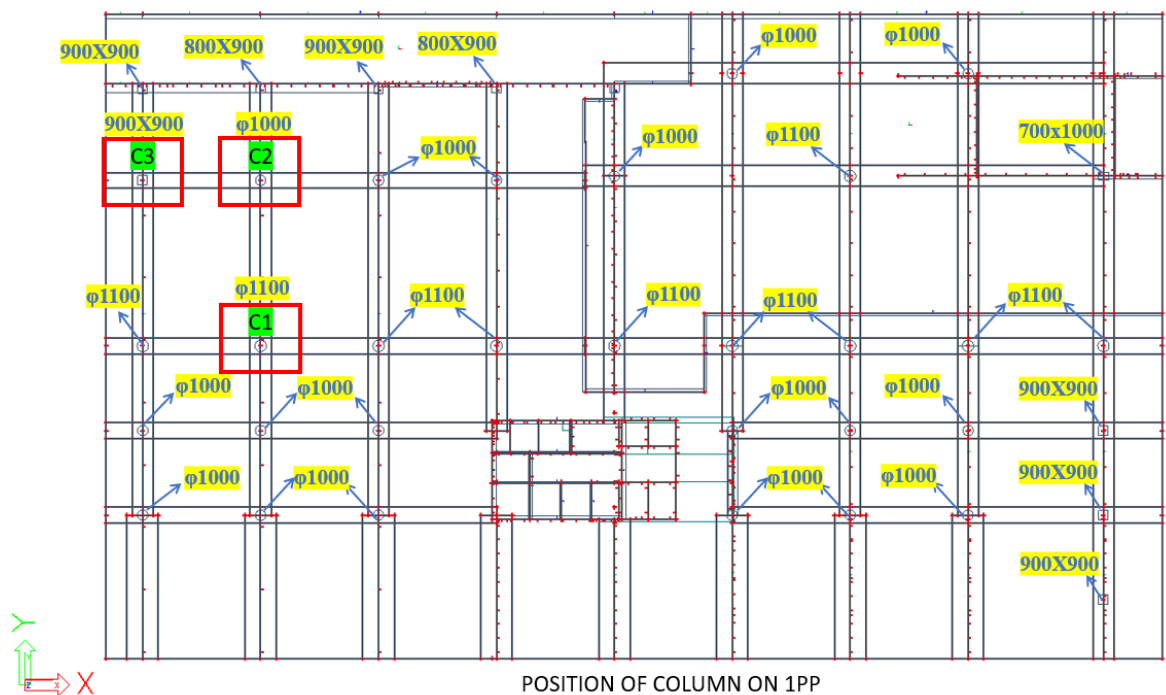

Figure 137: Layout of the 1PP showing the position of column

4.5.5.1 Material characteristics

Concrete: C45/55, XC1 – Dmax 16-S3

Steel: B500B

Concrete cover: 30mm

Concrete

Concrete C45/55, D_{max} 16mm (See 3.1)

Characteristic compressive strength of concrete (f_{ck}) = 45MPa

Design compressive strength of concrete (f_{cd}) = $\dfrac{f_{ck}}{\gamma_d} = \dfrac{45}{1.5} = 30MPa$

Steel

Steel B500B

Characteristic yield strength of reinforcement (f_{yk}) = 500MPa

Design yield strength of reinforcement (f_{yd}) = $\dfrac{f_{yk}}{\gamma_s} = \dfrac{500}{1.15} = 435MPa$

Cover of concrete layer: $C_{nom} = C_{min} + \Delta C_{dev}$

Where, allowance for design deviation = $\Delta C_{dev} = 10\ mm$

Degree of environmental influence:

Corrosion induced by carbonation: $XC1$

Construction class : S3

Total cover for concrete layer = $C_{nom} = C_{min} + \Delta C_{dev} = 20 + 10 = 30mm$

4.5.5.2 Design and check for reinforcement of column C1(ULS)

To design the column, first we need the axial force (N_{Ed}) and moments at top and bottom of the column, which is taken from the Scia Engineer.
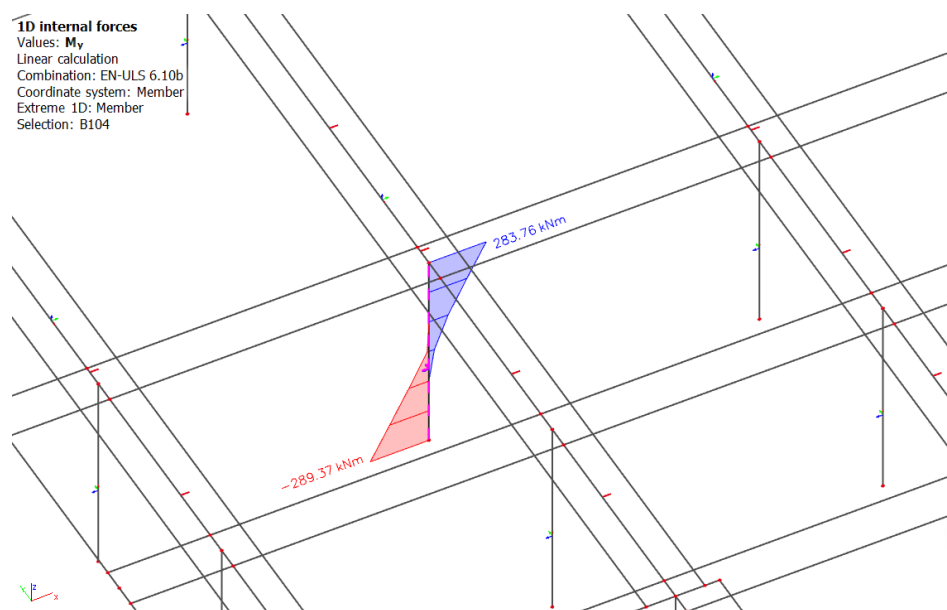

Figure 138: Display showing the moment my on selected column C2 due to ULS on 1PP

N_{Ed} = 17859.86kN

M_{top} = 283.76kNm

M_{bottom} = -289.37kNm

Diameter of column (d) = 1100mm

Now, first we need to check whether column is slender or not, for that as per Eurocode,

$$\lambda \geq \lambda_{lim} \ldots \ldots \ldots Slender\ column$$

Where,

$$\lambda = \frac{l_o}{i} = \frac{l_o}{\sqrt{\frac{I}{A_c}}},$$

$$For\ circular\ column = \frac{4 * l_o}{d} = \frac{4 * 4.6848}{1100} = 17.04$$

$$l = floor\ to\ floor\ height - thickness\ of\ slab = 7.57 - 0.25 = 7.32m = 7320mm$$
$$l_o = F * l = 0.64 * 7.320 = 4.6848$$

To calculate F, using the PD6687 method,

$$k = k1 = k2 = \frac{EI_c/L_c}{\sum \frac{2EI_b}{L_b}} = \frac{\frac{1100^4/12}{11975}}{\frac{2 * 11975 * 750^3/12}{11300}} = 0.1367 \cong 0.14$$
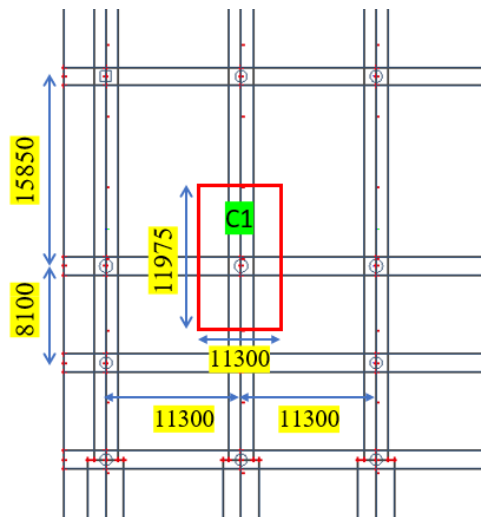

Figure 139: Area on which axial load which act on C1

150

k2	k1										
	0.10	0.20	0.30	0.40	0.50	0.70	1.00	2.00	5.00	9.00	Pinned
0.10	0.59	0.62	0.64	0.66	0.67	0.69	0.71	0.73	0.75	0.76	0.77
0.20	0.62	0.65	0.68	0.69	0.71	0.73	0.74	0.77	0.79	0.80	0.81
0.30	0.64	0.68	0.70	0.72	0.73	0.75	0.77	0.80	0.82	0.83	0.84
0.40	0.66	0.69	0.72	0.74	0.75	0.77	0.79	0.82	0.84	0.85	0.86
0.50	0.67	0.71	0.73	0.75	0.76	0.78	0.80	0.83	0.86	0.86	0.87
0.70	0.69	0.73	0.75	0.77	0.78	0.80	0.82	0.85	0.88	0.89	0.90
1.00	0.71	0.74	0.77	0.79	0.80	0.82	0.84	0.88	0.90	0.91	0.92
2.00	0.73	0.77	0.80	0.82	0.83	0.85	0.88	0.91	0.93	0.94	0.95
5.00	0.75	0.79	0.82	0.84	0.86	0.88	0.90	0.93	0.96	0.97	0.98
9.00	0.76	0.80	0.83	0.85	0.86	0.89	0.91	0.94	0.97	0.98	0.99
Pinned	0.77	0.81	0.84	0.86	0.87	0.90	0.92	0.95	0.98	0.99	1.00

Table 8: Chart to calculate the value k1 & k2

So, F = 0.64

$$\lambda_{lim} = \frac{20ABC}{\sqrt{n}} = \frac{20 * 0.7 * 1.1 * 1.8627}{\sqrt{0.6264}} = 36.24$$

$$= \qquad\qquad \ldots\ldots\ldots as\ per\ EN1992, clause\ 5.8.3.1(1)$$

Where,

A = 0.7 (default)

B = 1.1 (default)

C = 1.7 – r_m = 1.7 – (M_{01}/M_{02})

Additional moment due to imperfection = $N_{Ed} * e_i = N_{Ed} * \frac{l_o}{400} = 209.17 kNm$

So, $C = 1.7 - \left(\frac{-289.37+209.17}{283.76+209.17}\right) = 1.8627$

And, $n = \frac{N_{Ed}}{A_c * f_{cd}} = \frac{17859.86*10^3}{950331.77*30} = 0.6264$

$$\lambda(= 17.04) < \lambda_{lim}(= 36.24) \ldots\ldots\ldots NOT\ Slender\ column\ \&\ M2 = 0kNM$$

So, design moment $M_{Ed} = max(M_{o2};\ M_{0Ed} + M_2;\ M_{01} + 0.5M_2;\ N_{Ed}e_0)$

$$M_{Ed} = max(492.93, 263.7, -80.2, 654.92)$$

Where,

$$M_{o2} = M + e_i N_{Ed} = 283.76 + 209.17 = 492.93 kNm$$

$$M_{0Ed} = (0.6M_{02} + 0.4M_{01}) \geq 0.4M_{02}$$

$$M_{0Ed} = \left(0.6 * 492.93 + 0.4(-80.2)\right) = 263.678 > 197.172$$

$$M_{01} + 0.5M_2 = -80.2 + 0 = -80.2 kNm$$

Using design charts:

Require d_2/h, we can find the area of reinforcement,

Assume 25mm diameter bars as main reinforcement and 10mm bars as shear links.

$$d_2 = c_{nom} + link + \frac{\emptyset}{2} = 30 + 10 + 12.5 = 52.5$$

Require $\frac{d_2}{h} = \frac{52.5}{1100} = 0.0477 \cong 0.05$

$$\frac{M}{bh^2 f_{ck}} = \frac{492.93 * 10^6}{1100^3 * 45} = 0.008 \cong 0.01, \frac{N}{bhf_{ck}} = \frac{17859.86 * 10^3}{1100^2 * 45} = 0.33$$
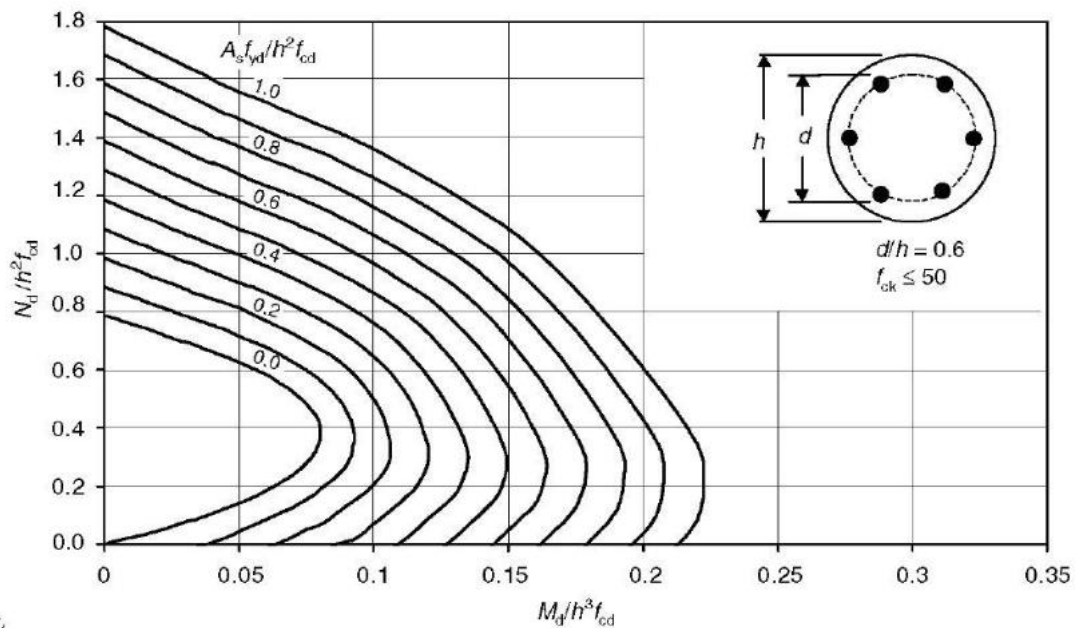
Figure 140: d/h design chart to find the area

From the values received, if we look into the chart for area we can see that,

$. \frac{A_s f_{yd}}{h^2 f_{cd}} = 0,$

So,

Minimum reinforcement as per EC, $A_s \geq \frac{0.1N_{Ed}}{f_{yd}}$ or $0.002A_c$

$$A_s = \frac{0.1N_{Ed}}{f_{yd}} = \frac{0.1*17859.86}{435} = 4105.72 mm^2 > 0.002A_c(= 1900.66)$$

$A_{smax} = 0.04A_c = 38013.27$

The maximum spacing, Smax should not be less than:

a) 20 times the minimum diameter of longitudinal bars = 500mm

b) the lesser dimension of the column

c) 400 mm

So, Try $9\emptyset 25mm \ at$ 400c/c

4.5.5.2 Design and check for reinforcement of column C2(ULS)

To design the column, first we need the axial force (N_{Ed}) and moments at top and bottom of the column, which is taken from the Scia Engineer.
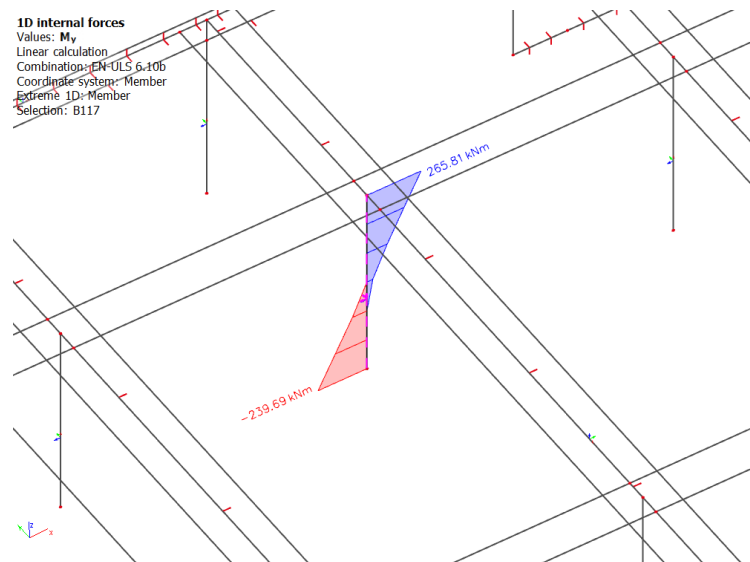

Figure 141: Display showing the moment my acting on the selected column C2 on 1PP

N_{Ed} = 17120.70kN

M_{top} = 265.81kNm

M_{bottom} = -239.69kNm

Diameter of column (d) = 1000mm

Now, first we need to check whether column is slender or not, for that as per Eurocode,

$$\lambda \geq \lambda_{lim} \ldots \ldots \ldots Slender \ column$$

Where,

$$\lambda = \frac{l_o}{i} = \frac{l_o}{\sqrt{\frac{I}{A_c}}},$$

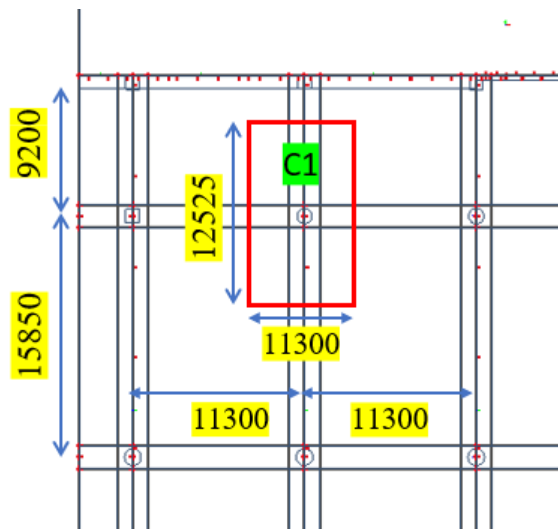$$For \ circular \ column = \frac{4 * l_o}{d} = \frac{4 * 4.6848}{1000} = 18.74$$

$$l = floor\ to\ floor\ height - thickness\ of\ slab = 7.57 - 0.25 = 7.32m = 7320mm$$

$$l_o = F * l = 0.64 * 7.320 = 4.6848$$

To calculate F, using the PD6687 method,

$$k = k1 = k2 = \frac{EI_c/L_c}{\sum \frac{2EI_b}{L_b}} = \frac{\frac{1000^4/12}{12525}}{\frac{2 * 12525 * 600^3/12}{11300}} = 0.1667 \cong 0.17$$

So, F = 0.64

$$\lambda_{lim} = \frac{20ABC}{\sqrt{n}} = \frac{20 * 0.7 * 1.1 * 1.784}{\sqrt{0.7266}} = 32.23$$

$$= \qquad\qquad\qquad ……….as\ per\ EN1992, clause\ 5.8.3.1(1)$$

Where,

A = 0.7 (default)

B = 1.1 (default)

C = 1.7 – r_m = 1.7 – (M_{01}/M_{02})

Additional moment due to imperfection = $N_{Ed} * e_i = N_{Ed} * \frac{l_o}{400} = 200.5kNm$

So, $C = 1.7 - \left(\frac{-239.69+200.5}{265.81+200.5}\right) = 1.784$

And, $n = \frac{N_{Ed}}{A_c*f_{cd}} = \frac{17120.70*10^3}{785398.1634*30} = 0.7266$

$$\lambda(= 18.74) < \lambda_{lim}(= 32.23) ………NOT\ Slender\ column\ \&\ M2 = 0kNM$$

So, design moment $M_{Ed} = max(M_{o2}; M_{0Ed} + M_2; M_{01} + 0.5M_2; N_{Ed}e_0)$

$$M_{Ed} = max(466.31, 264.11, -39.19, 570.69)$$

Where,

$$M_{o2} = M + e_i N_{Ed} = 265.81 + 200.5 = 466.31 kNm$$

$$M_{0Ed} = (0.6M_{02} + 0.4M_{01}) \geq 0.4M_{02}$$
$$M_{0Ed} = (0.6 * 466.31 + 0.4(-39.19)) = 264.11 > 186.524$$

$$M_{01} + 0.5M_2 = -39.19 + 0 = -39.19 kNm$$

Using design charts:

Require d_2/h, we can find the area of reinforcement,

Assume 25mm diameter bars as main reinforcement and 10mm bars as shear links.

$$d_2 = c_{nom} + link + \frac{\emptyset}{2} = 30 + 10 + 12.5 = 52.5$$

Require $\frac{d_2}{h} = \frac{52.5}{1000} = 0.0525 \cong 0.053$

$$\frac{M}{bh^2 f_{ck}} = \frac{466.31 * 10^6}{1000^3 * 45} = 0.0103 \cong 0.01, \frac{N}{bhf_{ck}} = \frac{17120.70 * 10^3}{1000^2 * 45} = 0.38 \cong 0.4$$
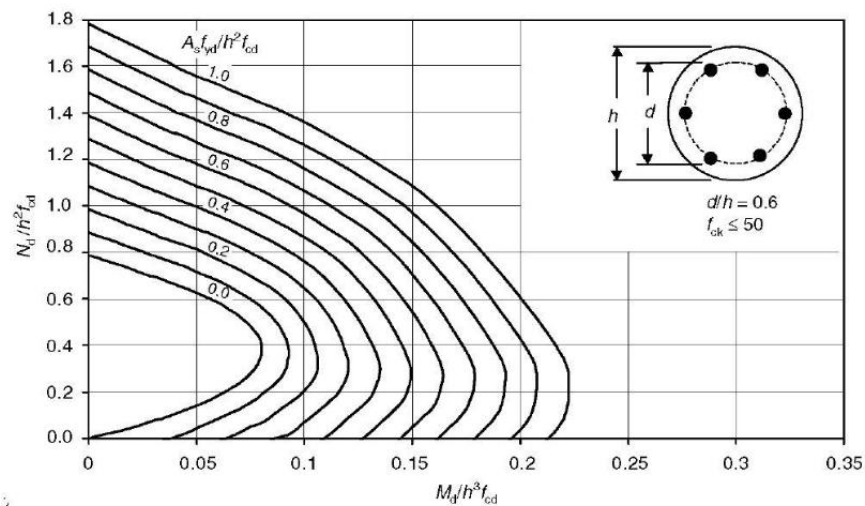

Figure 142: d/h design chart to find the area

From the values received, if we look into the chart for area we can see that, $\frac{A_s f_{yd}}{h^2 f_{cd}} = 0$,

Minimum reinforcement as per EC, $A_s \geq \frac{0.1N_{Ed}}{f_{yd}}$ or $0.002A_c$

$$A_s = \frac{0.1N_{Ed}}{f_{yd}} = \frac{0.1*17120.70*10^3}{435} = 3935.8mm^2 > 0.002A_c (= 1570.8)$$

$A_{smax} = 0.04A_c = 31416$

The maximum spacing, Smax should not be less than:

a) 20 times the minimum diameter of longitudinal bars = 500mm

b) the lesser dimension of the column

c) 400 mm

So, Try $9\emptyset25mm\ at\ 300$c/c

4.5.5.2 Design and check for reinforcement of column C3(ULS)

To design the column, first we need the axial force (N_{Ed}) and moments at top and bottom of the column, which is taken from the Scia Engineer.

$N_{Ed} = 15174.53$kN

$M_{top} = $ -300.57kNm

$M_{bottom} = 554.45$kNm

Size of column = 900x900

Now, first we need to check whether column is slender or not, for that as per Eurocode,

$$\lambda \geq \lambda_{lim} \dots \dots \dots Slender\ column$$

Where,

$$\lambda = \frac{l_o}{i} = \frac{l_o}{\sqrt{\frac{I}{A_c}}},$$

$$For\ rectangular\ column = \frac{3.46l_o}{h} = \frac{3.46 * 4.3188}{900} = 16.60$$

$$l = floor\ to\ floor\ height - thickness\ of\ slab = 7.57 - 0.25 = 7.32m = 7320mm$$
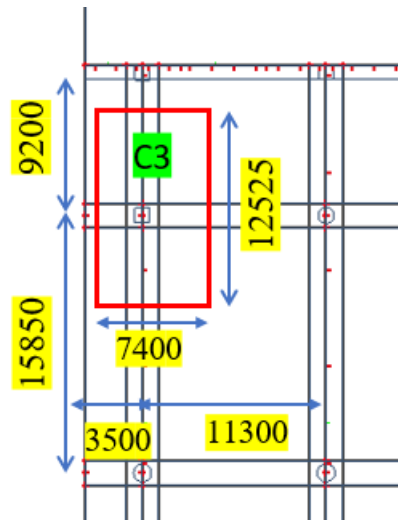
$$l_o = F * l = 0.59 * 7.320 = 4.3188$$

To calculate F, using the PD6687 method,

$$k = k1 = k2 = \frac{EI_c/L_c}{\sum \frac{2EI_b}{L_b}} = \frac{\frac{900^4/12}{12525}}{\frac{2 * 12525 * 600^3/12}{7400}} = 0.072$$

So, F = 0.59

$$\lambda_{lim} = \frac{20ABC}{\sqrt{n}} = \frac{20 * 0.7 * 1.1 * 1.89}{\sqrt{0.6244}} = 36.83$$

$$= \qquad\qquad \dots \dots \dots as\ per\ EN1992, clause\ 5.8.3.1(1)$$

Where,

A = 0.7 (default)

B = 1.1 (default)

C = 1.7 – r_m = 1.7 – (M_{01}/M_{02})

Additional moment due to imperfection = $N_{Ed} * e_i = N_{Ed} * \frac{l_o}{400} = 163.84 kNm$

So, $C = 1.7 - \left(\frac{554.45+163.84}{-300.57+163.84}\right) = 1.89$

And, $n = \frac{N_{Ed}}{A_c * f_{cd}} = \frac{15174.53*10^3}{810000*30} = 0.6244$

$$\lambda(= 16.60) < \lambda_{lim}(= 36.83) \dots \dots \dots NOT\ Slender\ column\ \&\ M2 = 0kNM$$

So, design moment $M_{Ed} = max(M_{o2};\ M_{0Ed} + M_2;\ M_{01} + 0.5M_2;\ N_{Ed}e_0)$

$$M_{Ed} = max(718.29, 264.11, -39.19, 570.69)$$

Where,

$$M_{o2} = M + e_i N_{Ed} = 665.45 + 163.84 = 718.29 kNm$$

$$M_{0Ed} = (0.6M_{02} + 0.4M_{01}) \geq 0.4M_{02}$$
$$M_{0Ed} = \left(0.6 * 718.29 + 0.4(-136.73)\right) = 376.28 > 287.316$$

$$M_{01} + 0.5M_2 = -136.73 + 0 = -136.73 kNm$$

Using design charts:

Require $\frac{d_2}{h}$, we can find the area of reinforcement,

Assume 25mm diameter bars as main reinforcement and 10mm bars as shear links.

$$d_2 = c_{nom} + link + \frac{\emptyset}{2} = 30 + 10 + 12.5 = 52.5$$

Require $\frac{d_2}{h} = \frac{52.5}{900} = 0.058 \cong 0.1$

$$\frac{M}{bh^2 f_{ck}} = \frac{718.29 * 10^6}{900^3 * 45} = 0.022, \qquad \frac{N}{bh f_{ck}} = \frac{15174.53 * 10^3}{900^2 * 45} = 0.42$$
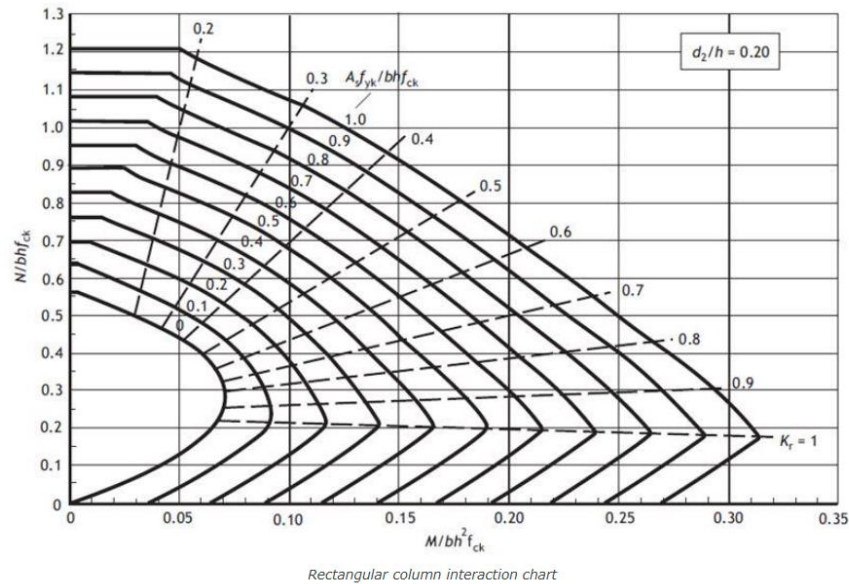

Rectangular column interaction chart

Figure 143: d/h design chart to find the area

From the values received, if we look into the chart for area we can see that,

$. \frac{A_s f_{yd}}{h^2 f_{cd}} = 0,$

So,

Minimum reinforcement as per EC, $A_s \geq \frac{0.1 N_{Ed}}{f_{yd}}$ or $0.002 A_c$

$A_s = \frac{0.1 N_{Ed}}{f_{yd}} = \frac{0.1 * 15174.53 * 10^3}{435} = 3488.4 mm^2 > 0.002 A_c (= 16200)$

$A_{smax} = 0.04 A_c = 32400$

The maximum spacing, Smax should not be less than:

a) 20 times the minimum diameter of longitudinal bars = 500mm

b) the lesser dimension of the column

c) 400 mm

So, Try $8\emptyset 25mm$ at 400c/c

4.5.6 Sheeting Design and Sheeting Check of structure using GEO5 Software

Sheet pile walls are thin preserving partitions (retaining walls) built to maintain earth, water, or another filler fabric. They're typically thinner than masonry or reinforced concrete retaining walls just like stake (cantilever) retaining partitions and may be built with the use of accouterments similar to a sword, concrete, or timber. strengthened concrete distance piles are a precast concrete members. The piles are pretty and displace a big volume of soil at some stage in riding. The most common place type of distance pile walls is steel distance piles. they have the advantage of being proof against high riding stresses advanced in difficult or rocky conformations. they are lighter in weight and can be reused numerous times in any sort of condition. metallic sheet piling is used in several types of brief workshops and endless systems. The named segment has to be designed to offer the maximum energy and continuity on the smallest feasible weight and appropriate riding charges [28]

There is various extraordinary makes use of sheet pile walls viz., for Basements, underground car parks, river management systems, ports & harbors, pumping stations, bridge abutments, avenue widening preserving walls, containment obstacles, and transient works.

1. Basements

   Sheet piling is an excellent material for constructing basement walls because it requires a minimum construction variety. Its parcels are completely employed in each transient and endless cases and it offers huge price and software savings. distance piles also can help perpendicular masses from the structure over.

2. Underground car parks

   One particular form of the basement in which sword distance piling has been installed to be specifically powerful is for the advent of underground vehicle premises. The truth is that sword distance piles may be driven tight against the boundaries of the factor and the wall itself has a minimum consistency approach in that the vicinity available for buses is maximized and the cost in line with the bay is minimized.

So, under the guidance of doc. Ing. Jan Záleský, CSc., for our model we compare the results in Geo5 Software by selecting Larssen (Sheeting walls Thyssenkrupp 700n) and by reinforced concrete sheet piles to check which is more suitable for such a large project.
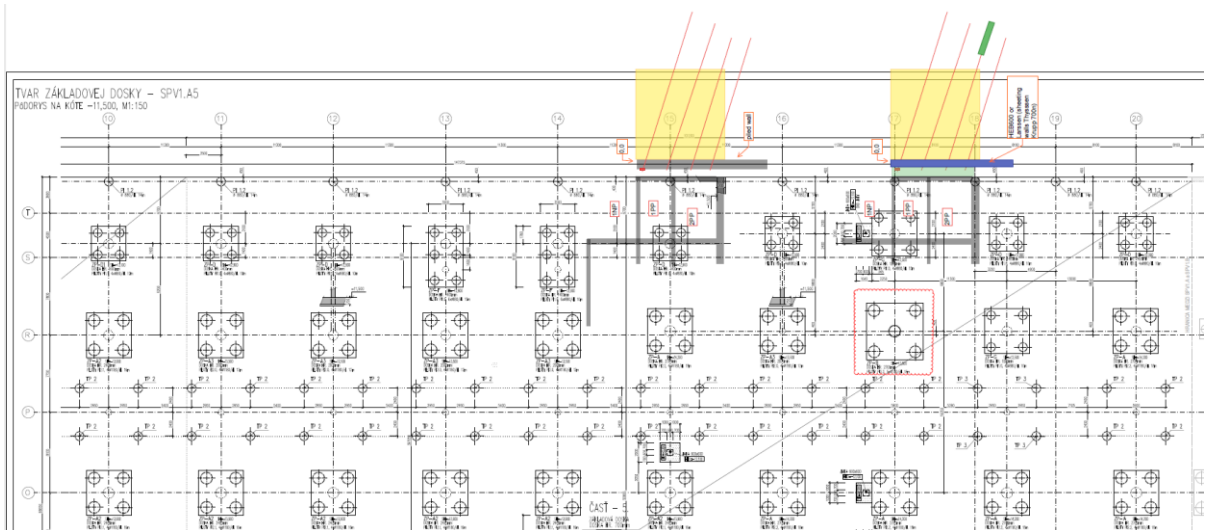
Figure 144: Layout of the pile group showing different groups of pile
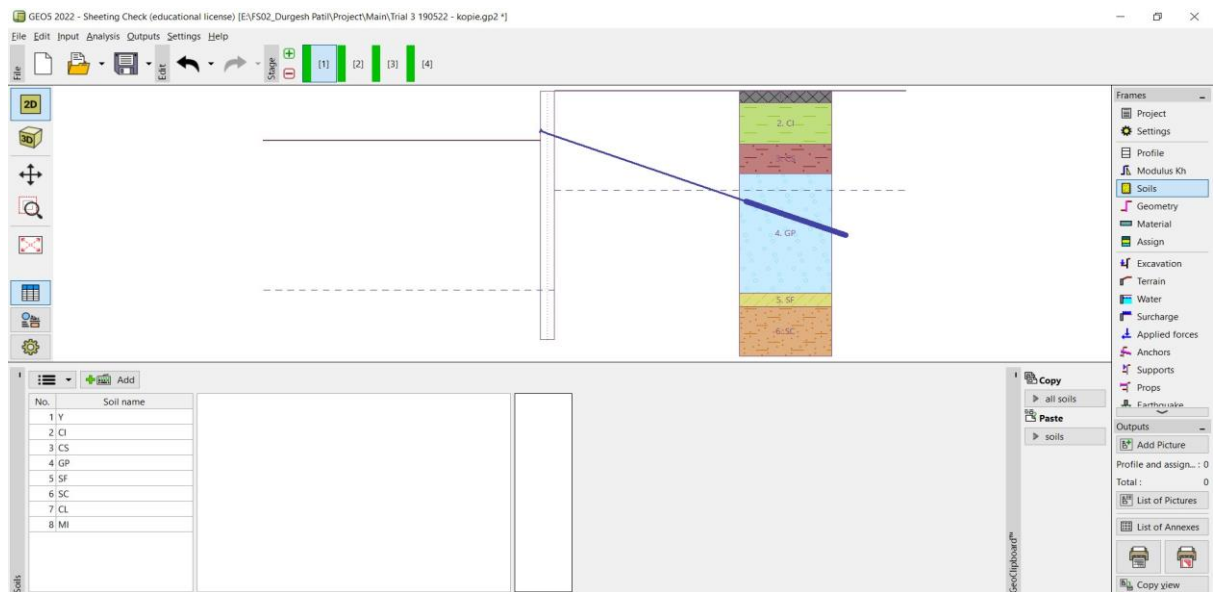
4.5.6.1 Soil Data

Figure 145: Display showing the assigning the soil data

After selection of type of sheeting wall, we assigned the soil data given by the site investigation report in GEO5 Software as shown in figure 145.

4.5.6.2 Geometry and Material Assign

As we discussed previously we design and check the sheeting walls for reinforced concrete and steel sheet, so in the beginning we assigned the geometry in which initially we choose the length of wall (L) 16m & h = 0.80m and material for RC rectangular wall as shown in the following figure 146 & 147.
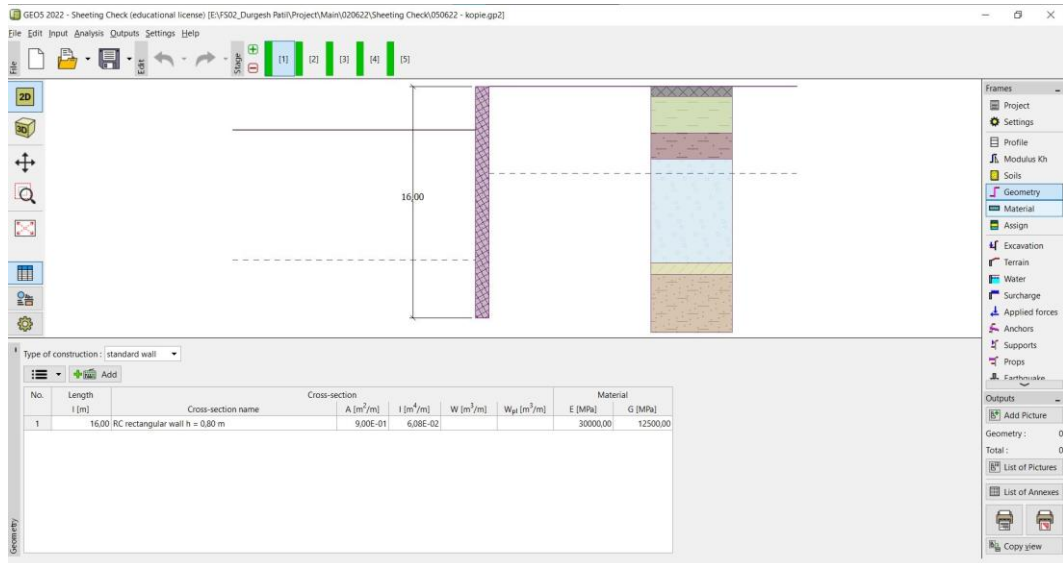
Figure 146: Display showing the geometry of the structure
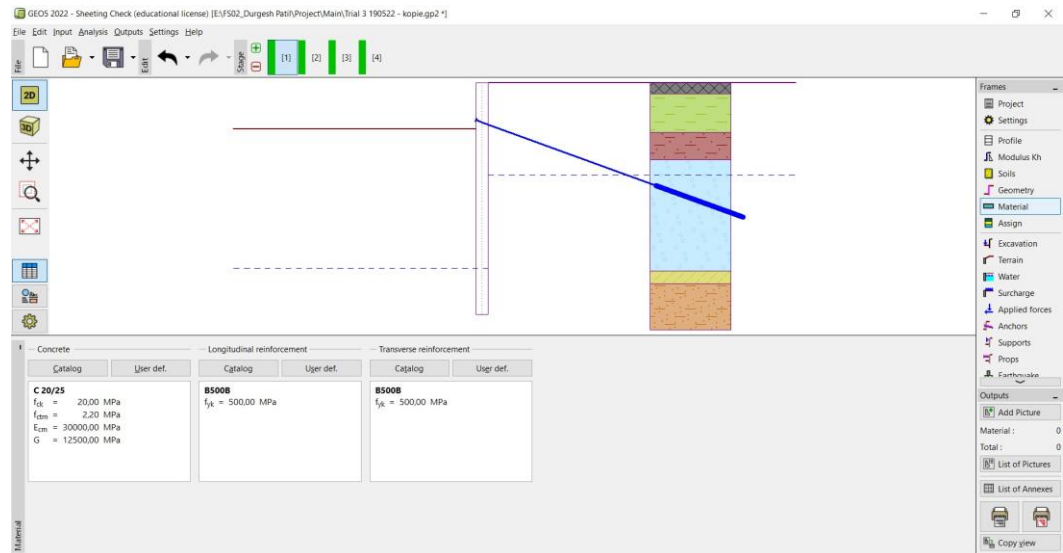

Figure 147: Display showing the material of the structure

4.5.6.5 Soil Assign

After successful geometry, the next step is to assign the soil present on the site, and as the investigation report we realized that there are total nine different types of soils are present varying with depth (or thickness) accordingly we managed to add the soil in the software as shown in the figure 148.
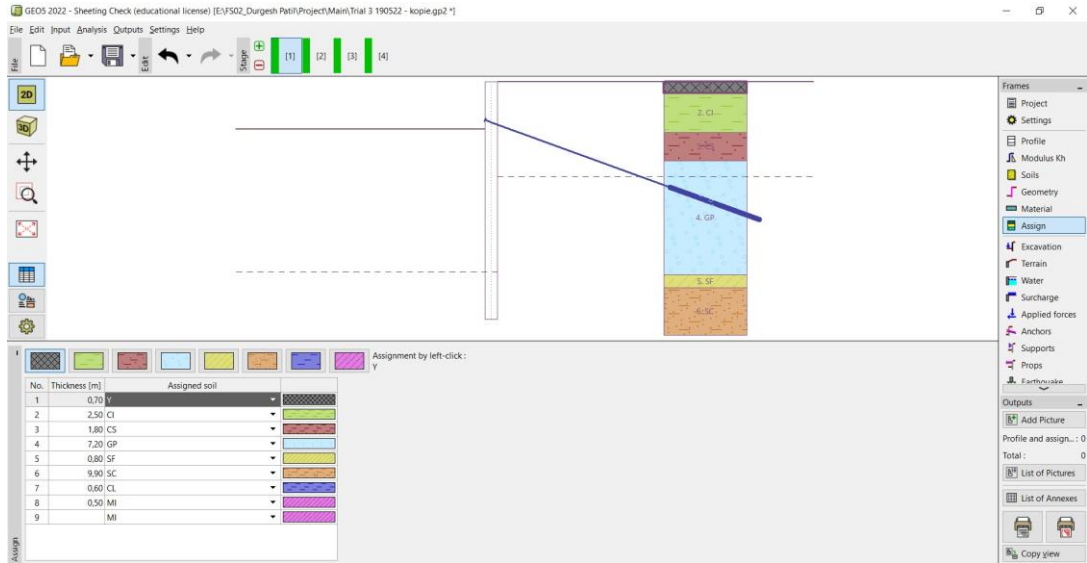
Figure 148: Display showing the soil assigning

4.5.6.6 Water Table Assign

In the next step, we looked for the water table and then we found that 6m of GWT is present behind the construction below ground level and 12m of GWT in front of construction so accordingly we putted it in the software as shown in Figure 149.
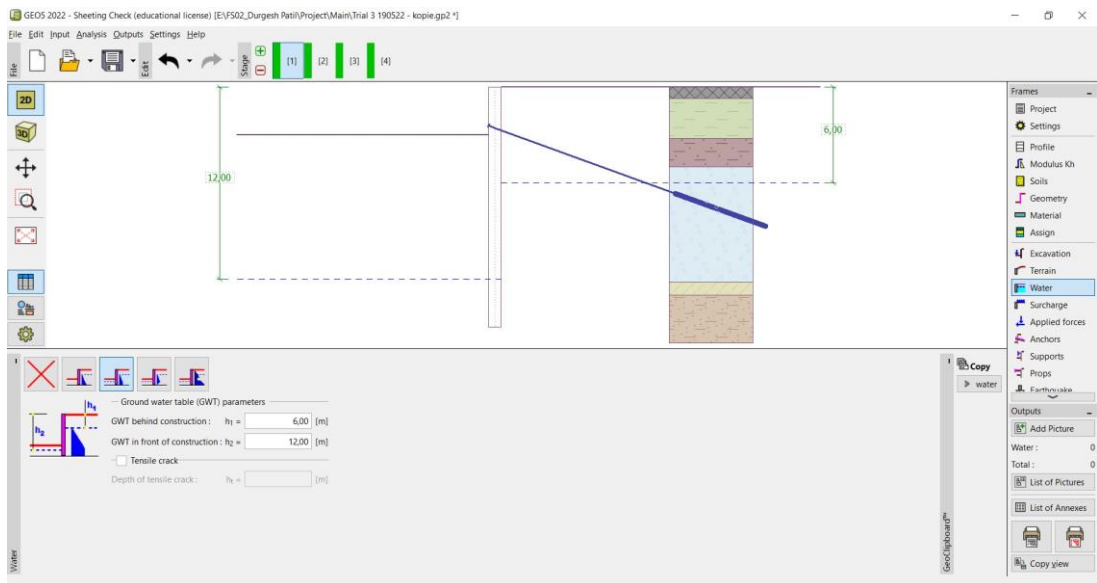

Figure 149: Display showing the GWT position behind and Infront of the construction
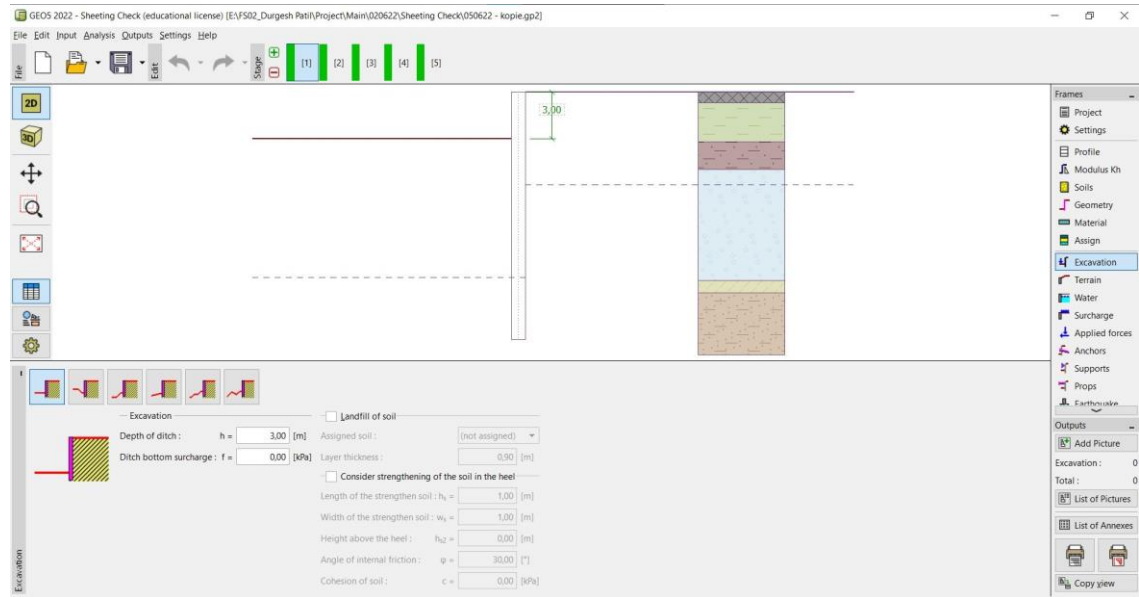
4.5.6.7 Excavation of Stage I

Figure 150: Display showing the excavation

Generally we can excavate the soil up to 3m at a time, so using the same approach we created five different excavation stages in the software from stage I with 3m, in the next stage further 3m and proceed up to stage V.

4.5.6.8 Analysis of Stages I -V

After the excavation, we analyzed it for all stages to know the maximum value of internal forces acting on the structure (shear force, moment) and displacement so that we can we get the idea how many number of anchors we need to provide and how it affect to water table as well.

Figure 151: Display showing the analysis of stage I

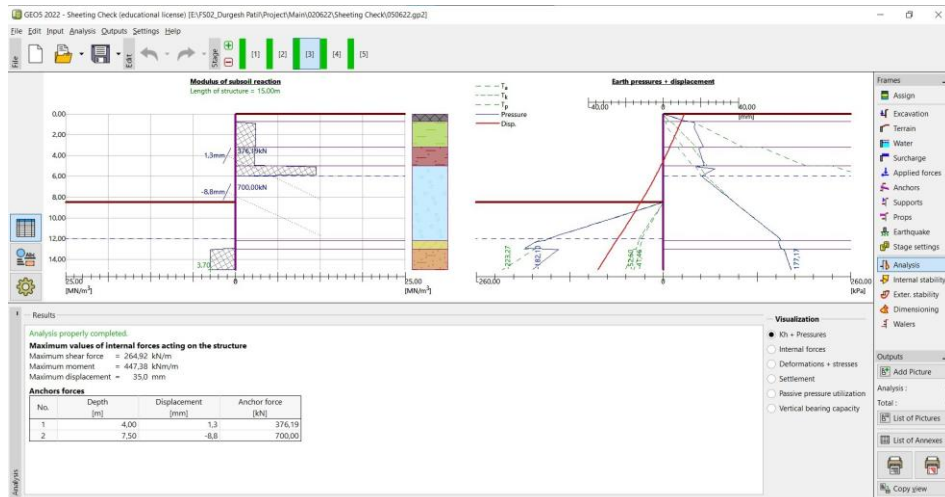Figure 152: Display showing the analysis of stage II

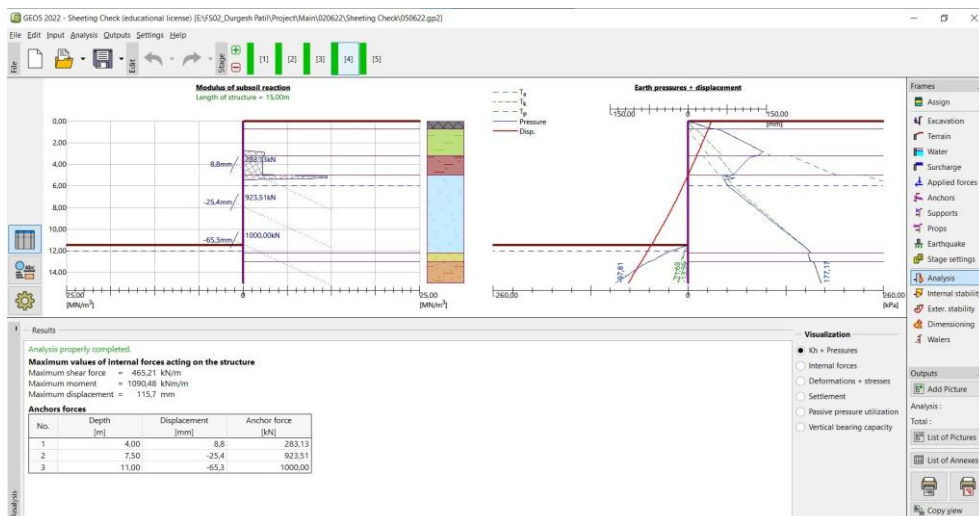Figure 153: Display showing the analysis of stage III

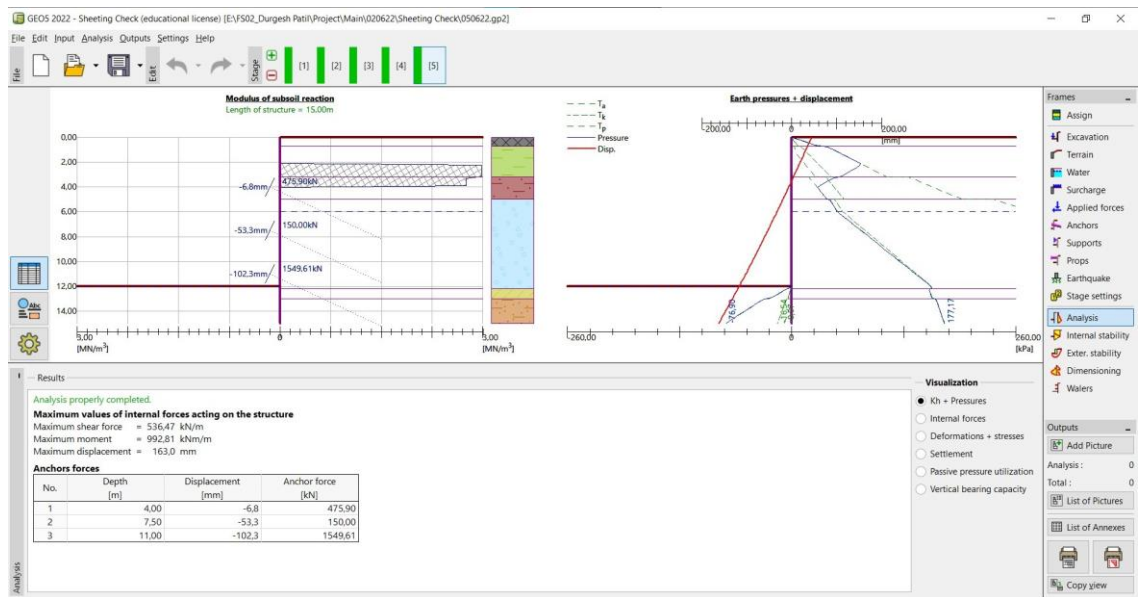

Figure 154: Display showing the analysis of stage IV

Figure 155: Display showing the analysis of stage V

4.5.6.9 Sheeting check after assigning the anchors

After the analysis, we got the clear idea that we need to at least three anchors at the different positions based on trial and error until we get the satisfactory stability. so, after the assigning the anchors we again analysis the structure and checked the three major sheeting checks as given below:

1. Internal stability

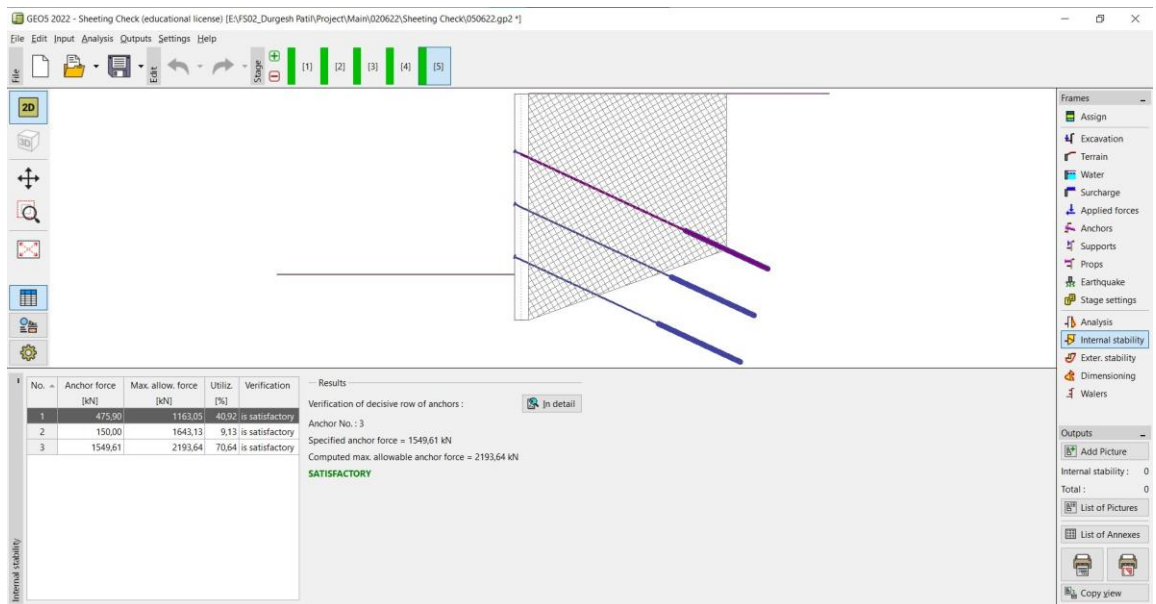In the internal stability we got the satisfactory results with three anchors as shown in the figure 156.

Figure 156: Display showing the internal stability of the RC Sheet wall

2. Dimensioning with crack

Then we looked it for crack to know whether with this three anchors and geometry that we choose is affect the structure or not with given water table and after the check we can say that for the selected data we got the satisfactory results as shown in the figure 157.
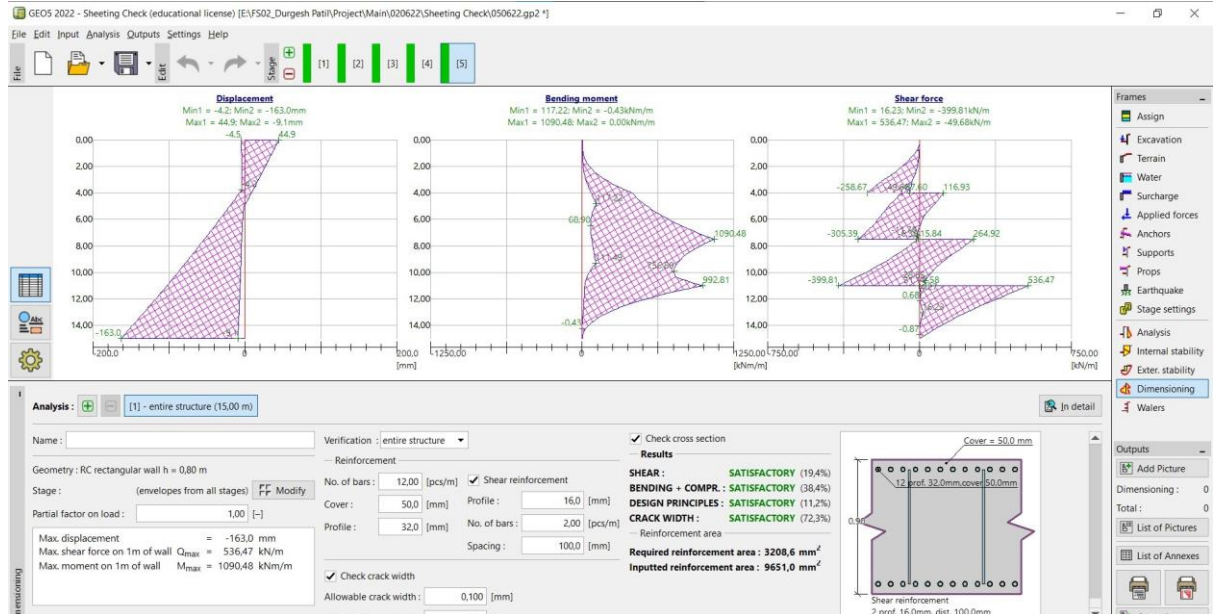

Figure 157: Display showing the dimensioning with crack of the RC Sheet wall

3. Slope Stability

The last check is slope stability, which is performed to check the design is safe or not that's felicity and reinforcement behavior. Stability of distance- pile walls is frequently veritably sensitive to seepage inflow. In the presence of seepage inflow, the reduction in unresistant pressure on one side and increase in active pressure on the other side of the wall increase the threat of the insecurity that may antecede precariousness due to pipeline or ground heaving.[31] So, first we check it for RC rectangular wall, and the we repeat the entire procedure which was explained above by using the steel sheet pile wall, and then compared the results of the both material.
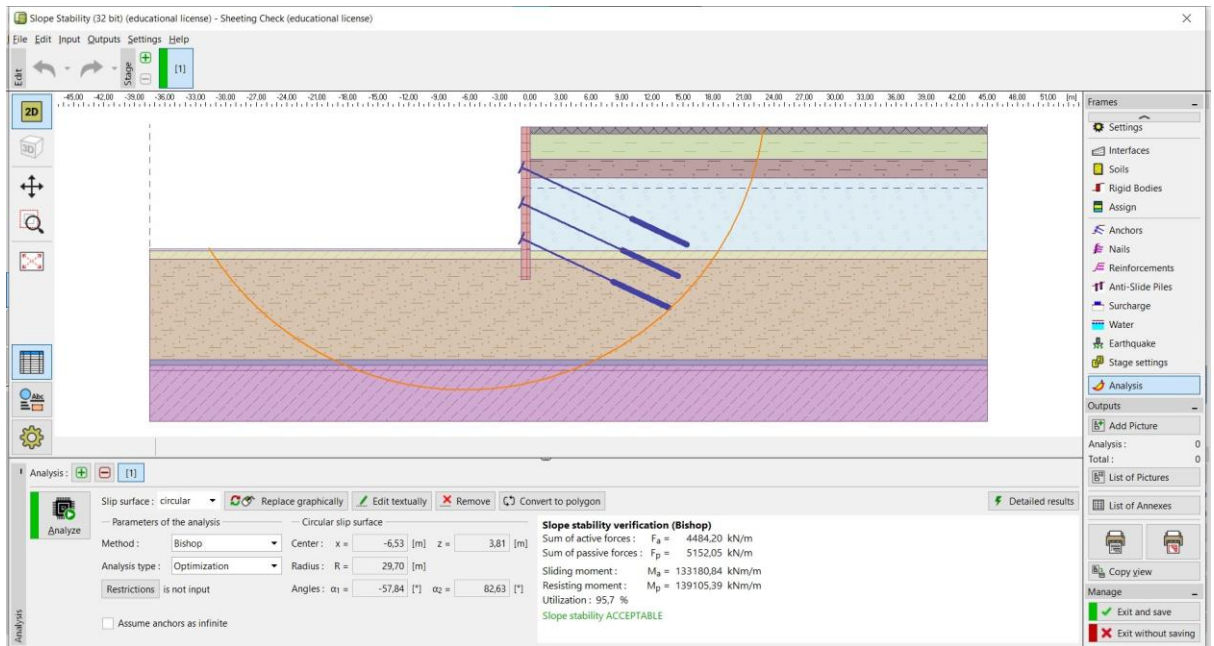
For RCC WALL

Figure 158: Display showing the slope stability of the RC Sheet wall
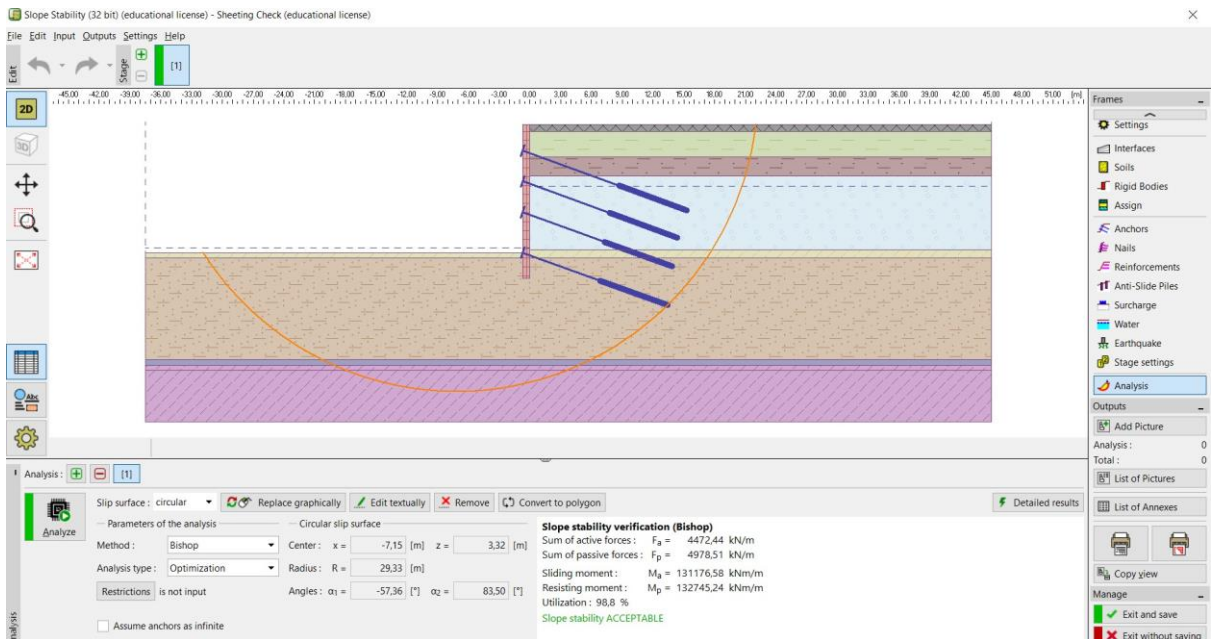
For Steel Sheet pile

Figure 159: Display showing the slope stability of the steel Sheet wall

From the above results, we can say that overall both the types of walls are suitable for our structure, but if we look in that slope utilization then we get to know almost 99% of utilization we got in steel sheet pile as compared to RC wall, but at the same time one additional anchor is required in the steel sheet pile. Moreover, there are some advantages also if we use steel sheet like resistant to high driving stresses developed in hard or rocky

formations, they are light in weight as compared to RC and can be reused several times in any type of condition.

But, if we provide additional length of wall in geometry in case of RC wall, then theoretically we can reduce the displacement, anchor force and also prevent the inflow of water from bottom as well, which will then make structure more stable.

4.5.7 Analysis of Pile Group

The building is based on a combination of mat and deep foundation construction, which consists of a base plate supported by large-diameter bored piles. Piles are designed not only for active and passive pressure transfer from vertical structures, but also for uplift pressure caused by groundwater. The base plate is mainly of uniform thickness, without expansion. In places of columns, the thickness of the base plate is increased due to the increase in load. In these places there are reactions from the superstructure transferred with the help of piles to the subsoil. The design of the foundation structures corresponds to the static design of the foundation of the building.
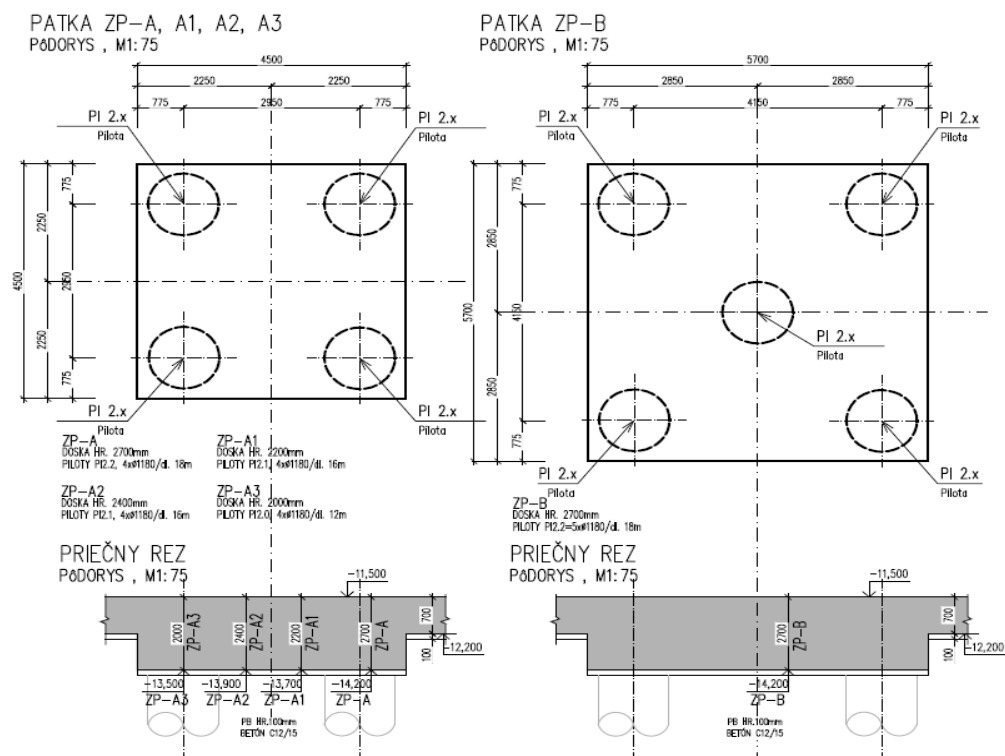

Figure 160: Geometry of the pile group

In the entire building, mostly 4 and 5 group of piles are used as per the drawings, so initially we did the calculations for both pile of groups using GEO5 Software.

First, we created the structure and geometry for the five and four group of pile in Geo5 software with help of given geometry of the pile (as shown in fig 161 & 162).
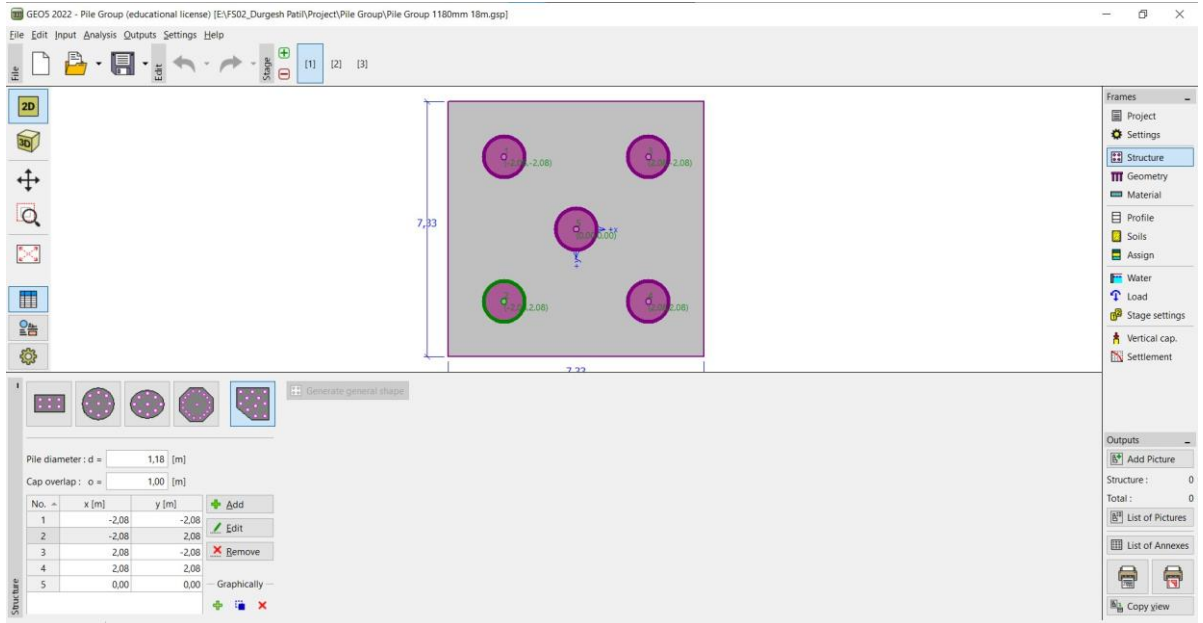
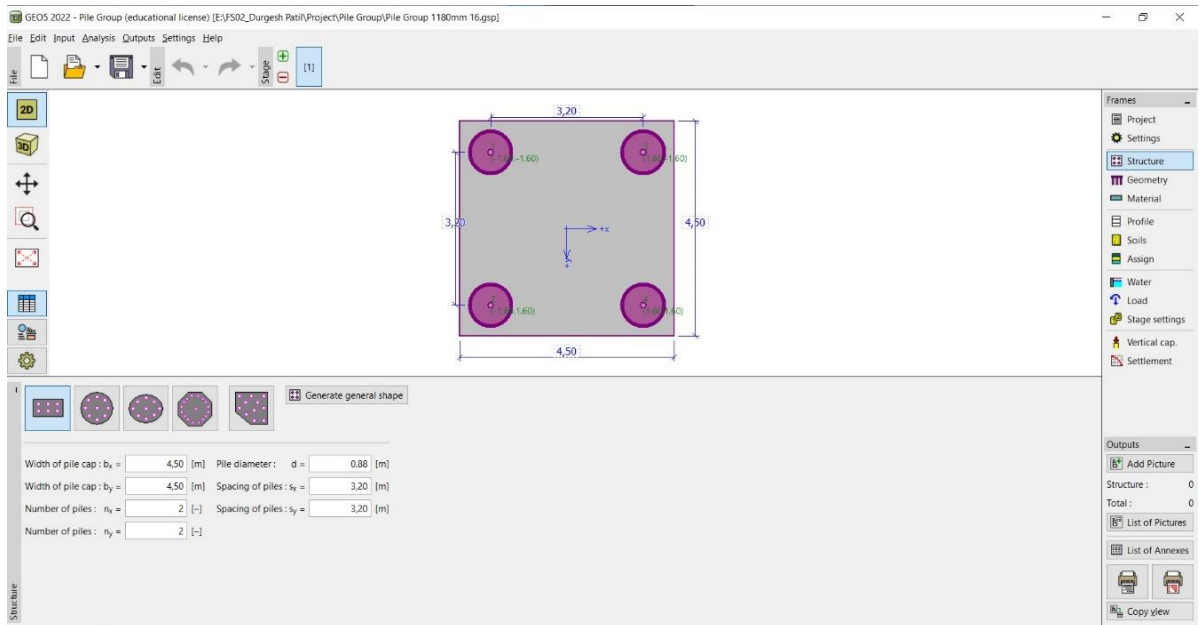

Figure 161: Structure for 4 group of pile

Figure 162: Structure for 5 group of pile

Then in the next step as per given data, material was assigned and profile is created for different layer of soil so that soil is assign to each different layer of soil and after applying the load on the pile vertical capacity is checked for the given structure and the results are given the figure 163.
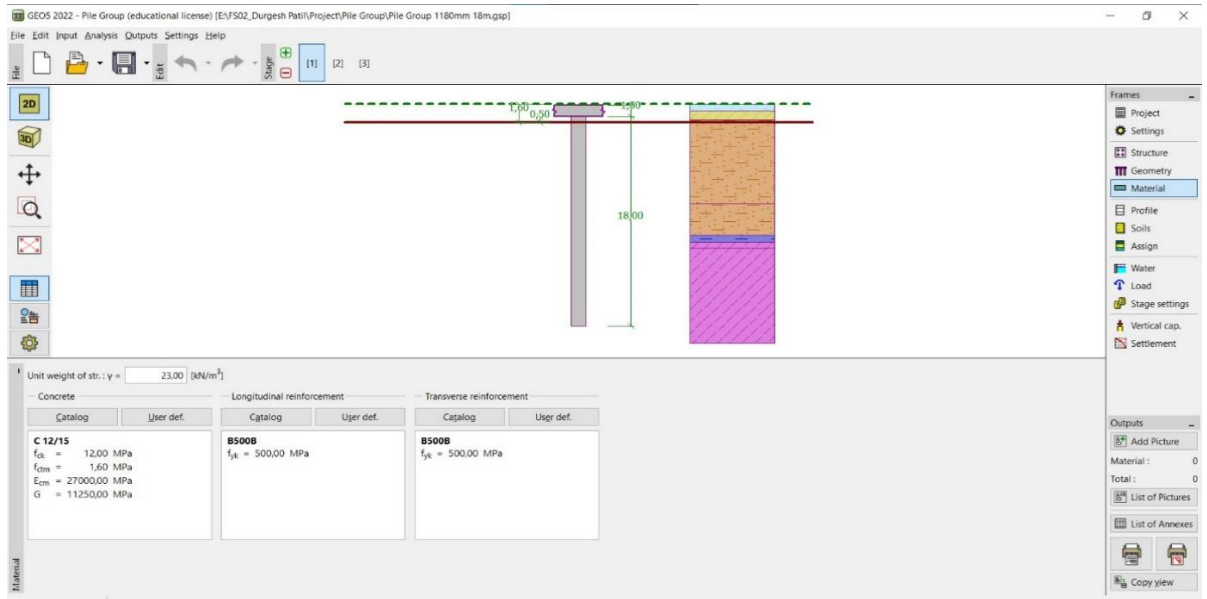
Figure 163: Material assigning for both group of pile

From the result of the vertical capacity, we can say that vertical bearing capacity of the pile group of five and four is satisfactory as shown in following figures 164 & 165.
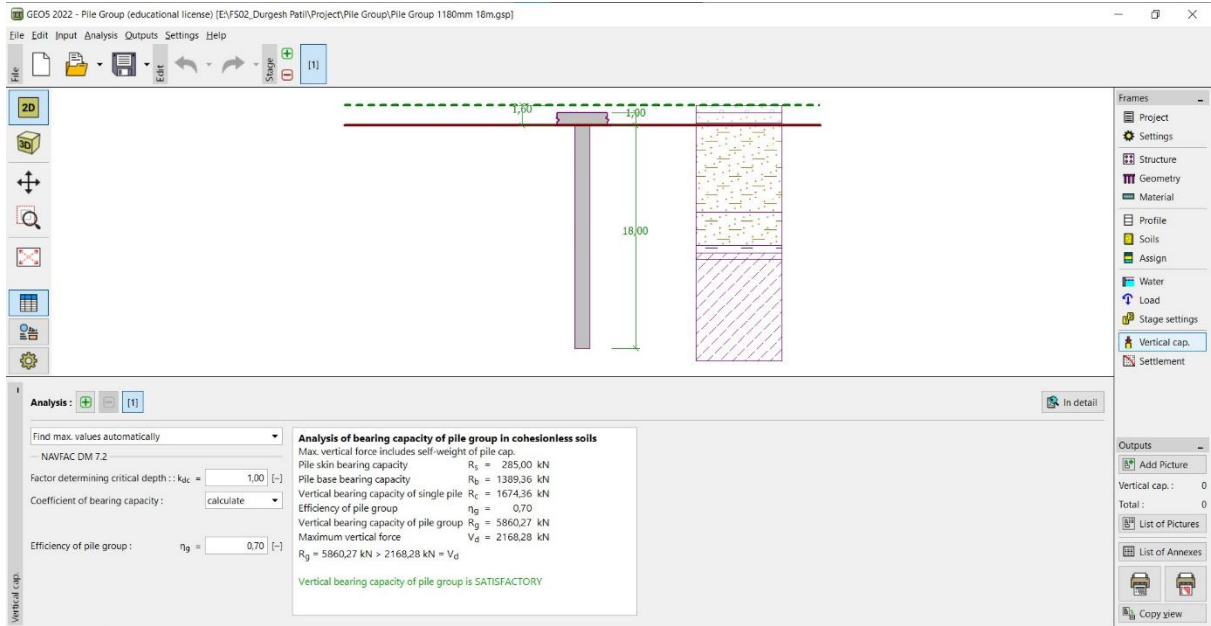
Figure 164: Result of vertical displacement for 5 group of pile
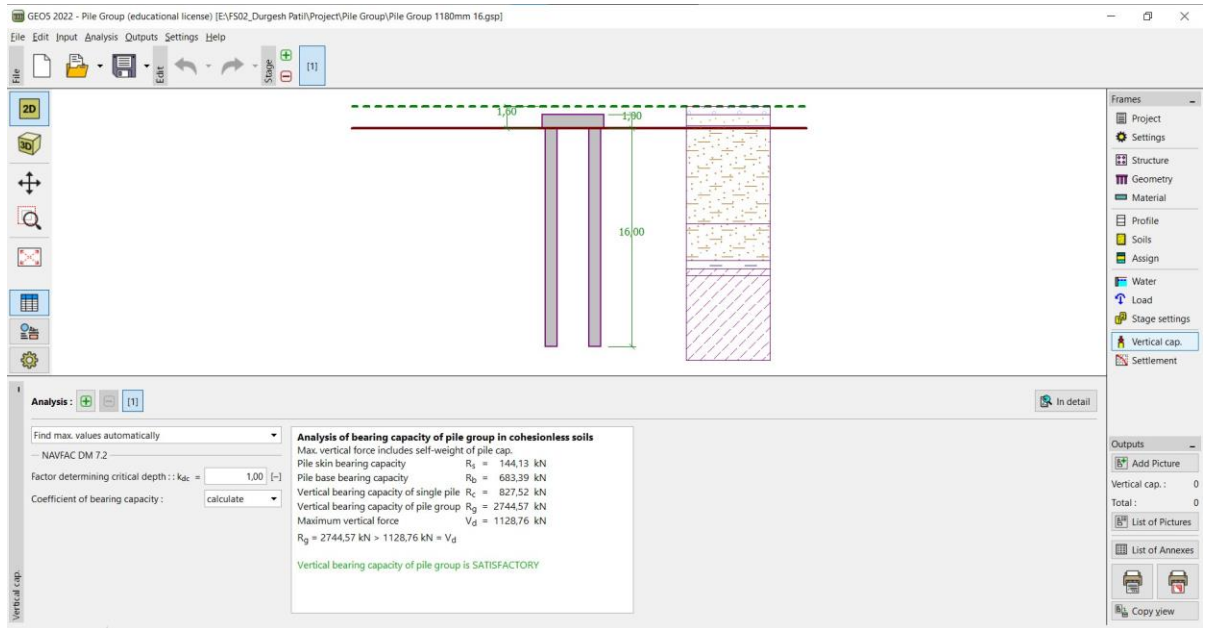
Figure 165: Result of vertical displacement for 4 group of pile

Next we looked for the settlement for both set of group pile and we found that the settlement in five group of pile (6.9mm) is less than group of four(21.9mm), but both the displacement are under the limit. However, we could say that probably it was due the axial load under four group of pile was higher due to the overall load which acts on it.
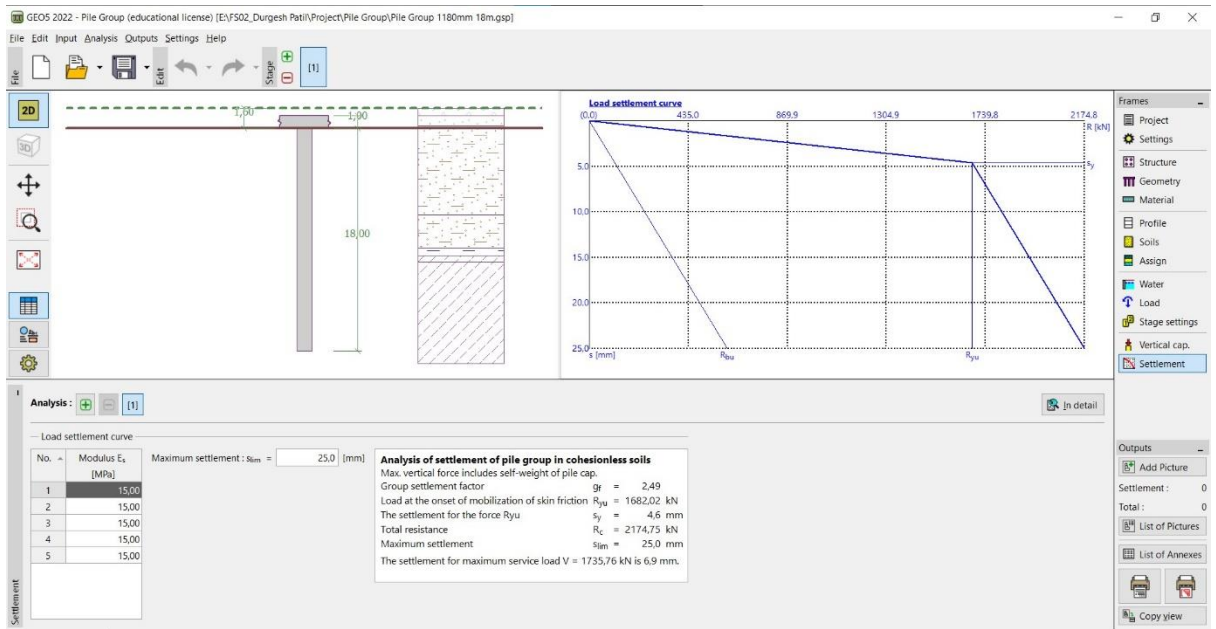
Figure 166: Result of settlement for 5 group of pile
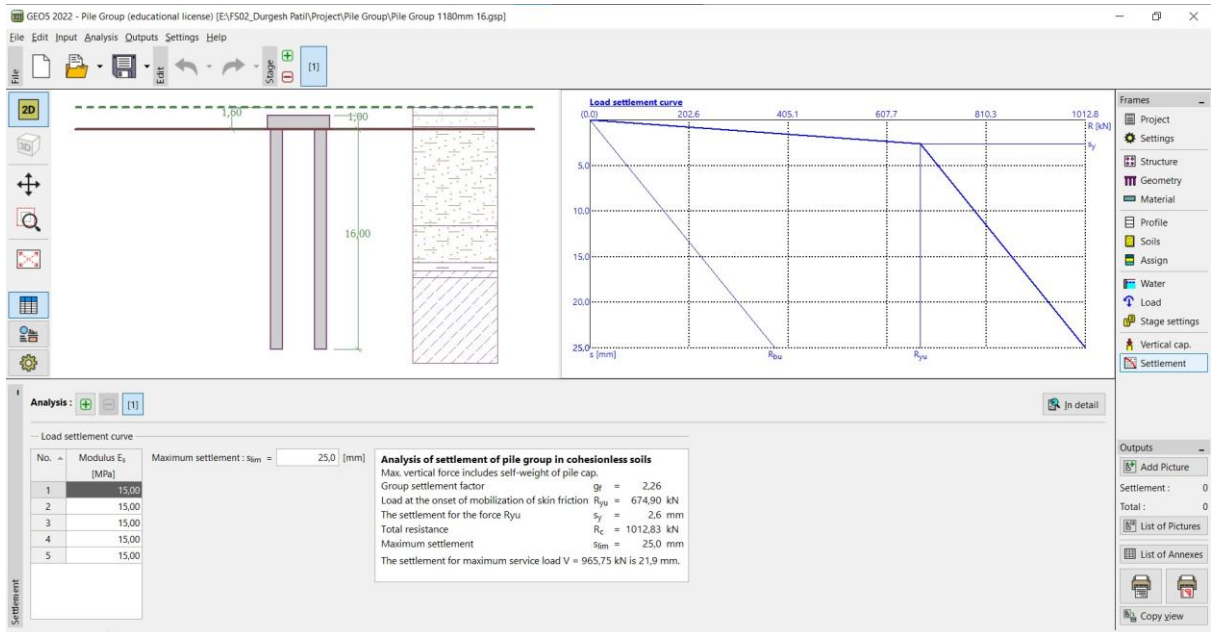
Figure 167: Result of settlement for 4 group of pile

Overall, in case of Pile group, as there was no further information about soil below 24m, so for the analysis we preliminary assumed the same soil which is on the last layer, but, for more accurate results we can search for deeper site investigation, also for next stage of site investigation – two bore holes well needed below toe of pile because of side friction, if this also not possible then need to do some checks before starting to find out the exact soil below toe.

5. CONCLUSION

The goal of this work was the prestressing design of the A5 expansion of the Mlynské Nivy Bus Station in Bratislava. On the morning of this work, we dealt with the exploration of the content of prestressed concrete. We anatomized the introductory specifics of the technology used, either in general or its use in connection with the assignment of work. In the coming part, we compactly described the design of the multifunctional house, its position, architectural result, and structural system. We created a model in the structure for the supporting structure of the structure, which we also anatomized and carried out a variant design of the supporting structure. For the design, we chose the most complex ceiling structure 1PP, which is specific to a supply yard with a high cargo, and at the same time, it's possible to apply the established design principles across the entire supporting structure. The main subject of the thesis was an annotated static computation, where we managed to justify the use of prestressed concrete technology in the assigned design, outlined the disadvantages of reinforced concrete long-span structures and, in particular, anatomized in detail the design of the prestressing of the beam A2, characteristic bearing element. The last step was the design of reinforced concrete rudiments (or elements) with the effect of prestressing in the answered section of the ceiling slab.

Next, we design the staircase which is available on each floor along with this the ramps which start from the 2NP to 4NP were designed with a detailed underpinning drawing. Likewise, columns were designed which are present on 1PP, and the shear wall near to staircase was designed to check out of total axial load it carries. Also, an analysis of sheeting pile walls was designed, and checked the stability and dimensioning for the crack range were to know the goods due to groundwater table, uplift pressure, and water seepage. And, also analysis of piles in groups was done to check the vertical bearing capacity of the structure and the settlement.

6. REFERENCE

1. https://en.wikipedia.org/wiki/Prestressed_concrete

2. Prestressed concrete (online)

   https://www.expertnotes.in/wp-content/uploads/2020/11/Prestressed-concrete-1.pdf

3. Multifunctional Object Mlynská Niva Bus Station,

   https://www.sieberttalas.com/cs/projekty/bus-station-twin-city

4. STANICA NIVY – a multifunctional project in the heart of Bratislava for the 21st century, Published: January 21, 2020, Ing. Jiří Koukal

   https://konstrukce.cz/realizace-staveb/stanica-nivy-multifunkcni-projekt-v-srdci-bratislavy-pro-21-stoleti-297

5. Cyclic shear behavior and strength capacity of prestressed concrete walls in high-rise buildings, Xiaowei Cheng, Xiaodong Ji, Ziguo Xu, Yixiu Wan, Tao Wang (online)

   https://reader.elsevier.com/reader/sd/pii/S0141029622007441?token=6734710A8C4FC96FC9B6AB21672E3A79190E55BCEF34365E235F6822E71A567E2621DC610EC6BCC79BE94BD8977CAB7A&originRegion=eu-west-1&originCreation=20220918101336

6. State-of-the-Art Report on Partially-Prestressed Concrete Earthquake-Resistant Building Structures for Highly-Seismic Region, I Gusti Putu Rakaa, Tavioa, Made Dharma Astawaa (online)

   https://reader.elsevier.com/reader/sd/pii/S1877705814032238?token=AF4F8594045D1B73BFA4A755B0F56EE47914E06BE08E035B423D6FC713DF7C35A7103362EEC272849E0CC56E25A77DC3&originRegion=eu-west-1&originCreation=20220918100137

7. Experimental study of prestressed steel-concrete composite beams with profiled steel decking, Marcela Moreira da Rocha Almeida, Alex Sander Clemente de Souza, Augusto Teixeira de Albuquerque

   https://reader.elsevier.com/reader/sd/pii/S0143974X22002036?token=9F155F8EAD69FDB2292E8200B2C7883EB3EFA644DE4BFB64AD885125B6FDF43F7A98B474CC16F06C4FB17F9770EE7245&originRegion=eu-west-1&originCreation=20220918100315

8. Experimental and numerical study on the axial compression performance of the prestressed sleeved members, Peng Gong, Wenhao Liu, Bin Zeng, Zhen Zhou

https://reader.elsevier.com/reader/sd/pii/S026382312200622X?token=717474DEA38
81BCFA8B3F8F9CBC9B44F325FB3590A93C789BD62E809671CBBD4E7EF9594
3750AF4BB8337E76D1A10D07&originRegion=eu-west-
1&originCreation=20220918100147

9. Serviceability Performance of Prestressed Concrete Buildings Taking into Account
   Long Term Behavior and Construction Sequence, H. L. YIP, F. T. K. AU, S. T.
   SMITH
   https://reader.elsevier.com/reader/sd/pii/S1877705811012513?token=0C11E3140196
   202FC3EB7D7B6A678A5D95CAA470818C0A8738CE5C8F6A3CB2BF1ECD838E
   2D8CFF59753C144434D25C79&originRegion=eu-west-
   1&originCreation=20220918100152

10. Experimental and numerical study on seismic behavior of prestressed concrete
    composite shear wall, Xin Zhang, Guangqiang Zhou, Shurong Li, Fang Zhang, Shuai
    Zhang
    https://reader.elsevier.com/reader/sd/pii/S0141029622006526?token=1E2554773CC
    AC12AFA28FC1DCD500DD5A2BA9CF7C85DB6EFF144915A9C278CB515E82A
    D1CF7E7F0BDF8366807E58295D&originRegion=eu-west-
    1&originCreation=20220918100309

11. Nonlinear numerical analysis of prestressed concrete beams and slabs, Amilton
    Rodrigues da Silva, João Paulo de Souza Rosa
    https://reader.elsevier.com/reader/sd/pii/S0141029619307047?token=4D1E0AEB5C8
    AB1BEAD31D0FD4862C6309D4C5D8AFB614B18BBF46351F1F05B5679A658FF
    7D0CA8883A081D285D4A90A1&originRegion=eu-west-
    1&originCreation=20220918111504

12. Eurocode: Basic of structural design (online)

13. Basic terminology of PSC, taken from the lecture notes of Prof. Marek Foglar,

14. Concrete structures 3 Foglar, Marek , Frantová, Michaela , Jiříček, Pavel

15. Navrátil,J.: Prestressed concrete structures, CERM. Brno, ISBN 80-7204-462-1, 2006

16. ČSN EN 1992-1-1 Eurocode 2:Designing concrete structures: part 1-1:General rules a
    rules for building structures = Eurocode2: Design of concrete structures - Part 1-1:
    General rules and rules for buildings

17. Mlynské Nivy bus station,
    https://sk.wikipedia.org/wiki/Autobusov%C3%A1_stanica_Mlynsk%C3%A9_Nivy

18. Brochure of bus terminal to gather the basic information,

    https://gallery.mailchimp.com/c95107f1b2e7f18a450844c61/files/6d1cd726-76c1-

    43be-84e5-a351214f1261/stanica_nivy_sk.pdf

19. SCIA CZ S.R.O. SCIA Engineer v19, v20 and v21-64bit,

    https://www.scia.net/cs/scia-engineer

20. Design of slab in Scia Engineer software,

    http://people.fsv.cvut.cz/www/stefarad/vyuka/133YBKC/YBKC_Deska.pdf

21. Freyssinet pre-switching system manual,

http://www.freyssinet.cz/gallery/predpinaci_system_freyssinet.pdf

https://www.freyssinet.co.nz/sites/default/files/freyssinet_prestressing.pdf(english version)

22. Design and check in Scia, online Scia help portal

https://help.scia.net/20.0/en/index.htm#rou/concrete15/concrete15_ec.htm%3FTocPath%3DDesign%2520and%2520check%7CConcrete%7CEC-EN%7C_____0

23. InDiOn - Interaction Diagram Online: A program for drawing an interactive cross-section diagram

https://people.fsv.cvut.cz/~holanjak/software/indion/program/

24. For making layout, drawings: AutoCAD V21

https://www.autodesk.cz/products/autocad/overview?term=1-YEAR&tab=subscription

25. Technical Report of Mlynske Nivy Bus terminal

26. Design of column (online)

https://structville.com/2020/10/design-of-reinforced-concrete-columns.html

27. Design of shear wall (online)

https://structurescentre.com/designing-a-shear-wall-to-eurocode/#:~:text=The%20Eurocode%20defines%20a%20wall,mm%20aid%20detailing%20and%20construction.

https://structville.com/2020/11/design-of-shear-walls.html

28. Analysis of Shear Walls-Worked Example (Online)

https://structurescentre.com/analysis-of-shear-walls-worked-example/

29. Derivation of Wind Load on Buildings (Online)

https://structurescentre.com/derivation-of-wind-loads-on-buildings/

30. Excel tool for 3D wind – Scia Garage (Online)

https://resources.scia.net/en/garage/exceltoolfor3dwindcz.htm

31. Sheet pile walls and their uses (online)

https://structville.com/2020/10/sheet-pile-walls-and-their-uses.html

32. Scia Manual – Construction stage (Online)

https://help.scia.net/15.2/cs/downloads/constructionstages_csy.pdf

Attached drawings

P1: Layout (shape) of the ceiling above 1PP (Solved ceiling slab)   M1:150

P2: Drawing of the prestressing of the solved section of the ceiling above 1PP

M1:150, M1:30

P3: Schematic of detailed process of stressing the tendons   M1:16, M1:10

P4: Drawing of bottom reinforcement of the ceiling above 1PP (Solved ceiling slab)

M1:150, M1:30, M1:10

P5: Drawing of top reinforcement of the ceiling above 1PP (Solved ceiling slab)

M1:150, M1:30, M1:10

P6: Drawing on design of staircase   M1:10, M1:5

P7: Drawing on design of the ramp -2NP   M1:150, M1:30, M1:10

P8: Drawing on design of column   M1:45, M1:20, M1:8

P9: Drawing on design of the shear wall   M1:20, M1:15